Production of novel protein therapeutics to improve targeted cancer therapy

Al-Qahtani, Alanod

Production of Novel Protein Therapeutics to Improve Targeted Cancer Therapy

PhD thesis

The research described in this thesis was financially supported by Qatar National Research Fund (QNRF) NPRP6065-3-012, Doha, Qatar.

The author gratefully thanks Groningen University and Anti-Doping Laboratory Qatar for facilitating and supporting the research, and Makery for printing the thesis.

مختبر مكافحة
المنشطات قطر
Anti Doping
Lab Qatar

Cover picture: Giovanni Cancemi/Shutterstock.com

Cover layout: Al-Anod Al-Qahtani

2018, Al-Anod Al-Qahtani, Doha, Qatar.

 ISBN: 978-94-034-1415-7 (Ebook)

ISBN: 978-94-034-1416-4 (printed book)

university of groningen

Production of Novel Protein Therapeutics to Improve Targeted Cancer Therapy

PhD thesis

to obtain the degree of PhD at the
University of Groningen
on the authority of the
Rector Magnificus prof. E. Sterken
and in accordance with the decision
by the College of Deans.

This thesis will be defended in public on

Monday 13 May 2019 at 11.00 hours

by

Alanod Dashin M F Al-Qahtani

born on 23 September 1986
in Doha, Qatar

Supervisors

Prof. A.S.S. Dömling
Prof. S.K. Goda

Assessment Committee

Prof. L. Chouchane
Prof. P.H. Elsinga
Prof. F. Kuipers

﴿ رَبِّ زِدْنِي عِلْمًا ﴾

[طه: 114]

This Thesis is dedicated to my parents and daughter

Table of Contents:

Chapter 1

General Introduction and Scope of the Thesis

General Introduction and Scope of the Thesis

Cancer is one of the leading causes of death worldwide and one of the top ten causes of death in Qatar. Cancer research worldwide aims to enhance the understanding of cancer and develop a more effective treatments, which targets cancer cells only, with tolerable side effects than the current chemotherapy and radiotherapy.

There are several pitfalls in the current cancer treatment that are either linked with the given drug or to the patient's immune system. Regarding the drug, it lacks selectively, i.e. it damages the healthy tissues as well as the cancer cells. The lack of selectivity can cause severe side effects which in many cases terminate the treatment.[1] The other pitfall is related to the fact that the drug should be given in cycles to the patient. This leads the patient's immune system to raise antibodies against the drug, which could hamper the efficacy and efficiency of the medicine.

Due to the above weaknesses of these conventional treatments the attention has been given to the targeted cancer therapy. In this approach, the drug will be

directed mainly to the cancer tissue limiting its side effects and make it more tolerable to the patient.

In this thesis, we focus on two approaches on targeted cancer therapy, one is known as the Antibody Directed Enzyme Prodrug Therapy (ADEPT) and the other one is Targeted Tumor Superantigens (TTS).

In **chapter 2,** we covered the literature in relation to the targeted cancer therapy including our work as shown in the above chapters. The review chapter focused on PEGylation and Albumin fusion as the two strategies to produce long acting drugs.

In **chapter 3, 4 and 5,** we successfully provided solutions to many limitations in the ADEPT, which will make it more effective and efficient. In **chapter 6**, we successfully managed to identify the part on the superantigen molecule which cause severe hypotension. This will lead to the production of novel superantigen variants to be used in TTS with less side effect.

Regarding the ADEPT, it is as a two-step approach in cancer treatment. The first step involves the administration of a cancer antibody-enzyme conjugate, which targets the tumor. Next, a prodrug is injected which will be activated by the enzyme at the site of the tumor, in an effort to circumvent the adverse impact on healthy tissues. The enzyme can activate many molecules of prodrug, which will result in a large amounts of drug being generated at the tumor vacinety.[2,3] The activation of the prodrug occurs extra cellular and can penetrate the cancer cell by diffusion causing cell death.[2]

One of the enzymes that is used in this technique is Carboxypeptidase G2 (CPG2) also known as glucarpidase. The enzyme CPG2 is a bacterial enzyme and a folate hydrolyzing enzyme.

On the other hand, the enzyme also can degrade the folate analogue, Methotrexate, which is used in chemotherapy treatment of cancer. CPG2, therefore, is not only

useful in targeted cancer therapy, but also in drug detoxification in case of a high doses.[3]

In **Chapter 3,** we successfully isolated a novel glucarpidase to be used in the detoxification of drugs and the ADEPT. We isolated novel glucarpidase producing bacteria from soil using folate as the only carbon or nitrogen source. We managed to isolate three novel enzyme producing bacterial. Two of the enzyme encoding genes, *Xenophilus azovorans* SN213 and *Stenotrophomonas sp* SA were cloned and molecularly characterized.

In **chapter 4,** we focused on the use of DNA shuffling to create enzyme variants with a new exerted feature, in our case, variants with higher enzyme activities.[4] DNA shuffling is a practical process to induce directed molecular evolution in vitro by mimicking natural recombination. In addition to recombination, the technique also introduces point mutations at a controlled rate, which broadens the possibilities for evolving improved genes.[5]

In **chapter 4**, we successfully implemented the DNA shuffling techniques to produce novel CPG2 variants with higher enzyme activity than the wild type. We produced a DNA library using the DNA shuffling techniques and screening over four thousand variants on folate containing media plates, the variants were isolated depending on the desired phenotype. The best three novel variants with higher activity glucarpidase were analyzed and sequenced, to recognize the effector mutation, and the kinetics of each variant.

In **Chapter 5,** we have managed to implement two techniques to extend the serum half-life of CPG2 in the ADEPT technique and the detoxification of MTX. The first

approach is through PEGylation by the attachment of polyethylene glycol (PEG). PEG is a water-soluble and biocompatible polymer, which is used expensively in drug delivery. PEG conjugation increases the circulation half-life without affecting its activity.[6] PEGylation prolongs the circulation time of the conjugated therapeutics by increasing its hydrophilicity, reducing the rate of glomerular filtration, and masking the antigenic sites. PEG is a non-biodegradable polymer and it is primarily excreted through the renal system, whereas higher molecular weight PEG chains get eliminated by fecal excretion.[6] Another approach that was used in our work, is the fusion of the Human Serum Albumin (HSA) to CPG2, HSA is an excellent carrier and is responsible for transporting endogenous and exogenous compounds with the feature of providing a long average serum half-life. It also tends to accumulate around tumors and inflamed tissue sites, which makes the fused albumin aid in targeting the therapeutic site of interest. Both new variants produced in this chapter have been tested for their, solubility, stability in serum and immunogenicity in comparison to the free CPG2.

In **Chapter 6,** we focused on the other targeted therapy technique (TTS) as mentioned above. We studied the possible production of a new superantigen for tolerable cancer immunotherapy. Superantigens (SAGs) are a class of immunostimulatory proteins with the ability to activate large fractions of the T cell population. Activation requires simultaneous interaction of the SAG with the V beta domain of the T cell receptor (TCR) and with major histocompatibility complex (MHC) class II molecules on the surface of the antigen-presenting cell.[7]

The SAGs are able to non-specifically activate up to 20% of resting T-cells, whilst conventional antigen present results in the activation of only 0.001 - 0.0001% of

the T-cell population.[8] This makes superantigens an excellent target for cancer immunotherapy. The use of these molecules however, has a sever side effect such as sever vasodilation and hypotension. The purpose of this part of the work is to identify the amino acid sequence(s) which contributing to the sever hypotension the aim of which is to produce a novel variant of superantigens to be used in tolerable cancer immunotherapy.

Four super antigens (SEA, SEB, SPEA and TSST-1) were codon optimized and overexpressed in *E .coli*. We synthesized peptides to cover the whole molecule and we mapped the region which causes vasodilation and therefore, hypotension.

Finally in **chapter 7, 8 and 9,** we provide in three different languages (English, Dutch and Arabic) a comprehensive summery of the results and conclusion as well as perspective for future work to be developed on the new and conventional CPG2 in cancer therapy.

References:

1. He, H.; Liang, Q.; Shin, M. C.; Lee, K.; Gong, J.; Ye, J.; Liu, Q.; Wang, J.; Yang, V. Significance and strategies in developing delivery systems for bio-macromolecular drugs. *Frontiers of Chemical Science and Engineering* **2013,** *7*, (4), 496-507.
2. Francis, R. J.; Sharma, S. K.; Springer, C.; Green, A. J.; Hope-Stone, L. D.; Sena, L.; Martin, J.; Adamson, K. L.; Robbins, A.; Gumbrell, L.; O'Malley, D.; Tsiompanou, E.; Shahbakhti, H.; Webley, S.; Hochhauser, D.; Hilson, A. J.; Blakey, D.; Begent, R. H. J. A phase I trial of antibody directed enzyme prodrug therapy (ADEPT) in patients with advanced colorectal carcinoma or other CEA producing tumours. *British journal of cancer* **2002,** *87*, 600.
3. Jeyaharan, D.; Brackstone, C.; Schouten, J.; Davis, P.; Dixon, A. M. Characterisation of the Carboxypeptidase G2 Catalytic Site and Design of New Inhibitors for Cancer Therapy. *ChemBioChem* **2018,** *19*, (18), 1959-1968.
4. Li, H.; Chu, X.; Peng, B.; Peng, X.-x. DNA shuffling approach for recombinant polyvalent OmpAs against V. alginolyticus and E. tarda infections. *Fish & Shellfish Immunology* **2016,** *58*, 508-513.
5. Marshall, S. H. DNA shuffling: induced molecular breeding to produce new generation long-lasting vaccines. *Biotechnology Advances* **2002,** *20*, (3), 229238.

6. Mishra, P.; Nayak, B.; Dey, R. K. PEGylation in anti-cancer therapy: An overview. *Asian Journal of Pharmaceutical Sciences* **2016,** *11*, (3), 337-348.
7. Li, H.; Llera, A.; Malchiodi, E. L.; Mariuzza, R. A. The structural basis of T cell activation by superantigens. *Annual review of immunology* **1999,** *17*, 435-66.
8. Papageorgiou, A. C.; Acharya, K. R. Superantigens as immunomodulators: recent structural insights. *Structure (London, England : 1993)* **1997,** *5*, (8), 991-6.

Chapter 2:

Strategies for the production of longacting therapeutics and efficient drug delivery for cancer treatment

Alanod D. AlQahtani[1, 2], David O'Connor [3], Alexander Domling[2], Sayed K. Goda[1, 4]

1. Anti-doping Lab-Qatar, Research Department, Protein Engineering unit, Doha, Qatar.
2. Drug Design Group, Department of Pharmacy, University of Groningen, Antonius Deusinglaan, AV Groningen, The Netherlands.
3. Xi'an Jiaotong-Liverpool University, Department of Biological Sciences, Science and Education Innovation District, Suzhou 215123, China
4. Cairo University, Faculty of Science, Giza, Egypt.

Biomedicine & Pharmacotherapy 2019;113:108750 doi https://doi.org/10.1016/j.biopha.2019.108750.

Contents

1. Abstract

Protein therapeutics play a significant role in treating many diseases. They, however, suffer from patient's proteases degradation and antibody neutralization which lead to short plasma half-lives. One of the ways to overcome these pitfalls is the frequent injection of the drug albeit at the cost of patient compliance which affects the quality of life of patients.

There are several techniques available to extend the half-life of therapeutics. Two of the most common protocols are PEGylation and fusion with human serum albumin. These two techniques improve stability, reduce immunogenicity, and increase drug resistance to proteases. These factors lead to the reduction of injection frequency which increases patient compliance and improve quality of life. Both techniques have already been used in many FDA approved drugs.

This review describes many technologies to produce long-acting drugs with the attention of PEGylation and the genetic fusion with human serum albumin. The report also discusses the latest modified therapeutics in the field and their application in cancer therapy. We compare the modification methods and discuss the pitfalls of these modified drugs.

2. Keywords

PEGylations, Human Serum Albumin, Targeted cancer cells, Drug Delivery, HalfLife Extension, Protein Immunogenicity.

3. Abstract Figure

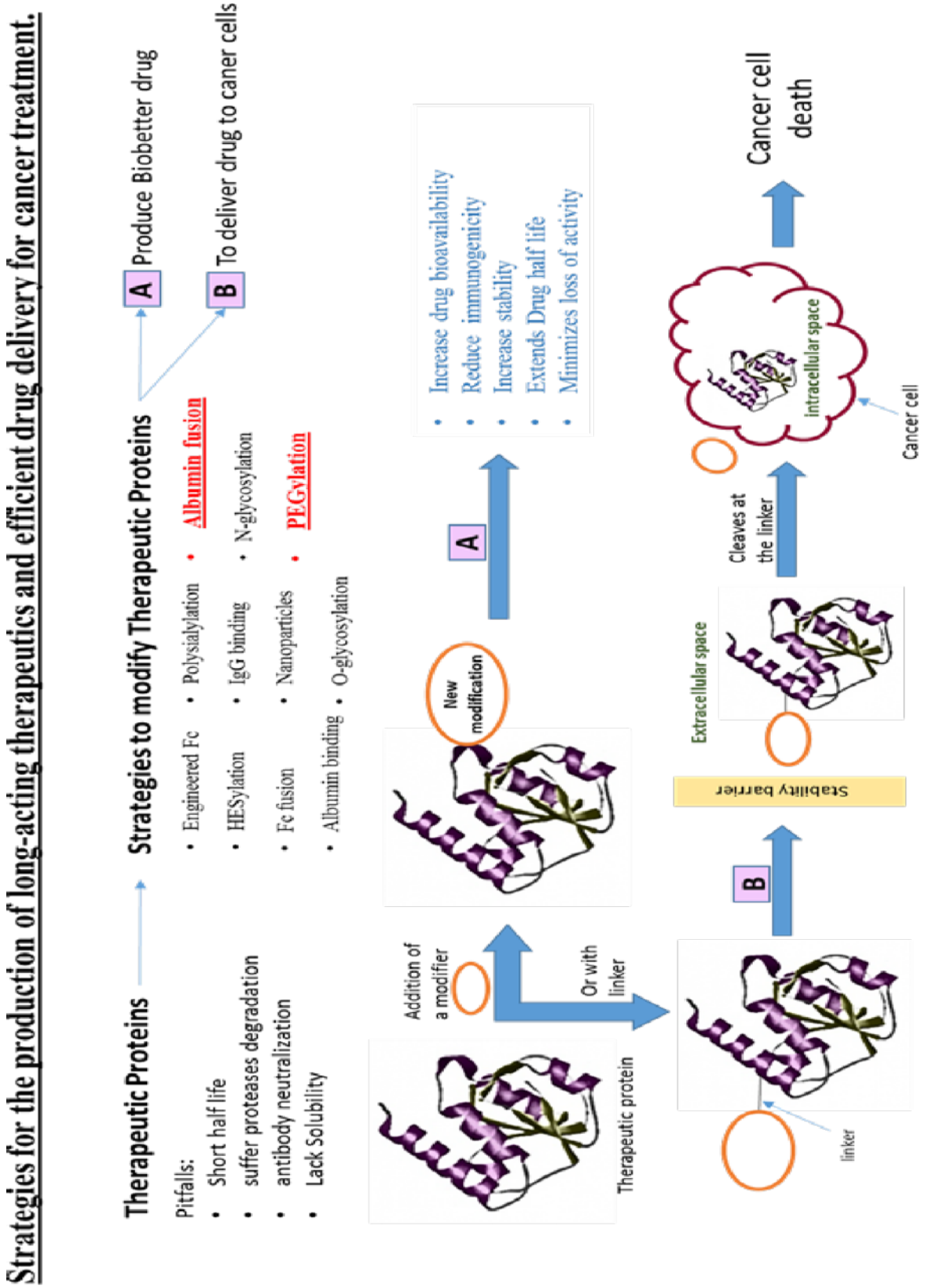

4. Introduction

Proteins therapeutic can be defined as proteins that are either naturally produced in the body or created in the laboratory and introduced into the patient with the aim of improving or curing a pathological condition. They are usually acquired from either microbial cells or by genetically modifying an animal or plant, and their uses range from oncology to inflammation to infectious diseases.[1] Proteins therapeutic also have the advantage that they function naturally as either pharmacokinetic or pharmacodynamic drugs, as they usually serve to replace an absent protein, and the body responds as if the protein is naturally occurring.[2]

Proteins often have multiple highly specific and complex functions that cannot be mimicked by simple chemical compounds. However, in common with small-molecule drugs, there are three major parameters influence their therapeutic efficacy: time (t1/2 or half-life), toxicity and targeted binding.[3]

The body produces many diverse proteins that are used as therapeutics. In the case of diseases caused by the mutation or deletion of a protein-coding gene, the protein therapeutic generally replaces the abnormal or missing protein in question without the need to go through gene therapy. Protein therapeutics have multiple advantages over small-molecule drugs. In particular, the clinical development and approval time of protein therapeutics by national drug approval agencies such as the Food and Drug Administration (FDA) is generally faster than that of small-molecule drugs.[1]

Protein therapeutics are categorized as having either an enzymatic or regulatory activity. They can have specifications based on their pharmacological activity, in which they

replace a protein that is deficient or abnormal. Alternatively, they can augment an existing pathway, provide a novel function or activity; interfere with a molecule or organism; or deliver other compounds (including other proteins), such as a radionuclide, cytotoxic drug, or effector protein.[4]

The first promoted recombinant therapeutic protein was human insulin (Humulin R) which was first produced in 1982 and has become one of the best-selling biologics worldwide after FDA approval.[5] There are now multiple approved protein therapeutics, and many of these proteins have molecular mass below 50 kDa and a short terminal halflife in the range of minutes to hours.[6] These limitations have led to the development and implementation of half-life extension approaches to lengthen the time that these recombinant proteins remain in the blood and to improve their pharmacokinetic properties as well.[7] To achieve therapeutically effective concentration over a prolonged period of time, the drug is typically applied at a local region or subcutaneously so that it is only slowly absorbed into the bloodstream. Thus, factors such as the clearance rate, volume of circulation and the bioavailability of the therapeutic drug all influence its effective half-life.[7]

This review discusses some key strategies to extend the half-lives of therapeutic proteins and their applications. In particular, it focuses on two approaches, the attachment of polyethylene glycol moieties to proteins (protein PEGylation) and fusion with human serum albumin, as these are most often used and have proved especially useful.

5. The need for modified therapeutic proteins and why they need to last longer in the body

Chemical and structural changes in therapeutic proteins are possible and are carried out frequently to accomplish pharmacological or clinical benefit. Such modifications are essential as the drug needs to pass through various membrane barriers, e.g. to reach a tumor. Active targeting of a drug is typically achieved by conjugating it to a target entity that improves bioavailability and reduces systemic toxicity.[8]

Half-life extension technologies are now entering the clinic. Importantly, they are allowing the implementation of new biologic therapies, especially those involving shortacting therapeutic agents that would otherwise require frequent dosing profiles, which is particularly beneficial for the treatment of chronic conditions.

Modified therapeutic proteins can also be applied in a technique called the Antibody Directed Enzyme Prodrug Therapy (ADEPT) for cancer targeted therapy. ADEPT therapies are designed to generate toxic chemotherapeutics at the site of malignancy, potentially improving efficacy and reducing side effects.[9, 10] The design of the modified therapeutic proteins aims to produce enzyme variants with good catalytic efficiency, highlevels of stability and reduced immunogenicity. Such extra features will often increase the protein's circulatory half-life, i.e. the time that the protein will circulate in the blood. This lead to the decrease of the number of doses required to be given to the patient, thereby reducing the possibility that the patient will generate antibodies to the modified protein and limiting the time available for the targeted cancer cells to mutate and hence avoid or resist the treatment as in case of glucarpidase. It has been shown that

protein modification using PEGylation or HSA gene fusion of glucarpidase produces forms of the enzyme with a much longer half-life and more resistant to proteases.[11]

6. Advantages of modified proteins over unmodified ones

In contrast to small-molecule drugs, proteins are readily amenable to site-specific alterations through genetic engineering. In principle, therefore, it is possible to build in features that allow them to remain active for longer in the body and or to improve their tolerance. These features include: resistance to proteolysis; delayed clearance; reduced capacity to cause local irritation; increased half-life; lower toxicity; increased stability and solubility, and decreased immunogenicity.[12, 13]

Many of protein therapeutic drugs have now been developed and approved. Many exhibit short half-lives in plasma and hence strategies to improve their pharmacokinetic properties, which influence distribution and excretion,[13] are becoming increasingly important. Increasing the size and hydrodynamic radius of the protein, or peptide aims to decrease kidney filtration and to increase the net negative charge of the target protein or peptide has a similar effect, as the net charge of the protein contributes to renal filtration. It has been suggested that the proteoglycans of the endothelial cells and the glomerular basement membrane contribute to an anionic barrier, which partially prevents the passage of negatively-charged plasma macromolecules.[14]

Another approach is to increase the degree to which the therapeutic peptide or protein interacts with serum components, e.g. albumin or immunoglobulins, which tends to increase the half-life of the circulating targeted protein.[15, 16] Both serum albumin and

immunoglobulins (particularly IgG1, IgG2 and IgG4) have extraordinarily long half-lives – around 19 days - in humans.[17] Use of neonatal Fc receptor is another approach that can be used to promote interactions with albumin or with the Fc region of IgG in a pHdependent manner. FcRn binding can protect albumin and IgG from degradation in the lysosomal compartment and redirects them to the plasma membrane. Thus, such binding can extend or modulate the half-life of the protein that is attached to it.[18]

7. Strategies for producing long-acting protein therapeutics

Significant effort has been expended to discover different approaches to extend the halflives of protein drugs, not least by evading or interfering with their common clearance pathway. Modifications to protein drugs that prolong their half-lives include conjugation or fusion to specific moieties and the discovery of variants of the therapeutic protein drugs.[4]

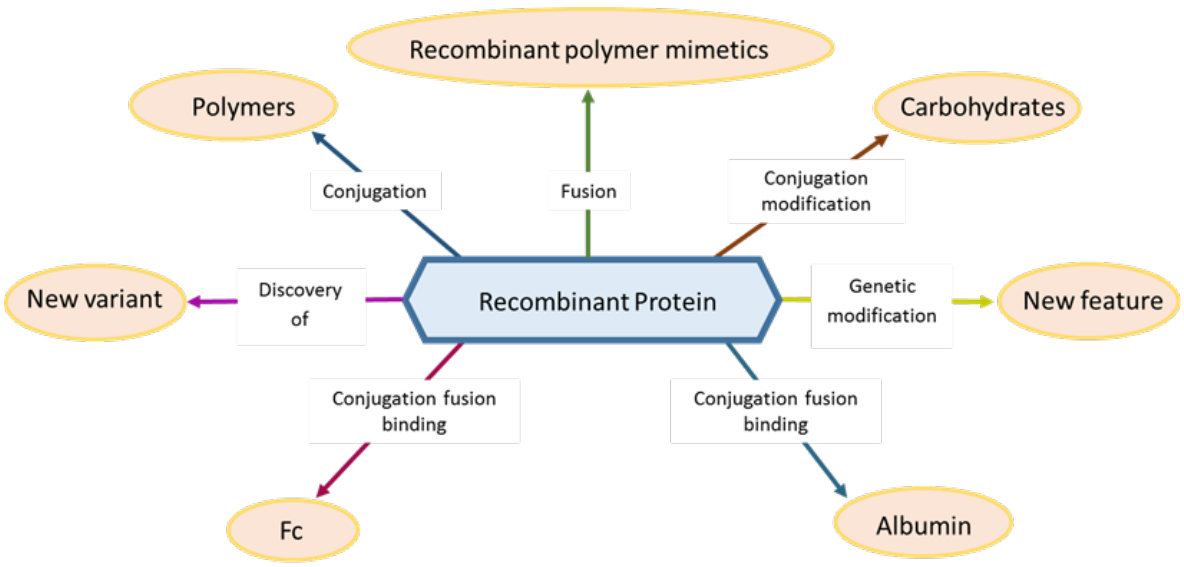

Figure 1: Different strategies to extend the half-life of therapeutic proteins.

These strategies also include chemical coupling of polymers and carbohydrates, posttranslational modifications such as N -glycosylation[19], and fusion to recombinant polymer mimetics.[20, 21] (**Figure 1**; **Table 1**).[22] On the other hand, changes in structure or sequence of protein molecules (e.g. through glycosylation or PEGylation) may cause changes in the pharmacokinetic properties of these compounds. The size of a therapeutic protein may hinder its passage across a biological membrane. Other factors that affect its half-life include its immunogenicity, the level of the corresponding endogenous protein, the period of drug administration, and the rate and site of drug delivery.[13]

Gene modification can be used to create therapeutic proteins with altered isoelectric points and protein dynamics.[23] Such mutations can also modulate both enzyme selectivity and the intrinsic activity of the enzyme. In one example, both the activity and the specificity of Neprilysin, a protease that degrades amyloid beta and hence might be of use in the treatment of Alzheimer's disease, were altered through site-specific mutagenesis. The engineered Neprilysin double mutant G399V/G714K showed a ~20-fold increase in activity on amyloid beta 1–40 but a ~3,200-fold reduction in activity on other peptides. Further, this therapeutic drug is therefore, a promising candidate for the in vivo treatment of Alzheimer's disease.[24]

One strategy which is different from the above is to isolate a similar enzyme to the one under study which will not be recognized by the antibody of the original protein. This approach will lead to prolonging an enzyme's activity. For example, a novel variant of Carboxypeptidase G2 (CPG2), which has been used in drug detoxification and ADEPT is used in targeted therapy for cancer, especially in the ADEPT strategy mentioned above. [10] A leading approach to improving the half-life of a protein therapeutic is to reduce its

renal clearance rate, e.g. by increasing its size above the renal cut-off of 40– 50 kDa. Several ways can achieve this, including chemical and post-translational modification as well as by genetic engineering.[7] **Table 1** lists different modifications that can create favorable new features in therapeutic proteins. Two of the wildly used approaches to extend the half-life of therapeutics and improve drug delivery, are PEGylation and albumination, this review will focus on the use of the two techniques and discuss their application in cancer therapy. This part will include our recent work on the glucarpidase PEGylation and albumination.

8. Protein PEGylation using polyethylene glycol (PEG)

Polyethylene glycol (PEG) is a neutral polyether polymer. Because it is water soluble, nonionic and biocompatible, it is widely employed in the field of polymer-based drug delivery. PEG moieties are made from multiple units of ethylene oxide that create long chains of amphiphilic inert molecules.[44] In 1990 the FDA approved the first PEGylated product, and ever since it has been extensively used in post-production modification methodology to improve the physicochemical properties, and hence the biomedical efficacy, of therapeutic proteins. PEGylated pharmaceuticals have proven their applicability and safety over many years. Thus, PEGylation plays an essential role in prolonging the residence time in the circulation of the relatively small therapeutic drugs such as peptides, proteins, nanobodies and scaffolds, which is achieved by increasing their molecular size to above that needed for half-life extension.[45] As indicated above, a key advantage of using PEGylated proteins is that patients require fewer doses to maintain the necessary therapeutic levels in the circulation.

More recently, releasable PEG moieties have been developed that can be removed from a therapeutic protein under controlled conditions. This strategy allows administration of the protein in a pro-drug format prior to reconstitution of the native protein under appropriate conditions.[46] A wide range of biologically important molecules have been conjugated to PEG to take advantage of its advantages (**Table 1**). Moreover, site-specific PEGylation offers opportunities to create novel proteins and peptides and peptides of medicinal interest.[47]

It is essential to add a functional group to the PEG at one or both termini which will enable its conjugation to a protein . By choosing the functional group judiciously, it is possible to attach PEG moieties to specific amino acid side chains or to the N-terminus of a protein (**Figure 2**).

Table 1: Strategies to modify the half-lives of therapeutic products [22]

Strategy	**Target**	**Examples**	**Effect**	**Treatment**
PEGylation	Small molecule	Metal Nanoparticle Surfaces	Reduction in Nonspecific Cell Uptake	brain glioma cancer cells[25]
	Affinity ligands	protein A	Improved selectivity in affinity chromatography	Staohylococcus aureus Disease[26]
	Peptide	glycosaminoglycan (GAG)-binding enhanced transduction (GET)	Improved safety profile and efficient gene transfer of a reporter luciferase plasmid, enhanced gene expression, and enhanced transfection efficiency	Lung gene therapy[27]

	Protein	carboxypeptidase G2 (glucarpidase)	Avoidance of the immune system and increased the half-life.	Targeted Cancer Treatment[11]
		interferon β-1a	Increased half-life and hence decreased frequency of administration.	multiple sclerosis [28]
	Saccharides	radix ophiopogonis polysaccharide (ROP)	Suppression of elimination from plasma	myocardial ischemia[29]
	Oligonucleotides	interleukin-17A (IL-17A)	Better stability in blood circulation.	systemic inflammatory disease[30]
	Lipids	Synthetic highdensity lipoprotein nanoparticles (sHDLs)	Increased half-life	Targeted Cancer Treatment[31]
	Liposomes and particulates	DC-Chol/DOPE cationic liposomes	Enhanced silencing of the target gene at tumor sites and substantial suppression of tumor growth.	ovarian cancer therapy[32]
Polysialylation	protein	Erythropoietin	Significantly prolonged circulating half-life, improved stability against proteases and thermal stress, reduced clearance, and enhanced in vivo efficacy	anemia[33]
Fc fusion	Protein	Thymosin alpha 1 (Tα1)	Increased half-life and stronger activity.	Melanoma and Breast Cancer[34]
		recombinant human growth hormone (rhGH)	Increased half-life, and less dosage	human growth hormone

				(rhGH) therapy[35]
Engineered Fc	protein	proprotein convertase subtilisin kexin type 9 (PCSK9)	Increased serum halflife and enhanced efficacy in vivo, enabling less frequent or lower dosing into the blood.	lower plasma LDL levels[36]
IgG binding	protein	interferon-α	Increased serum halflife with significantly	viral infections[37]
			improved bioavailability	
Albumin fusion	protein	factor VIII and factor IX	Increased half-life	replacement therapy in hemophilia A and B[38]
Albumin binding	protein	Triclocarban (TCC)	Transport, and distribution	Toxix effect of humans[39]
	Peptide	[177Lu]LuDOTATATE peptide receptor	Enhanced residence time in blood. Increased tumor uptake, and a higher kidney uptake.	Targets Tumers[40]
	saccharides	Ganoderma lucidum polysaccharides (GLP)	Increased thermal stability	Growth Hormone Deficiency [41]
Nanoparticles	protein	recombinant tissue plasminogen activator (rtPA)	increased the half-life of the conjugate and targeted delivery system	thrombosis[42]
	Small molecule drugs	paclitaxel (PTX)	targeted therapy and increased half-life	osteosarcoma targeted therapy[43]

Figure 2: Modification of the protein. A) Using PEG derivatives carrying appropriate functional groups, it is possible to target specific sites / amino acid residues within a protein. Alternatively, the PEG moiety can be attached via an enzyme-mediated

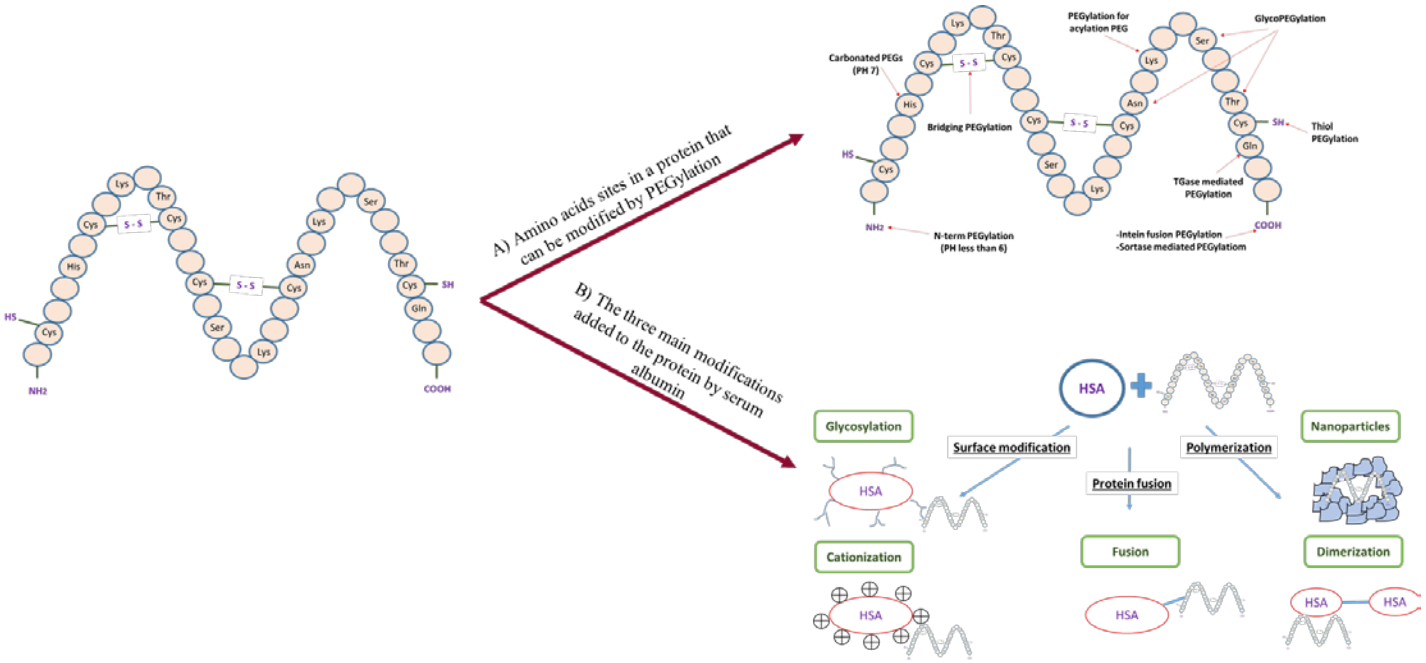

reaction.[48] B) The three main modifications to the serum albumin protein used to improve drug delivery (modified as mentioned elsewhere).[49]

PEGylation of proteins can be performed by chemically reacting a specific chemical functionalities within a protein (e.g. the side chains of lysine, histidine, arginine, cysteine, aspartic acid, glutamic acid, threonine, tyrosine, and serine as well as the N-terminal amino and the C-terminal carboxylic acid groups) with a suitable PEGylation reagent.[16] As the degree of modification increases, the likelihood of antigenicity generally decreases whereas the circulatory half-life of the therapeutic protein is extended. Due to reactions with different nucleophilic groups on the protein, even mono-PEGylation leads to positional isomers that can differ significantly in their biological and biomedical properties mainly in body residence time and immunogenicity. However, it should be noted that conjugation might sometimes lead to the formation of new epitopes as a consequence of, e.g., partial protein denaturation after conjugation or the use of an inappropriate spacer between protein and PEG chain.[45]

PEG derivatives are often attached to the amino groups of lysine and the N-terminus of polypeptide molecules. PEG derivatives are suitable for amine modifications includes Nhydroxysuccinimidyl-activated esters, which produce an amide linkage between PEGepoxide, and PEG-aldehyde, PEG-tresylate and PEG-carbonyl imidazole, which will provide a urethane linkage. The activated PEG compound will react with one or all exposed free amino groups contained within the protein groups, with regards to steric hindrance. By regulating the concentration of the reagents whether through the protein, or reaction conditions, in reference to the standard methods of amine condensation, one can control the degree of PEGylation of the free amino groups exposed on the folded protein.

Another option is to use the thiol groups of cysteine residues, which can be modified by use of PEG-maleimide and vinyl sulfone. However, changes in PEGylation interactions or reaction conditions can result in changes in the functional properties of the therapeutic proteins. [50-52]

A study was conducted to optimize site-specific PEGylation of Exendin-4 (Ex4-Cys), an analogue of glucagon-like peptide-1 (GLP-1) with anti-diabetic properties, using a highmolecular-weight trimeric PEG. PEGylation of the C-terminus (C40-tPEG-Ex4-Cys) was carried out using Ex4-Cys and activated trimeric PEG. The resulting C40-tPEG50K-Ex4Cys derivative had a better t1/2 in circulating blood (7.53-fold increase) and its AUC_{inf} (a measure of total exposure to the drug) relative to Ex4-Cys was increased over 45-fold. Further, its hypoglycemic duration, a measure of its pharmacologic activity, was increased 8-fold relative to that of native Ex4-Cys, with a dose of 25 nM/kg.[52]

9. Fusion to Human Serum Albumin

Human serum albumin (HSA) is one of the best-characterized proteins in the pharmaceutical field. It is responsible for transporting endogenous and exogenous compounds and has a long average half-life (around 19 days). In part, this is due to its size – it is around 66 kDa, which is almost at the boundary of the kidney's filtration capacity – and also the fact that it is the most abundant protein in plasma. It tends to accumulate around tumors and inflamed tissues sites, and this feature opens the potential of fusing albumin to a target protein to aid targeting to the therapeutic site of interest.[49] It is widely used as an excipient, especially for biotechnology products. Recombinant versions of the protein are available, which alleviate any potential concerns about the transmission of infectious agents associated with the human plasma-derived protein.[53]

Many researchers have developed methods to improve novel albumin-based drug carriers and these can generally be categorized into three main categories: (1) low-molecularweight proteins fused with albumin; (2) polymerization; (3) surface modification (**Figure 2**).[54] I has recently emerged as an adaptable carrier for drug delivery to transport therapeutic peptides and proteins against diabetes, cancer, and infectious diseases.[55]

Therapeutic compounds have been pharmaceutically enhanced by multiple techniques using albumin to improve their distribution, bioavailability and the half-life. For example, non-covalent interactions allow the binding of the albumin to a broad range of endogenous and exogenous ligands. Albumin dimerization in particular has significant potential and advantages for clinical applications, as both a plasma expander and as a

drug carrier. Such dimers are present at elevated levels in the circulating blood of patients with chronic renal disease and also result from oxidative damage in the blood.[56] Many molecules of therapeutic interest bind to endogenous albumin in the blood through its fatty acid binding sites, thereby prolonging their half-life and bioavailability. For example, the human insulin analogue, Detemir (marketed by Novo Nordisk as Levemir), is longacting due to the myristic acid moiety bound to the Lys residue at position B29 of insulin. The attached fatty acid facilitates binding to albumin thereby prolonging the circulatory half-life of this insulin derivative in blood.[57, 58]

Covalent binding of a drug to albumin can be achieved either through direct chemical conjugation or via the use of a small molecule to link the two components. Alternatively, it can be achieved through gene fusion to create a chimeric protein that is expressed in a suitable host, resulting in the production of a single polypeptide.[59] The gene fusion approach has been used to attach albumin to the N- and or C-termini of several proteins of therapeutic interest, to extend their half-life. Examples of therapeutic proteins that have been attached to HSA include interferons[60], growth factors[61], hormones, cytokines, coagulation factors[62], and antibody fragments.[21]

Various domains of the HSA molecule have also been used to make bioconjugates with increased stability, better targeting properties, and/or extended half-lives in blood. For example, domain I of HSA has been used in the preparation of antibody conjugates. This was achieved through the use of a cyclohexene sulfonamide compound that siteselectively labels Lys64 in this HSA domain.[63] Similarly, the half-life the of granulocyte colony stimulating factor (G-CSF) was prolonged by genetic fusion to domain III of I to its N-terminus.[64]

10. Diseases that have been treated with PEGylated proteins

Several PEGylated molecules have been approved for clinical use. For example, PEGylated interferon for such infections, PEG-interferon alfa-2b, was approved by the FDA in August 2001.[55] **Table 2** lists some PEGylated products that have received FDA approval.[8]

Table 2: FDA approved PEGylated and albuminated protein therapeutics [8, 53, 54]

Trade name	**Conjugate**	**FDA Approval date**	**FDA approved date/clinical trial status and use**
Sylatron™	PEG-interferon α-2b	March 9, 2011	Approved as adjuvant therapy for resected stage III melanoma
Pegasys®	PEG-interferon α-2a	October 2002	Phase I for melanoma and phase II as for chronic myelogenous leukemia
Neulasta®	PEG-filgrastim	January 31, 2002	Used to treat neutropenia during chemotherapy
Oncaspar®	PEG-asparaginase	July 24, 2006	February 1994, acute lymphoblastic leukemia, and on July 24, 2006 the first-line treatment for acute lymphoblastic leukemia

Levemir®	The albumin-binding derivative of human insulin	Apr 2, 2012	Pregnancy Category Change for Women with Diabetes
Abraxane®	Albumin–paclitaxel nanoparticle	Sep 6, 2013	For Late-Stage Pancreatic Cancer
albinterferon alfa-2b	Fusion protein of albumin and interferon-α-2b	October 2010	For the treatment of chronic hepatitis C
Vasovist® (Schering AG, Berlin, Germany)	Gadofosveset reversibly binds to human serum albumin	December 22, 2008	As in magnetic resonance angiography (MRA)

10.1. PEGylation to improve drug delivery and targeting of cancer cells

The number of therapeutics involving drug delivery has increased markedly, especially for cancer treatment (**Table 3**).[65] While most of the PEGylated products to date are nonprotein-based, the use of peptide- and protein-based PEGylated products is now being investigated. In principle, PEGylation of proteins, due to its enhanced permeability and retention (EPR) effect, is an excellent way to achieve a longer circulation time and for drug delivery to a tumor site.[66]

For example, a succinimide-activated PEG derivative has been used to PEGylate the εamino groups of lysine residues of xanthine oxidase, which mediates anticancer activity because of its ability to generate cytotoxic reactive oxygen species. In animal studies, this derivative exhibited 2.8-fold higher tumor accumulation at solid tumors when compared to the native enzyme in a 24 hr injection period.[65]

Bispecific antibodies have been studied as a method in cancer immunotherapy, and the use of PEGylation is an effective method to improve their antitumor efficiency. Sitespecific PEGylation has been used to modify a bispecific single-domain antibody-linked Fab (S-Fab), which was designed to link an anti-carcinoembryonic antigen (anti-CEA) nanobody with an anti-CD3 Fab. The resulting construct, polyethylene glycol-S-Fab (PEGylated S-Fab), had slightly decreased tumor cell cytotoxicity *in vitro* when compared to the free S-Fab, but an increased half-life (t1/2) - 12-fold – resulting in effective inhibition of tumor growth *in vivo*.[68]

PEGylation can be combined with other strategies to improve drug delivery. For example, it has been used in conjunction with niosomes, i.e. non-ionic surfactant-based vesicles that can carry various drugs within them, to improve cell targeting. Niosomes are first rendered magnetic with Fe_3O_4@SiO_2 nanoparticles prior to modifying their surface by PEGylation. In this case, the role of PEGylation increases the bioavailability of niosomes, and magnetization makes them capable of targeting specific tissues. In one application, carboplatin, an antitumor drug, was loaded into PEGylated magnetic niosomes, leading to an increased drug release rate (**Figure 3**). Moreover, using an external magnetic field significantly increases their toxicity towards cancerous cells.[69]

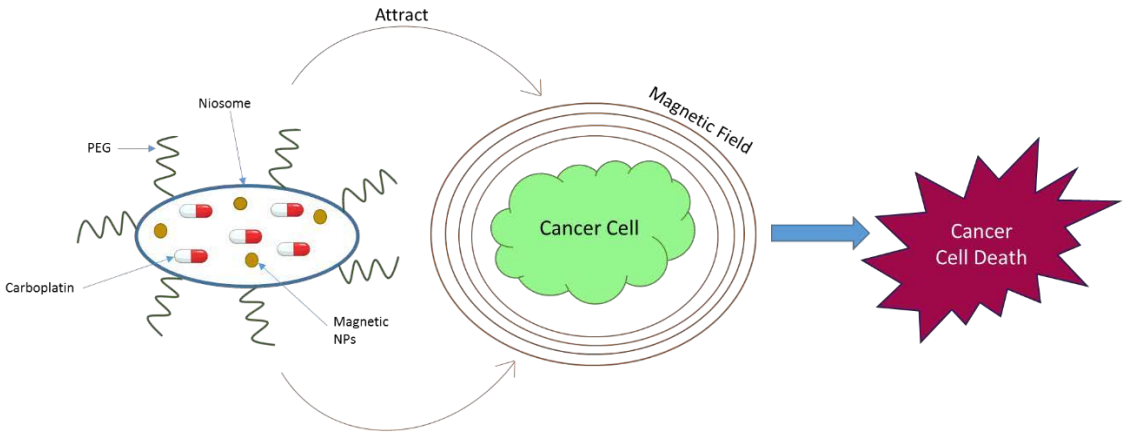

Figure 3: Use of PEG-coated noisome magnetic nanoparticles to deliver carboplatin to tumor cells. Application of an external magnetic field in the vicinity of the tumor leads to a significant increase in the local concentration of niosomes, which release the antitumor agent carboplatin over time (based on figure mentioned elsewhere, permission was given by the author and journal) [69]

In addition to the use of drug encapsulation using a vesicular carrier, drugs can be delivered to a tumor site by attaching them to a drug delivery module via acid-cleavable linkers, which can be hydrolyzed in the acidic environment of the tumor. Alternatively, some other type of specialized linkage can be used that permits the drug to be released *in situ* within the tumor microenvironment. Thus, both pro-drug and active targeting strategies can be used.[12] To minimize the loss of activity reversible PEGylation has been developed and a large number of cleavable linkages, mediated in vivo by specific enzymes, hydrolytic cleavage or reduction, have been identified.[8, 70, 71]

The use of pH sensitive cleavable PEG has proved to be an effective approach in which cleavage of a PEG-lipid moiety is triggered in the vicinity of the tumor. In order to achieve a tumor-specific cleavable PEG system, the enzymes specifically expressed in the tumor have also been exploited for cleavage, e.g. matrix metalloproteinases (MMP).[66] Another comparable example in facilitating drug delivery to tumor cells is the peptide-loaded pHsensitive PEGylation to liposomes (PEG-PpHL) which are characterized and delivered

to cis-platinum resistant ovarian cancer C13 cells. The carrier entraps the drug and exhibits a pH-dependent release in the tumor site. Moreover, the PEGylated PpHL behaved differently against macrophage cells due to its ability to protect liposomes from the cells of the reticuloendothelial system.[72]

11. Diseases which have been treated with proteins linked to HAS

A number of therapeutic products conjugated to HSA have now been approved for clinical use (**Table 2**). For example, fatty acid derivatives of human insulin bound to HSA have applications in the treatment of diabetes while paclitaxel-HSA nanoparticles have been used to treat various cancers such as metastatic breast cancer and advanced pancreatic cancer. It has even proved possible to use HSA to deliver a bioactive gas, nitric oxide (NO), to treat ischemic/reperfusion injury, cancer, and bacterial infections. While endogenous S-nitrosated HSA occurs naturally in blood plasma and serves as a NO donor, analogues have been developed in which the HSA molecule has many conjugated SNO groups (polySNO-HSA). Interestingly, while SNO-HSA inhibits apoptosis, poly-SNO-HSA possesses very strong pro-apoptotic effects against tumor cells.[73]

Albiglutide, a glucagon-like peptide-1 agonist (GLP-1 agonist) for the treatment of type 2 diabetes (marketed as Tanzeum and as Eperzan and the US and Europe, respectively), was one of the first HSA-peptide or protein fusion product to be approved for clinical use. Whereas the half-life of pharmacologically active native GLP-1 is 1–2 min, albiglutide's half-life is 4–7 days, which allows it to be administered weekly rather than more frequently.[74] IL-2, which is used in passive cancer immunotherapy, is another successful example. One of the IL-2 limitations is its low serum half-life, which necessitates high

doses that have severe side-effects. To overcome these issues, Adabi *et al.* therefore fused IL-2 to an albumin-binding domain from streptococcal protein G. The resulting fusion protein, ABD-rIL-2, binds to serum albumin, and had a three-fold increase in its terminal half-life in serum relative to recombinant IL-2, when tested in BALB/c mice.[75]

TV-1106 is a recombinant form of human growth hormone (rhGH) that has been genetically fused to recombinant HSA. Again, this fusion resulted in a long plasma halflife for rhGH in the systemic circulation. In the case of GH deficiency, TV-1106 has been developed for the treatment of this disease. This modified drug provides sustained exposure which will lead to the reduction of the frequency of injection and therefore will improve patient's compliance and quality of life. A phase 1 clinical trial demonstrated that the TV-1106 is well tolerated, has a prolonged plasma half-life, and is hormonally active in GH-deficient adult patients.

The side effects of GH therapy were reported to be rare and it was shown to have a favorable overall safety profile.[76]

11.1 HSA fusion to improve drug delivery and targeting of cancer cells

Fusion of therapeutic proteins to HSA has proved to be a viable and effective way to increase the solubility and/or delivery of molecules for cancer therapy.[77] The physicochemical properties of HSA, which facilitate coupling to drugs, and its preferential uptake in tumor tissue make it an almost ideal carrier for drug delivery.[78]

In pancreatic cancer chemotherapy the gemcitabine (GEM) nanocarriers have received extensive attention in recent years. Linking HSA to GEM/IR780 resulted in a complex

that had elevated levels in blood and a long-term circulation in tumor tissues when compared to the free IR780. [79]

Fusion with HSA can also be used to target and inhibit essential intracellular pathways. It has been recently reported that a fusion protein consisting of HSA linked to p53reactivating peptide (p53i) interferes with at least four intracellular targets, making it a viable therapeutic protein for the treatment of a variety of cancers. It retains the ability to bind to MDM2 and MDMX, resulting in p53 transcription-dependent apoptosis, and additionally, is able to bind and neutralize anti-apoptotic Bcl-2 family proteins, Bcl-xL and Mcl-1.[77]

HSA has evolved to bind many natural ligands and this propensity can be exploited to allow it to carry anti-cancer agents. For example, it readily binds the chemotherapeutic entity Cu^{II} nalidixic acid–DACH. It should be noted, however, that binding in this case results in significant shape-changes in HSA as evidenced by UV–vis, fluorescence, CD, FTIR spectroscopy. It remains to be seen if such changes result in the production of new epitopes in HSA. If they do then such conjugates may provoke adverse immune reactions following repeated administration. [80]

12. Immune responses of patients towards the modified drugs

12.1 Effects of the PEG moiety on protein immunogenicity and stability

Conjugation of PEG to a protein inevitably results in a new macromolecule with significantly changed physicochemical characteristics. These changes are typically

reflected by reduced immunogenicity.[81, 82] The PEG 'tail' is quite flexible and can shield a protein from recognition by the immune system. Additionally, it can reduce the chance of reticuloendothelial clearance, sterically hinder binding to cellular receptors, and reduce the degradation by proteolytic enzymes. These properties collectively lead to decreased renal, enzymatic, and cellular clearance, resulting in prolonged circulation half-lives in the bloodstream.[83] In the case of antibodies, although the PEG moiety is chemically linked to a position as far as possible from the antigen binding site, it is still possible that the flexible polymer sterically blocks the binding interface via interactions that change the plasticity or surface charge distribution of the molecule. Similar principles apply once a PEGylated antibody molecule binds to its antigen on a surface - the polymer tail acts intermolecularly to hinder binding of antibodies to adjacent antigen molecules.[62]

It was demonstrated that very high doses of PEG-protein conjugates might induce renal tubular vacuolization. However, this phenomenon is not associated with functional abnormalities and disappears after the treatment has been completed. Therefore, PEGprotein conjugates are regarded as immunologically safe and non-toxic.[84]

In one study the effect of PEGylation on the antibodies was monitored via competitive ELISA. In this method, the modified or unmodified antibodies were mixed with HRPattached polyclonal antibodies, specific to human serum IgG (hsIgG) or to IgY, and incubated in ELISA plate coated with the unmodified hsIgG or IgY. The concentration of the free unmodified antibodies competing with the modified antibody lowered the resulting OD to a value of 0.4, which is considered to reflect 100% detection by secondary antibody. The percentage of the reduction of detection by secondary antibody was calculated using the ratio of modified/unmodified free antibody concentration needed to

lower the OD value to 0.4. Conjugation with PEG5 and PEG20 reduced the detection of hsIgG to 12.5% and 3.1% of unmodified hsIgG, respectively, and that of IgY to 2% and 1.6%, of unmodified IgY respectively. This implies that *in vitro* the PEG molecules mask some of the exposed epitopes on the hsIgG and IgY, and possibly sterically prevent detection and binding of the antibodies to the relevant epitope on the PEGylated protein.[56] However, this is not the case *in vivo*. Unexpectedly, PEGylation of IgY was found to elevate the immune response via both administration routes (i.v. and i.m.) investigated. PEGylation of hsIgG with PEG5 did not reduce the primary or secondary immune response following administration in BALB/c mice. Interestingly, PEGylation with PEG20 significantly increased the antibody titer when administrated i.m., and significantly decreased it when administrated i.v. The immune response to hsIgG carrying PEG5 was also tested in C57BL/6 mice. In this strain, in contrast to BALB/c, PEG induced an elevation in antibody response.[85]

There are various factors that can influence the properties of PEG such as the number of PEG chains attached to the polypeptide, the structure of PEG chains attached to the polypeptide, the location of the PEG sites on the polypeptide and the chemistry used to attach the PEG to the polypeptide.[86]

PEGylation is considered as one of the best approaches for passive targeting of anticancer therapeutics, based upon the concentration gradient between the intracellular and extracellular space that is created due to the high concentration of the drug in the tumor area.[8]

The clearance of the PEG chain depends on its seizes. The molecule less than 400 Da would be degraded by alcohol dehydrogenases and lead to the formation of toxic

metabolites. The elimination mechanism of longer PEG chains, depends on their molecular mass. PEG below 20 kDa, are eliminated by renal filtration. The PEGylated proteins conjugated with PEG molecule larger than 20kDa are cleared by different pathways such as liver uptake and degradation of the protein part by proteases. It is also the same mechanism for clearing of large protein molecules with molecular masses above 70 kDa.[84]

Generally the elimination half-life and the absorption of the PEG-protein is directly proportional with the PEG chain. It was shown that branched PEGs have longer elimination half-life than linear PEGs of the same molecular weight.[45] However, the stabilizing effect of PEGs on proteins is a delicate balance between the two opposing effects: stabilizing effect due to steric exclusion and destabilizing effect due to hydrophobic interaction.[87]

It has been established that despite all advantages of the protein PEGylation as drug life extender the patient immune system produces antibodies against the PEG moiety (antiPEG Abs), including both pre-existing and treatment-induced Abs.[88] This unfortunately has been correlated with loss of therapeutic efficacy and an increase in adverse effects in several clinical reports examining different PEGylated therapeutics.[88]

The reason(s) for the presence of pre-existing antibodies specific for PEG in individuals who have never received any formal treatment with PEGylated therapeutics remains largely unknown. However, as a ‘generally regarded as safe’ (GRAS) product, PEG is widely used in cosmetics, processed foods, pharmaceuticals, agriculture, and industrial manufacturing. Because PEG is found in so many domestic and hygiene products, it is reasonable to assume that repeated exposure to PEG could lead to the development of

anti-PEG Abs. However, the constant exposure does not clearly clarify the real mechanism underlying anti-PEG immunity. Due to the abundant presence of PEG, it is very likely to be present at or introduced to the inflammation site. The occurrence of PEG in close vicinity to highly active immune cells may be enough to elicit the stimulation of anti-PEG Abs. Successive exposure to PEG-containing products could prompt a robust memory immune response to the polymer.[89]

The presence of both pre-existing and induced anti-PEG Abs is a significant challenge to the clinical efficacy of PEGylated therapeutics.[90] There is now a large body of evidence indicating that potent and specific antibody reactions against the PEG polymer, which reduce the circulatory half-life circulation and lower the therapeutic efficacy of the PEGylated drugs in both animal models and humans. Addressing this challenge should be a priority in future studies in this area [89]

PEGloticase, a PEGylated form of recombinant porcine uricase, is approved for the treatment of refractory gout. In a phase one study, 13 of 30 patients (43%) produced antibodies against PEGloticase that were specific to the PEG component rather than the uricase moiety. Such antibodies caused rapid elimination of the PEGloticase from plasma, which in turn resulted in a loss of efficacy and a doubled risk of infusion reactions. The anti-PEG antibodies appeared after the first dose, but 5 of the 10 responders had preexisting antibodies, even though they had not previously been exposed to PEGloticase. In phase 3 trials, high levels of antibodies to PEGloticase was the main reason for the loss of efficacy. [91]

As indicated above, the enzyme-linked immunosorbent assays (ELISA) technique is an efficient method to analyze anti-PEG antibody responses. Direct and competitive ELISAs

can be used in combination to determine the PEG-specificity of Ab responses induced after treatment with a PEGylated protein (PEG-Pr), as well as pre-existing anti-PEG Abs. Both anti-PEG IgM and IgG can bind to polymers composed of repeated subunits.[89]

PEG-modified recombinant mammalian urate oxidase (PEG-uricase), a treatment for patients with chronic gout, was investigated for the presence of anti-PEG antibodies. In 5 of 13 patients, low-titer IgM and IgG antibodies against PEG-uricase were detected. This correlated with the plasma uricase activity being not detectable beyond ten days after injection. As in the other study [106], the elicited antibodies were directed against the PEG moiety rather than the uricase protein. Conversely, the relatively low titer antibodies did not inhibit uricase catalytic activity. Instead, the uricase activity was decreased due to rapid clearance of the circulating uricase. This is due to the binding of the antibody against the unabsorbed PEG-uricase at the injection site after dosing. (**Figure 4**) [92]

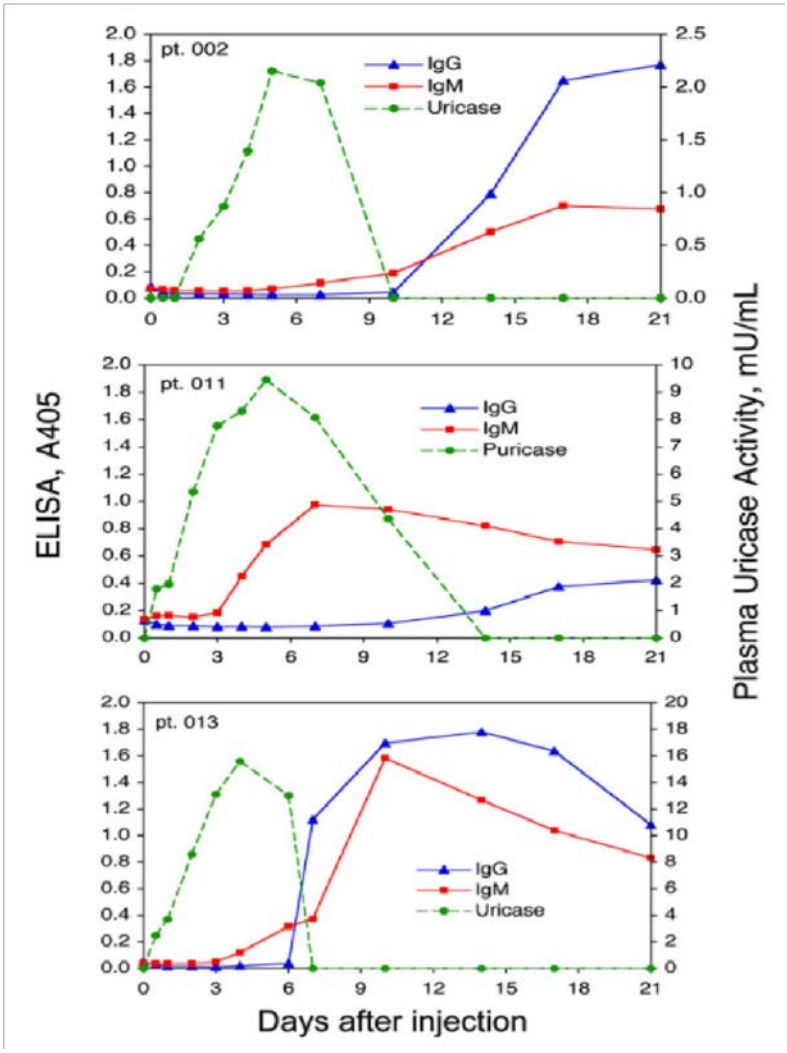

Figure 4: The appearance of anti-PEG-Uricase antibodies and plasma uricase activity in subjects 002, 011, and 013. Subject 002 at 4 mg, and subjects 011 and 013 at 12 mg, of PEG-modified recombinant mammalian urate oxidase (PEG-uricase), (reproduced with the permission of the journal).[92]

Due to the immunogenicity problem towards the PEG it is essential to consider effective therapeutic options for patients exhibiting anti-PEG antibodies. One possibility is the infusion of a compound that can block or suppress anti-PEG before the administration of a PEG-conjugated drug. In many clinical cases, where anti-PEG antibody response is induced, the clearance rate of the PEG-conjugated drug should be carefully monitored

and doses adjusted to compensate. Alternatively, it may be possible to replace the PEGconjugate with a non-PEGylated version of the therapeutic agent.[93]

12.2 Effects of the HSA moiety on protein immunogenicity and stability

HSA is the only therapeutic protein that is stable as a liquid at room temperature. This stability is primarily due to the presence of 17 disulfide linkages present in the molecule. The stability of albumin makes its storage and handling easier than typical proteins, thus making itself well suited as an excipient. The high stability of the protein also allows it to be heated at a temperature of 60°C for 10 hours, without significant denaturation, which facilitates virus inactivation during manufacturing. HSA is used as a stabilizer for proteins due to its amphiphilic properties, which makes it appropriate as an additive to prevent adsorption of the active protein, via the competitive adsorption mechanisms. HSA may also stabilize the native conformation of the active molecule, thereby helping it to maintain its bioactivity throughout the product shelf life.[94]

While HSA is largely non-immunogenic, the same cannot be said of proteins that bind to HSA. For example, the albumin binding domain of streptococcal protein G is of concern due to its bacterial origin. Accordingly, it has been engineered to reduce its immunogenicity by removing the T-cell epitopes. Based on the existing literature and use of in silico programs for predicting T-cell epitopes, several derivatives have been

produced and one (ABD094) is currently being clinically evaluated.[95]
Besides, its long serum half-life, HSA has been found to accumulate in many tumors as a result of their enhanced vascular permeability and the increased retention of albumin in tumor interstitium.[96, 97] These findings have been validated by radiolabeled or

dyeconjugated albumins, which have been shown to have high uptake into tumors.[98] Based on this property, HSA is considered to be a suitable system for drug delivery to tumor tissue.[99, 100] By implication, it is assumed that fusion proteins bearing albumin binding domains will also accumulate inside tumors following their association with HSA. In the case of constructs such as ABD-rIL-2, this induces the recruitment of cytotoxic T cells to tumor sites.[75]

Studies indicate that the position of the fusion has an essential influence on the subsequent activity of the therapeutic protein. Human brain natriuretic peptide (BNP), which is used in the treatment of acute decompensated congestive heart failure, illustrates this point. Four fusion proteins, BNP-HSA, $(BNP)_2$-HSA, $(BNP)_4$-HSA, and HSA-$(BNP)_2$, were constructed, with different numbers of BNP molecules and fusion orientations. Fusion with HSA successfully prolonged the bioactivity of BNP, stimulating intracellular cGMP expression over 24 h and activating human natriuretic peptide receptor A (NPRA). The HSA-$(BNP)_2$, with two BNP molecules fused in tandem at the C-terminus of HSA, had the highest and most prolonged BNP bioactivity in activating human NPR-A.[101] In contrast, the other three fusion proteins only slightly increased the activity of NPR-A. Currently, there is no way of predicting which fusion structure will be most effective – it is necessary to use trial and error to test different constructs and determine which is best.

Similarly, although serum albumin has a half-life in humans of about 19 days, the halflives of therapeutic proteins fused with HSA is generally much lower. For example, the

fusion protein proalbiglutide, a drug marketed for diabetes 2, only has a circulatory halflife of about 5 days. Other proteins tested such as CTP, ELP, or XTEN, their fusion proteins have not shown any better half-life than 2.5, 4–5, and 4–5 days, respectively.[74]

13. Advantages of PEGylation and HSA fused drug

Rival strategies often have complementary advantages and disadvantages; PEGylation and linkage to HSA are no exception.

PEGylation creates relatively simple changes in a protein's structure. However, such changes can have significant effects on functions such as signaling, targeting, catalysis, and catabolism, circulation time in the blood, the degree of immunogenicity/antigenicity, body-residence time and stability. In part these effects are due to the fact that PEG shields the protein surface from degradative agents and from the immune system. Additionally, the increased hydrodynamic radius that results from PEGylation usually decreases the efficiency of kidney clearance of the protein in question.[16]

The widespread acceptance of PEG conjugates can be attributed to the exceptionally favorable combination of physicochemical and biological properties of the polymer. This includes its solubility in aqueous and most organic solvents, biocompatibility, lack of toxicity and (usually) low immunogenicity.[67] The favorable properties of PEG also result in peptide and protein conjugates that are soluble and active in organic solvents and that have reduced levels of absorption to surfaces. This last property is particularly useful in the case of PEGylated liposomes and niosomes, greatly increasing their utility for drug delivery.[47]

The FDA approval of several PEGylated therapeutic proteins highlights their advantages. Some of the most important advantages are their prolonged body-residence time, which allows a drug to be administered less frequently, which arises from their increased resistance to degradative agents such as proteases or nucleases, and decreases in immunogenicity. Given these advantages, it is perhaps unsurprisingly that PEGylation has allowed the creation of blockbuster products such as Pegasys (peginterferon alfa-2a) and PEG-Intron (PEG-Intron (Peginterferon alfa-2b).[16]

The unusually long circulation time of HSA (19 days) has similarly encouraged researchers to use it to prolong the serum half-lives of other proteins either through genetic fusion or by chemical conjugation.[102]. It has been known for some time that HSA's longevity in serum is due in large part to its electrostatic repulsion in kidneys and to FcRnmediated recycling in the endothelium.[14-16, 103] However, it was initially unclear if fusion with HSA would increase the longevity of other proteins attached to it or if this would simply result in a decrease in HSA longevity. Fortunately, subsequent investigations proved these concerns to be largely unfounded.

In contrast to PEGylated proteins which tend to have reduced absorption in the body relative to their native counterparts, proteins conjugated to albumin tend to accumulate in certain locales *in vivo*. This means that albumin-based drug carrier systems have particular applications in the field of chemotherapy as they can improve the passive tumor targeting properties of anti-cancer drugs. Proliferating tumor cells utilize albumin and other plasma proteins for their nutrition and take up albumin by fluid phase endocytosis at a greater rate than normal tissues. After lysosomal digestion, the derived amino acids serve as a source for nitrogen and energy in the tumor cells. These favorable properties make albumin an attractive choice as a drug carrier where the conjugates enjoy the same favorable tumor targeting properties as albumin itself, e.g. high tumor uptake rates, low liver uptake rates and a very long biologic half-life.

Both approaches have the ability to conjugate to proteins without comprising the critical property of the target protein. In mice, the serum half-life using the HSA and the PEG was typically around 9- and 7-fold greater, respectively, than that of the sfGFP-WT. Although the binding affinity of HSA to a mouse is much greater than that of a human, it is still much greater than that of a PEG-conjugated protein in human. A disadvantage in both techniques is that the handling and chemical modification of HSA during modification can lead to slight denaturation which may generate a significant immune response.[21]

The hydrophobic moieties present on the polymers can bind to proteins through hydrophobic interactions (e.g., PEG with aromatic groups). Additionally, these polymers can also destabilize the native protein conformation by stabilizing unfolded protein conformations. Protein excipients, for example human serum albumin (HSA), stabilize biopharmaceuticals by competitively adsorbing to surfaces and interfaces and preventing interface induced aggregation of the drug product.[55]

The production of long-acting protein therapeutics using techniques such as PEGylation, and others to overcome the patient's immunogenicity has been established and covered extensively in the literature. We successfully produced two forms of long-acting glucarpidase using PEGYlation and HSA fusion with glucarpidase. The two forms produced are more resistant to proteases than the free enzyme (**Figure 5**). They also less immunogenic than the free glucarpidase (**Figure 6**)[11]

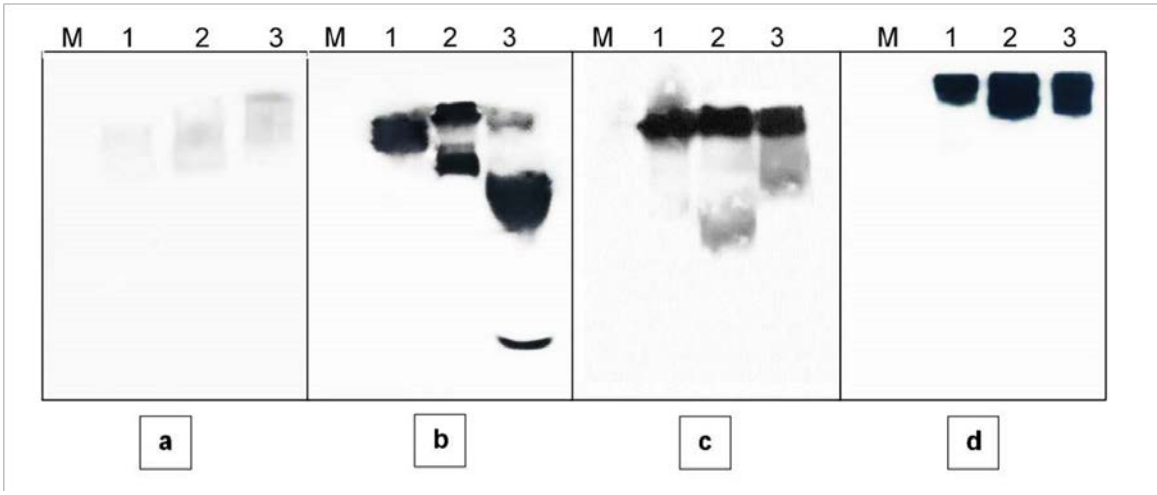

Figure 5: Stability of different CPG2 Forms after incubation in normal human serum. The samples were collected on 0, 10 and 15 days, which are 1, 2, and 3 respectively. Lane M, SeeBlue Plus2 Prestained ladder (198-10 kDa); a: serum only as control; b: XenCPG2; c: PEG-Xen-CPG2; and d: HSA-Xen-CPG2. The samples were analyzed by western blotting using the anti Xen-CPG2 antibody.

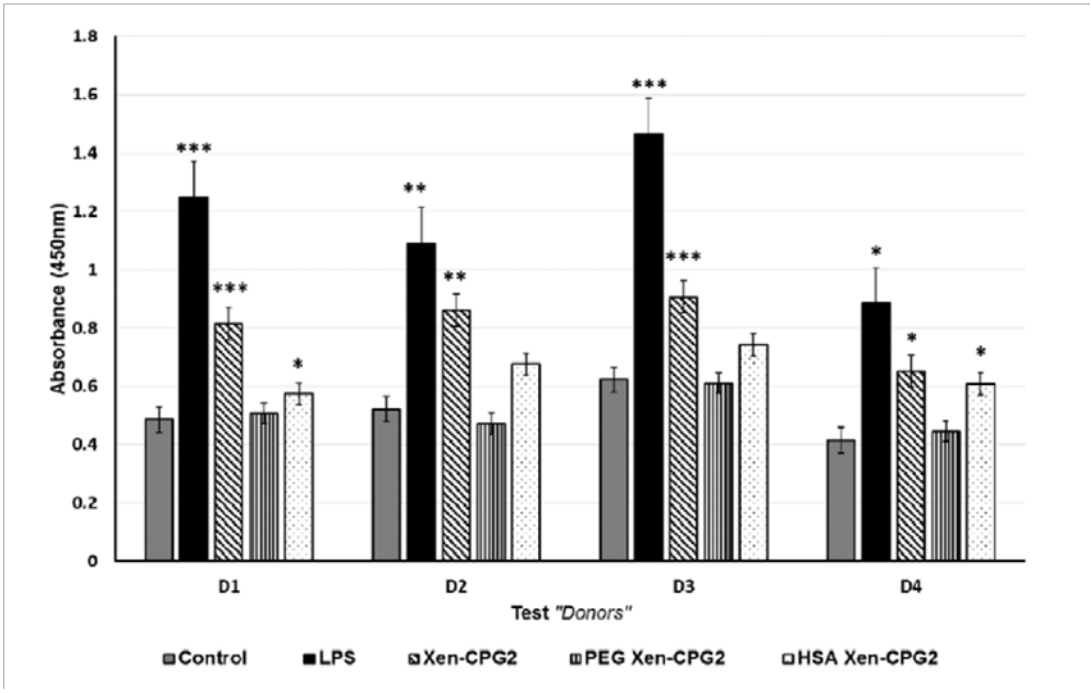

Figure 6: Immunogenicity testing using healthy Human PBMC proliferation assay. The positive control, Lipopolysaccharide (LPS) showed a significant increase when compared with all control groups with the vehicle only. The negative control, PEG Xen-CPG2 treated cells in all groups showed no significant increase in proliferation. The cells treated with HSA Xen-CPG2 gave a similar result except in two donors. $P < 0.05$ was considered statistically significant, ** $P < 0.01$, *** $P < 0.0001$.

In our recent work, we established a different and new strategy to overcome the immunogenicity problem. We showed that isolation of a novel form of the protein used with different epitops could also minimize the patient immune response. We showed that the antibody of one form of the enzyme does not neutralize the other form (**Figure 7**).[10] We therefore proposed that the two forms of the proteins or the enzymes could be used consecutively instead of using one form of the enzyme.

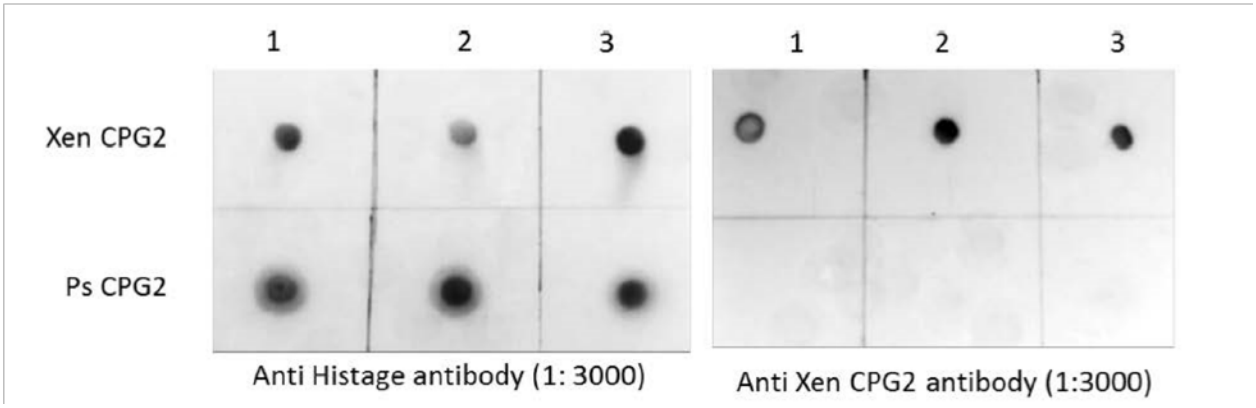

Figure 7: Dot blot using anti his tag and anti Xen CPG2 antibodies. 1-3 concentrations 0.05, 0.1, and 0.2 mg/mL of pure Xen CPG2 and Ps CPG2

14. Nanonization and Drug development

We discussed different strategies to overcome the immunogenicity of drugs and many problems related to drug development and their clinical applications

Another major obstacle to drug development is poor water solubility of many therapeutics. This poor water solubility affects the drug bioavailability which in turn reduce its efficiency. This presents another major pitfall to their clinical applications.

Many conventional formulations to improve solubility may lead to poor pharmacokinetics and low or loss of bioavailability. Drug PEGylation, in addition to many advantages, may increase solubility.

Nanonization techniques, however, offers an efficient way to overcome problems related to drug development.

Different methods of drug nanonization have been established.[104-108] The use of nanonization to improved drug development and drug delivery and to overcome the solubility problem have been successful in several drugs.[105, 109-117]

In summary, the use of techniques such as drug PEGylation and fusion with human serum albumin followed by drug nanonization could solve many problems related to drug development such as immunogenicity, proteases degradation and drug bioavailability.

15. Conclusions

Modification of therapeutic molecules by chemical conjugation with Human serum albumin (HSA), polyethylene glycol (PEG) or other known molecules has been established to enhance the drug pharmaceutical properties. This has been shown in the successful approval of more than 12 modified drugs by the FDA. Despite the fact that the added moiety improves the pharmacologic and pharmaceutical properties of the drug, most of the adverse effects of the modified drugs are due to the active part of the medicine and not to the added moiety. The use of external moieties, such as PEG and HSA, as delivery of the drug to the cancer cell is an added advantage of the process and will pave the way for more research in this area.

16. Acknowledgements

• QNRF grant number NPRP6-065-3-012, Qatar National Research Fund, Doha Qatar for funding some of the work that is presented in this paper.

17. References

1. Kontermann, R. E. Alternative antibody formats. *Current opinion in molecular therapeutics* **2010,** *12*, (2), 176-83.
2. DeFrees, S.; Wang, Z. G.; Xing, R.; Scott, A. E.; Wang, J.; Zopf, D.; Gouty, D. L.; Sjoberg, E. R.; Panneerselvam, K.; Brinkman-Van der Linden, E. C.; Bayer, R. J.; Tarp, M. A.; Clausen, H. GlycoPEGylation of recombinant therapeutic proteins produced in Escherichia coli. *Glycobiology* **2006,** *16*, (9), 833-43.
3. Jana, S.; Mandlekar, S.; Marathe, P. Prodrug design to improve pharmacokinetic and drug delivery properties: challenges to the discovery scientists. *Current medicinal chemistry* **2010,** *17*, (32), 3874-908.
4. Dimitrov, D. S. Therapeutic proteins. *Methods in molecular biology (Clifton, N.J.)* **2012,** *899*, 1-26.
5. Quianzon, C. C.; Cheikh, I. History of insulin. *Journal of community hospital internal medicine perspectives* **2012,** *2*, (2), 10.3402/jchimp.v2i2.18701.
6. Dozier, J. K.; Distefano, M. D. Site-Specific PEGylation of Therapeutic Proteins. *International Journal of Molecular Sciences* **2015,** *16*, (10), 25831-25864.
7. Half-Life Modulating Strategies–An Introduction. In *Therapeutic Proteins*.
8. Fee, C. J.; Van Alstine, J. M. PEG-proteins: Reaction engineering and separation issues. *Chemical Engineering Science* **2006,** *61*, (3), 924-939.
9. Osipovitch, D. C.; Parker, A. S.; Makokha, C. D.; Desrosiers, J.; Kett, W. C.; Moise, L.; Bailey-Kellogg, C.; Griswold, K. E. Design and analysis of immune-evading enzymes for ADEPT therapy. *Protein engineering, design & selection : PEDS* **2012,** *25*, (10), 613-23.
10. Rashidi, F. B.; AlQhatani, A. D.; Bashraheel, S. S.; Shaabani, S.; Groves, M. R.; Dömling, A.; Goda, S. K. Isolation and molecular characterization of novel glucarpidases: Enzymes to improve the antibody directed enzyme pro-drug therapy for cancer treatment. *PLoS ONE* **2018,** *13*, (4), e0196254.
11. AlQahtani, A. D.; Al-Mansoori, L.; Bashraheel, S. S.; Rashidi, F. B.; Al-Yafei, A.; Elsinga, P.; Domling, A.; Goda, S. K. Production of "biobetter" glucarpidase variants to improve drug detoxification and antibody directed enzyme prodrug therapy for cancer treatment. *European journal of pharmaceutical sciences : official journal of the European Federation for Pharmaceutical Sciences* **2018,** *127*, 79-91.
12. Wen, H.; Jung, H.; Li, X. Drug Delivery Approaches in Addressing Clinical Pharmacology-Related Issues: Opportunities and Challenges. *The AAPS journal* **2015,** *17*, (6), 1327-40.
13. Mahmood, I.; Green, M. D. Pharmacokinetic and pharmacodynamic considerations in the development of therapeutic proteins. *Clinical pharmacokinetics* **2005,** *44*, (4), 33147.
14. Tryggvason, K.; Wartiovaara, J. How does the kidney filter plasma? *Physiology (Bethesda, Md.)* **2005,** *20*, 96-101.
15. Schellenberger, V.; Wang, C. W.; Geething, N. C.; Spink, B. J.; Campbell, A.; To, W.; Scholle, M. D.; Yin, Y.; Yao, Y.; Bogin, O.; Cleland, J. L.; Silverman, J.; Stemmer, W. P. A recombinant polypeptide

extends the in vivo half-life of peptides and proteins in a tunable manner. *Nature biotechnology* **2009,** *27*, (12), 1186-90.
16. Veronese, F. M.; Pasut, G. PEGylation, successful approach to drug delivery. *Drug discovery today* **2005,** *10*, (21), 1451-8.
17. Andersen, J. T.; Dalhus, B.; Viuff, D.; Ravn, B. T.; Gunnarsen, K. S.; Plumridge, A.; Bunting, K.; Antunes, F.; Williamson, R.; Athwal, S.; Allan, E.; Evans, L.; Bjoras, M.; Kjaerulff, S.; Sleep, D.; Sandlie, I.; Cameron, J. Extending serum half-life of albumin by engineering neonatal Fc receptor (FcRn) binding. *The Journal of biological chemistry* **2014,** *289*, (19), 13492-502.
18. Roopenian, D. C.; Akilesh, S. FcRn: the neonatal Fc receptor comes of age. *Nature reviews. Immunology* **2007,** *7*, (9), 715-25.
19. Nakamura, H.; Oda-Ueda, N.; Ueda, T.; Ohkuri, T. Introduction of a glycosylation site in the constant region decreases the aggregation of adalimumab Fab. *Biochem Biophys Res Commun* **2018,** *503*, (2), 752-756.
20. Abdiche, Y. N.; Yeung, Y. A.; Chaparro-Riggers, J.; Barman, I.; Strop, P.; Chin, S. M.; Pham, A.; Bolton, G.; McDonough, D.; Lindquist, K.; Pons, J.; Rajpal, A. The neonatal Fc receptor (FcRn) binds independently to both sites of the IgG homodimer with identical affinity. *mAbs* **2015,** *7*, (2), 331-43.
21. Yang, B.; Lim, S. I.; Kim, J. C.; Tae, G.; Kwon, I. Site-Specific Albumination as an Alternative to PEGylation for the Enhanced Serum Half-Life in Vivo. *Biomacromolecules* **2016,** *17*, (5), 1811-7.
22. Pisal, D. S.; Kosloski, M. P.; Balu-Iyer, S. V. Delivery of therapeutic proteins. *Journal of pharmaceutical sciences* **2010,** *99*, (6), 2557-75.
23. Ishida, T. Effects of point mutation on enzymatic activity: correlation between protein electronic structure and motion in chorismate mutase reaction. *Journal of the American Chemical Society* **2010,** *132*, (20), 7104-18.
24. Webster, C. I.; Burrell, M.; Olsson, L. L.; Fowler, S. B.; Digby, S.; Sandercock, A.; Snijder, A.; Tebbe, J.; Haupts, U.; Grudzinska, J.; Jermutus, L.; Andersson, C. Engineering neprilysin activity and specificity to create a novel therapeutic for Alzheimer's disease. *PLoS One* **2014,** *9*, (8), e104001.
25. Vodyanoy, V.; Daniels, Y.; Pustovyy, O.; MacCrehan, W. A.; Muramoto, S.; Stan, G. Engineered metal nanoparticles in the sub-nanomolar levels kill cancer cells. *International journal of nanomedicine* **2016,** *11*, 1567-1576.
26. Kim, H. K.; Emolo, C.; DeDent, A. C.; Falugi, F.; Missiakas, D. M.; Schneewind, O. Protein A-specific monoclonal antibodies and prevention of Staphylococcus aureus disease in mice. *Infection and immunity* **2012,** *80*, (10), 3460-3470.
27. Osman, G.; Rodriguez, J.; Chan, S. Y.; Chisholm, J.; Duncan, G.; Kim, N.; Tatler, A. L.; Shakesheff, K. M.; Hanes, J.; Suk, J. S.; Dixon, J. E. PEGylated enhanced cell penetrating peptide nanoparticles for lung gene therapy. *Journal of controlled release : official journal of the Controlled Release Society* **2018,** *285*, 35-45.
28. Furber, K. L.; Van Agten, M.; Evans, C.; Haddadi, A.; Doucette, J. R.; Nazarali, A. J. Advances in the treatment of relapsing-remitting multiple sclerosis: the role of pegylated interferon beta-1a. *Degenerative neurological and neuromuscular disease* **2017,** *7*, 4760.
29. Sun, G.; Lin, X.; Shen, L.; Wu, F.; Xu, D.; Ruan, K.; Feng, Y. Mono-PEGylated radix ophiopogonis polysaccharide for the treatment of myocardial ischemia. *European journal of pharmaceutical sciences : official journal of the European Federation for Pharmaceutical Sciences* **2013,** *49*, (4), 629-36.
30. Haruta, K.; Otaki, N.; Nagamine, M.; Kayo, T.; Sasaki, A.; Hiramoto, S.; Takahashi, M.; Hota, K.; Sato, H.; Yamazaki, H. A Novel PEGylation Method for Improving the Pharmacokinetic Properties of Anti-Interleukin-17A RNA Aptamers. *Nucleic acid therapeutics* **2017,** *27*, (1), 36-44.
31. Tang, J.; Kuai, R.; Yuan, W.; Drake, L.; Moon, J. J.; Schwendeman, A. Effect of size and pegylation of liposomes and peptide-based synthetic lipoproteins on tumor targeting. *Nanomedicine : nanotechnology, biology, and medicine* **2017,** *13*, (6), 1869-1878.

32. Lee, J.; Ahn, H. J. PEGylated DC-Chol/DOPE cationic liposomes containing KSP siRNA as a systemic siRNA delivery Carrier for ovarian cancer therapy. *Biochem Biophys Res Commun* **2018,** *503*, (3), 1716-1722.
33. Meng, H.; Lockshin, C.; Jain, S.; Shaligram, U.; Martinez, J.; Genkin, D.; Hill, D. B.; Ehre, C.; Clark, D.; Hoppe, H. Clinical application of polysialylated therapeutic proteins. *Recent patents on drug delivery & formulation* **2018**.
34. Wang, F.; Yu, T.; Zheng, H.; Lao, X. Thymosin Alpha1-Fc Modulates the Immune System and Down-regulates the Progression of Melanoma and Breast Cancer with a Prolonged Half-life. *Scientific reports* **2018,** *8*, (1), 12351.
35. Kim, S. J.; Kwak, H. H.; Cho, S. Y.; Sohn, Y. B.; Park, S. W.; Huh, R.; Kim, J.; Ko, A. R.; Jin, D. K. Pharmacokinetics, Pharmacodynamics, and Efficacy of a Novel Long-Acting Human Growth Hormone: Fc Fusion Protein. *Molecular pharmaceutics* **2015,** *12*, (10), 3759-65.
36. Shen, Y.; Li, H.; Zhao, L.; Li, G.; Chen, B.; Guo, Q.; Gao, B.; Wu, J.; Yang, T.; Jin, L.; Su, Y. Increased half-life and enhanced potency of Fc-modified human PCSK9 monoclonal antibodies in primates. *PLoS One* **2017,** *12*, (8), e0183326.
37. Zong, Y.; Tan, X.; Xiao, J.; Zhang, X.; Xia, X.; Sun, H. Half-life extension of porcine interferon-alpha by fusion to the IgG-binding domain of streptococcal G protein. *Protein expression and purification* **2019,** *153*, 53-58.
38. Graf, L. Extended Half-Life Factor VIII and Factor IX Preparations. *Transfusion medicine and hemotherapy : offizielles Organ der Deutschen Gesellschaft fur Transfusionsmedizin und Immunhamatologie* **2018,** *45*, (2), 86-91.
39. Guan, J.; Yan, X.; Zhao, Y.; Sun, Y.; Peng, X. Binding studies of triclocarban with bovine serum albumin: Insights from multi-spectroscopy and molecular modeling methods. *Spectrochimica acta. Part A, Molecular and biomolecular spectroscopy* **2018,** *202*, 112.
40. Rousseau, E.; Lau, J.; Zhang, Z.; Uribe, C. F.; Kuo, H. T.; Zhang, C.; Zeisler, J.; Colpo, N.; Lin, K. S.; Benard, F. Effects of adding an albumin binder chain on [(177)Lu]LuDOTATATE. *Nuclear medicine and biology* **2018,** *66*, 10-17.
41. Battelino, T.; Rasmussen, M. H.; De Schepper, J.; Zuckerman-Levin, N.; Gucev, Z.; Savendahl, L. Somapacitan, a once-weekly reversible albumin-binding GH derivative, in children with GH deficiency: A randomized dose-escalation trial. *Clinical endocrinology* **2017,** *87*, (4), 350-358.
42. Deng, J.; Mei, H.; Shi, W.; Pang, Z. Q.; Zhang, B.; Guo, T.; Wang, H. F.; Jiang, X. G.; Hu, Y. Recombinant Tissue Plasminogen Activator-conjugated Nanoparticles Effectively Targets Thrombolysis in a Rat Model of Middle Cerebral Artery Occlusion. *Current medical science* **2018,** *38*, (3), 427-435.
43. Zhao, L.; Bi, D.; Qi, X.; Guo, Y.; Wang, X.; Han, M. Polydopamine-based surface modification of paclitaxel nanoparticles for osteosarcoma targeted therapy. *Nanotechnology* **2019**.
44. D'souza, A. A.; Shegokar, R. Polyethylene glycol (PEG): a versatile polymer for pharmaceutical applications. *Expert opinion on drug delivery* **2016,** *13*, (9), 1257-1275.
45. Jevsevar, S.; Kunstelj, M.; Porekar, V. G. PEGylation of therapeutic proteins. *Biotechnology journal* **2010,** *5*, (1), 113-28.
46. Filpula, D.; Zhao, H. Releasable PEGylation of proteins with customized linkers. *Adv Drug Deliv Rev* **2008,** *60*, (1), 29-49.
47. Schrama, D.; Reisfeld, R. A.; Becker, J. C. Antibody targeted drugs as cancer therapeutics. *Nature reviews. Drug discovery* **2006,** *5*, (2), 147-59.
48. Pasut, G.; Veronese, F. M. State of the art in PEGylation: The great versatility achieved after forty years of research. *Journal of Controlled Release* **2012,** *161*, (2), 461-472.
49. Taguchi, K.; Giam Chuang, V. T.; Maruyama, T.; Otagiri, M. Pharmaceutical Aspects of the Recombinant Human Serum Albumin Dimer: Structural Characteristics, Biological Properties, and Medical Applications. *Journal of pharmaceutical sciences* **2012,** *101*, (9), 3033-3046.
50. Veronese, F. M. Peptide and protein PEGylation: a review of problems and solutions. *Biomaterials* **2001,** *22*, (5), 405-17.

51. Veronese, F. M.; Pasut, G. PEGylation: Posttranslational bioengineering of protein biotherapeutics. *Drug discovery today. Technologies* **2008,** *5*, (2-3), e57-64.
52. Kim, T. H.; Jiang, H. H.; Lim, S. M.; Youn, Y. S.; Choi, K. Y.; Lee, S.; Chen, X.; Byun, Y.; Lee, K. C. Site-specific PEGylated Exendin-4 modified with a high molecular weight trimeric PEG reduces steric hindrance and increases type 2 antidiabetic therapeutic effects. *Bioconjugate chemistry* **2012,** *23*, (11), 2214-20.
53. Park, K. Albumin: a versatile carrier for drug delivery. *Journal of controlled release : official journal of the Controlled Release Society* **2012,** *157*, (1), 3.
54. Tang, L.; Persky, A. M.; Hochhaus, G.; Meibohm, B. Pharmacokinetic aspects of biotechnology products. *Journal of pharmaceutical sciences* **2004,** *93*, (9), 2184-204.
55. Nguyen, N. T.; Lee, J. S.; Yun, S.; Lee, E. K. Separation of mono- and di-PEGylate of exenatide and resolution of positional isomers of mono-PEGylates by preparative ion exchange chromatography. *Journal of chromatography. A* **2016,** *1457*, 88-96.
56. Ogasawara, Y.; Namai, T.; Togawa, T.; Ishii, K. Formation of albumin dimers induced by exposure to peroxides in human plasma: A possible biomarker for oxidative stress. *Biochemical and Biophysical Research Communications* **2006,** *340*, (2), 353-358.
57. Sleep, D.; Cameron, J.; Evans, L. R. Albumin as a versatile platform for drug half-life extension. *Biochimica et biophysica acta* **2013,** *1830*, (12), 5526-34.
58. Elsadek, B.; Kratz, F. Impact of albumin on drug delivery--new applications on the horizon. *Journal of controlled release : official journal of the Controlled Release Society* **2012,** *157*, (1), 4-28.
59. Kratz, F.; Elsadek, B. Clinical impact of serum proteins on drug delivery. *Journal of controlled release : official journal of the Controlled Release Society* **2012,** *161*, (2), 429-45.
60. Sung, C.; Nardelli, B.; LaFleur, D. W.; Blatter, E.; Corcoran, M.; Olsen, H. S.; Birse, C. E.; Pickeral, O. K.; Zhang, J.; Shah, D.; Moody, G.; Gentz, S.; Beebe, L.; Moore, P. A. An IFN-beta-albumin fusion protein that displays improved pharmacokinetic and pharmacodynamic properties in nonhuman primates. *Journal of interferon & cytokine research : the official journal of the International Society for Interferon and Cytokine Research* **2003,** *23*, (1), 25-36.
61. Osborn, B. L.; Sekut, L.; Corcoran, M.; Poortman, C.; Sturm, B.; Chen, G.; Mather, D.; Lin, H. L.; Parry, T. J. Albutropin: a growth hormone-albumin fusion with improved pharmacokinetics and pharmacodynamics in rats and monkeys. *European journal of pharmacology* **2002,** *456*, (1-3), 149-58.
62. Rasmussen, K. C.; Højskov, M.; Johansson, P. I.; Kridina, I.; Kistorp, T.; Salling, L.; Nielsen, H. B.; Ruhnau, B.; Pedersen, T.; Secher, N. H. Impact of Albumin on Coagulation Competence and Hemorrhage During Major Surgery: A Randomized Controlled Trial. *Medicine* **2016,** *95*, (9), e2720.
63. Patterson, J. T.; Wilson, H. D.; Asano, S.; Nilchan, N.; Fuller, R. P.; Roush, W. R.; Rader, C.; Barbas, C. F., 3rd. Human Serum Albumin Domain I Fusion Protein for Antibody Conjugation. *Bioconjugate chemistry* **2016,** *27*, (10), 2271-2275.
64. Zhao, S.; Zhang, Y.; Tian, H.; Chen, X.; Cai, D.; Yao, W.; Gao, X. Extending the serum half-life of G-CSF via fusion with the domain III of human serum albumin. *BioMed research international* **2013,** *2013*, 107238.
65. Sawa, T.; Wu, J.; Akaike, T.; Maeda, H. Tumor-targeting chemotherapy by a xanthine oxidase-polymer conjugate that generates oxygen-free radicals in tumor tissue. *Cancer research* **2000,** *60*, (3), 666-71.
66. Hatakeyama, H.; Akita, H.; Harashima, H. The polyethyleneglycol dilemma: advantage and disadvantage of PEGylation of liposomes for systemic genes and nucleic acids delivery to tumors. *Biological & pharmaceutical bulletin* **2013,** *36*, (6), 892-9.
67. Khan, T.; Gohel, A. Pegylation: Concept and applications in cancer therapeutics. *Indian Drugs* **2014,** *51*, (04), 5.

68. Pan, H.; Liu, J.; Deng, W.; Xing, J.; Li, Q.; Wang, Z. Site-specific PEGylation of an antiCEA/CD3 bispecific antibody improves its antitumor efficacy. *International journal of nanomedicine* **2018,** *13*, 3189-3201.
69. Davarpanah, F.; Khalili Yazdi, A.; Barani, M.; Mirzaei, M.; Torkzadeh-Mahani, M. Magnetic delivery of antitumor carboplatin by using PEGylated-Niosomes. *Daru : journal of Faculty of Pharmacy, Tehran University of Medical Sciences* **2018,** *26*, (1), 57-64.
70. Palumbo, E. Pegylated Interferon and Ribavirin Treatment for Hepatitis C Virus Infection. *Therapeutic Advances in Chronic Disease* **2011,** *2*, (1), 39-45.
71. Santi, D. V.; Schneider, E. L.; Reid, R.; Robinson, L.; Ashley, G. W. Predictable and tunable half-life extension of therapeutic agents by controlled chemical release from macromolecular conjugates. *Proceedings of the National Academy of Sciences of the United States of America* **2012,** *109*, (16), 6211-6.
72. Sacchetti, F.; Marverti, G.; D'Arca, D.; Severi, L.; Maretti, E.; Iannuccelli, V.; Pacifico, S.; Ponterini, G.; Costi, M. P.; Leo, E. pH-Promoted Release of a Novel Anti-Tumour Peptide by "Stealth" Liposomes: Effect of Nanocarriers on the Drug Activity in CisPlatinum Resistant Cancer Cells. *Pharmaceutical research* **2018,** *35*, (11), 206.
73. Ishima, Y.; Maruyama, T. [Human Serum Albumin as Carrier in Drug Delivery Systems]. *Yakugaku zasshi : Journal of the Pharmaceutical Society of Japan* **2016,** *136*, (1), 39-47.
74. Strohl, W. R. Fusion Proteins for Half-Life Extension of Biologics as a Strategy to Make Biobetters. *BioDrugs : clinical immunotherapeutics, biopharmaceuticals and gene therapy* **2015,** *29*, (4), 215-39.
75. Adabi, E.; Saebi, F.; Moradi Hasan-Abad, A.; Teimoori-Toolabi, L.; Kardar, G. A. Evaluation of an Albumin-Binding Domain Protein Fused to Recombinant Human IL-2 and Its Effects on the Bioactivity and Serum Half-Life of the Cytokine. *Iranian biomedical journal* **2017,** *21*, (2), 77-83.
76. Czerwiński, M.; Amunom, I.; Piryatinsky, V.; Hallak, H.; Sahly, Y.; Bar-Ilan, O.; Bolliger, P.; Bassan, M. Direct and cytokine-mediated effects of albumin-fused growth hormone, TV-1106, on CYP enzyme expression in human hepatocytes in vitro. *Pharmacology Research & Perspectives* **2018,** *6*, (3), e00397.
77. Roscoe, I.; Parker, M.; Dong, D.; Li, X.; Li, Z. Human serum albumin and p53-derived peptide fusion protein promotes cytotoxicity irrespective of p53 status in cancer cells. *Molecular pharmaceutics* **2018**.
78. Sepehri, N.; Rouhani, H.; Ghanbarpour, A. R.; Gharghabi, M.; Tavassolian, F.; Amini, M.; Ostad, S. N.; Ghahremani, M. H.; Dinarvand, R. Human serum albumin conjugates of 7-ethyl-10-hydroxycamptothecin (SN38) for cancer treatment. *BioMed research international* **2014,** *2014*, 963507.
79. Han, H.; Wang, J.; Chen, T.; Yin, L.; Jin, Q.; Ji, J. Enzyme-sensitive gemcitabine conjugated albumin nanoparticles as a versatile theranostic nanoplatform for pancreatic cancer treatment. *Journal of colloid and interface science* **2017,** *507*, 217-224.
80. Yousuf, I.; Bashir, M.; Arjmand, F.; Tabassum, S. Multispectroscopic insight, morphological analysis and molecular docking studies of Cu(II) based chemotherapeutic drug entity with Human Serum Albumin (HSA) and Bovine Serum Albumin (BSA). *Journal of biomolecular structure & dynamics* **2018**, 1-31.
81. Fishburn, C. S. The pharmacology of PEGylation: balancing PD with PK to generate novel therapeutics. *Journal of pharmaceutical sciences* **2008,** *97*, (10), 4167-83.
82. Hamidi, M.; Rafiei, P.; Azadi, A. Designing PEGylated therapeutic molecules: advantages in ADMET properties. *Expert opinion on drug discovery* **2008,** *3*, (11), 1293-307.
83. Kubetzko, S.; Sarkar, C. A.; Pluckthun, A. Protein PEGylation decreases observed target association rates via a dual blocking mechanism. *Molecular pharmacology* **2005,** *68*, (5), 1439-54.
84. Caliceti, P.; Veronese, F. M. Pharmacokinetic and biodistribution properties of poly(ethylene glycol)-protein conjugates. *Adv Drug Deliv Rev* **2003,** *55*, (10), 1261-77. 85. Gefen, T.; Vaya, J.; Khatib, S.; Harkevich, N.; Artoul, F.; Heller, E. D.; Pitcovski, J.; Aizenshtein, E. The impact of

PEGylation on protein immunogenicity. *International Immunopharmacology* **2013,** *15*, (2), 254-259.
86. Allen, T. M. Ligand-targeted therapeutics in anticancer therapy. *Nature reviews. Cancer* **2002,** *2*, (10), 750-63.
87. Ohtake, S.; Kita, Y.; Arakawa, T. Interactions of formulation excipients with proteins in solution and in the dried state. *Adv Drug Deliv Rev* **2011,** *63*, (13), 1053-73.
88. Zhang, P.; Sun, F.; Liu, S.; Jiang, S. Anti-PEG antibodies in the clinic: Current issues and beyond PEGylation. *Journal of Controlled Release* **2016,** *244*, 184-193.
89. Yang, Q.; Lai, S. K. Anti-PEG immunity: emergence, characteristics, and unaddressed questions. *Wiley interdisciplinary reviews. Nanomedicine and nanobiotechnology* **2015,** *7*, (5), 655-677.
90. Garay, R. P.; El-Gewely, R.; Armstrong, J. K.; Garratty, G.; Richette, P. Antibodies against polyethylene glycol in healthy subjects and in patients treated with PEGconjugated agents. *Expert opinion on drug delivery* **2012,** *9*, (11), 1319-23.
91. Hershfield, M. S.; Ganson, N. J.; Kelly, S. J.; Scarlett, E. L.; Jaggers, D. A.; Sundy, J. S. Induced and pre-existing anti-polyethylene glycol antibody in a trial of every 3-week dosing of pegloticase for refractory gout, including in organ transplant recipients. *Arthritis Research & Therapy* **2014,** *16*, (2), R63-R63.
92. Ganson, N. J.; Kelly, S. J.; Scarlett, E.; Sundy, J. S.; Hershfield, M. S. Control of hyperuricemia in subjects with refractory gout, and induction of antibody against poly(ethylene glycol) (PEG), in a phase I trial of subcutaneous PEGylated urate oxidase. *Arthritis Research & Therapy* **2006,** *8*, (1), R12-R12.
93. Armstrong, J. K.; Hempel, G.; Koling, S.; Chan, L. S.; Fisher, T.; Meiselman, H. J.; Garratty, G. Antibody against poly(ethylene glycol) adversely affects PEG-asparaginase therapy in acute lymphoblastic leukemia patients. *Cancer* **2007,** *110*, (1), 103-11.
94. David Mead, D. P., Maree devine. Recombinant human albumin: applications as a biopharmaceutical excipient. **2007,** *22*.
95. Frejd, F. Y., Half-Life Extension by Binding to Albumin through an Albumin Binding Domain. In *Therapeutic Proteins*, 2012.
96. Greish, K. Enhanced permeability and retention of macromolecular drugs in solid tumors: a royal gate for targeted anticancer nanomedicines. *Journal of drug targeting* **2007,** *15*, (7-8), 457-64.
97. Kratz, F. Albumin as a drug carrier: design of prodrugs, drug conjugates and nanoparticles. *Journal of controlled release : official journal of the Controlled Release Society* **2008,** *132*, (3), 171-83.
98. Alakhova, D. Y.; Kabanov, A. Y. Drug Delivery in Oncology. From Basic Research to Cancer Therapy. 3 Volumes. Edited by Felix Kratz, Peter Senter and Henning Steinhagen. *Angewandte Chemie International Edition* **2014,** *53*, (14), 3547-3548.
99. Kratz, F. Albumin, a versatile carrier in oncology. *International journal of clinical pharmacology and therapeutics* **2010,** *48*, (7), 453-5.
100. Larsen, M. T.; Kuhlmann, M.; Hvam, M. L.; Howard, K. A. Albumin-based drug delivery: harnessing nature to cure disease. *Molecular and cellular therapies* **2016,** *4*, 3.
101. Ding, Y.; Peng, Y.; Deng, L.; Wu, Y.; Fu, Q.; Jin, J. The effects of fusion structure on the expression and bioactivity of human brain natriuretic peptide (BNP) albumin fusion proteins. *Current pharmaceutical biotechnology* **2014,** *15*, (9), 856-63.
102. Lim, S. I.; Hahn, Y. S.; Kwon, I. Site-specific albumination of a therapeutic protein with multi-subunit to prolong activity in vivo. *Journal of controlled release : official journal of the Controlled Release Society* **2015,** *207*, 93-100.
103. Peters, T., 2 - The Albumin Molecule: Its Structure and Chemical Properties. In *All About Albumin*, Peters, T., Ed. Academic Press: San Diego, 1995; pp 9-II.
104. Savkare, A. D.; Bhavsar, M. R.; Gholap, V. D.; Kukkar, P. M. Liquisolid technique: A review. *International Journal of Pharmaceutical Sciences and Research* **2017,** *8*, (7), 2768-2775.

105. Mustapha, O.; Din, F. U.; Kim, D. W.; Park, J. H.; Woo, K. B.; Lim, S. J.; Youn, Y. S.; Cho, K. H.; Rashid, R.; Yousaf, A. M.; Kim, J. O.; Yong, C. S.; Choi, H. G. Novel piroxicam-loaded nanospheres generated by the electrospraying technique: physicochemical characterisation and oral bioavailability evaluation. *Journal of microencapsulation* **2016,** *33*, (4), 323-30.
106. Serrano, D. R.; Gallagher, K. H.; Healy, A. M. Emerging Nanonisation Technologies: Tailoring Crystalline Versus Amorphous Nanomaterials. *Current topics in medicinal chemistry* **2015,** *15*, (22), 2327-40.
107. Mugheirbi, N. A.; Paluch, K. J.; Tajber, L. Heat induced evaporative antisolvent nanoprecipitation (HIEAN) of itraconazole. *International journal of pharmaceutics* **2014,** *471*, (1-2), 400-11.
108. Keck, C. M.; Muller, R. H. Drug nanocrystals of poorly soluble drugs produced by high pressure homogenisation. *European journal of pharmaceutics and biopharmaceutics : official journal of Arbeitsgemeinschaft fur Pharmazeutische Verfahrenstechnik e.V* **2006,** *62*, (1), 3-16.
109. Mukherjee, R.; Dutta, D.; Patra, M.; Chatterjee, B.; Basu, T. Nanonized tetracycline cures deadly diarrheal disease 'shigellosis' in mice, caused by multidrug-resistant Shigella flexneri 2a bacterial infection. *Nanomedicine : nanotechnology, biology, and medicine* **2018**.
110. Kankala, R. K.; Chen, B. Q.; Liu, C. G.; Tang, H. X.; Wang, S. B.; Chen, A. Z. Solutionenhanced dispersion by supercritical fluids: an ecofriendly nanonization approach for processing biomaterials and pharmaceutical compounds. *International journal of nanomedicine* **2018,** *13*, 4227-4245.
111. Jia, L. Nanoparticle Formulation Increases Oral Bioavailability of Poorly Soluble Drugs: Approaches Experimental Evidences and Theory. *Current nanoscience* **2005,** *1*, (3), 237-243.
112. Chen, B.-Q.; Kankala, R. K.; Wang, S.-B.; Chen, A.-Z. Continuous nanonization of lonidamine by modified-rapid expansion of supercritical solution process. *The Journal of Supercritical Fluids* **2018,** *133*, 486-493.
113. Yadav, D.; Kumar, N. Nanonization of curcumin by antisolvent precipitation: process development, characterization, freeze drying and stability performance. *International journal of pharmaceutics* **2014,** *477*, (1-2), 564-77.
114. Pan, S.; Takebe, G.; Suzuki, M.; Takamoto, H.; Ge, J.; Liu, C.; Hiramatsu, M. Nanonization of poorly water-soluble drug clobetasone butyrate by using femtosecond laser. *Optics Communications* **2014,** *313*, 152-156.
115. Chen, H.; Khemtong, C.; Yang, X.; Chang, X.; Gao, J. Nanonization strategies for poorly water-soluble drugs. *Drug discovery today* **2011,** *16*, (7-8), 354-60.
116. Sylvestre, J. P.; Tang, M. C.; Furtos, A.; Leclair, G.; Meunier, M.; Leroux, J. C. Nanonization of megestrol acetate by laser fragmentation in aqueous milieu. *Journal of controlled release : official journal of the Controlled Release Society* **2011,** *149*, (3), 273-80.
117. Kalepu, S.; Nekkanti, V. Improved delivery of poorly soluble compounds using nanoparticle technology: a review. *Drug delivery and translational research* **2016,** *6*, (3), 319-32.

Chapter 3:

Isolation and Molecular Characterization of Novel Glucarpidases: Enzymes to improve the antibody directed enzyme pro-drug therapy for cancer treatment

Alanod D AlQhatani [1,3], Fatma B Rashidi [1,2], Sara S Bashraheel[1,3], Shabnam Shaabani[3], Matthew R Groves[3], Alexander Dömling[3] and Sayed K Goda[1,2]

1 Anti-doping Lab-Qatar, Research Department, Protein Engineering unit, Doha, Qatar PO Box 27775

2 Cairo University, Faculty of Science, Giza, Egypt

3 Drug Design Group, Department of Pharmacy, University of Groningen, Antonius Deusinglaan 1, 9713 AV Groningen, The Netherlands

PLoS One. 2018 Apr 26;13(4):e0196254. doi: 10.1371/journal.pone.0196254.

Abstract

Repeated cycles of Antibody Directed Enzyme Pro-drug Therapy (ADEPT) and the use of glucarpidase in the detoxification of cytotoxic methotrexate (MTX) are highly desirable during cancer therapy but are hampered by the induced human antibody response to glucarpidase. Novel variants of glucarpidase (formal name: carboxypeptidase G2, CPG2) with epitopes not recognized by the immune system are likely to allow repeated cycles of ADEPT for effective cancer therapy.

Towards this aim, over two thousand soil samples were collected and screened for folate hydrolyzing bacteria using folate as the sole carbon and/or nitrogen source. The work led to the isolation and the characterization of three new glucarpidase producing strains, which were designated as: *Pseudomonas lubricans* strain SF168, *Stenotrophomonas* sp SA and *Xenophilus azovorans* SN213. The *CPG2* genes of *Xenophilus azovorans* SN213 (named *Xen CPG2*) and *Stenotrophomonas sp* SA (named *Sten CPG2*) were cloned and molecularly characterized. Both Xen CPG2 and Sten CPG2 share very close amino acid sequences (99%); we therefore, focused on the study of Xen CPG2.

Finally, we demonstrated that a polyclonal antibody raised against our new CPG2, Xen CPG2, does not react with the CPG2 from *Pseudomonas sp*. strain RS-16 (Ps CPG2) that are currently in clinical use. The two enzymes, therefore could potentially be used consecutively in the ADEPT protocol to minimize the effect of the human antibody response that hampers current treatment with Ps CPG2. The identified novel CPG2 in this study will, therefore, pave the way for safer antibody directed enzyme pro-drug therapy for cancer treatment.

Introduction

Cells use derivatives of folic acid as essential cofactors that are involved in the synthesis of DNA, RNA, proteins, and phospholipids [1, 2]. Mammals cannot synthesize folic acid and thus need to obtain it from their diets. Dietary folate is then converted to various tetrahydrofolate derivatives via a folate pathway.

There are three main enzymes in the folate pathway that are considered as targets for antifolate drugs: Dihydrofolate reductase (DHFR), thymidylate synthase (TS) and glycinamide ribonucleotide formyltransferase (GARFT). Inhibition of DHFR leads to a deficiency of dTMP which, in turn, results in deficient DNA synthesis, DNA breakdown and cell death. Similarly, inhibition of TS will lead to a deficiency in dTMP and cell death. Direct inhibition of GARFT leads to depletion of purine nucleotides, which also leads to cell death [3].

The synthetic folate analog Methotrexate (MTX) is an essential component of many chemotherapeutic regimes that are used for the treatment of patients with neoplastic diseases and has been in clinical use since 1948 [4]. The cytotoxic action of both MTX and its active metabolites is through the inhibition of DHFR, leading to the inhibition of DNA synthesis, repair, and cellular replication. Malignant cells are actively proliferating tissue and, in general, more sensitive to this cellular interference by MTX. Additionally, MTX has an immunomodulating effect and, hence, is used in the treatment of some other diseases such as rheumatoid arthritis, multiple sclerosis and psoriasis [5,

6].

There are also different analogs for MTT in various stages of preclinical and clinical development [7, 8]. Pemetrexed, a potent polyglutamate classic antifolate TS inhibitor formerly

called LY23154 [9], is an interesting new antifolate. The novel structure of Pemetrexed makes it different from other antifolates and, in contrast to MTX, Pemetrexed can inhibit several enzymes that are involved in the synthesis of purines and pyrimidines. Pemetrexed, similarly to MTX and other antifolates, has an unacceptable level of toxicity, creating major drawbacks in clinical use [10].

The ability to degrade antifolate drugs rapidly in vivo would have major clinical advantages. It would minimize toxicity, allowing a higher dose of antifolate compounds to be administered, potentially leading to a higher clinical efficacy. Enzymatic degradation to remove the excess of these drugs is considered a highly effective mechanism and can be achieved through the therapeutic use of glucarpidases [10].

Glucarpidase (also known as carboxypeptidase G2 or CPG2, Ps CPG2) is produced from *Variovorax paradoxus* (*Pseudomonas sp*. strain RS-16), it has no mammalian equivalent and is a zinc-dependent dimeric protein composed of two subunits of 41kDa [11, 12]. Glucarpidase has a relatively restricted substrate specificity and hydrolyzes the Cterminal glutamic acid residue of folic acid, poly-glutamyl derivatives of folic acid and folate analogs, including methotrexate and sub-fragments of folic acid, e.g., *p*aminobenzoyl glutamate [13] to yield pteroate derivatives. Glucarpidase converts methotrexate into a less toxic product, pteroate, leading to a rapid decrease in MTX levels in the serum in both animal models and in humans. Accordingly, the enzyme is a powerful rescue agent in patients receiving toxic doses of MTX, and glucarpidase treatment might be clinically attractive for MTX dose escalation studies [4].

Another important medical application of glucarpidase is its use in targeted cancer therapy. There are two major obstacles in systemic cancer therapies: a lack of tumor selectivity and drug resistance. Antibody Directed Enzyme Pro-drug Therapy (ADEPT) [14-18] is a therapy

that solves these two problems by generating a powerful agent in the vicinity of the tumor site. ADEPT has been successfully used in animal tumor models of human choriocarcinoma, as well as colonic and breast carcinoma. Glucarpidase is the most widely used enzyme in the ADEPT-based clinical trials [19-22]. The activity of glucarpidase can be exploited to cleave glutamic acid moieties of a variety of pro-drugs to release potent nitrogen mustards. Of these, 4-[(2-chloroethyl)(2-mesyloxyethyl)amino]benzoyl-L-glutamic acid (CMDA), is cleaved by Ps CPG2 to a cytotoxic agent, 4-[(2chloroethyl)(2-mesyloxyethyl)amino benzoic acid. Additionally, a variety of glucarpidaseantibody chemical conjugates targeting CPG2 activity to tumors have been evaluated [23]. However, treatment with glucarpidase results in a severe immune response following repeated use, limiting its therapeutic applicability. Thus, new CPG2s that differ in their immunogenicity relative to Ps CPG2 would increase the chances of success in repeated cycles of ADEPT by triggering a lower human antibody response.

To address this problem, we screened for new glucarpidase-producing bacteria from soils followed by the isolation, cloning and overexpression of their novel glucarpidase(s) for functional investigation and characterization.

Materials and Methods

Growth media, Enzymes, Chemicals and Antibodies

Folate minimal medium (FMM) contains per liter: 3g KH_2PO_4, 6g Na_2HPO_4 (anhydrous), 1g NaCl, 0.13g $MgSO_4.7H_2O$ and 0.01g $FeSO_4.7H_2O$. All salts were dissolved in distilled water, the pH of the solution was adjusted to 7.2 and the volume was adjusted to 1 liter with further distilled water prior to autoclaving at 121 °C at 15 p.s.i. for 15 min; filter-sterilized 0.5% (v/v)

folic acid (Sigma) was then added as the sole carbon source. The medium was solidified with 1.5% (w/v) Bacto-agar when necessary.

Enzymes for cloning and expression of the glucarpidase genes were purchased from Thermo Scientific, with the exception of *Sau*3AI, *Bam*H1 and a PCR master mix (2x) kit, which were purchased from Promega. Ni-NTA resin was purchased from Sigma. GelPilot 1 kb DNA ladder (100) was purchased from Thermo Scientific, Wizard® SV Gel and PCR Clean-Up System Kit were purchased from Promega. GeneJET Plasmid Miniprep Kit was obtained from Thermo Scientific. All other chemicals were of a high analytical grade.

The Mass spectroscopy (MS) analysis was carried out at the Toxicology and Multipurpose Labs, ADL-Qatar. Anti-Xen CPG2 Polyclonal Antibodies were produced by Eurogentec, Belgium, anti-Rabbit IgG (whole molecule)–Peroxidase antibody produced in goat (Sigma) Catalog No. 40545 was used as the secondary conjugated antibody. 6x His Epitope Tag Antibody (HIS. H8) (Thermo Scientific) Catalog No. MA1-21315 was used for detection of the purified 6 His tagged CPG2 and Polyclonal Rabbit Anti-Mouse Immunoglobulins/HRP (Dako) ref. code P0260 was used as secondary antibody.

Isolation of glucarpidase producing bacteria

Bacterial Sample Collection

More than two thousands soil samples were collected from the surface layer (0-15 cm) of thirty different agricultural sites in Egypt and Qatar. The samples were collected from private agricultural lands after the permission of the owners in both countries. The field studies did not involve endangered or protected species. These fields were previously cultivated with fruits and vegetables rich in folates such as oranges, asparagus and broccoli.

Isolation of folate hydrolyzing bacteria by an enrichment technique

After thorough mixing, preparations were incubated at 37°C for five days in 5 mL growth media to increase the probability of identifying folate-hydrolyzing bacteria. Subsequently, 1 mL was used to inoculate 50 mL autoclaved M9 minimal salt medium (MSM) [24] containing folate (0.5%) as the sole carbon source. Cultures were then incubated in an orbital shaker for three days at 37 °C and 160 rpm. After three days, cultures were allowed to settle for one hour, and 1 mL of each supernatant was used to inoculate another 9 mL of fresh enrichment medium prior to incubation for an additional five days under the same conditions. After three subsequent enrichments in the same media, cultures were serially diluted (10^{-4}-10^{-8}) and plated on the same media. Plates were incubated at 37 °C until bacterial colonies became visible. Selected isolates were stored at 4 °C.

Identification of isolated bacterial strains by *16S rDNA*

Three isolates - NS1 and FS3 and AS1 - were subsequently selected for further molecular characterization and identification by Vitek 2 Compact (GN kit) from bioMérieux, PCR amplification and partial sequence analysis of their *16S rRNA*genes.

A single colony of each strain was re-suspended in 1 mL of PCR-grade water and boiled for 10 min. The diluted lysate was used as a template for PCR amplification of *16S rDNA* using primer pair 27F (5' AGAGTTTGATCATGGCTCAG 3') and 1492R (5' CGGTTACCTTGTTACGACTT 3'). PCR was carried out using a GeneAmp PCR System 9700 (Applied Biosystems, Foster City, CA, USA) with the following amplification conditions: initial denaturation at 94 ^{o}C for 5 min, 35 cycles of 30 sec denaturation at 94 ^{o}C, 30 sec annealing at 60 ^{o}C and 1 min extension at 72 ^{o}C, followed by a final extension at 72 ^{o}C for 10 min. The PCR product was cloned into pGEM-T vector (Promega, UK) following the manufacturer's

instructions and transformed into *E. coli* JM109 competent cells. Following isolation of the transformants, plasmid DNA was purified and sequenced. *16S rDNA* sequence of each strain was submitted to a BLAST search of the NCBI (National Center for Biotechnology Information) GenBank database (www.blast.ddbj.nig.ac.jp/) to identify the organism.

Native Glucarpidase Activity Assay

Determination of glucarpidase activity in the three identified strains

Cells of strains NS1, FS3 and AS1 were sonicated in 0.1 M Tris-hydrochloride (pH 7.3) containing 0.2 mM $ZnSO_4$, and the soluble fraction tested for glucarpidase activity. Glucarpidase activity was determined using methotrexate (MTX) as the substrate by the modification of the method of McCullough [25]. 590 µl of 0.1 M Tris-HCl pH 7.3 containing 0.2 mM $ZnSO_4$ and 5 µl of MTX (0.45 mM) was equilibrated at 37^{o}C for 10 minutes, then the total protein extract of each strain (50 µg/mL) was added and incubated at 37^{o}C. Samples were taken at 10 min intervals, and the decrease in absorbance at 320 nm was measured using a NANODROP 1000 spectrophotometer (Thermo Scientific). The same protocol was performed to analyze the activity of the pure recombinant CPG2 using 3 µg/mL protein. The obtained data was plotted using GraphPad Prism6.

Effect of zinc ion on glucarpidase activity

A 1-mL reaction cuvette containing 0.1 mL of 0.45 mM MTX and 0.9 mL of 0.1 M Tris-hydrochloride (pH 7.3) in the presence of 0.2 mM $ZnSO_4$ was equilibrated at 37 °C. Protein extract, 20 µl of 1 mg/mL, was added and the decrease in absorbance at 320 nm was measured with a Pye-Unicam SP1800 double-beam spectrophotometer. The same experiment also was done in the presence of 0.5 mM EDTA.

New *Xen* and *Sten CPG2* gene(s) Isolation and Cloning into vector pET28a

Genomic DNA library construction and screening

Genomic DNA from *Xenophilus sp.* SN213 and *Stenotrophomonas sp* AS was isolated using a DNA extraction kit (Thermo Scientific), partially digested by *Sau*3AI, and fragments in the range of 2-4 kb were isolated by gel electrophoresis. The resulting fragments were cloned into *Bam*H1-digested pET28a, (pET28a has been used successfully in our laboratory for cloning and overexpression of many genes) and then transformed into competent cells of *E. coli* BL21 (DE3) RIL. The transformants were screened on LB-Kan-folate-IPTG plates (containing 32 μg/mL kanamycin, 0.5% (v/v) folate and 0.1% IPTG). Positive clones of yellow color were picked and plasmids isolated as described above.

Sequence analysis, isolation, and cloning of the Xen CPG2 and Sten CPG2

The selected constructs were sequenced using universal primers T7 promoter and terminator. ORF searches and sequence analysis were performed using the DNASTAR program and the obtained sequences were subjected to homology search using the National Centre for Biotechnological Information (NCBI) on-line program BLAST. Sequence comparison was performed using pairwise and multiple sequence alignment program CLUSTAL W [26, 27]. Primers were designed based on the ORF of the two new CPG2, and unique restriction enzymes (*Nde*I/*Hind*III) were introduced to facilitate the cloning of the gene(s).

CPG2-Fwd 5' ACC GGA TCC CAT ATG CAG AAG CGC GAC AAC GTG CTG TTC C 3' (the underlined sequence is *Nde*I site).

CPG2-Rev 5' CCT AAG CTT TCA CTT GCC GGC GCC CAG ATC CAT G 3' (the underlined sequence is *Hind*III site).

The PCR program used for amplification was 94 °C for 5 min (1 cycle), followed by 35 cycles of 94 °C denaturation for 1 min, 64 °C annealing for 1 min and 72 °C extension for 1.5 min, followed by a final extension at 72 °C for 10 min (1 cycle). The purified PCR product was digested with *Nde*I and *Hind*III and ligated into similarly digested, dephosphorylated pure pET28a DNA using T4 DNA ligase.

The ligated mixtures were transformed into chemically competent *E. coli* and spread over LB-agar plates supplemented with 32 μg/mL kanamycin and incubated at 37 °C overnight. Plasmid DNA was extracted from randomly selected colonies, following the manufacturer's (Thermo Scientific) recommended protocol. Miniplasmid preparations were checked for the presence of the gene of interest by double restriction digestion reaction using *Nde*I/*Hind*III. Finally, the constructs of both new *CPG2*, *Xen CPG2* and *Sten CPG2* were confirmed by DNA sequencing using universal T7 promoter and terminator primers.

Xen CPG2 Protein Expression and Recombinant Protein Purification

Protein expression

The pET28a-Xen CPG2 was transformed into the expression host *E. coli* BL21(DE3)RIL according to the manufacturer's instructions (Stratagene) and transformants were selected on LB-agar plates supplemented with Kanamycin (Kan) and Chloramphenicol (Cam) at final

concentration of 32 µg/mL each at 37 ºC. A single colony was incubated in 10 mL LB medium supplemented with the required antibiotics at 37 °C. 50 mL of fresh autoclaved LB-broth supplemented by the corresponding antibiotics was inoculated with 250 µl of the overnight culture. The culture was incubated at 37 ºC in an incubator shaker until the optical density at 600nm reached 0.5-0.6. Induction of recombinant CPG2 was initiated by the addition of isopropyl-β-D-thiogalactopyranoside (IPTG) at a final concentration of 1 mM then incubated for further four hours at 37 °C with shaking at 200 rpm. Cells were collected by centrifugation at 4000rpm for 20 min at 4 ºC. Cell pellets were re-suspended in 20 mM Tris buffer pH 7.5 containing 50 mM NaCl and then were disrupted by sonication on ice, 5 cycles of 30 sec sonication pulses followed by I min rest. The soluble fraction was separated by centrifugation at 14,000 rpm for 20 min at 4 °C. The soluble and insoluble fractions were mixed with 2X sample buffer and boiled for 10 minutes at 95 °C, then applied to SDS-PAGE analysis. Protein expression was performed, where the induction step with IPTG at 20 °C was carried out identically to assess the effect of temperature to improve soluble protein expression. The CPG2 expressed in the soluble form was used for all our studies. We did not carry out refolding of the inclusion bodies.

Ni-NTA Purification

To facilitate the purification of Xen CPG2, the gene was sub-cloned into the *Nde*I/*Hind*III sites of pET-28a, creating a gene that encoded an *N*-terminal His_6 tag. The soluble protein was subjected to purification by Ni^{2+} affinity chromatography using NiNTA resin. About 1 mL of the resin was washed with distilled water and activated by binding and washing buffer A (20 mM Tris pH 8, 50 mM NaCl, 5 mM BME, and 20 mM imidazole), then the total soluble protein was combined with the activated resin and gently agitated for 20 min at 4 °C to allow the protein to

bind to the column resin. The resin was separated by gravity, the flow-through was collected, and the resin was washed 3 times with buffer A. The target protein (bound to the resin) was collected by adding ice-

cold elution buffer B (20 mM Tris pH 8, 50 mM NaCl, 5 mM BME and 400 mM imidazole). The eluted protein was dialyzed against 100 mM Tris-HCl pH 7.3 containing 0.2 mM $ZnSO_4$. All fractions of the protein purification were analyzed by SDS-PAGE analysis. Hydrolytic activity of the pure recombinant glucarpidase (at conc. 3 µg/mL) was assayed spectrophotometrically using MTX (substrate) as described above.

Pseudomonas sp. strain RS-16, Ps CPG2 Protein expression and Purification

A synthetic gene for *Pseudomonas* CPG2 codon-optimized for maximum expression in *E. coli* B21(DE)3RIL[28], was cloned, overexpressed and purified following the same procedures used for Xen CPG2.

MS of folate degradation by Xen and Ps CPG2

The insoluble materials formed from folate degradation by Xen CPG2 or Ps CPG2 containing bacteria were collected and dissolved in NaOH pH 9. 3 µl aliquot of each sample was injected onto a 2.1 x 50 mm Acquity BEH C18 (1.7 um particle size) UPLC column using the following eluents: A= water + 0.1% formic acid and B= acetonitrile + 0.1 % formic acid. Eluent flow was 300 µl/min operating in an isocratic mode consisting of 7% B. The column was thermostatted at 40 ^{o}C. The UHPLC was a Dionex UniMate 3000 Binary RSLC (Thermo Fisher Scientific).

Eluent from the UPLC column was passed to a HESI II electrospray ion source operating in the positive ion mode. Data were acquired on a QExactive Classic HRAM orbitrap mass spectrometer (Thermo Fisher Scientific) in full scan high resolution (70,000 mass resolution) accurate mass mode (HRAM). Accurate mass results were acquired with external calibration. Protonated parent ion current profiles for the targeted parent masses were extracted with a mass tolerance of +/- 5 ppm. Background subtracted spectra showed protonated parent masses with a mass accuracy of better than 3 ppm (external calibration).

Kinetics Properties of Xen CPG2 and Ps CPG2

Methotrexate was used for determination of the Michaelis constant (K_m) and the rate of reaction (V_{max}). Both purified enzymes, Xen CPG2 and Ps CPG2 (2.12 µg/mL), were assayed at various methotrexate concentration (0.03 up to 0.42 mM) in 0.1 M TrisHCl pH 7.3 and 0.2 mM $ZnSO_4$ using Nunc 96 plates with UV transparent flat bottom wells. All reactions were carried out at 37 °C for 2 min and the decrease in absorbance at 320 nm was determined using Infinite M200 PRO NanoQuant Plate Reader (TECAN).

Apparent K_m, V_{max} and K_{cat} values of each protein were determined by fitting to the Michaelis-Menten equation using GraphPad PRISM 6 software.

One unit of the enzyme represents the hydrolysis of 1mM of MTX per min at 37 °C. The enzyme activity per ml of extract was calculated by using an extinction coefficient for MTX of 8,300.

Biophysical Characterization of Xen CPG2 by Circular Dichroism

Sample preparation

Pure Xen CPG2 was re-dialyzed against sterile milli-Q water; then the protein was centrifuged 30 min. at 4 °C to get rid of any aggregates. The protein concentration was measured using Nanodrop 2000 spectrophotometer (Thermo Scientific) and adjusted to about 0.5 mg/mL with water. The extinction coefficient for glucarpidase was taken as ε = 23380 M^{-1} cm^{-1} for Xen CPG2 and 24870 M^{-1} cm^{-1} for Ps CPG2.

Circular dichroism (CD)

All CD experiments were carried out at 20 °C using a Chirascan™ Plus CD Spectrometer (Applied Photophysics). Protein concentrations of 0.5 mg/mL to 0.6 mg/mL were measured in a SUPRASIL Quartz demountable rectangular (Hellma®) cuvette of 0.2 mm light-path length (sample volume ~60 µl).The used CD parameters were: bandwidth 1 nm and a scan time per point of 0.5 s. Four average and smoothed scans per sample were measured using the Chirascan analysis software. Additionally, an averaged buffer (water) CD signal over the same wavelength region was determined and used as a buffer baseline, and each averaged CD spectrum was corrected for the buffer baseline by subtraction. The resulting molar ellipticity [θ] was calculated per spectrum by applying the molar protein concentration [M] and the pathlength of the used cuvette (0.02 cm) and following the equation:

$$\text{Molar Ellipticity } [\Theta] = (100 \times \theta) \,/\, (Conc \times Pathlength)$$

Where θ is the ellipticity measured in degrees, Conc. is concentration measured in mole/L, the pathlength is measured in cm, and molar ellipticity has units of $deg.cm^2.dmol^{-1}$.

CD spectra deconvolution method

Protein secondary structure was estimated by CD data deconvolution analysis using the CDNN (version 2.1) software tool to deconvolute the CD data spectra in the far UV spectral region. Deconvolution of the CD data was done in the 190–260 nm spectral region. In the deconvolution calculations, the number of amino acids/residues was taken for Xen CPG2 as 392 AAs, with a molecular weight of 41.76148 kDa and for Ps CPG2; 394 AAs, with 41.91174, protein conc. (0.58 mg/mL) and 0.02 cm light-pathlength of the cuvette was used. Four repeat scans were measured per sample and then averaged.

Homology modeling of Xen CPG2

Homology modeling was performed using SWISS-MODEL, a fully automated protein structure homology-modeling server, accessible via the ExPASy web server, or from the program DeepView (Swiss Pdb-Viewer) [29]. Briefly, we searched for templates matching our target Azo CPG2 sequence. The closest enzyme, carboxypeptidase G2 (PDB ID 1CG2) with a sequence homology of 94% was used to build a model. The model quality evaluation was performed using GMQE (Global Model Quality Estimation). The model was visualized using PyMol.

Immunoblotting of Xen CPG2 and Ps CPG2 using Anti His and Anti Xen CPG2 antibodies

Xen CPG2 or Ps CPG2 were separated by SDS-PAGE and transferred to PVDF membranes overnight at 30 V using a Bio-Rad Mini-Trans-Blot tank and Tris-glycine buffer (25 mM Tris, 192 mM glycine, pH 8.3). For detection of each CPG2 protein, a polyclonal anti-$(His)_6$ antibody (Sigma) or a polyclonal anti CPG2 were used separately as the primary antibody (1:3000 dilution), with HRP-conjugated ECL anti-rabbit antibody (GE Healthcare, 1:10,000 dilution) used as the secondary antibody. Detection was performed using ECL chemiluminescent

detection reagent as described by the supplier (GE Healthcare). In addition, dot blots were carried out at different protein concentrations (0.05, 0.1, and 0.2 mg/mL) and at different anti Xen CPG2 dilutions (1:20 000, 1:10 000 and 1:3000).

Results

Isolation and Characterization of Glucarpidase Producing Bacterial Strains

Seven folate hydrolyzing bacterial strains (NS1-3, FS1-3, and AS1) were successfully isolated using the described enrichment technique. A clear halo appeared around colonies capable of hydrolyzing folate, which indicates the presence of glucarpidase activity in the isolated bacteria. Due to the larger halos formed around NS1, FS3 and AS1, these isolates were chosen for further studies.

The screened isolates NS1, FS3, and AS1 showed growth after two days on minimum folate media (FMM) agar-plate and showed complete degradation of the folate after 5 days (data not shown).

Fig 1A & B shows the colorless areas around the growing bacterial strain FS3 as brightblue fluorescence under UV light resulting from the accumulation of lumazine-6carboxylic acid, which was confirmed by analyzing cell extracts by gel electrophoresis (Fig 1C).

We also confirmed the hydrolysis of folate by glucarpidase containing strains, and the production of DAMPA (2, 4-diamino-N-10-methyl pteroic acid) the insoluble product by mass-

spectroscopy (MS). (Fig 2a) Shows a mass of 313.1 m/z, corresponding to the calculated mass of DAMPA H^+ from one strain. Similar results were obtained from the recombinant *E. coli* containing glucarpid

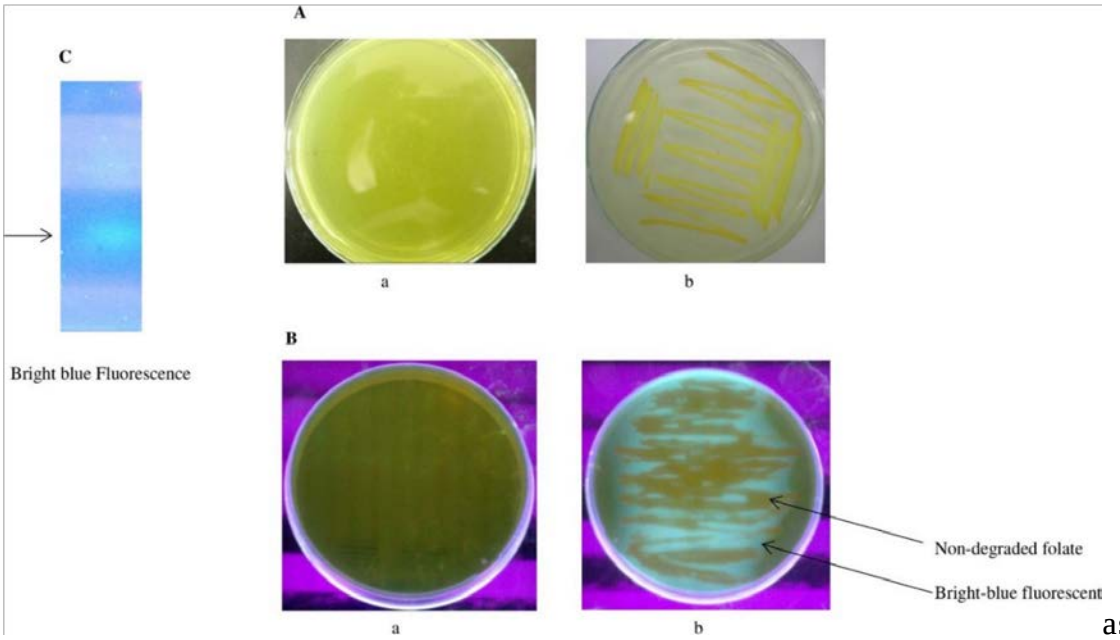

ase(s) (Xen and Ps CPG2) (Fig 2b-c).

Fig 1. Growth of glucarpidase producing bacteria. 1A. Bacterial growth on folate as the only carbon source LB/agar plate. (a) Before the bacterial growth and (b) the bacterial growth after several days.**1B**. A bright-blue fluorescence under U.V. light. (a) The Folate media under UV light while (b) is the growing bacteria on folate plate showing the bright-blue fluorescence of lumazine-6-carboxylic acid resulting from folate hydrolysis by the growing strain. **1C**. 1% Agarose gel electrophoresis of the cell extract of one isolate showing bright blue fluorescence (lumazine6-carboxylic acid) under U.V. light, resulting from folate degradation by the isolated strain.

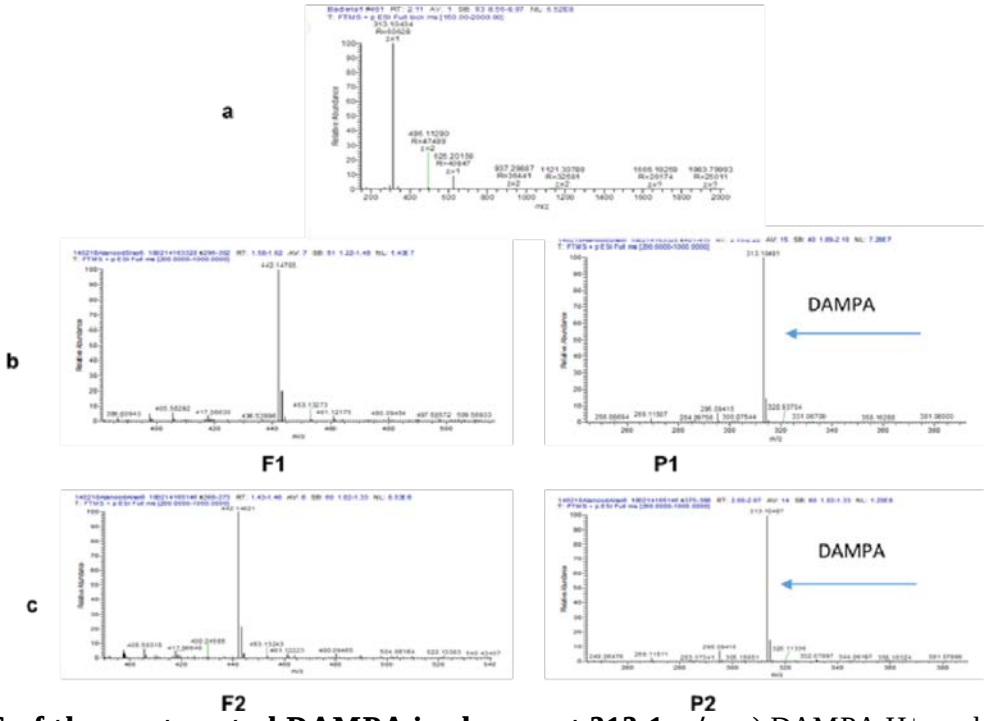

Fig 2. MS of the protonated DAMPA is shown at 313.1m/z. a) DAMPA H^+ peak is the product of folate hydrolysis by the isolated strain. b and c) P1, P2 are DMPA H^+ produced by recombinant CPG2 (new and Ps CPG2) and F1, F2 are the folate before hydrolysis

Microbiological and Isolates Identification: PCR Amplification and Sequence Analysis of *16S rRNA* Gene for

Results from microbiological identification of the isolate(s) using Vitek 2 Compact and DNA sequence similarity analysis of the PCR products from the *16S rRNA* genes of the NS1, AS1, and FS3 isolates indicated that the 1317 bp of *16S rRNA* gene of NS1 is most closely related to *Xenophilus azovorans* strain KF46F (98%) and was identified as *Xenophilus azovorans* SN213. The results of the sequence similarity analysis indicated that the 1254 bp of *16S rRNA* gene of FS3 was identical to that of *Pseudomonas lubricans* (100%) and *Pseudomonas sp.* PASS-camb (99%). This analysis indicated that strain FS3 belonged to *Pseudomonas* species and was identified as *Pseudomonas lubricans* strain SF168. The AS1 strain is 100% identical to

Stenotrophomonas sp. AB1 and was named as *Stenotrophomonas sp.* AS. To establish the phylogenetic position of the isolated strain(s), their 16s rRNA sequence(s) were compared with other sequences of their closely related species retrieved from the GenBank database. Their resulting phylogenetic tree based on the Fast Minimum Evolution Method is shown in supplementary data.

GenBank Accession Numbers

The sequence and the name of the identified strains were then deposited to the NCBI GenBank, (*Pseudomonas lubricans* Strain SF168, accession number FJ600733 and *Xenophilus azovorans* SN213, Accession number EU650684).

Zinc Dependence of the Native Glucarpidase Activity

The data in Fig 3 indicate that the total protein extract of *Pseudomonas lubricans* strain SF168 and *Xenophilus azovorans* SN213 showed no glucarpidase activity towards the substrate methotrexate in the absence of Zn^{2+} ions. However, when Zn^{2+} was added to the assay mixture, glucarpidase activity could be measured. We carried out the same experiment in the presence of 10 mM EDTA. No enzyme activity was detected in the presence of EDTA.

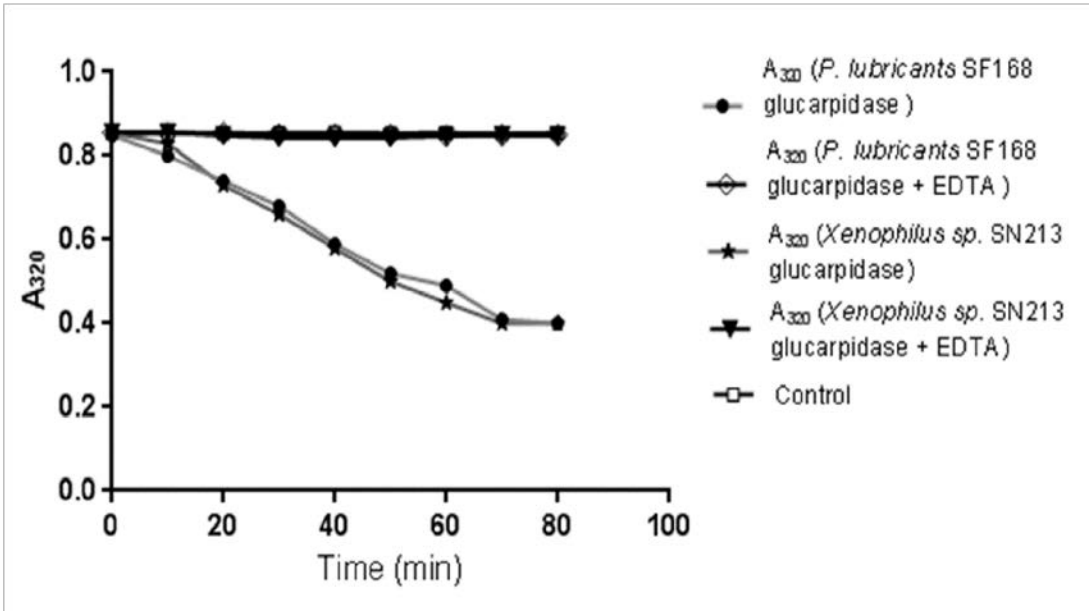

Fig 3. Glucarpidase activity in the total soluble protein of the two novel glucarpidase producing bacteria. MTX substrate solution and total soluble protein of *Pseudomonas lubricants* strain SF168 in presence of Zn^{2+} (filled ball) and in presence of Zn^{2+} and EDTA (diamond). MTX substrate solution and total soluble protein from *Xenophilus* sp. SN213 in the presence of Zn^{2+} (star), and in the presence of Zn^{2+} and EDTA (filled triangle), and control of MTX and enzyme buffer (square) are shown. The data in this figure indicates that both strains (*Pseudomonas lubricans* strain SF168 and *Xenophilus* sp. SN213) show CPG2 activity through methotrexate hydrolysis.

Cloning and Overexpression of the New Glucarpidases from *Xenophilus azovorans* SN213 and *Stenotrophomonas sp.* SA

To clone the *CPG2* genes from the newly isolated strains, chromosomal DNA libraries from both isolated strains were prepared and screened for CPG2 producing colonies using media where folate is the only carbon source. The resultant recombinant plasmids were designated pCPGxen16 and pCPGsten8, for CPG2 from *Xenophilus azovorans* SN213 and *Stenotrophomonas sp.* SA respectively. Determination of the nucleotide sequence of each fragment in both plasmids revealed the amino acid sequences of each recombinant protein. In

each case, the identified open reading frame is 1,176 nucleotides long and encodes proteins with 392 amino acids.

Partial nucleotides and amino acid sequence data for CPGxen16 appear in the DDBJ/ GenBank database under accession numbers JX192958 and AGI21725, respectively.

The calculated molecular mass of the deduced amino acid sequence of the CPGxen16 was 41761.4 Da, which is in close agreement with that of the native enzyme [12]. A search of the protein database using the program BLAST revealed that the deduced amino acid sequence of the Xen CPG2 exhibits a high identity (94%) to that of CPG2 from the strain of *Pseudomonas sp*. Strain RS-16 [12, 30]. CPG2sten8 exhibits 99% similarity with CPGxen16. Their amino acid sequence alignment is shown in Fig 4.

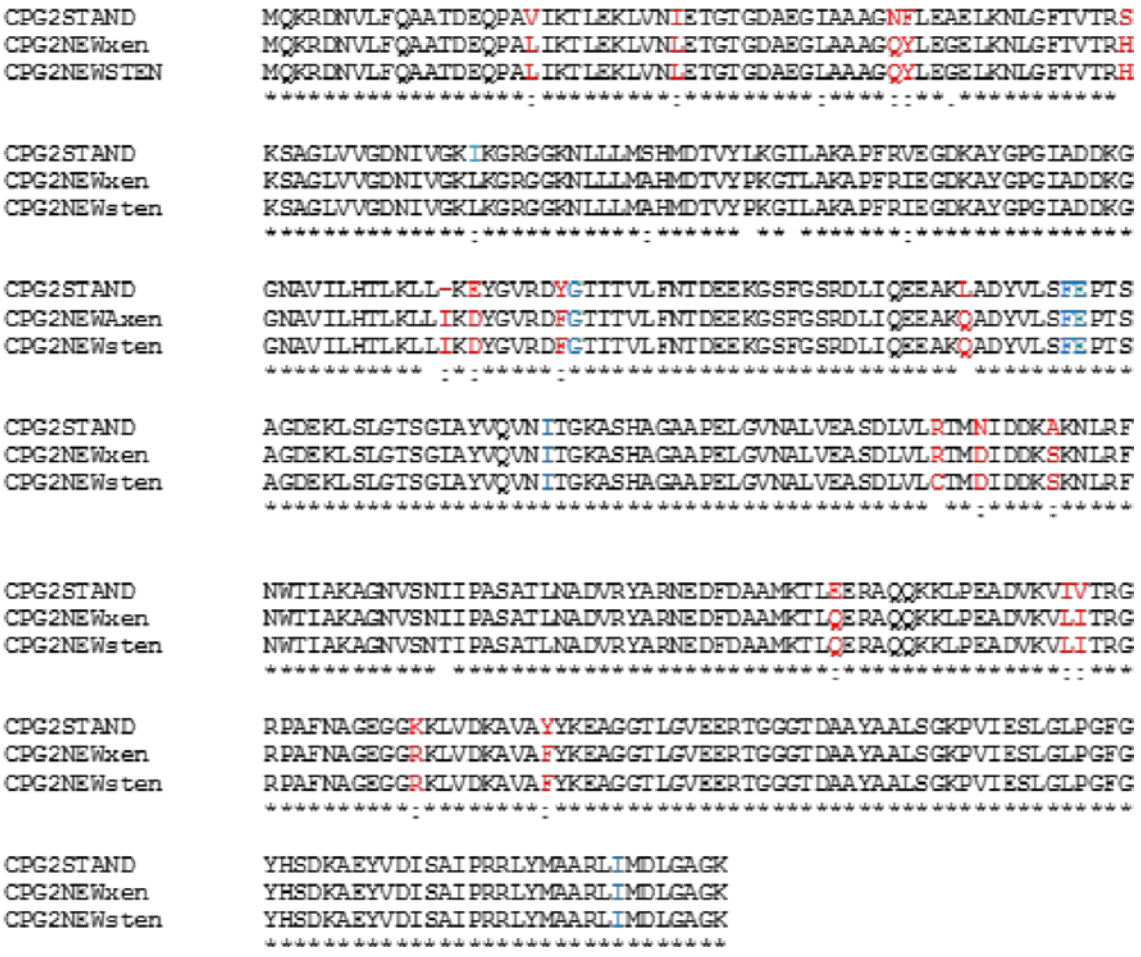

Fig 4. Amino acids sequence alignment of glucarpidase genes: the uppermost sequence encodes the glucarpidase from *Pseudomonas sp*. Strain RS-16 (12), the lower sequences encode the new glucarpidases isolated from *Xenophilus azovorans SN213* and *Stenotrophomonas sp SA*, respectively (this work). Amino acid differences between the sequences are highlighted in red. Amino acids in blue are involved in the active site of the enzyme where two zinc ions and a bridging water molecule binds (30).

SDS-PAGE analysis showed that a high level of protein expression (160 mg/L) was observed (Fig 5a). The CPG2s of both new strains were overexpressed but about 80% of the protein was present as inclusion bodies. The expression of soluble CPG2 did not improve by varying the IPTG concentration (data not shown). However, when cells were induced at 20 °C for overnight, we found that soluble CPG2 expression was significantly increased (80 mg/L) (Fig 5b). The molecular weight of over-expressed glucarpidase was about 41 kDa, as determined by

SDS-PAGE, and is consistent with the calculated molecular mass from the deduced amino acid sequence of the isolated gene.

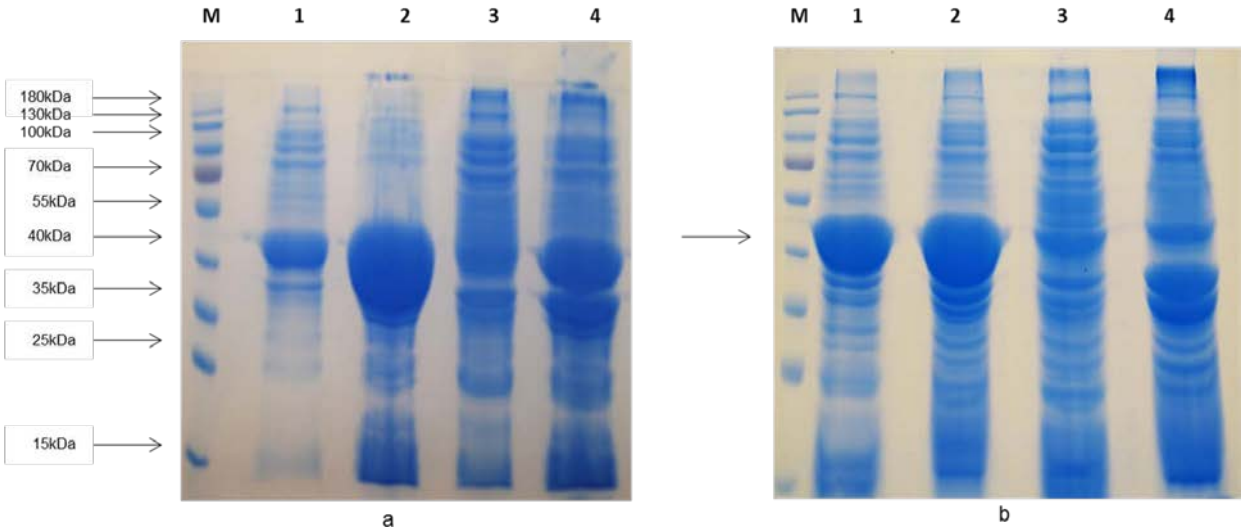

Fig 5. CPG2 Protein expression of the gene isolated from *Xenophilus azovorans* SN213. **a**. Coomassie blue staining of 10% SDS-PAGE of *E. coli* BL21(DE3)RIL-CPG2 protein expression at 37 °C of the gene isolated from *Xenophilus azovorans* SN213. M is the PageRuler Prestained Protein Ladder (10 to 180 kDa), lanes 1 and 2 are the induced soluble and insoluble fractions respectively, and lanes 3 and 4 are the uninduced soluble and insoluble fractions respectively. **b**. Protein expression at 20 °C of the gene isolated from *Xenophilus azovorans*. SN213. M is the prestained protein ladder, lanes 1 and 2 are the induced soluble and insoluble fractions respectively, and lanes 3 and 4 are the uninduced soluble and insoluble fractions respectively.

Protein Purification and Activity Assay of the Newly Isolated Glucarpidase, Xen CPG2

The isolated recombinant Xen CPG2 showed high glucarpidase activity toward folate degradation on agar plates (Fig 6) in comparison to the Ps CPG2 recombinant enzyme in a negative control (empty vector). Therefore, we isolated the recombinant glucarpidases to test their activity *in vitro*.

We found that single step purification by Ni-affinity chromatography was sufficient to obtain highly pure Xen CPG2 (Fig 7a).

Fig 6. Recombinant CPG2 activity on folate agar plate. The activity of the isolated recombinant CPG2 in comparison to Ps CPG2 of *Pseudomonas sp* strain RS-16 and in the presence of negative control (vector only) on LB/KAN/CAM/IPTG/Folate in the presence of 0.2 mM $ZnSO_4$.

We also optimized the overexpression of the Ps CPG2 and purified the recombinant protein (Fig7b).

The activity of the isolated enzyme on methotrexate was studied as shown in (Fig 8) and indicates that the isolated glucarpidases are metalloenzymes and require Zn^{2+} for activity.

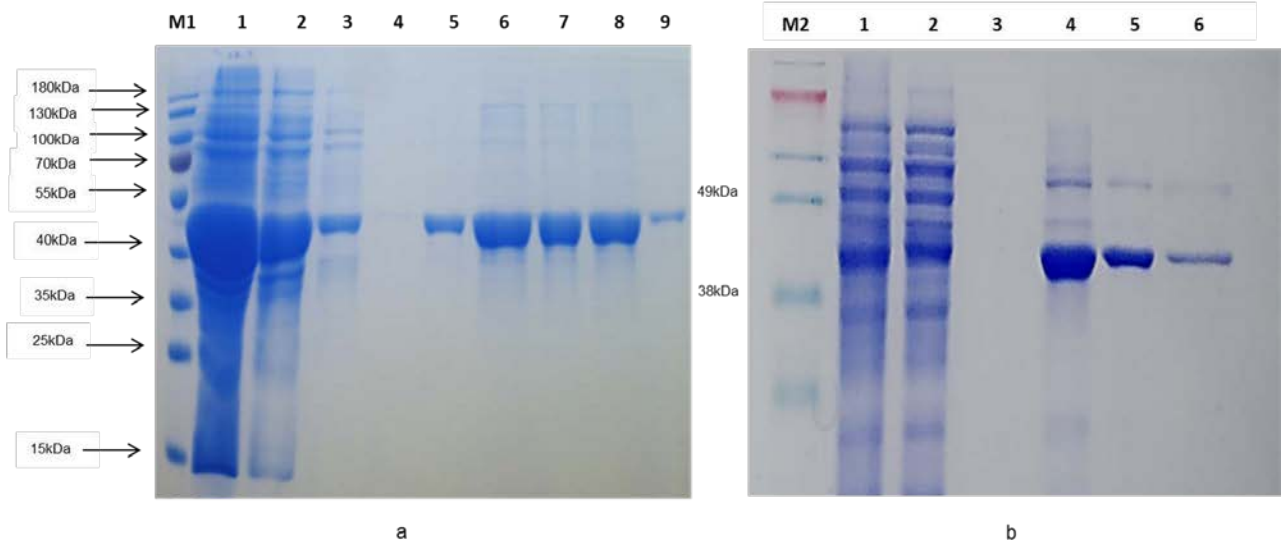

Fig 7. Purification of recombinant new glucarpidase relative to Ps CPG2: Coomassie blue staining of a 10% SDS-PAGE gel. M; Size markers in kiloDaltons; M1 is PageRuler Prestained Protein

Ladder (10 to 180 kDa) and M2 is SeeBlue Plus prestained standard (3 to 198 kDa). **a)** Xen CPG2 purification; lane 1 is total soluble fraction of glucarpidase after centrifugation; 2, flow through; 3–4, wash 1 and wash 5; 5-9, eluted fractions from the Ni-NTA column with 400 mM imidazole. **b)** Ps CPG2 purification; lanes 1, 2, 3 are total, flow through, wash, lanes 4-6 are elution fractions.

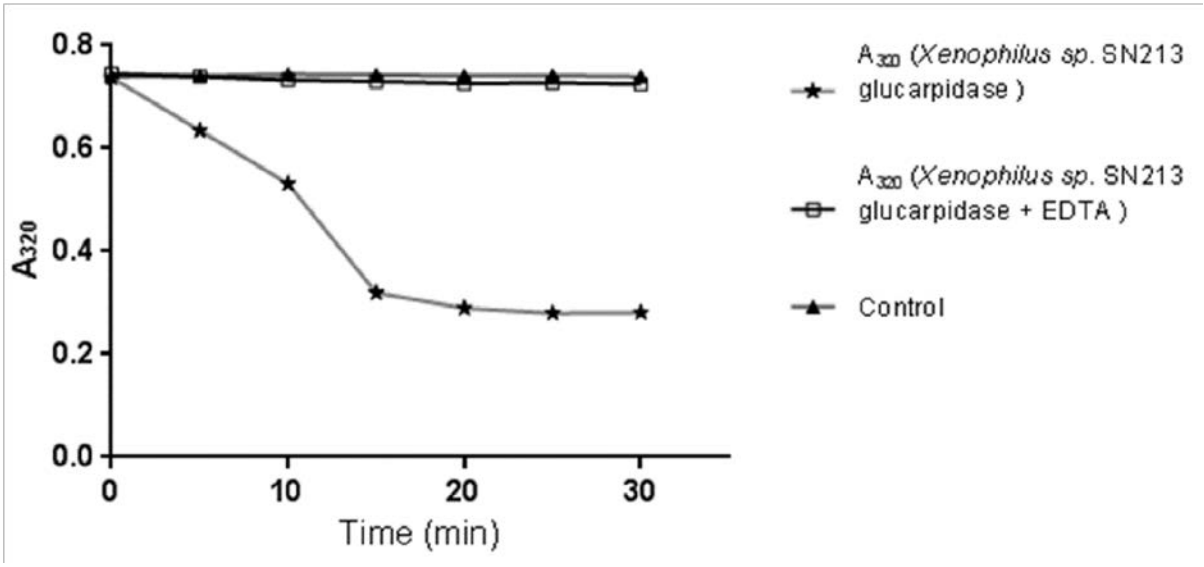

Fig 8. Carboxypeptidase G2 activity is Zn^{2+} dependent. MTX substrate solution and pure CPG2 in the presence of Zn^{2+} (star), control reaction of MTX substrate solution and buffer (filled triangle) and MTX substrate solution and pure CPG2 in the presence of Zn^{2+} and 10 mM EDTA (square) are shown. New isolated CPG2 is Zn^{2+} dependent.

Kinetic Properties of Xen CPG2 and Ps CPG2

Kinetic studies of the enzymes, Xen CPG2 and Ps CPG2 were carried out using a range of methotrexate substrate concentrations (0.03 - 0.42 mM) under standard assay conditions. Using the Lineweaver–Burk plot, the K_m and V_{max} values of 50.5 µM and 24.3 µM/min for Xen CPG2 and 171.7 µM and 52.6 µM/min for Ps CPG2 were obtained. The K_{cat} for both enzymes, Xen CPG2 and Ps CPG2 are 11.49 S^{-1} and 24.83 S^{-1}. In addition, the specific activities of Xen CPG2 and Ps CPG2 were determined to be 28.84 nmol/min/mg and 62.6 nmol/min/mg, respectively.

Circular dichroism (CD) spectral analysis

The changes in the obtained CD magnitude (i.e. chirality of the signal, either positive or negative). In addition, the characteristic shape of the detected far UV CD signals for Ps CPG2 and Xen CPG2 (Fig 9) give insight about the extent to which they differed in the individual proteins' inter-molecular secondary structure. CD deconvolution results displaying the relative percentage of each secondary structure are shown in the attached table in Figure 9.

The percentage change of the four main secondary structures calculated by CDNN deconvolution analysis of the spectra is shown in Fig 9, that consists of 69.3% alpha helix, 1.2% antiparallel, 3.2% parallel, 11.3% beta turn, and 14.9% random coil for Xen CPG2, and 34.2% helix, 8.5% antiparallel, 8.5% parallel, 16.6% beta turn, and 32.3% random coil for Ps CPG2.

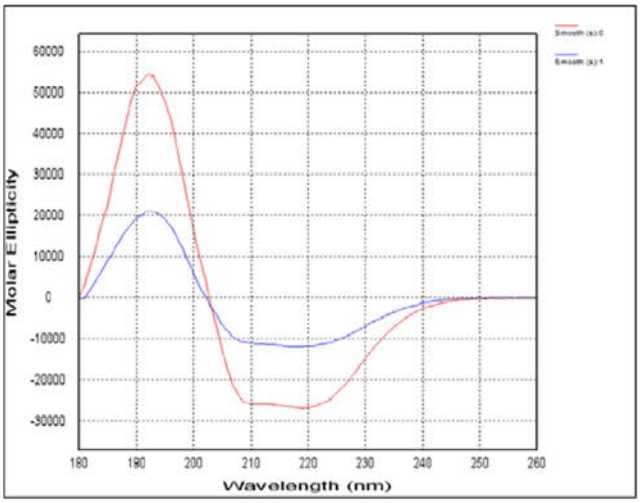

A

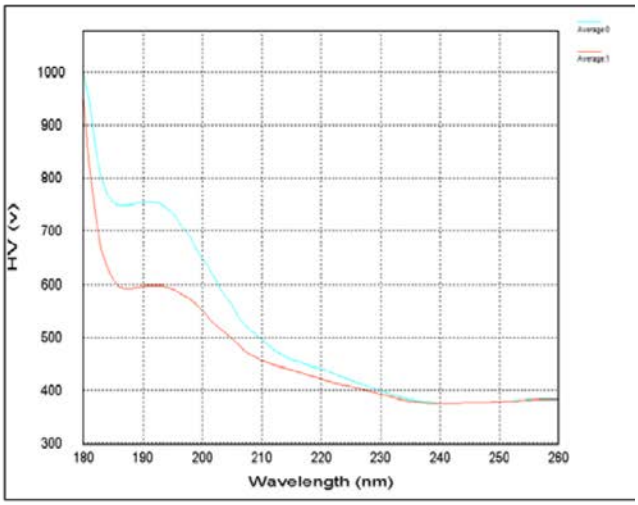

B

	Helix	Antiparallel	parallel	Beta Turn	Random Coil	Total
Xen CPG2	69.3%	1.2%	3.2%	11.3%	14.9%	99.9%
Ps CPG2	34.2%	8.5%	8.5%	16.6%	32.3%	100%

Fig 9. CD spectra and High voltage of Xen CPG2 and Ps CPG2. A) Combined CD spectra data of Xen CPG2 and Ps CPG2 in molar ellipticity relative the wavelength in far UV region, the spectra obtained by dragging their spectral data over each other, where smooth 0 is molar ellipticity of Xen CPG2 and smooth 1 is for CD spectra of Ps CPG2. All Spectral data are corrected for the baseline buffer, B) represents the combined High voltage (HV) for both enzymes where average 0 is Xen CPG2 and average 1 is Ps CPG2. Also the table shows the calculated protein secondary structure of Xen CPG2 and Ps CPG2 by CDNN deconvolution analysis using their CD spectral data.

Homology Modeling of Xen CPG2

Homology modeling was performed to produce the X ray structure of the Xen CPG2 and the alignment with the Ps CPG2 is shown in Figure 10.

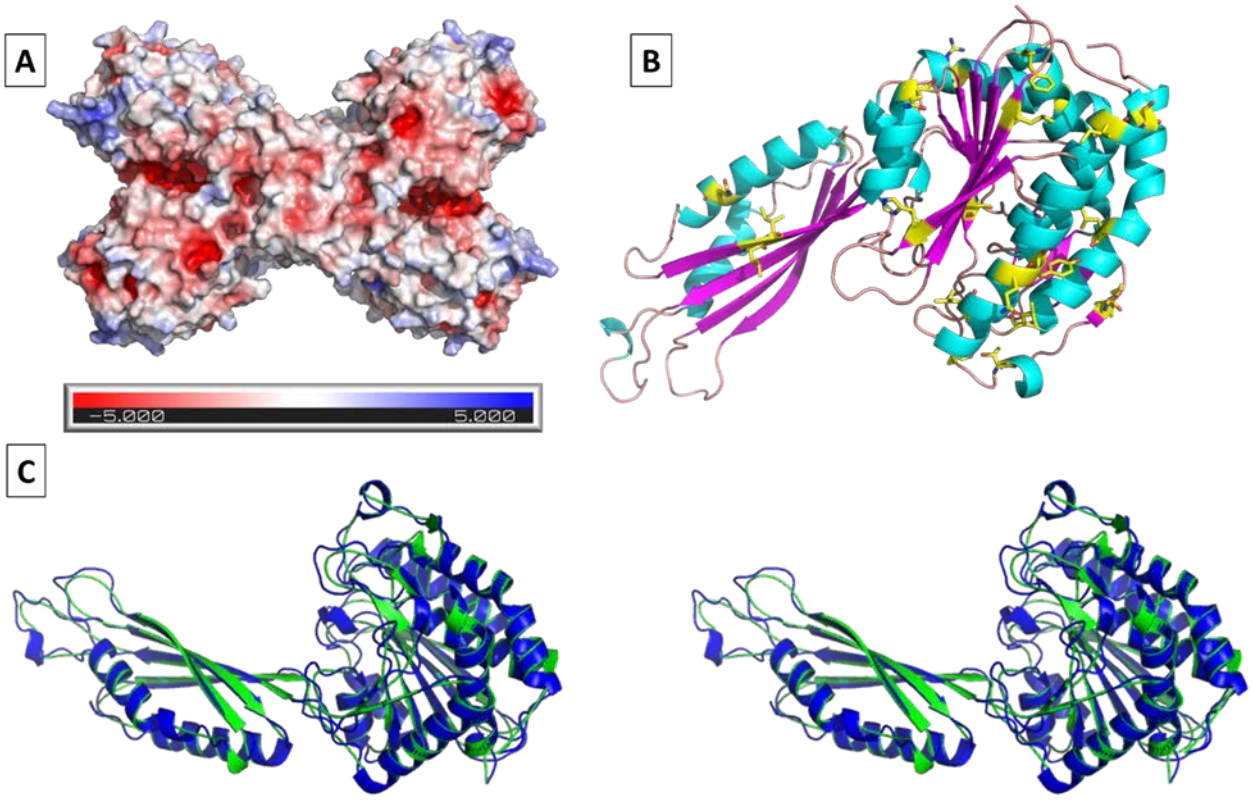

Fig 10. Homology modeling of Xen CPG2. **A.** Electrostatic surface presentation of the Xen CPG2 tetramer. Positive and negative charges are shown in blue and red, respectively. **B.** Color rendering of a Xen CPG2 monomer. Helix in cyan, b-sheet in pink, loops in brown and amino acids which differ from the model carboxypeptidase G2 are shown as yellow sticks. Rendering was performed using PyMol. **C.** Stereoview of the alignment of CPG2 Pseudomonas sp. Strain RS-16 (blue cartoon, PDB ID 1CG2) with the model of Xen CPG2 (green cartoon, RMS = 0.084 (374 to 374 atoms)).

Anti Xen CPG2 Polyclonal Antibody Response to Ps CPG2

To test whether Ps CPG2, which is in current clinical use, was recognized by the antibody raised against the new CPG2 (Xen CPG2), we carried out dot blots and western blots on both enzymes (at different protein concentrations; 0.05, 0.1, and 0.2 mg/mL) using the Anti His tag

antibody (positive control) and the Anti Xen CPG2 antibody as primary antibodies. In both cases (dot blot and Western Blot), the Anti His antibody bound to both CPG2s whereas the Anti Xen CPG2 bound strongly to the new CPG2 but showed little or no binding to the Ps CPG2 (Fig 11).

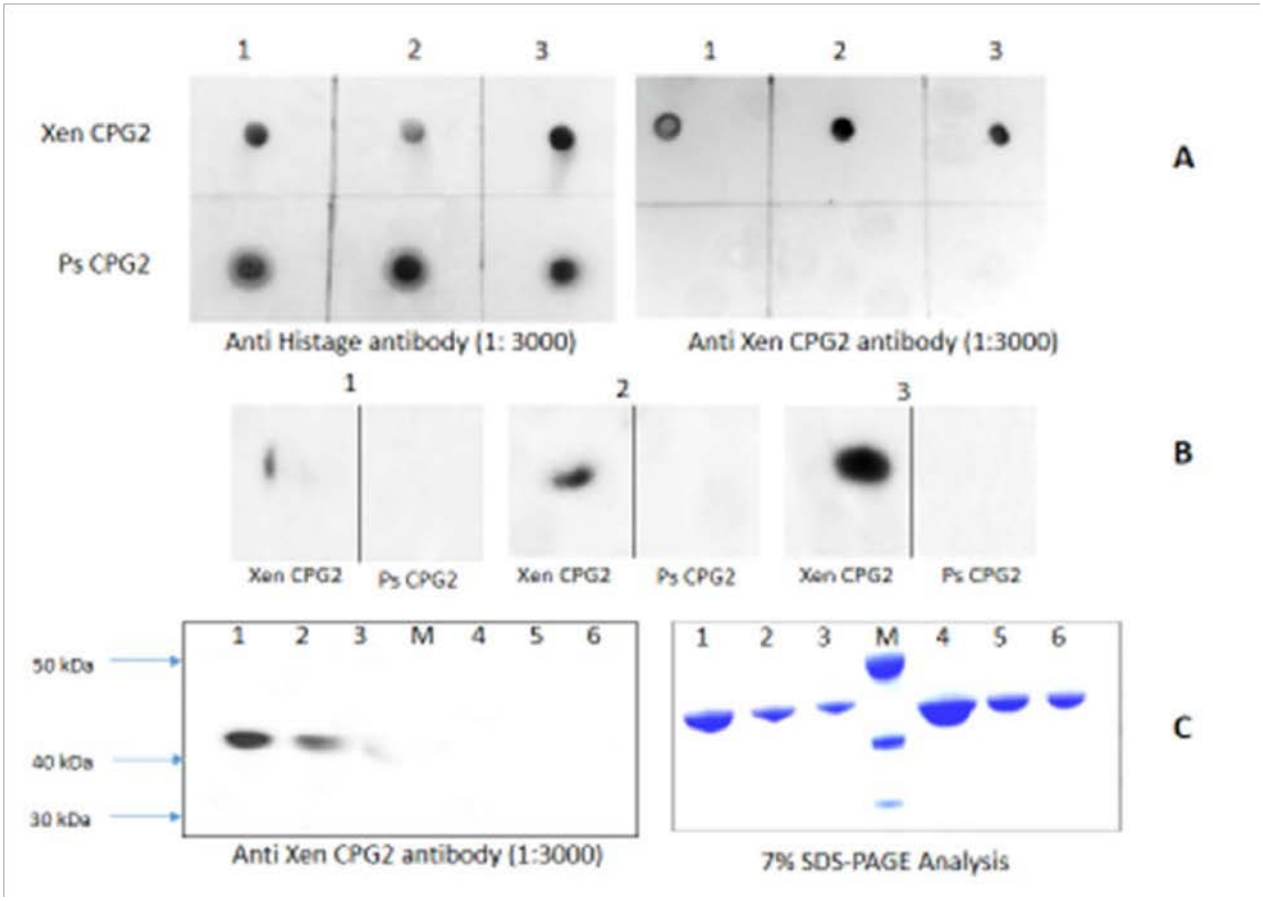

Fig 11. Antibody detection of newly isolated CPG2 relative to Ps CPG2. A. Dot blot using anti His tag antibody and using anti Xen CPG2 antibody where 1, 2, and 3 are pure protein (Xen CPG2 and Ps CPG2) at concentrations (0.05, 0.1, and 0.2 mg/mL). **B.** Dot blot at different concentration of anti Xen CPG2 antibody where 1, 2, and 3 are blotting at dilutions 1:20 000, 1:10 000 and 1:3000 in blocking buffer. **C.** SDS-PAGE and Western blot analysis of the pure protein (Xen CPG2 and Ps CPG2) where M is PageRuler™ Unstained Protein Ladder (10-200 kDa), lanes 1, 2, 3 are 0.25, 0.1, and 0.05 mg/mL of Xen CPG2 and lanes 4, 5, 6 are the same series of protein concentrations of Ps CPG2.

Discussion

Targeted therapies have great advantages over the conventional chemotherapy and radiotherapy in significantly reducing systemic toxicity, and severe side effects. To be effective, targeted therapy requires repeated cycles of administration of the protein drug.
Such repeated cycles, however, will lead to the development of an antibody response which undermines the efficacy of the therapy. The antibody response development against a protein eventually involves the differentiation of the B-cell with antibody receptor with binding capacity to the epitopes on the protein therapeutics.

A number of strategies have been pursued to overcome the antibody response by modifying the therapeutic protein to minimize its immunogenicity [31, 32]. However, the modification of a protein therapeutic to avoid or minimize the immune response can be laborious and is sometimes difficult to achieve.

We propose in this study a different strategy to overcome the immunogenicity problem of CPG2 in cancer therapy. CPG2 can be used in cancer treatment in two ways: firstly, in rescue therapy to remove any overdose of methotrexate by the hydrolysis of methotrexate to the less harmful product. Secondly, in targeted cancer treatment, by coupling CPG2 to antibodies specific for tumor cells, and the use of a pro-drug that would be activated by the enzyme in the vicinity of the cancer. Both applications utilize the ability of CPG2 to cleave C-terminal glutamate moieties. The use of CPG2 in antibody directed enzyme pro-drug therapy and detoxification of methotrexate is hampered by the host immune system response against CPG2. The detoxification process will also benefit greatly from variants with higher specific activity than that currently in use.

We propose that the unwanted immunogenicity towards the CPG2 in the ADEPT technique could be circumvented by using different CPG2s sharing the same function but with different epitopes. These CPG2s could be used consecutively, and therefore any antibody produced in response to the previously used CPG2 will not neutralize a subsequent CPG2 with disrupted or different epitope(s), nor will it provoke an undesired immune reaction in the patient.

Because the CPG2 is a bacterial enzyme, we propose that screening for new and different CPG2 producing bacteria from soil, and isolation and cloning of the CPG2 might lead to a new CPG2 with different epitope(s).

The identification of the newly isolated strains was carried out by biochemical and the *16s rRNA* analysis. The *16s rRNA* analysis showed that the first strain shares 98% DNA homology with a strain *Xenophilus azovorans* and 97% homology with *Variovorax paradoxus*. From these results, it was evident that strain SN1 is a new strain and may belong to the family *Comamonadaceae*. We could not find any strain with identical *16s RNA* DNA sequencing. We, therefore, named this isolated strain as *Xenophilus azovorans* SN213 and the novel *16s RNA* was deposited in the GeneBank database with accession number EU650684. *16s rRNA* DNA analysis of the second strain indicates that the strain SF3 is a *Pseudomonas* species, therefore its named was proposed to be *Pseudomonas lubricans* strain SF168 and was deposited with FJ600733 accession number in the GeneBank database. The *16s rRNA* DNA analysis shows that the third strain has 100% homology with *Stenotrophomonas sp*. AB1 and therefore the third new strain was named *Stenotrophomonas sp*. SA.

Glucarpidase is Zn^{2+}-dependent enzyme [12, 33]. We demonstrated that the isolated new strains are glucarpidase producers by showing that their protein extracts degrade methotrexate

and also that the activity is Zn^{2+} dependent (Fig 3). After the successful isolation and the confirmation of three CPG2 producers, we embarked on the isolation, cloning and molecular characterization of the genes from two of these CPG2 isolated strains, the gene from the *Xenophilus azovorans* SN213 (*Xen CPG2*) and the *Stenotrophomonas sp* SA (*Sten CPG2*). Molecular characterization of the two new glucarpidases, Xen CPG2 and Sten CPG2, revealed that Xen CPG2 encode a putative peptide of 415 amino acids, with about 94% similarity to the corresponding polypeptides of the *Pseudomonas sp*. Strain RS-16 glucarpidase (Fig 4) [12] which is currently in clinical use.

The amino acid sequence of Sten CPG2 shows a difference of three amino acids with the Xen CPG2. The predicted molecular weights of each recombinant protein are ≈ 41.761 kDa and 41.696 kDa for Xen CPG2 and Sten CPG2, respectively. These values are similar to those of other glucarpidases [11, 12].

The two new glucarpidases were cloned and overexpressed, in a soluble form exceeding 40% of the total soluble protein. The overexpression of the Xen CPG2 is shown in Figure 5. Due to the high expression of the CPG2 in the soluble form, we carried out all our studies on the soluble part and we did not perform a refolding process of the inclusion bodies. The new CPG2 (Xen CPG2) exerts higher activity towards folate hydrolysis on folate agar plate than Ps CPG2 (Fig 6), indicating that either the new CPG2 is much more active than Ps CPG2, or the Xen CPG2 was expressed in more soluble form than the Ps CPG2. The kinetic studies are consistent with the later explanation that the Xen CPG2 was expressed in a soluble form more than the Ps CPG2. At the same time, its pure recombinant protein (Fig 7a) confirmed that Xen CPG2 is a Zn^{2+} dependent metalloenzyme [34] as it showed maximum hydrolytic activity for MTX in the presence of Zn^{2+} ion that completely depleted upon chelation by addition of EDTA (Fig 8).

We also managed to optimize the condition to overexpress the codon optimized Ps CPG2 in *E. coli* [28] (Fig 7b) and testing its hydrolysis of folate relative to the newly isolated glucarpidase (this study) and testing by mass spectrometry (Fig 2b-c).

The soluble active recombinant Ps CPG2 we obtained in this study was used to investigate whether it is detected by a polyclonal antibody raised against Xen CPG2 and also to carry out a comparison study on both CPG2s: Xen CPG2 and Ps CPG2.

The change in secondary structure components as calculated by the deconvolution analysis software of CD spectra of Xen CPG2 and Ps CPG2 showed a significant increase in the alpha helix calculated component rather than the other secondary structure components, namely β-sheet (both parallel and anti-parallel), β-turn, and random coil of Xen CPG2 (69.3%) relative to Ps CPG2 (34.2%) indicating that Xen CPG2 has more folding structure than that of Ps CPG2 (Fig 9).

We also predicted the structure of Xen CPG2 based on its sequence (Fig 10). The best model based on the primary structure of Xen CPG2 we found was carboxypeptidase G2 (PDB ID 1CG2) with a sequence homology of 94%. This was used as a template to predict the tertiary and quaternary structure of Xen CPG2 (Fig 10A-B). We also did the structural alignment of the predicted structure of Xen CPG2 with CPG2 from *Pseudomonas sp*. strain RS-16. (PDB ID 1CG2) [30]. Not surprisingly we found an overall very good structural match with an RSM = 0.084. The only significant changes of the alignment were found in the flexible loop, C- and N-terminal regions (Fig 10C). The MS analysis of the insoluble materials formed from the CPG2 degradation of bacteria carrying Xen CPG2 and Ps CPG2 were identical with the formation of DAMPA with mass at 313.1m/z which consistent with the calculated value (Fig 2b-c).

The kinetic studies of the two CPG2s showed that at the same protein concentration Xen CPG2 has lower K_m value (50 µM) in comparison to Ps CPG2 (170 µM), indicating its higher affinity towards MTX than Ps CPG2 and although Xen CPG2 shows a lower turnover number K_{cat} (11.49 S^{-1}) than Ps CPG2 (24.83 S^{-1}), Xen CPG2 shows about double the kinetic efficiency (kinetic perfection) of Ps CPG2 based on their calculated

values K_{cat}/K_m.

The strategy of mutating B-cell epitopes to reduce immunogenicity has also been implemented successfully [35-37] and promises to be a useful technique that has a wide range of applications for recombinant cancer therapy and other diseases. The work presented here, however, to the best of our knowledge, is the first to report upon the characterization of two different but related protein therapeutics with the same function but with different epitope structures. Although the data reported here (Fig 11) needs to be confirmed using blood sera from patients treated with the Ps CPG2, it strongly suggests that the two enzymes are likely to have different epitopes and hence may be of clinical value.

Methotrexate is a potent and effective therapeutic drug, not only in cancer therapy, but also in rheumatoid arthritis (RA), diabetes mellitus, and other inflammatory diseases. The availability of new glucarpidases could be of great importance in improving its therapeutic usefulness in cancer therapy and will provide the opportunity for dose studies that, in turn, might lead to the escalation of methotrexate doses for more efficient treatment.

References

1. Jolivet J, Cowan KH, Curt GA, Clendeninn NJ, Chabner BA. The pharmacology and clinical use of methotrexate. N Engl J Med. 1983;309(18):1094-104. Epub 1983/11/03. doi: 10.1056/NEJM198311033091805. PubMed PMID: 6353235.

2. Pinedo HM, Zaharko DS, Bull JM, Chabner BA. The reversal of methotrexate cytotoxicity to mouse bone marrow cells by leucovorin and nucleosides. Cancer Res. 1976;36(12):441824. Epub 1976/12/01. PubMed PMID: 1087180.
3. Kisliuk RL. Deaza analogs of folic acid as antitumor agents. Current pharmaceutical design. 2003;9(31):2615-25. Epub 2003/10/08. PubMed PMID: 14529545.
4. Bleyer WA. The clinical pharmacology of methotrexate: new applications of an old drug. Cancer. 1978;41(1):36-51. Epub 1978/01/01. PubMed PMID: 342086.
5. Dasgupta S, Mazumder B, Ramani YR, Bhattacharyya SP, Das MK. Evaluation of the role of erythropoietin and methotrexate in multiple sclerosis. Indian journal of pharmacology. 2011;43(5):512-5. Epub 2011/10/25. doi: 10.4103/0253-7613.84955. PubMed PMID: 22021991; PubMed Central PMCID: PMC3195118.
6. Rekedal LR, Massarotti E, Garg R, Bhatia R, Gleeson T, Lu B, et al. Changes in glycosylated hemoglobin after initiation of hydroxychloroquine or methotrexate treatment in diabetes patients with rheumatic diseases. Arthritis and rheumatism. 2010;62(12):3569-73. Epub 2010/08/20. doi: 10.1002/art.27703. PubMed PMID: 20722019; PubMed Central PMCID: PMC2992611.
7. McGuire JJ, Haile WH, Valiaeva N, Bartley D, Guo J, Coward JK. Potent inhibition of human folylpolyglutamate synthetase by a phosphinic acid mimic of the tetrahedral reaction intermediate. Biochemical pharmacology. 2003;65(3):315-8. Epub 2003/01/16. PubMed PMID: 12527324.
8. Gustavsson B, Carlsson G, Swartling T, Kurlberg G, Derwinger K, Bjorkqvist H, et al. Phase 1 dose de-escalation trial of the endogenous folate [6R]-5,10-methylene tetrahydrofolate in combination with fixed-dose pemetrexed as neoadjuvant therapy in patients with resectable rectal cancer. Investigational new drugs. 2015;33(5):1078-85. Epub 2015/07/21. doi: 10.1007/s10637-015-0272-0. PubMed PMID: 26189513; PubMed Central PMCID: PMC4768212.
9. Calvert AH. Biochemical pharmacology of pemetrexed. Oncology. 2004;18(13 Suppl 8):13-7. Epub 2005/01/20. PubMed PMID: 15655931.
10. Lansiaux A, Lokiec F. [Pemetrexed: from preclinic to clinic]. Bull Cancer. 2007;94 Spec No Actualites:S134-8. Epub 2007/09/13. PubMed PMID: 17845983.
11. Kalghatgi KK BJ. Folate-degrading enzymes: a review with special emphasis on carboxypeptidase G. Holcenberg JS, Roberts J (eds) Enzyme as drugsJohn Wiley and Sons, New York. 1981:P77–102.
12. Minton NP, Atkinson T, Sherwood RF. Molecular cloning of the Pseudomonas carboxypeptidase G2 gene and its expression in Escherichia coli and Pseudomonas putida. Journal of bacteriology. 1983;156(3):1222-7. Epub 1983/12/01. PubMed PMID: 6358192; PubMed Central PMCID: PMC217971.
13. Sherwood RF, Melton RG, Alwan SM, Hughes P. Purification and properties of carboxypeptidase G2 from Pseudomonas sp. strain RS-16. Use of a novel triazine dye affinity method. European journal of biochemistry. 1985;148(3):447-53. Epub 1985/05/02. PubMed PMID: 3838935.
14. Bagshawe KD, Springer CJ, Searle F, Antoniw P, Sharma SK, Melton RG, et al. A cytotoxic agent can be generated selectively at cancer sites. British journal of cancer. 1988;58(6):700-3. Epub 1988/12/01. PubMed PMID: 3265633; PubMed Central PMCID: PMC2246864.
15. Syrigos KN, Epenetos AA. Antibody directed enzyme prodrug therapy (ADEPT): a review of the experimental and clinical considerations. Anticancer research. 1999;19(1A):605-13. Epub 1999/05/05. PubMed PMID: 10226606.
16. Cheng TL, Wei SL, Chen BM, Chern JW, Wu MF, Liu PW, et al. Bystander killing of tumour cells by antibody-targeted enzymatic activation of a glucuronide prodrug. British journal of cancer. 1999;79(9-10):1378-85. Epub 1999/04/03. doi: 10.1038/sj.bjc.6690221. PubMed PMID: 10188879; PubMed Central PMCID: PMC2362709.

17. Jung M. Antibody directed enzyme prodrug therapy (ADEPT) and related approaches for anticancer therapy. Mini reviews in medicinal chemistry. 2001;1(4):399-407. Epub 2002/10/09. PubMed PMID: 12369965.
18. Denny WA. Tumor-activated prodrugs--a new approach to cancer therapy. Cancer investigation. 2004;22(4):604-19. Epub 2004/11/30. PubMed PMID: 15565818.
19. Bagshawe KD. Antibody-directed enzyme prodrug therapy for cancer: its theoretical basis and application. Molecular medicine today. 1995;1(9):424-31. Epub 1995/12/01. PubMed PMID: 9415191.
20. Coelho V, Dernedde J, Petrausch U, Panjideh H, Fuchs H, Menzel C, et al. Design, construction, and in vitro analysis of A33scFv::CDy, a recombinant fusion protein for antibody-directed enzyme prodrug therapy in colon cancer. International journal of oncology. 2007;31(4):951-7. Epub 2007/09/06. PubMed PMID: 17786329.
21. Zhang Q, Zhang SH, Su MQ, Bao GQ, Liu JY, Yi J, et al. Guided selection of an antigamma-seminoprotein human Fab for antibody directed enzyme prodrug therapy of prostate cancer. Cancer immunology, immunotherapy : CII. 2007;56(4):477-89. Epub 2006/07/27. doi: 10.1007/s00262-006-0202-2. PubMed PMID: 16868778.
22. Sharma SK, Bagshawe KD. Translating antibody directed enzyme prodrug therapy (ADEPT) and prospects for combination. Expert opinion on biological therapy. 2017;17(1):1-13. Epub 2016/10/16. doi: 10.1080/14712598.2017.1247802. PubMed PMID: 27737561.
23. Martin J, Stribbling SM, Poon GK, Begent RH, Napier M, Sharma SK, et al. Antibodydirected enzyme prodrug therapy: pharmacokinetics and plasma levels of prodrug and drug in a phase I clinical trial. Cancer chemotherapy and pharmacology. 1997;40(3):189201. Epub 1997/01/01. doi: 10.1007/s002800050646. PubMed PMID: 9219501.
24. Sambrook J FE, Maniatis T. Molecular Cloning: A Laboratory Manual, 2nd ed. Cold Spring Harbor, New York: Cold Spring Harbor Laboratory Press. 1989.
25. McCullough JL, Chabner BA, Bertino JR. Purification and properties of carboxypeptidase G 1. J Biol Chem. 1971;246(23):7207-13. Epub 1971/12/10. PubMed PMID: 5129727.
26. Thompson JD, Higgins DG, Gibson TJ. CLUSTAL W: improving the sensitivity of progressive multiple sequence alignment through sequence weighting, position-specific gap penalties and weight matrix choice. Nucleic Acids Res. 1994;22(22):4673-80. Epub 1994/11/11. PubMed PMID: 7984417; PubMed Central PMCID: PMCPMC308517.
27. Thompson R, Wray NR, Crump RE. Calculation of prediction error variances using sparse matrix methods. J Anim Breed Genet. 1994;111(1-6):102-9. Epub 1994/01/12. doi: 10.1111/j.1439-0388.1994.tb00443.x. PubMed PMID: 21395757.
28. Goda SK, Rashidi FA, Fakharo AA, Al-Obaidli A. Functional overexpression and purification of a codon optimized synthetic glucarpidase (carboxypeptidase G2) in Escherichia coli. Protein J. 2009;28(9-10):435-42. Epub 2009/11/17. doi: 10.1007/s10930-009-9211-2. PubMed PMID: 19911261.
29. Biasini M, Bienert S, Waterhouse A, Arnold K, Studer G, Schmidt T, et al. SWISS-MODEL: modelling protein tertiary and quaternary structure using evolutionary information. Nucleic Acids Res. 2014;42(Web Server issue):W252-8. Epub 2014/05/02. doi: 10.1093/nar/gku340. PubMed PMID: 24782522; PubMed Central PMCID: PMCPMC4086089.
30. Rowsell S, Pauptit RA, Tucker AD, Melton RG, Blow DM, Brick P. Crystal structure of carboxypeptidase G2, a bacterial enzyme with applications in cancer therapy. Structure. 1997;5(3):337-47. Epub 1997/03/15. PubMed PMID: 9083113.
31. Chirino AJ, Ary ML, Marshall SA. Minimizing the immunogenicity of protein therapeutics. Drug Discov Today. 2004;9(2):82-90. Epub 2004/03/12. doi: 10.1016/S13596446(03)02953-2. PubMed PMID: 15012932.
32. Mayer A, Sharma SK, Tolner B, Minton NP, Purdy D, AmLot P, et al. Modifying an immunogenic epitope on a therapeutic protein: a step towards an improved system for antibody-directed

enzyme prodrug therapy (ADEPT). Br J Cancer. 2004;90(12):2402-10. Epub 2004/05/27. doi: 10.1038/sj.bjc.6601888. PubMed PMID: 15162148; PubMed Central PMCID: PMCPMC2409521.
33. Sharma SK, Bagshawe KD, Begent RH. Advances in antibody-directed enzyme prodrug therapy. Current opinion in investigational drugs. 2005;6(6):611-5. Epub 2005/07/07. PubMed PMID: 15997480.
34. Turra KM, Pasqualoto KF, Ferreira EI, Rando DG. Molecular modeling approach to predict a binding mode for the complex methotrexate-carboxypeptidase G2. J Mol Model. 2012;18(5):1867-75. Epub 2011/08/26. doi: 10.1007/s00894-011-1196-z. PubMed PMID: 21866317.
35. Moola ZB, Scawen MD, Atkinson T, Nicholls DJ. Erwinia chrysanthemi L-asparaginase: epitope mapping and production of antigenically modified enzymes. Biochem J. 1994;302 (Pt 3):921-7. Epub 1994/09/15. PubMed PMID: 7945221; PubMed Central PMCID: PMCPMC1137318.
36. Mehta RK, Verma S, Pati R, Sengupta M, Khatua B, Jena RK, et al. Mutations in subunit interface and B-cell epitopes improve antileukemic activities of Escherichia coli asparaginase-II: evaluation of immunogenicity in mice. J Biol Chem. 2014;289(6):355570. Epub 2013/12/04. doi: 10.1074/jbc.M113.486530. PubMed PMID: 24297177; PubMed Central PMCID: PMCPMC3916557.
37. Hu X, Zhang M, Zhang C, Long S, Wang W, Yin W, et al. Removal of B-cell epitopes for decreasing immunogenicity in recombinant immunotoxin against B-cell malignancies. J BUON. 2016;21(6):1374-8. Epub 2017/01/01. PubMed PMID: 28039694.

Chapter 4:

Production of “biobetter” variants of glucarpidase with enhanced enzyme activity.

Alanod D Al-Qahtani[1,2], Sara S Bashraheel[1,2], Fatma B Rashidi[3], C. David O’Connor[4], Atilio Reyes Romero[2], Alexander Domling[2] and Sayed K Goda[1,3]

[1] Protein Engineering Unit, Life and Science Research Department, Anti-Doping LabQatar (ADLQ), Doha, Qatar.
[2]Drug Design Group, Department of Pharmacy, University of Groningen, Groningen, Netherlands
[3]Cairo University, Faculty of Science, Chemistry Department, Giza, Egypt
[4]Department of Biological Sciences, Xi'an Jiaotong-Liverpool University, Science and Education Innovation District, Suzhou 215123, China

Biomedicine & Pharmacotherapy 2019;112:108725 doi https://doi.org/10.1016/j.biopha.2019.108725.

Abstract

Glucarpidase, also known as carboxypeptidase G_2, is a Food and Drug Administrationapproved enzyme used in targeted cancer strategies such as antibody-directed enzyme prodrug therapy (ADEPT). It is also used in drug detoxification when cancer patients have excessive levels of the anti-cancer agent methotrexate. The application of glucarpidase is limited by its potential immunogenicity and limited catalytic efficiency. To overcome these pitfalls, mutagenesis was applied to the glucarpidase gene of *Pseudomonas* sp. strain RS-16 to isolate three novels "biobetter" variants with higher specific enzyme activity. DNA sequence analysis of the genes for the variants showed that each had a single point mutation, resulting in the amino acid substitutions: I100T, G123S and T239A. $K_{m,}$ V_{max} and K_{cat} measurements confirmed that each variant had increased catalytic efficiency relative to wild type glucarpidase.

Additionally, circular dichroism studies indicated that they had a higher alpha-helical content relative to the wild type enzyme. However, three different software packages predicted that they had reduced protein stability, which is consistent with having higher activities as a tradeoff. The novel glucarpidase variants presented in this work could pave the way for more efficient drug detoxification and might allow dose escalation during chemotherapy. They also have the potential to increase the efficiency of ADEPT and to reduce the number of treatment cycles, thereby reducing the risk that patients will develop antibodies to glucarpidase.

Production of "biobetter" variants of glucarpidase with enhanced enzyme activity.

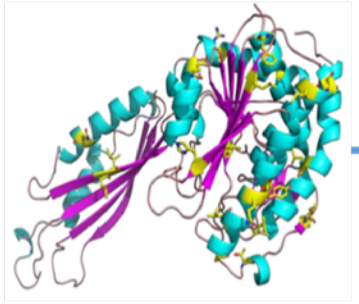

Glucarpidase

Isolation of three new variants, I100T, G123S, T329A; with enhanced enzyme activities

Purification of the new variants and the wild type Enzyme activity assay

Enzyme activity assay of the wild type and the I100T, G123S, T329A variances

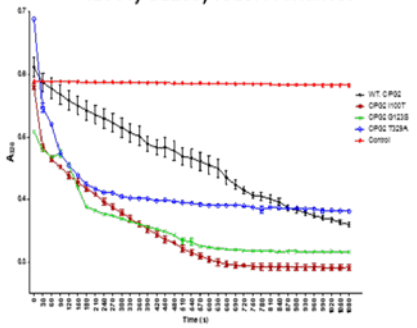

In silico stability study using three different programs

Kinetic studies

Program used	CPG2 I100T ΔΔG	CPG2 G123S ΔΔG	CPG2 T329A ΔΔG
mCSM [16]	-2.127Kcal/mol (destabilizing)	-2.205 Kcal/mol (destabilizing)	-0.535 Kcal/mol (destabilizing)
SDM [17]	-2.66 Kcal/mol (destabilizing)	-2.23 Kcal/mol (destabilizing)	0.16 Kcal/mol (stabilizing)
DUET [18]	-2.34 Kcal/mol (destabilizing)	-2.246Kcal/mol (destabilizing)	-0.283 Kcal/mol (destabilizing)

Enzyme	Kinetic parameter			
	K_m	V_{max}	K_{cat}	R^2
WT CPG2	171.7±65.66	52.6±8.484	24.83±0.9149	0.8791
CPG2 I100T	62.68±10.26	55.34±2.504	26.11±0.3592	0.9317
CPG2 G123S	71.38±13.85	57.69±3.344	27.21±0.4570	0.9123
CPG2 T329A	82.41±15.07	57.09±3.237	26.93±0.4453	0.9175

Keywords

Biobetter glucarpidase, DNA shuffling, glucarpidase, error-prone PCR, drug detoxification, ADEPT, targeted cancer therapy.

Introduction

Several strategies for targeted cancer therapy involving glucarpidase, also known as Carboxypeptidase G2 (CPG2), have been put into clinical practice in recent years. [1] (Glucarpidase or CPG2 will be used interchangeably throughout the text).

Glucarpidase has proved particularly useful in Antibody Directed Enzyme Prodrug Therapy (ADEPT), in which it accumulates at the site of a tumor via a tumor-specific antibody, after that it converts a prodrug into an active drug.[2-4]

In contrast, in cases of methotrexate-induced toxicity, glucarpidase is administered to convert this anti-cancer agent to a less harmful compound (4-deoxy-4-amino-N10methylpteroic acid) that is excreted via a hepatic pathway. The enzyme is typically given in high doses to patients, thereby decreasing the risk of renal failure.[5-9]

Although clinically useful, patients treated with glucarpidase often develop antibodies against it, which limits the number of times it can be administered.

Additionally, the wild-type enzyme has limited catalytic efficiency and hence must be given in relatively high doses. For both reasons, it would be desirable to develop variants of CPG2 that have increased specific activity but different immunogenic properties due to their altered structures.

Such variants might escape recognition by the patients' immune system and might also allow clinicians to decrease the amount of CPG2 that is administered.

The re-assortment of mutations to produce favorable combinations that can undergo natural selection is a critical component of biological evolution. This process can be simulated by directed evolution, which has proved to be an effective strategy for improving or altering the activity of biomolecules for industrial, research and therapeutic applications. The evolution of proteins in the laboratory uses error-prone DNA replication *in vitro* to generate genetic diversity and specific screens to identify protein variants with desired properties.[10] Where necessary, the genes for these variants can then be shuffled in a process akin to homologous recombination to achieve further improvements.[10] In several instances, chimeric enzymes with improved activity and stability have been isolated from libraries constructed using DNA shuffling.[11-14] In other cases, the method resulted in libraries with either too many mutations in each gene [15] or too few crossovers [16] to be useful.

DNA shuffling can take advantage of orthologous proteins to repurpose functional diversity from nature, i.e. in addition to using error-prone replication in vitro, it can be used to shuffle distantly related existing sequences to take advantage of the natural diversity that exists within a population and to provide a means to eliminate deleterious mutations that may accumulate in strains.[17]. On the other hand, it is limited by the degree of sequence homology shared by the existing sequence variants[10].

This paper describes the production of novel CPG2 variants with increased activity, which may also have structural alterations, and hence altered immunogenicity, thereby allowing additional cycles of therapy. The novel highly active glucarpidase(s) were sub-cloned, overexpressed and functionally characterized.

Materials and Methods

Growth media, Enzymes, Chemicals and Antibodies

LB Media was from Formedium (Norfolk, UK) and where necessary was solidified with 1.5% (w/v) Bacto-agar (Fermentas; Waltham, Massachusetts, USA). Enzymes for cloning and expression of the glucarpidase genes were purchased from Thermo Scientific, with the exception of *Sau*3AI, *Bam*H1 and a PCR master mix (2×) kit, which was purchased from Promega (Fitchburg, Wisconsin, USA). Ni-NTA resin was purchased from SigmaAldrich (Saint Louis, Missouri, USA). GilPilot 1 kb DNA ladder (100) was purchased from

Thermo Scientific (Waltham, Massachusetts, USA), Wizard® SV Gel and PCR Clean-Up System Kit were purchased from Promega. GeneJET Plasmid Miniprep Kit was obtained from Thermo Scientific. All other chemicals were of a high analytical grade. The mass spectroscopy (MS) analysis was carried out at the Toxicology and Multipurpose Labs, ADL-Qatar. Anti-Xen CPG2 Polyclonal Antibodies were produced by Eurogentec, Belgium, anti-Rabbit IgG (whole molecule)–Peroxidase antibody produced in goat

(Sigma-Aldrich) was used as secondary conjugated antibody. 6× His Epitope Tag Antibody (HIS. H8) (Thermo Scientific) was used for detection of the purified 6-Histagged CPG2 and Polyclonal Rabbit Anti-Mouse Immunoglobulins/HRP (Dako Labs, Santa Clara, California, USA) was used as the secondary antibody.

Mutagenesis and recombination by DNA shuffling

DNA shuffling was carried out essentially according to the Stemmer method [18] using as a template a synthetic version of the CPG2/glucarpidase gene from *Pseudomonas putida* that had been codon-optimized for expression in *E. coli* [19]. First, to enhance the natural mutation rate, libraries of

glucarpidase mutants were constructed by error-prone PCR. 30 pmol of each primer flanking the glucarpidase gene set (CPGF; 5'-ACC GGA TCC CAT ATG GCG CTG GCC CAG AAA CG-3', and CPGR 5-CTT AAG CTT TTA TTT GCC CGC ACC CAG ATC C-3'), 5 mM $MgCl_2$, 0.2 mM of each dATP and dGTP, 1 mM of each dTTP and dCTP, and 0.5 µl *Taq* polymerase was used in the PCR reactions. The thermal cycling parameters were: 95^{o}C for 2 min (1 cycle), 95^{o}C for 1 min, 55^{o}C for 1 min, 72^{o}C for 2 min (30 cycles) and 72^{o}C for 5 min (1 cycle). The PCR products were purified using a PCR purification kit (Thermo Scientific). 44 µl of purified DNA template was then mixed with 2.5 µl of 1 M Tris−HCl (pH 7.5), 2.5 µl of 200 mM $MnCl_2$ and brought to a final volume of

49 µl with deionized water. The mixture was equilibrated at 15^{o}C for 5 min. Subsequently, 1 µl DNase I (10 U/µl) diluted to 1:100 in deionized water for digestion at 15^{o}C was added. Aliquots (10 µl) was taken after 30 s, 1, 2, 3 and 5 min of incubation and immediately mixed with 5 µl of ice-cold stop buffer containing 50 mM EDTA and 30% (v/v) glycerol. Large scale DNase digest was carried out and the fragments were separated by electrophoresis in 2% agarose gels and DNA fragments in the 200-300bp size range were cut from the gel and extracted. Then, a primerless PCR reaction was carried out, in which 10 µl of purified fragments were combined with 5 µl of 10× *Pfu* buffer, 5 µl of 10× dNTP mixture (2 mM of each dNTP) and 0.5 µl of *Pfu* polymerase to a total volume of 50 µl and then PCR reaction was performed. PCR conditions were: 1 cycle at 95^{o}C for 3 min, 40 cycles of 95^{o}C for 30 s, 55^{o}C for 1 min, 72^{o}C for 1 min + 5 (s per cycle) and 72^{o}C for 5 min (1 cycle). Recombinant genes were amplified in a standard PCR reaction using serial dilutions of the assembly reaction. The PCR reaction conditions were: 1 µl serial diluted templates, 10 pmol of each primer set, 5 µl of 10× *Pfu* buffer, 1 µl of 10× dNTP mixture (2 mM of each dNTP) and 0.5 µl of *Pfu* polymerase in the total volume of 50 µl. The thermal cycling parameters was 95^{o}C for 2 min (1 cycle), 95^{o}C for 1 min, 55^{o}C for 1 min, 72^{o}C for 2 min (30 cycles) and 72^{o}C for 5 min (1 cycle).

Sub-cloning of shuffled glucarpidase (S-glucarpidase) mutants

The PCR products were purified using a gel extraction kit (Thermo Scientific) and doubledigested with the restriction enzymes *Nde*I and *Hind*III. After further gel purification, the digested glucarpidase gene fragments were ligated into the *Nde*I/*Hind*III sites of the pET28a expression vector and transformed into competent *E. coli*. Plasmid minipreps were purified and sequenced using T7 promoter and terminator primers to screen for mutations.

Screening for functional S-glucarpidase(s)

Derivatives of the expression vector pET28a expression vector containing variant genes for the shuffled glucarpidase (variants) were selected, transformed into the expression host *E. coli* BL21(DE3) RIL, and then plated on LB/agar plates containing 0.1 mM isopropyl-β-D-thiogalactopyranoside (IPTG), folate and the required antibiotics. The plates were incubated at 37$_{o}$C overnight, and colonies that were surrounded by clear zones were selected for protein expression and activity assays using cell-free extracts, as previously described.[20] Priority was given to colonies with large 'halo zones', on the assumption that these either produced more glucarpidase or corresponded to variants with increased enzymatic activity.

Recombinant protein expression and characterization

E. coli BL21(DE3) RIL cells contain pET28a-CPG2, or the same expression vector contain a variant, were incubated with shaking (200 rpm) at 37°C in 250 ml of LB medium supplemented kanamycin and chloramphenicol (both at 32 µg/ml) until the optical density at 600 nm reached 0.5-0.6. Induction of expression of recombinant CPG2 was initiated by the addition of IPTG at a final concentration of 1 mM, whereupon the culture was incubated for a further four hours at 37°C with shaking. Cells were collected by centrifugation at 4,000 rpm for 20 min at 4°C and the pellets were re-suspended in Tris buffer (pH 7.5), 50 mM NaCl. Lysis was achieved by sonication, using Soniprep 150 plus, on ice (5 cycles of 30 sec sonication pulses followed by 1 min rest). The soluble fraction

was separated by centrifugation at 14,000 rpm for 20 min at 4°C. The soluble and insoluble fractions were mixed with 2× sample buffer, boiled for ten minutes at 95°C, and then analyzed by SDS-PAGE. Protein expression in cells incubated at 20°C was carried out identically to assess the effect of temperature on improving soluble protein expression.

Purification using nickel affinity chromatography

Protein extracts from *E. coli* BL21 (DE3) RIL cells containing pET28a-CPG2, or the same expression vector containing a variant, were subjected to purification by Ni^{2+} affinity chromatography using Ni-NTA resin. About 1 ml of the resin was washed with distilled water and activated by binding and washing buffer A (20 mM Tris pH 8, 50 mM NaCl, 5 mM β-mercaptoethanol (BME), and 20 mM Imidazole) then the total soluble protein was combined with the activated resin and gently agitated for 20 min at 4 °C to allow the protein to bind to the column resin. The resin was separated by gravity, the flow-through was collected, and the resin was washed 3 times with buffer A. The target protein (bound to the resin) was collected by adding ice-cold elution buffer B (20 mM Tris pH 8, 50 mM NaCl, 5 mM BME and 400 mM Imidazole). The eluted protein was dialyzed against 100 mM Tris-HCl pH 7.3 containing 0.2 mM $ZnSO_4$. All fractions from the protein purification were analyzed by SDS-PAGE. MTX hydrolysis the pure recombinant glucarpidase was assayed using as described below.

Assay of wild-type and mutant glucarpidase activity using methotrexate

The glucarpidase activity of each of the shuffled variants was determined using MTX as substrate. The assay was a modification of the method described by McCullough [21]. 0.1 M Tris-HCl (pH 7.3), 0.2 mM $ZnSO_4$ was used as a dilution buffer for 5 µl of MTX (0.45 mM, final concentration). After equilibration of the reaction mixture at 37°C for 10 minutes, a total protein extract from the expressed shuffled variant (50 µg/ml) was added and incubated at 37°C. Samples were taken at 10

min intervals, and the decrease in absorbance at 320 nm was measured using a NANODROP 1000 spectrophotometer (Thermo Scientific). The same protocol was used to analyze the activity of the pure recombinant CPG2 using 3 µg/ml protein. The Michaelis-Menten equation was used for determination of the actual values of K_m, K_{cat}, and V_{max} of each protein using GraphPad PRISM 6 software (San Diego, California, USA). One unit of the enzyme represents the amount of enzyme in mg required for hydrolysis of 1 mM of MTX per min at 37°C. The enzyme activity per ml of protein was calculated using 8300 as the molar extinction coefficient for MTX.

Circular Dichroism of the shuffled CPG2

a. Pre-CD Scanning

The wild-type CPG2 and the three variant proteins were purified and dialyzed against Milli-Q water 4 times, 18 hours each, then clarified by centrifugation at 14000 rpm for 30 min at 4°C. To measure the protein concentration a NanoDrop 2000 spectrophotometer (Thermo Scientific) was used to achieve the required concentration of about 6 µM for the

CD measurement. The extinction coefficients were calculated as ε 24870 M^{-1} cm^{-1} for the four proteins WT, CPG2I100T, CPG2T329A and CPG2G123S.

b. Circular Dichroism (CD)

CD measurements were obtained using a Chirascan™ Plus CD Spectrometer (Applied Photophysics). Scanning of the proteins (6 µM, final concentration) in the far UV spectral region (260 to 180 nm) was performed in a rectangular demountable SUPRASIL Quartz cuvette (Hellma®) of 0.2 mm light-path length (sample volume ~70 µl). The applied CD parameters were: bandwidth 1 nm and scan time per point of 0.5 sec at 20°C. Four scans were taken per sample, and the readings were averaged and smoothed using the CD analysis software. The produced spectra were subtracted from an averaged CD spectra of the blank baseline (Milli Q water).

c. CD- deconvolution method

Protein secondary structures of the pure shuffled CPG2 were calculated by CD data and the deconvolution analysis using the CDNN (version 2.1) software tool. A spectral range of (180–260 nm) was used for the deconvolution calculation. The number of residues and molecular weight were taken as 394 AAs, with 41.9117, 41.8996, 41.8817, 41.9417 kDa for the WT, CPG2I100T, CPG2T329A and CPG2G123S, respectively, and the light-path length of the cuvette used was 0.2cm.

Prediction of the impact of the single point mutation on glucarpidase

To find a possible correlation with the results of the activity assays, three software packages, mCSM [22], SDM [23], and DUET [24], were used to predict the effects of the mutations on glucarpidase stability and to generate environment-specific substitution tables (ESST) and thermodynamic stability data for glucarpidase mutants.

Prediction of Hydrogen bond networking of the mutants

The models were generated using Modeller package [25-28] from the crystal structure of carboxypeptidase G2 (PDB: 1CG2). Polar contacts are depicted in red dotted lines and the picture was rendered with Pymol (Version 2.2 Schrödinger, LLC).

Statistical analysis

Data are presented as mean ± standard error of the mean (S.E.M) of “3” observations. All graphs were constructed using GraphPad Prism 6 software (San Diego, CA, USA). Statistical analysis was performed using Student T-test or two-way ANOVA as appropriate. P values < 0.05 were considered statistically significant.

Results

Mutagenesis of the Glucarpidase Gene

Error-prone PCR was used to mutate the CPG2 gene of *Pseudomonas putida*, which has previously been codon-optimised for expression in *E. coli* [20]. The mutated genes were fragmented, and then primer-less and conventional PCR was used in an attempt to produce shuffled DNA, and to amplify full-length genes containing mutations (see Materials and Methods for further details) (Supplemental Fig. S1). Following cloning into the expression vector pET28a, DNA sequence analysis was used to confirm mutation and shuffling of the CPG2 gene (data not shown).

Isolation of variants with enhanced CPG2 activity pET28a plasmids containing CPG2 variants were transformed into BL21(DE3)RIL and screened for glucarpidase activity on folate-containing agar plates. Approximately four thousand colonies containing variants were screened for hydrolysis of folate by searching for clear zones and yellow precipitates around colonies. 73% of the four thousand colonies grown on folate containing media plates formed clear zones and, of this set, three colonies displayed a significantly darker coloration after two days of incubation relative to cells harboring the original pET28a-CPG2 construct (Supplemental Fig. S2). This suggested that the isolates either produced more glucarpidase or that the glucarpidase in question had a higher level of activity against the folate substrate.

The mutations in the CPG2 genes of three variants that were selected for the further study were identified by sequencing (Supplemental Fig. S3). Each mutant had a single but different codon change relative to the wild-type CPG2 sequence, corresponding to the following amino acid changes:

C100T, G123S, and T329A. Accordingly, the mutants were named CPG2I100T, CPG2G123S, and CPG2T329A.

Purification of the glucarpidase mutants and Western Blot analysis

The three mutant enzymes were overexpressed and purified by affinity chromatography using Ni columns. **Figure 1** shows a representative purification for the wild-type and CPG2 I100T mutant while **Figure 2** shows the corresponding Western blot analysis using an anti-His antibody.

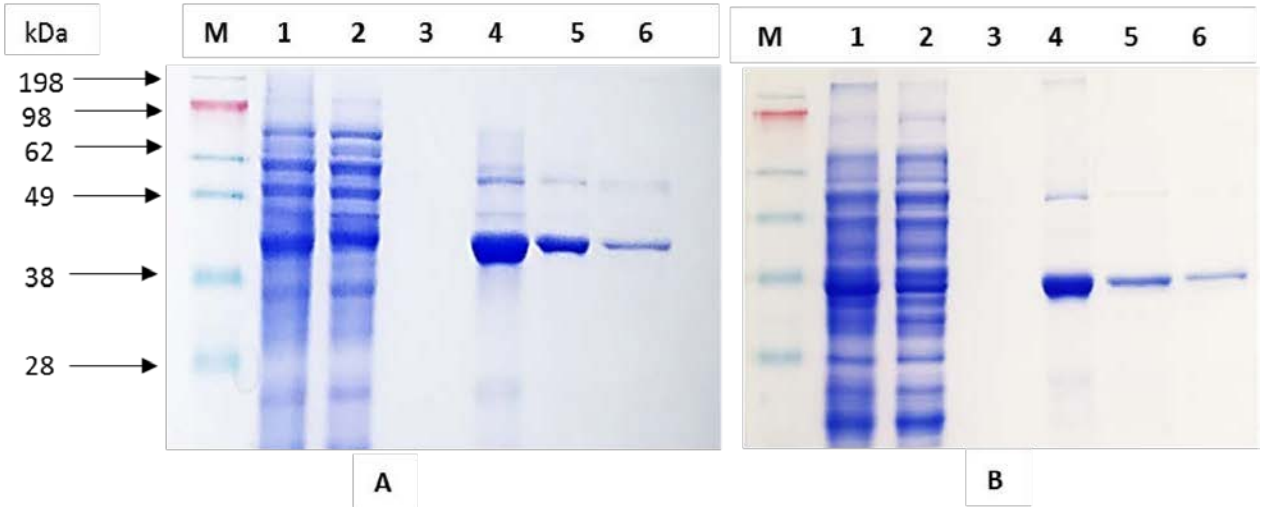

Fig. 1. Ni-NTA Protein purification of CPG2 (*P. putida* and one of the shuffled variant, I100T) in Bl21(DE3)RIL. **A**. protein purification of *P. putida* CPG2, and **B**. an example of a protein purification of a mutant protein, where M is SeeBlue Plus2 Pre-Stained Protein Standard (3-198 kDa), lanes 1, 2, 3, 4, 5, and 6 are total soluble, flow-through, wash, and elutions (E1, E2, and E3 for CPG2 of *P. putida*) respectively.

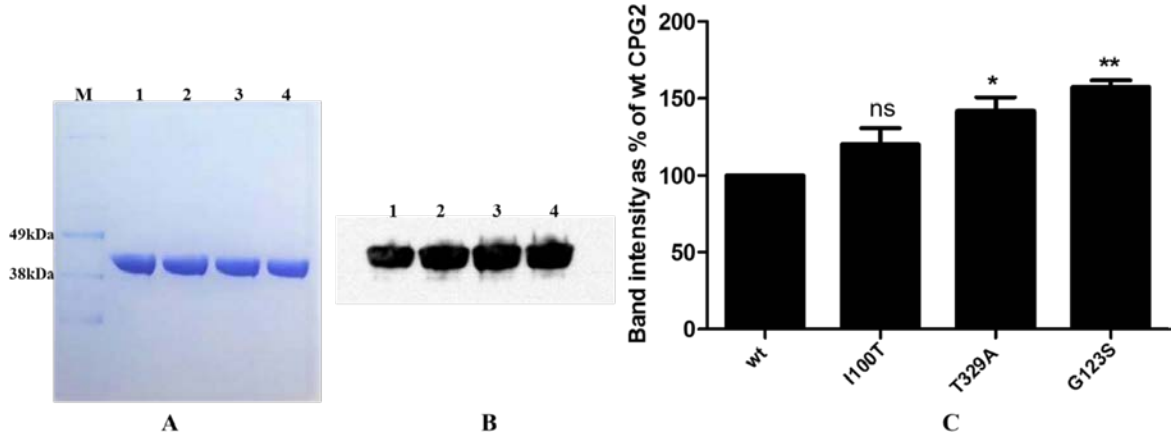

Fig 2 Western blotting analysis of the shuffled CPG2s relative to WT-CPG2. A) Shows the relevant gel image after SDS-PAGE while B) the corresponding immunoblot. Lanes 1, 2, 3 and 4 are WTCPG2, CPG2I100T, CPG2T329A and CPG2G123S, respectively. C) Densitometric quantification of bands was carried using GASepo analysis software. Results are expressed as the percentage of WTCPG2 band intensity and are presented as mean ± standard error of the mean (S.E.M) of 3 independent experiments. Statistically significant difference: *$p<0.05$ and **$p<0.01$ while ns is not significant. Ex-#1, Ex-#2, and Ex-#3, three independent western blot replicates are shown in the supplement section.

Activity of mutant glucarpidases relative to the wild-type enzyme

Equal amounts of protein extracts containing the wild-type and mutant CPG2 enzymes were assayed for glucarpidase activity using MTX as a substrate in the presence of Zn^{2+} ions, as described in the Materials and Methods section. The results indicated that each of the mutants had a higher glucarpidase activity than the wild type enzyme (**Figure 3**). The I100T and G123S mutants showed the largest increases in enzyme activity. However, the T329A mutant also had a significantly increased activity relative to wild-type CPG2 but less activity than the other two mutants.

Two-way ANOVA statistical analysis of the Enzyme Activity Assay showed a significant difference in activity between the four enzymes $p<0.001$. When compared with the WTCPG2, there was a significant difference in activity at time 60- 780, 150-660 and 180270 for CPG2I100T, CPG2G123S and CPG2T329A, respectively. Details are provided in the (**Table 1).**

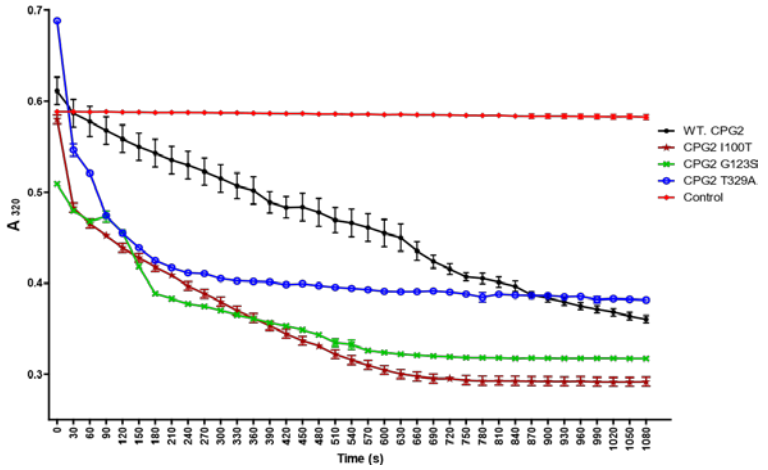

Fig. 3. Activity assay of wild type glucarpidase (wt-CPG2) and the three mutant enzymes using MTX as a substrate. Total protein extracts (50 µg/ml) from cells expressing the proteins were added to MTX (0.45 mM, final concentration), and the change in absorbance at 320 nm recorded. The plot shows the relative activities of WT-CPG2 (black), CPG2I100T (dark red), CPG2T239A (blue) and CPG2G123S (Green) in the presence of Zn^{+2} relative to the control in the absence of enzyme (red).

Table 1. The difference in activities between the wild type CPG2 and the three novel mutants and the corresponding p-value.

Time [S]			
WTCPG2 vs CPG2I100T	**WTCPG2 vs CPG2G123S**	**WTCPG2 vs CPG2T329A**	**P-value**
60-210, 720-780	660	180-270	<0.05
240-510, 660-690	150, 300-630	None	<0.01
540-630	180-270	None	<0.001

Kinetic studies of the mutants and comparison with WT-CPG2

More detailed kinetic studies were carried out to characterize the variants further. Specifically, the K_m, V_{max} and K_{cat} values for the mutants were determined using methotrexate as a substrate and compared with the wild-type enzyme (**Table 2)**.

Table 2: Comparison of the kinetic parameters of the wild-type and mutant CPG2 enzymes using methotrexate as a substrate (± S.E.M, R^2 coefficient of determination).

Enzyme	Kinetic parameter			
	K_m	V_{max}	K_{cat}	R_2
WT CPG2	171.7±65.66	52.6±8.484	24.83±0.9149	0.8791
CPG2 I100T	62.68±10.26	55.34±2.504	26.11±0.3592	0.9317
CPG2 G123S	71.38±13.85	57.69±3.344	27.21±0.4570	0.9123
CPG2 T329A	82.41±15.07	57.09±3.237	26.93±0.4453	0.9175

Circular Dichroism spectroscopy and secondary structure determination

Given the significant changes in the specific activities of the mutants CPG2 enzymes, it was of interest to see if they also had significant changes in their secondary structures. Accordingly, we obtained and compared CD data in the far UV region for the wild-type and mutant proteins to estimate such changes (**Figure 4**). All three of the mutant proteins gave more negative chiral CD signals, relative to the wild-type, in 208-230 nm region. Overall, however, the CPG1I100T and CPG2G123S mutants had similar profiles to the wild type whereas the CPGT329A mutant was markedly different. The estimated percentage values for the secondary structure components of the proteins were deduced by CD deconvolution (**Table 3**). In keeping with the spectral analysis, CPGT329A was estimated to have significantly more alpha-helical content relative to the other proteins.

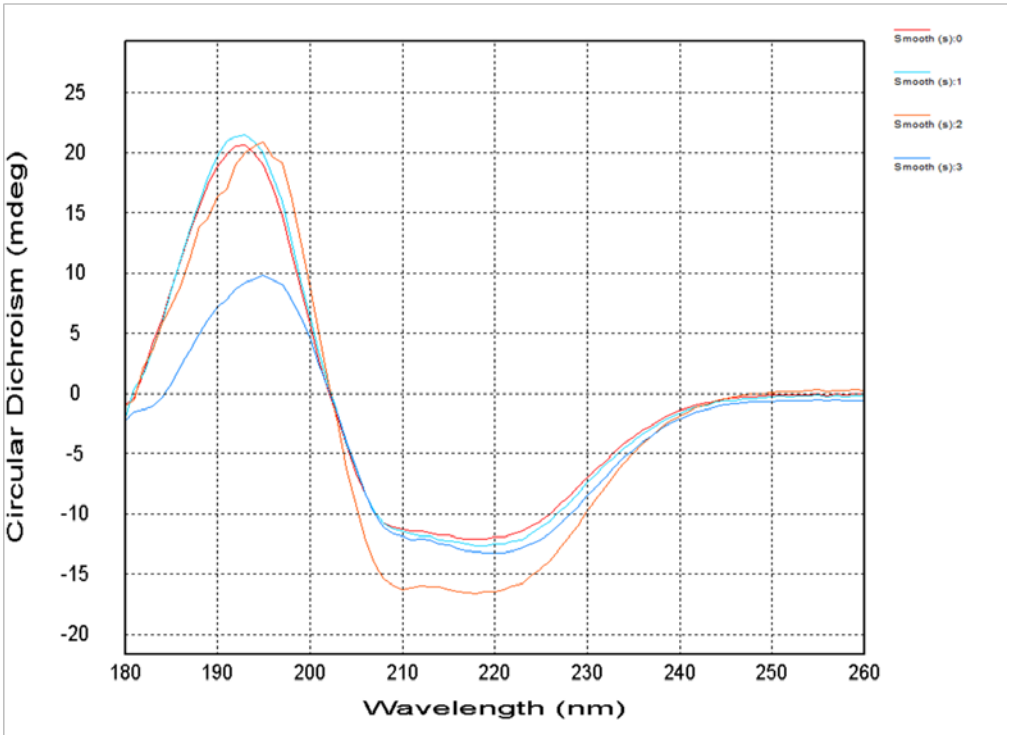

Fig. 4. CD analysis in the far UV region of wt CPG2 and the three mutants. The red, cyan, orange and dark blue curves correspond to wild-type CPG2, CPG1I100T, CPGT329A, and CPG2G123S enzymes, respectively. The baseline corrected CD (mdeg) molar ellipticity [Θ] displayed more negative chiral CD signals with shuffled proteins relative to the wild-type enzyme at the same protein concentration (0.58 mg/ml).

Table 3: Estimated secondary structure changes in the three mutants relative to the wild-type CPG2 enzyme

	Estimated secondary structure (%)					
	Alpha-helical	**Anti-parallel**	**Parallel**	**Beta-turn**	**Random**	**Total**
Wild-type CPG2	34.2	8.5	8.5	16.6	32.3	100
CPG2I100T	36.2	7.6	8.2	16.2	31.5	99.6
CPG2G123S	36.4	7.5	8.1	16.0	31.7	99.7
CPG2T329A	40.7	6.6	7.2	15.5	28.5	98.5

The relative amounts of secondary structure in each of the proteins was estimated by CDNN deconvolution analysis using the data shown in **Figure 4**. The average values (as percentages) of each secondary structure component for four sets of measurements is shown.

The impact of the single point mutations on glucarpidase stability

Given the differences in secondary structure indicated by the CD studies, we checked the predicted impact of the amino acid alterations on the stability of the glucarpidase variants (**Table 4)**. Three software packages were used to predict whether the amino acid changes were likely to stabilize or destabilize the protein structure of CPG2. Although programs mostly predicted the changes to be destabilizing, the Site Directed Mutator (SDM) package predicted that T329A change would be stabilizing.

Table 4: Predicted stabilities of the mutant CPG2 enzymes

Program used for predicting stability change	CPG2 I100T ΔΔG	CPG2 G123S ΔΔG	CPG2 T329A ΔΔG
mCSM [22]	-2.127Kcal/mol (destabilizing)	-2.205 Kcal/mol (destabilizing)	-0.535 Kcal/mol (destabilizing)
SDM [23]	-2.66 Kcal/mol (destabilizing)	-2.23 Kcal/mol (destabilizing)	0.16 Kcal/mol (stabilizing)
DUET [24]	-2.34 Kcal/mol (destabilizing)	-2.246Kcal/mol (destabilizing)	-0.283 Kcal/mol (destabilizing)

Prediction of the hydrogen bond network of glucarpidase mutants

Visual inspection of the predicted models disclosed new hydrogen bond network forming between the mutated amino acids and adjacent residues as shown in the figure panel of **Figure 5**.

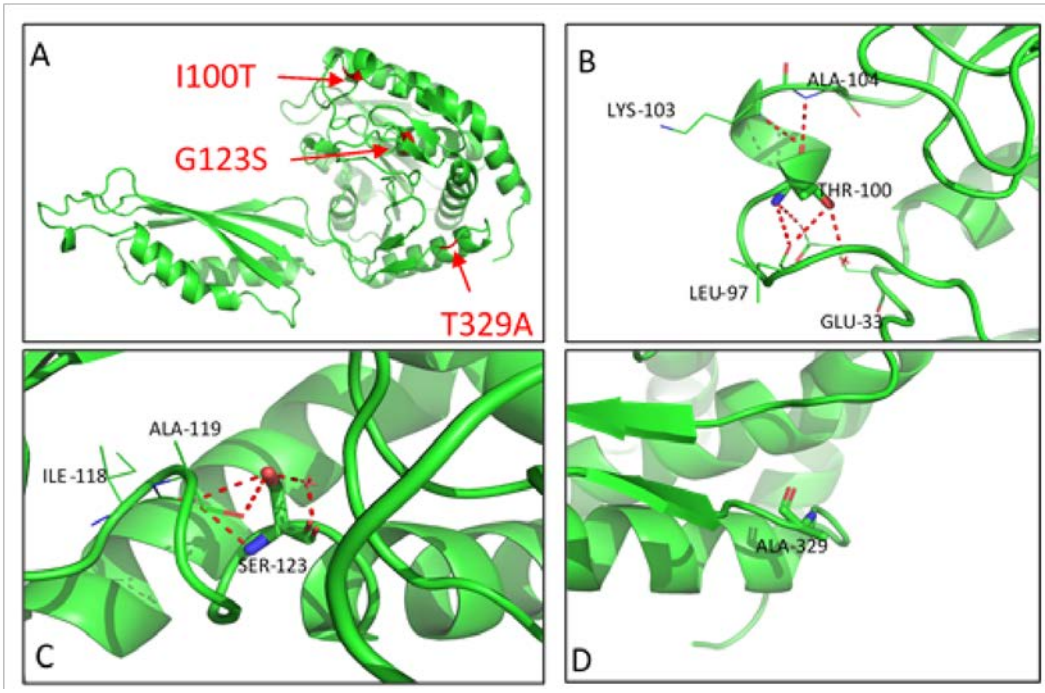

Figure 5 Figure panel is showing the modelled prediction of hydrogen bond network following point mutation in the various mutants. (**A**) Cartoon representation of chain A of glucarpidase. Red arrows indicate where the single point mutations were made. (**B**) Compared to the native type, the mutant I100T acquires a new hydrogen bond between the hydroxyl group of threonine and the carboxyl group of Leu-97. (**C**) The mutant G123S forms a hydrogen bond with Ile-118 similarly to the unmutated form but interacts with Ala-119 and loses the hydrogen bond with Val127. (**D**) On the contrary, in mutant T329A no extra hydrogen bonds with neighbored residues were observed.

Discussion

Glucarpidase, the recombinant form of CPG2, has been used for more than two decades as a detoxifying agent for MTX and also in targeted cancer therapies such as ADEPT. However, its usefulness in both treatment regimens has been limited by its relatively low specific activity and the fact that patients often develop antibodies against it after repeated administration. In our previous study [29], we successfully produced two longacting variants of glucarpidase, PEGylated glucarpidase and HSA-fused Glucarpidase. We demonstrated that both “biobetter” glucarpidases are less immunogenic and had prolonged half-lives relative to the native enzyme. However, the study did not address the

question of the native enzymes relatively low specific activity. In the present work, we used mutagenesis techniques to produce further “biobetter” glucarpidase variants with improved activity.

Following mutagenesis of the glucarpidase gene of *Pseudomonas* sp. strain RS-16 [30], approximately 73% of the clones retained enzyme activity, as indicated by the clear zones and yellow precipitate surrounding their colonies. However, there were very few that had ‘halos’ around colonies that were darker than that of the wild-type, which would be indicative either of more active glucarpidase variants or variants that over-produced the enzyme relative to the wild-type construct. DNA sequence analysis of the three mutants taken for further study indicated that each had a single point mutation leading to the alteration of a single amino acid at the protein level (Supplemental Fig. S3). The fact that only single point mutations were present suggests that the error-prone PCR may have contributed more than the DNA shuffling procedure to the production of these particular mutants. Alternatively, it is possible that combining two or more individual mutations into a single gene may have resulted in mutant enzymes with little or no enzyme activity.

The three mutant enzymes, named CPG2 I100T, CPG2 G123S, and CPG2 T329A, were then characterized in greater detail. In keeping with their colony phenotypes, each had a higher specific activity in enzyme assays, and this was supported by the results of studies to determine their kinetic parameters. Specifically, the three mutants had higher substrate affinity as shown by their lower K_m values relative to the wild-type enzyme (**Table 2**). It remains to be seen if combining two or more of the mutations into the same CPG2 gene results in a further increase in enzyme activity.

Having established that the mutants had increased enzyme activity against the substrate MTX, it was then of interest to determine the extent to which their structures had been perturbed. Accordingly, we carried out a CD study to check for alterations in secondary structure, and also analyzed their predicted amino acid sequences using programs designed to predict changes in protein stability. For two of the mutants, CPG2 I100T and CPG2 G123S, the alterations in secondary structure appear to be modest although it is likely that they are slightly destabilizing.

The analysis of the three web servers to predict the effect of a single mutant [22-24], the prediction shows a higher destabilizing effect in position 100 and 123 compared to 329 of the three mutants. In contrast, CD analysis of the third mutant, CPG2 T329A, suggests that it has a marked increase in alpha-helical content, which, interestingly, might even lead to a modest increase in its structural stability, as indicated by analysis with the SDM software package (**Table 4**).

It has previously been shown [31] that amino acids in a protein that is involved in enzyme catalysis are not optimized for stability. Thus, replacement of specific residues may reduce the activity of an enzyme but concomitantly increase its stability. Alternatively, the replacement of residues involved in protein stability could lead to higher enzyme activity. The results presented in this work are consistent with these findings. The three randomly produced glucarpidase mutation substitution, I100T, G123S and T329A, increased the enzyme activity in each case but are predicted to decrease the stability of each mutant (**Figure 3**, **Table 4**).

Our study may also suggest the involvement of the isoleucine, glycine and alanine at positions 100, 123 and 329, respectively, in glucarpidase catalysis. It has previously been shown that [32] proteins with specific sites known as flexibility hotspots are important for both binding and stability.

The predicted structure (**Figure 5**) shows that in the two mutations, I100T and G123S, hydrophobic and neutral side chains respectively, are replaced replace with a polar functional group. As previously observed[33], only certain amino acids show a specific propensity to become part of an alpha helix[33]: according to the proposed scale, the helical penalty of threonine and serine are 0.66 Kcal/mol and 0.50 Kcal/mol. Such thermodynamic penalties can be related to steric clashes and the formation of new hydrogen bonds, as we propose in our models. The substitution with such amino acids can therefore lead to a destabilization to the wild type, and this reinforces the validity of the model calculated for the I100T and G123S which were found to be more active to cleave the methotrexate compared to T329A.

Further information on these points will probably require X-Ray crystallographic or NMR studies on the mutants. Such studies might also open a rational pathway for further changes to produce other variants with different features.

Conclusion

In this study, we produced three novel glucarpidase variants with improved enzyme activity. The mutants may be beneficial in MTX detoxification and may also have applications in targeted cancer strategies such as ADEPT.

Conflict of interest

All authors declare that they have no conflict of interest

Acknowledgements

QNRF grant number NPRP6-065-3-012, Qatar National Research Fund, Doha Qatar for funding this work with grant number NPRP No.: NPRP6-065-3-012.

Author Contribution

ADA and SSB designed the experiment under the supervision of AD and SG, performed the experiments and analyzed the data and wrote the first draft: FBR, performed experimental work, supervision, and contributed to the data analysis. ARR performed the X ray prediction work, DOC, writing – review & editing the manuscript, AD and SKG supervised the work, and SKG the overall supervision of the project

All authors discussed the manuscript and approved it for publications.

Appendix A. Supplementary data

The following is Supplementary data to this article:

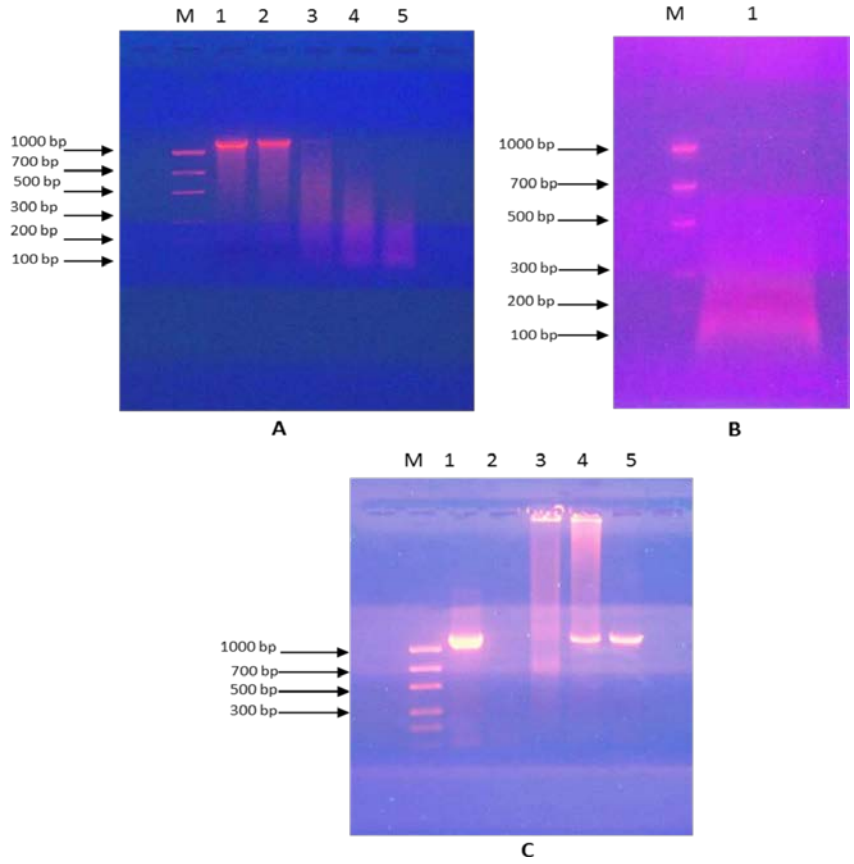

Supplemental Figure S1. DNA shuffling of glucarpidase**. A.** Time course of DNase digestion of the purified error-prone CPG2 DNA analysed by 2% agarose gel electrophoresis. M is the MassRuler™ Express DNA Ladder LR Forward (100-1000 bp); lanes 1-5 contain samples digested with DNase I for 30- sec, 1, 2, 3 and 5 min. (see experimental section for more details), **B.** Large scale DNase digestion of the error-prone PCR product where the 200-300bp size fragments were cut, and the DNA fragments were eluted, **C.** An overall summary of the entire DNA mutagenesis process, showing different stages in the production of variants of the CPG2 gene. M is the MassRuler™ Express DNA Ladder LR Forward (100-1000 bp); lane 1, error-prone PCR product; lane 2, DNase I fragments; lane 3, self-reassembled (primerless) PCR; lane 4, amplified PCR product obtained using specific primers for CPG2; lane 5 , purified shuffled PCR product ready for cloning.

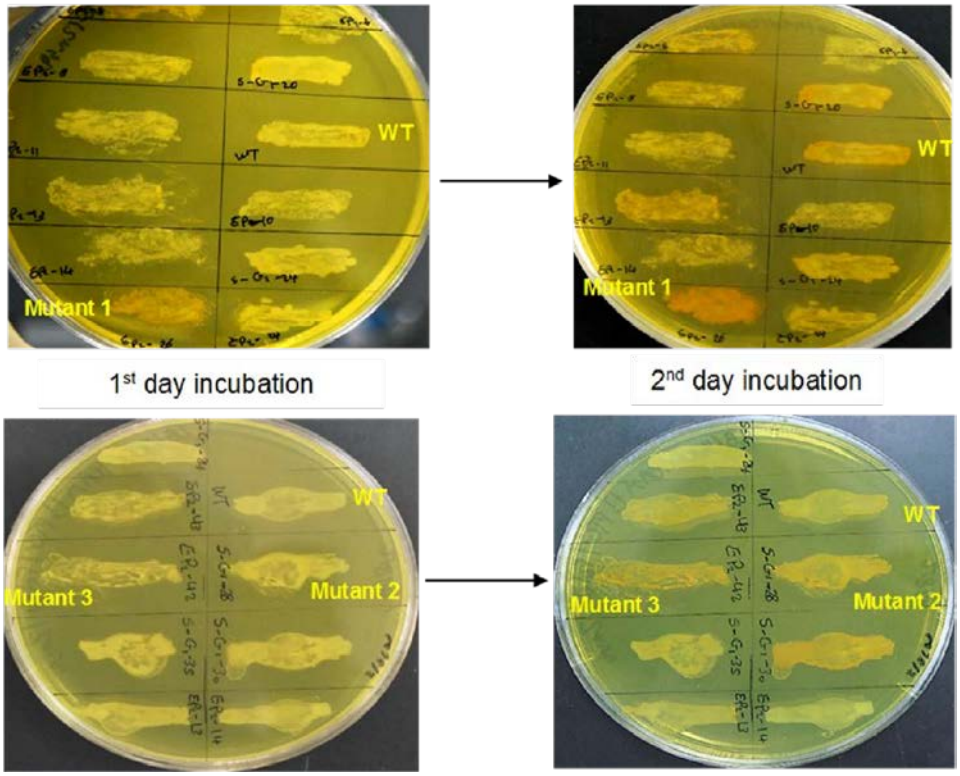

Supplemental Figure S2. Screening of the mutant CPG2 constructs in *E. coli* BL21(DE3)RIL by growth on LB plates supplemented with kanamycin, chloramphenicol, folate and IPTG. The arrow indicates an isolate that shows significantly darker coloration after two days of incubation relative to cells harboring the original pET28a-CPG2 construct. The higher the activity of glucarpidase, the more insoluble material will be produced and hence the darker the color formed.

Supplemental Figure S3. Multiple alignments of the amino acid sequences of the active glucarpidase gene mutants - CPG2I100T, CPG2G123S, and CPG2T329A - relative the wild type. Substituted amino acids, produced by shuffling, are underlined in red.

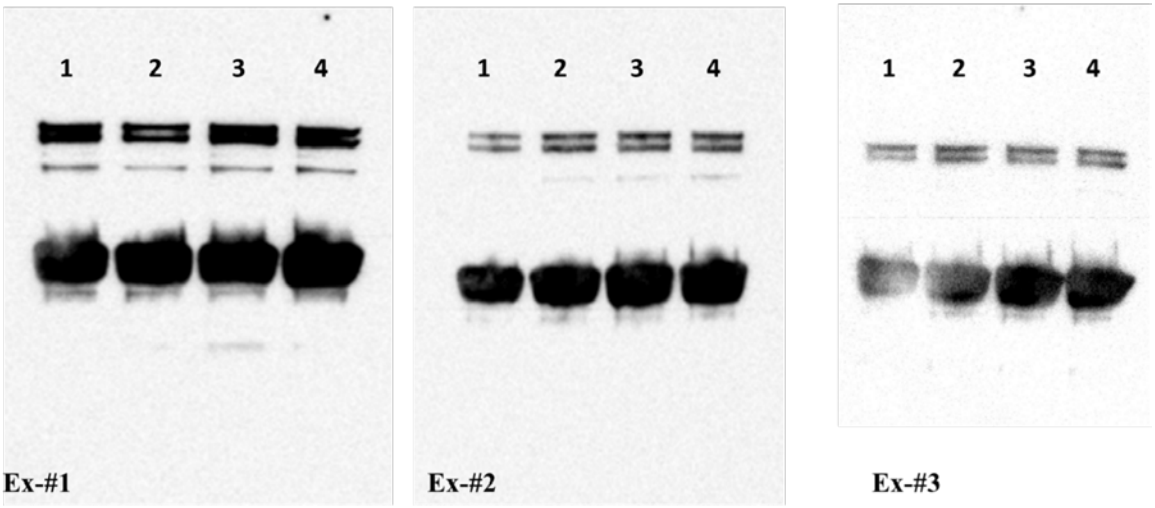

Supplemental Figure S4. Ex-#1, Ex-#2, and Ex-#3 are three independent western blot replicates. Lanes 1, 2, 3 and 4 are WT CPG2, CPG2 I100T, CPG2 T329A and CPG2 G123S, respectively

References

1. Burke PJ. The potential use of carboxypeptidase G2 in the treatment of cancer. Expert Opinion on Therapeutic Patents. 2000;10(2):209-14. doi: 10.1517/13543776.10.2.209.
2. Sharma SK, Bagshawe KD. Antibody Directed Enzyme Prodrug Therapy (ADEPT): Trials and tribulations. Adv Drug Deliv Rev. 2017;118:2-7. doi: 10.1016/j.addr.2017.09.009. PubMed PMID: 28916498.
3. Sharma SK, Bagshawe KD. Translating antibody directed enzyme prodrug therapy (ADEPT) and prospects for combination. Expert Opin Biol Ther. 2017;17(1):1-13. doi: 10.1080/14712598.2017.1247802. PubMed PMID: 27737561.
4. Mishra AP, Chandra S, Tiwari R, Srivastava A, Tiwari G. Therapeutic Potential of Prodrugs Towards Targeted Drug Delivery. Open Med Chem J. 2018;12:111-23. doi: 10.2174/1874104501812010111. PubMed PMID: 30505359; PubMed Central PMCID: PMCPMC6210501.
5. Mohty M, Peyriere H, Guinet C, Hillaire-Buys D, Blayac JP, Rossi JF. Carboxypeptidase G2 rescue in delayed methotrexate elimination in renal failure. Leukemia & lymphoma. 2000;37(3-4):441-3. Epub 2000/04/07. doi: 10.3109/10428190009089446. PubMed PMID: 10752997.
6. Buchen S, Ngampolo D, Melton RG, Hasan C, Zoubek A, Henze G, et al. Carboxypeptidase G2 rescue in patients with methotrexate intoxication and renal failure. British journal of cancer. 2005;92:480. doi: 10.1038/sj.bjc.6602337.
7. Ramsey LB BF, O'Brien MM, Schmiegelow K, Pauley JL, Bleyer A, Widemann BC, Askenazi D, Bergeron S, Shirali A, Schwartz S, Vinks AA, Heldrup J Consensus Guideline for Use of Glucarpidase in Patients with High-Dose Methotrexate Induced Acute Kidney Injury and Delayed Methotrexate Clearance. Oncologist. 2018 Jan;23(1):52-61. doi: 10.1634/theoncologist.2017-0243.
8. Dijkman MA dLD, de Vries I. Do not exclude glucarpidase too soon in the context of high-dose methotrexate induced nephrotoxicity. Neth J Med. 2018 May;76(4):204.
9. Garcia H LV, Goldwasser F, Bouscary D, Raffoux E, Boissel N, Broutin S, Joly D. Renal toxicity of high-dose methotrexate]. Nephrol Ther 2018 Apr;14(Suppl 1):S103-S13. doi: 10.1016/j.nephro.2018.02.015.

10. Packer MS, Liu DR. Methods for the directed evolution of proteins. Nature Reviews Genetics. 2015;16:379. doi: 10.1038/nrg3927.
11. Chang CC, Chen TT, Cox BW, Dawes GN, Stemmer WP, Punnonen J, et al. Evolution of a cytokine using DNA family shuffling. Nature biotechnology. 1999;17(8):793-7. Epub 1999/08/03. doi: 10.1038/11737. PubMed PMID: 10429246.
12. Ness JE, Welch M, Giver L, Bueno M, Cherry JR, Borchert TV, et al. DNA shuffling of subgenomic sequences of subtilisin. Nature biotechnology. 1999;17(9):893-6. Epub 1999/09/03. doi: 10.1038/12884. PubMed PMID: 10471932.
13. Christians FC, Scapozza L, Crameri A, Folkers G, Stemmer WP. Directed evolution of thymidine kinase for AZT phosphorylation using DNA family shuffling. Nature biotechnology. 1999;17(3):259-64. Epub 1999/03/30. doi: 10.1038/7003. PubMed PMID: 10096293.
14. Bruhlmann F, Chen W. Tuning biphenyl dioxygenase for extended substrate specificity. Biotechnology and bioengineering. 1999;63(5):544-51. Epub 1999/07/09. PubMed PMID: 10397810.
15. Zhao H, Arnold FH. Optimization of DNA shuffling for high fidelity recombination. Nucleic acids research. 1997;25(6):1307-8. Epub 1997/03/15. PubMed PMID: 9092645; PubMed Central PMCID: PMCPMC146579.
16. Kikuchi M, Ohnishi K, Harayama S. Novel family shuffling methods for the in vitro evolution of enzymes. Gene. 1999;236(1):159-67. Epub 1999/08/06. PubMed PMID: 10433977.
17. Tong Q-Q, Zhou Y-H, Chen X-S, Wu J-Y, Wei P, Yuan L-X, et al. Genome shuffling and ribosome engineering of Streptomyces virginiae for improved virginiamycin production. Bioprocess and Biosystems Engineering. 2018;41(5):729-38. doi: 10.1007/s00449-0181906-3.
18. Stemmer WP. DNA shuffling by random fragmentation and reassembly: in vitro recombination for molecular evolution. Proceedings of the National Academy of Sciences of the United States of America. 1994;91(22):10747-51. Epub 1994/10/25. PubMed PMID: 7938023; PubMed Central PMCID: PMCPMC45099.
19. Goda SK, Rashidi FA, Fakharo AA, Al-Obaidli A. Functional overexpression and purification of a codon optimized synthetic glucarpidase (carboxypeptidase G2) in Escherichia coli. The protein journal. 2009;28(9-10):435-42. Epub 2009/11/17. doi: 10.1007/s10930-009-9211-2. PubMed PMID: 19911261.
20. Rashidi FB, AlQhatani AD, Bashraheel SS, Shaabani S, Groves MR, Dömling A, et al. Isolation and molecular characterization of novel glucarpidases: Enzymes to improve the antibody directed enzyme pro-drug therapy for cancer treatment. PLoS ONE. 2018;13(4):e0196254. doi: 10.1371/journal.pone.0196254. PubMed PMID: PMC5919439.
21. McCullough JL, Chabner BA, Bertino JR. Purification and properties of carboxypeptidase G 1. The Journal of biological chemistry. 1971;246(23):7207-13. Epub 1971/12/10. PubMed PMID: 5129727.
22. Pires DE AD, Blundell TL. mCSM: predicting the effects of mutations in proteins using graph-based signatures. Bioinformatics. 2014;30(3):335-42. doi: 10.1093/bioinformatics/btt691.
23. Pandurangan AP, Ochoa-Montano B, Ascher DB, Blundell TL. SDM: a server for predicting effects of mutations on protein stability. Nucleic acids research. 2017;45(W1):W229-w35. Epub 2017/05/20. doi: 10.1093/nar/gkx439. PubMed PMID: 28525590; PubMed Central PMCID: PMCPMC5793720.
24. Pires DE AD, Blundell TL. DUET: a server for predicting effects of mutations on protein stability using an integrated computational approach. Nucleic acids research. 2014;42(web Server issue):W314-9. doi: 10.1093/nar/gku411.
25. Sali A, Blundell TL. Comparative protein modelling by satisfaction of spatial restraints. Journal of molecular biology. 1993;234(3):779-815. Epub 1993/12/05. doi:

10.1006/jmbi.1993.1626. PubMed PMID: 8254673.
26. Marti-Renom MA, Stuart AC, Fiser A, Sanchez R, Melo F, Sali A. Comparative protein structure modeling of genes and genomes. Annual review of biophysics and biomolecular structure. 2000;29:291-325. Epub 2000/08/15. doi: 10.1146/annurev.biophys.29.1.291. PubMed PMID: 10940251.
27. Fiser A, Do RK, Sali A. Modeling of loops in protein structures. Protein science : a publication of the Protein Society. 2000;9(9):1753-73. Epub 2000/10/25. doi: 10.1110/ps.9.9.1753. PubMed PMID: 11045621; PubMed Central PMCID: PMCPMC2144714.
28. Webb B, Sali A. Protein Structure Modeling with MODELLER. Methods in molecular biology (Clifton, NJ). 2017;1654:39-54. Epub 2017/10/08. doi: 10.1007/978-1-49397231-9_4. PubMed PMID: 28986782.
29. AlQahtani AD, Al-Mansoori L, Bashraheel SS, Rashidi FB, Al-Yafei A, Elsinga P, et al. Production of "biobetter" glucarpidase variants to improve drug detoxification and antibody directed enzyme prodrug therapy for cancer treatment. European journal of pharmaceutical sciences : official journal of the European Federation for Pharmaceutical Sciences. 2018;127:79-91. Epub 2018/10/22. doi: 10.1016/j.ejps.2018.10.014. PubMed PMID: 30343151.
30. Minton NP, Atkinson T, Sherwood RF. Molecular cloning of the Pseudomonas carboxypeptidase G2 gene and its expression in Escherichia coli and Pseudomonas putida. Journal of bacteriology. 1983;156(3):1222-7. Epub 1983/12/01. PubMed PMID: 6358192; PubMed Central PMCID: PMCPMC217971.
31. Tokuriki N SF, Serrano L, Tawfik DS. How protein stability and new functions trade off. PLoS Comput Biol. 2008 4(2):e1000002. doi: 10.1371/journal.pcbi.1000002
32. Teilum K, Olsen JG, Kragelund BB. Protein stability, flexibility and function. Biochimica et biophysica acta. 2011;1814(8):969-76. Epub 2010/11/26. doi: 10.1016/j.bbapap.2010.11.005. PubMed PMID: 21094283.
33. Pace CN, Scholtz JM. A helix propensity scale based on experimental studies of peptides and proteins. Biophys J. 1998;75(1):422-7. Epub 1998/07/02. PubMed PMID: 9649402; PubMed Central PMCID: PMCPMC1299714.

Chapter 5:

Production of “biobetter” glucarpidase variants to improve Drug Detoxification and Antibody Directed Enzyme Prodrug Therapy for Cancer Treatment

Alanod D. AlQhatani[1,2] , Layla Al-mansoori[1,3] , Sara S Bashraheel[1,2], Fatma B Rashidi[4], Afrah Al-Yafei[1], Philip Elsinga[3], Alexander Domling[2] and Sayed K Goda[1]

[1] Protein Engineering Unit, Life and Science Research Department, Anti-Doping LabQatar (ADLQ), Doha, Qatar.

[2]Drug Design Group, Department of Pharmacy, University of Groningen, Groningen, Netherlands

[3]University of Groningen, University, Medical Center Groningen (UMCG), Groningen, Netherlands.

[4]Cairo University, Faculty of Science, Chemistry Department, Giza, Egypt

Eur J Pharm Sci. 2019 Jan 15;127:79-91. doi:10.1016/j.ejps.2018.10.014.

Table of Contents

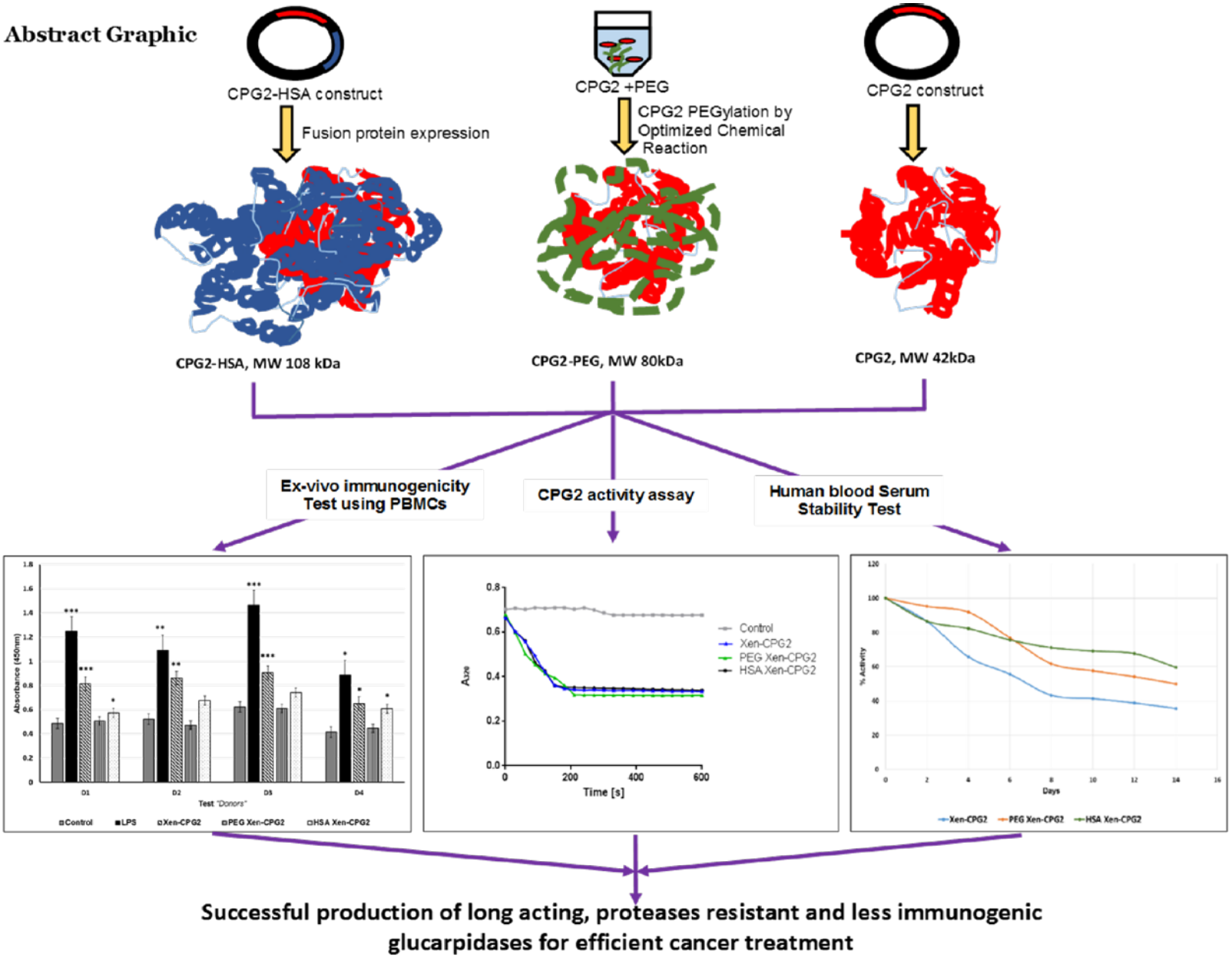
Abstract Graphic
CPG2-HSA construct
Fusion protein expression
CPG2 +PEG
CPG2 PEGylation by Optimized Chemical Reaction
CPG2 construct
CPG2-HSA, MW 108 kDa
CPG2-PEG, MW 80kDa
CPG2, MW 42kDa
Ex-vivo immunogenicity Test using PBMCs
CPG2 activity assay
Human blood Serum Stability Test
Absorbance (450nm)
Test "Donors"
D1
D2
D3
D4
Control
LPS
Xen-CPG2
PEG Xen-CPG2
HSA Xen-CPG2
Azo
Time [s]
Control
Xen-CPG2
PEG Xen-CPG2
HSA Xen-CPG2
% Activity
Days
Xen-CPG2
PEG Xen-CPG2
HSA Xen-CPG2
Successful production of long acting, proteases resistant and less immunogenic glucarpidases for efficient cancer treatment

Abstract

Recombinant glucarpidase (formerly: Carboxypeptidase G2, CPG2) is used in Antibody Directed Enzyme Prodrug Therapy (ADEPT) for the treatment of cancer. In common with many protein therapeutics, glucarpidase has a relatively short half-life in serum and, due to the need for the repeated cycles of the ADEPT, its bioavailability may be further diminished by neutralizing antibodies produced by patients. PEGylation and fusion with human serum albumin (HSA) are two approaches that are commonly employed to increase the residency time of protein therapeutics in blood, and also to increase the half-lives of the proteins in vivo. To address this stability and the immunogenicity problems, 'biobetter' glucarpidase variants, mono-PEGylated glucarpidase, and HSA fused glucarpidase by genetic fusion with albumin, were produced. Biochemical and bioactivity analyses, including anti-proliferation, bioassays, circular dichroism, and in vitro stability using human blood serum and immunoassays, demonstrated that the functional activities of the designed glucarpidase conjugates were maintained. The immunotoxicity studies indicated that the PEGylated glucarpidase did not significantly induce T-cell proliferation, suggesting that glucarpidase epitopes were masked by the PEG moiety. However, free glucarpidase and HSA-glucarpidase significantly increased T-cell proliferation compared with the negative control. In the latter case, this might be due to the type of expression system used or due to trace impurities associated with the highly purified (99.99%) recombinant HSAglucarpidase. Both PEGylated glucarpidase and HSA-glucarpidase exhibit more stability in human serum and were more resistant to key human proteases relative to native glucarpidase. To our knowledge, this study is the first to report stable and less immunogenic glucarpidase variants produced by PEGylation and fusion with HSA. The results suggest that they may have better

efficacy in drug detoxification and ADEPT, thereby improving this cancer treatment strategy.

Keywords

Carboxypeptidase G2; CPG2; Antibody Directed Enzyme Prodrug Therapy; ADEPT; PEGylation; human serum albumin; HSA; HSA-glucarpidase; PEGylated glucarpidase; Cancer.

Introduction

The US Food and Drug Administration has approved more than 180 therapeutic peptides and proteins for many applications and disease treatments. Because most of these proteins and peptides are smaller in size than the kidney filtration cutoff of ~70 kDa, they do not have optimal pharmacokinetics. Thus, these protein and peptide therapeutics have short half-lives *in vivo*, due to the action of proteases and the generation of antibodies against them [1].

Due to these features, therapeutic proteins and peptides needed to be injected frequently and in high dose. This not only results in the need for more frequent treatments, often leading to patient non-compliance, but it also results in reduced drug efficacy.

One of the therapeutic proteins used in cancer therapy is glucarpidase, also known as Carboxypeptidase G2, CPG2, which originates from the bacterium *Variovorax paradoxus* (old name, *Pseudomonas* sp. strain RS-16). It has no mammalian equivalent [2, 3] and is a zinc-dependent dimeric protein with two subunits of 41 kDa [4, 5]. Glucarpidase has a relatively restricted specificity and hydrolyzes the Cterminal glutamic acid residue of folic acid and folate analogues such as methotrexate [6]. The mechanism of action of glucarpidase is, therefore, to lower systemic methotrexate levels by rapidly causing methotrexate to be converted to glutamate and 4-deoxy-4-amino-N 10-methylpteroic acid (DAMPA), both of which undergo hepatic metabolism.

Glucarpidase, consequently, provides an alternative route for methotrexate elimination in patients with impaired renal function. This action of glucarpidase on methotrexate makes the enzyme not only a powerful rescue agent in patients receiving

high doses of methotrexate but also helps to avoid life-threatening toxicity in patients with methotrexate intoxications.

The enzyme can also be used in a targeted cancer therapy technique known as Antibody Directed Enzyme Prodrug Therapy (ADEPT), which has already been implemented for cancer treatment [7].

ADEPT consists of two steps (fig. 1), which result in the production of a powerful cytotoxic drug only in the vicinity of the tumor. In the first step, a tumor-selective antibody is chemically linked to an enzyme and then administered intravenously to the patient. The second step includes the injection of a non-toxic drug precursor (Prodrug).

The enzyme, which accumulates at the tumor site via the tumor-specific antibody, converts the prodrug into an active drug. This therapy, therefore, produces a powerful cytotoxic drug in the vicinity of the tumor with little toxicity elsewhere in the patient body. One of the enzymes that has been used in the ADEPT is the glucarpidase from *V. paradoxus* strain RS-16, which when applied has been shown to result in antitumor activity in different types of cancer [8-11].

The use of glucarpidase in the ADEPT and the drug detoxification are effective but have limitations. The treatment requires repeated cycles, which results in a severe immune response against the glucarpidase and, additionally, proteases present in patients' blood degrade the enzyme thereby limiting its therapeutic applicability.

We recently isolated a new glucarpidase that shares 94% amino acid identity with the one produced by *V. paradoxus* strain RS-16 [13]. We also demonstrated that antibodies

raised against the newly isolated glucarpidase do not react with the one from *V. paradoxus* strain RS-16.

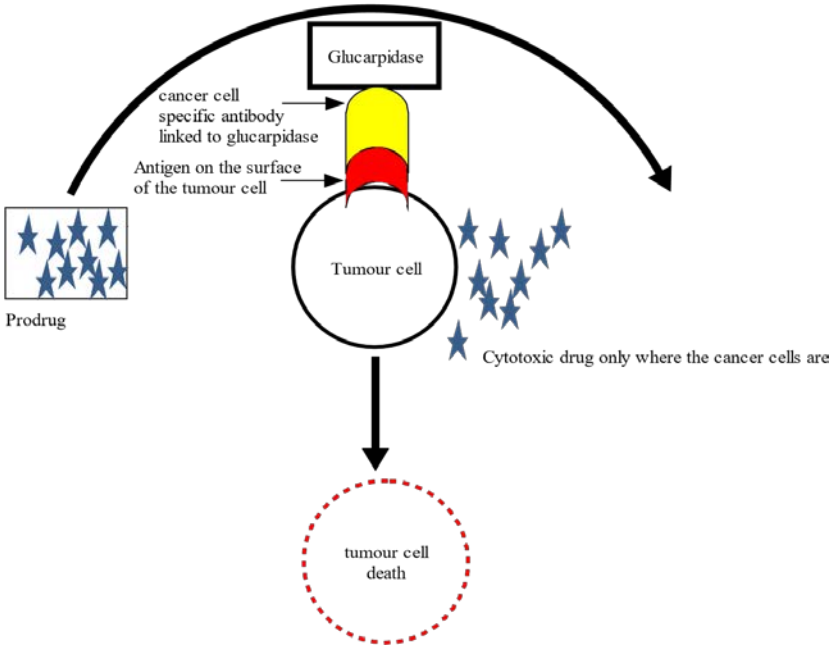

Fig. 1. The principle of ADEPT. The first step is the injection of the antibody-enzyme fusion protein, which localizes to tumors. The second step is the injection of a prodrug, following clearance of the fusion protein from the blood. The localized glucarpidase converts the prodrug into the cytotoxic drug, which can diffuse through the tumor and kill antigen-containing tumor cells as well as tumor cells that are nearby but do not express the relevant antigen, thus giving a "bystander" effect [12].

In this work, we report the production of long-acting variants of our glucarpidase to overcome the complications related to the multiple cycles of ADEPT. A number of strategies have been developed to address the issue of immunogenicity and to improve the pharmacokinetics of protein and peptide therapeutics. These include PEGylation, i.e. the attachment of polyethylene glycol (PEG) polymer chains, fusion with human serum albumin (HSA), fusion with non-structured polypeptides, and fusion with the constant fragment (Fc) domain of a human immunoglobulin (Ig)G [14]. In this study, we focused our work on the production of 'biobetter' glucarpidases by using PEGylation (PEG) and fusion with the Human serum albumin (HSA).

PEGylation technology has already been used successfully to produce long-acting proteins. For example, PEGylated forms of interferon α2b and interferon α2a, which are known commercially as Pegintron and Pegasys respectively, have been used for the treatment of treatment of patients with melanoma and hepatitis B. Similarly, a PEGylated version of granulocyte colony-stimulating factor has been used for the treatment of chemotherapy-induced neutropenia [15-17].

Human serum albumin, which has a circulation half-life of nineteen days[18], has also been used to extend the half-life of biopharmaceuticals and to maintain their bioactivity[19, 20]. Protein therapeutics that have been improved using this strategy include vascular endothelial growth factor [21], interferon [22, 23], and interleukin-2 [24].

In this study, we implemented the two strategies, PEGylation of Lys residues and genetic fusion with human serum albumin, to produce long-acting glucarpidases to overcome current problems with ADEPT in cancer treatment.

Glucarpidase is clinically important enzyme in the antibody directed enzyme prodrug therapy and also in drug detoxification. Both applications have several pitfalls. We report, for first time, the production of novel glucarpidase variants with long acting and higher stability features than the free enzyme. Our work will pave the way for clinical investigation and in vivo studies.

Experimental Section

Bacterial strains, plasmids, and growth conditions.

The following strains of *E. coli*: Mach1™ T1R cells, DH5α™ *E. coli*, both from Thermo Fischer Scientific were used as cloning hosts and for plasmid propagation. Other strains such as BL21(DE3) RIL, Bl21 (DE3) and Rosetta™(DE3) Competent Cells

(Novagen) were used for protein expression of the recombinant proteins. The plasmid pEX-K4 (Eurofins) was used for subcloning of the CPG2 to be conjugated with HSA, and pET28a (Novagen, Stratagen) was used for recombinant protein expression in *E. coli*. All recombinant bacterial strains were grown in Luria Bertani broth (Sigma life sciences) for liquid culture, which was solidified with agar (Sigma life sciences) for solid culture media.

Restriction enzymes, Antibodies and other chemicals

Restriction endonucleases and other enzymes required for cloning were from New England Biolabs. *Nde*I/*Hin*dIII were used for subcloning of CPG2 into pEX-K4HSA, and *Kpn*I/ *Eco*R1 and *Hin*dIII were used to release the new conjugate into pET28a for expression study, and Calf Intestinal Alkaline phosphatase was used for vector dephosphorylation. T4 DNA ligase (Thermo Fischer Scientific) was used for the ligation step. T7 promoter: 5´-TAATACGACTCACTATAGGG-3´ and T7 terminator 5´-GCTAGTTATTGCTCAGCGG-3´ primers were obtained from Eurofins and used as universal primers for sequencing and subcloning confirmation. For protein purification by nickel affinity chromatography, Ni-NTA resin (Sigma) was used. Quick-Load® Purple 1 kb DNA Ladder (NEB) was used as the DNA marker while the SeeBlue Plus2 Prestained ladder (198-10 kDa) (Thermo Fischer Scientific) was used as protein markers. The GeneJET Plasmid Miniprep and Gel Extraction Kits (Thermo Fischer Scientific) were used for plasmid mini preparations and for DNA extraction and purification from gels, respectively. NuPAGE 10% Bis-Tris Gel Novex (Life Technologies) was used for SDS-PAGE Nitrocellulose Membrane (Thermo Fischer Scientific) was used for immunoblotting. Dialysis tube (Spectra/Por 7 Dialysis Tubing, 10 kDa MWCO, 24 mm Flat-width, 5 meters/roll (16 ft) (Spectrum) and dialysis tube of 50 kDa MWCO (Fischer Scientific) were used for exchanging buffers for proteins.

The PEGylation reagent used was Y-shape (MPEG20K) 2-Succinimidyl Carboxymethyl Ester, MW 40000 (JenKem Technology). The following antibodies were used: mouse 6x-His Tag Monoclonal Antibody (HIS.H8) (Invitrogen) (1:2000 dilution), rabbit polyclonal anti Xen-CPG2 antibody (GE Healthcare) (1:2000 dilution), mouse anti-human serum albumin antibody [15C7] (ab10241) (Abcam) (1:500 dilution), rabbit anti-polyethylene glycol antibody [PEG-B-47] (ab51257) Abcam (1:2000 dilution) were used as primary antibodies for protein detection and goat anti-Mouse IgG H&L (HRP) (ab205719) from Abcam (1:4000 dilution) and goat anti-Rabbit IgG H&L (HRP) (ab6721) from Abcam (1:5000 dilution) were used as secondary conjugated antibodies. An ECL chemiluminescent detection reagent (GE Healthcare) was used as the substrate for detection of bound antibodies in western blotting.

Designing and construction Human Serum Albumin (HSA) to Xen-CPG2

The Human Serum Albumin (HSA) gene was custom synthesized by Eurofins genomics and inserted into the vector pEX-K4. The resulting construct was transformed into competent *E. coli* DH5alpha for propagation. pEX-K4-HSA was digested using *Nde*I/ *Hin*dIII and used as the receiving vector for insertion of a similarly digested DNA fragment carrying Xen-CPG2, which originated from a pET28a vector. Plasmid DNA from the resulting construct, designated pEX-K4HSA-CPG2 and carrying a gene coding for an HSA-CPG fusion, was digested with *Kpn*I/*Hin*dIII to release the HSA-CPG2 gene fusion and then further digested with *Eco*RI prior to insertion into the *Eco*RI/*Hin*dIII digested expression vector pET28a. The structure of the resulting construct, pET28a-Xen CPG2-HSA, was checked by

restriction digestion and sequencing using T7 promoter and terminator universal primers.

Protein Expression of HSA Xen-CPG2 protein

E. coli BL21(DE3)RIL cells containing the pET28a-Xen CPG2-HSA were grown in LB medium supplemented with kanamycin and chloramphenicol at final concentrations of 33 µg/mL and 34 µg/mL, respectively. Following overnight incubation at 37 °C with shaking (200 rpm), 5 ml of the culture was added to 1L of fresh LB-broth containing the required antibiotics. The culture was incubated at 37 °C for 4 hours in an incubator shaker until the optical density at 600 nm was 0.5-0.6, at which point the culture was induced using isopropyl-β-Dthiogalactopyranoside (IPTG) at a final concentration of 0.5 mM or left uninduced as the control. Following further incubation for four hours at 37 °C at 200 rpm, cells were harvested by centrifugation for 15 min at 4 °C and 4000 rpm. Cell pellets were re-suspended in 20 mM Tris buffer, pH 8 and 50 mM NaCl and were disrupted by sonication (MSE Soniprep 150 Plus) on ice (8 cycles of 30 sec pulses followed by 30 sec rest). Cell lysates were centrifuged at 14,000 rpm for 30 min at 4 °C for separation of the soluble and insoluble fractions. Each fraction was mixed with an equal volume of 2X sample buffer, denatured by boiling for 10 minutes at 95 °C, and then analyzed by SDS-PAGE. For maximum soluble protein production, cultures were induced with IPTG overnight at 20 °C.

Ni-NTA Purification of the HSA Xen-CPG2

The Xen-HSA CPG2 fusion protein was designed with a six-histidine tag at its Nterminus. Consequently, this protein was purified by Ni-NTA affinity

chromatography. The resin was washed with sterile Milli-Q water and activated using a binding-washing buffer containing Tris (20 mM) pH 8, NaCl (50 mM), BME (5 mM), and imidazole (20 mM). Total soluble protein from *E. coli* BL21(DE3)RIL cells containing the pET28a-Xen CPG2-HSA was incubated with the resin with gentle agitation for 30 min at 4 °C. The combined resin was separated by gravity, the flow-through collected, and then the resin was washed repeatedly with wash buffer. The target protein bound to the resin was released by adding ice-cold elution Tris buffer containing 400 mM imidazole. The eluted protein was dialyzed against 100 mM Tris-HCl pH 7.3 containing 0.2 mM $ZnSO_4$ for activity assay. All collected fractions of protein purification steps were analyzed by SDS-PAGE.

Conjugation of Poly Ethylene Glycol (PEG) into Xen-CPG2

The purified CPG2, at a concentration of 0.5mg/ml, was dialyzed against 1X PBS pH 6 and subjected PEGylation by addition 1–5 fold molar excess of PEGylation reagent Y-shape (MPEG20K)2 Succinimidyl Carboxymethyl (SCM) Ester of MW 40,000 (JenKem Technology) in 100 mM sodium phosphate at pH 6, at room temperature for 30 min – 4 h. The same reaction was carried out at 30 ^{o}C, The PEGylation reaction was followed by SDS Gel analysis and the incubation time was prolonged to optimize the PEG binding to the CPG2 protein using a modification of the previous method[25].

. Larger scale PEGylation was achieved by mixing of 5 mg/ml of the CPG2 protein with a 3-fold molar excess of PEGylation reagent Y-shape (Y-SCM-40K), with rapid and thorough shaking by vortex followed by incubation at 30 ^{o}C in an incubator shaker at 200 rpm for 10 hours. The PEGylated CPG2 mixture was then subjected to Ni-NTA purification to remove the excess non-reactive PEGylation reagent and further purified by gel filtration using an AKTA purifier. Finally, the purified PEGylated CPG2

conjugate was isolated and quantified. Determination of PEGylated and HSA conjugated CPG2 catalytic enzyme kinetics

The glucarpidase activities of the pure recombinant HSA-CPG2 (≈2 μg/ml) and PEG-CPG2 (≈2 μg/ml) was determined by measuring methotrexate hydrolytic activity using Tris buffer (0.1 M Tris-HCl pH 7.3 and 0.2 mM ZnSO4) containing

Methotrexate (MTX) (0.27 mM) as substrate and measured spectrophotometrically using Plate Reader Infinite M200 PRO NanoQuant (TECAN) at 320 nm, 37 ^{o}C for 1 hour.

Kinetic studies of these modified CPG2 (HSA Xen-CPG2 and PEG Xen-CPG2 of ≈2 μg/ml), were also assayed by testing their activities at different MTX concentrations (30-420 μM) in the required Tris-$ZnSO_4$ buffer using Nunc 96 plates with UV transparent flat bottom wells, to determine the stability constant (Km) and the rate of reaction (Vmax). All reactions were carried out at 37 °C for 2 min and the decrease in absorbance at 320 nm was monitored using Plate reader, Infinite M200 PRO NanoQuant. The Michaelis-Menten equation was used for determination of the actual values of Km, Kcat, and Vmax of each protein using GraphPad PRISM 6 software.

One unit of the enzyme represents the amount of enzyme in mg required for hydrolysis of 1 mM of MTX per min at 37 ^{o}C. The enzyme activity per ml of protein was calculated using 8,300 as the molar extinction coefficient for MTX.

Circular Dichroism and secondary structure analyses of the modified CPG2

a) Pre-CD Scanning

Purified preparations of the CPG2 (HSA Xen-CPG2 and PEG Xen-CPG2) proteins were dialyzed against Milli-Q water 4 times each for 18 hours, followed by centrifugation for 30 min. at 4 °C. A NanoDrop 2000 spectrophotometer (Thermo Scientific) was used for measuring the protein concentration and the required concentration for CD measurement for each protein was adjusted to about 8-10

μM. The extinction coefficients were taken as ε = 66305 and 23380 M^{-1} cm^{-1} for HSA Xen-CPG2 and PEG Xen-CPG2, respectively.

b) Circular dichroism (CD)

Measurements were made using Chirascan™ Plus CD Spectrometer (Applied Photophysics). CD scanning of the modified CPG2 in far UV spectral region was measured using a SUPRASIL Quartz cuvette demountable rectangular (Hellma®) of 0.2 mm light-path length (sample volume ~70 μl). Scans were made from 260 to 180 nm. All proteins were tested at conc. 8-10 μM at 20 °C. The applied CD parameters were as follows: bandwidth 1 nm and scan time per point of 0.5 sec. Four scans were taken per one sample, and these readings were averaged and smoothed using the CD analysis software. The produced spectra were subtracted from an averaged CD spectra of the used blank (Milli Q water) baseline.

c) CD- deconvolution method

Protein secondary structure of the pure recombinant modified CPG2 were calculated by CD data deconvolution analysis using the CDNN (version 2.1) software tool. The Deconvolution calculation was carried out in the spectral range of (180–260 nm). The parameters used in the deconvolution calculations, the number of residues and molecular weight were taken as 1018 AAs, with 112.38344 kDa for HSA Xen-CPG2 and

81.76148 kDa and 392 AAs for PEG Xen-CPG2 respectively, and 0.02 cm light-pathlength of the cuvette was used.

Mass Spectra analysis of HSA-glucarpidase fusion protein

The purified fusion protein was analyzed on 8% SDS-PAGE electrophoresis. The extracted band-containing HSA-glucarpidase protein was subjected to protein digestion with Trypsin Gold (mass spec grade, Promega) using in gel digestion protocol according to manufacturer's instruction.

The digested proteins were then analyzed by tandem mass spectrometry (LCMS/MS) using LC/MS LTQ-Orbitrap Elite.

Extracted data was analyzed to identify the protein sequence against protein database using PEAKS Studio software.

CPG2 and its modified forms stability assay

The structural stability of resulting purified proteins was determined by incubation of the 0.1µg/µl purified free Xen-CPG2, PEG Xen-CPG2 and HSA Xen-CPG2 with human serum samples from a normal donor at 37 ^{o}C. Samples collected every 5 days for 15 days and analyzed by western blotting. Samples (1µg/lane) were separated on non-denatured gels (native-PAGE) and transferred to nitrocellulose membranes electrostatically. The resulting membranes were blocked with 5% nonfat milk in 1x PBS for 1 hour at room temperature, then incubated with rabbit anti Xen-CPG2 antibody (1:2000) in 1% non-fat milk for 1 hour at room temperature. Following washing, the membranes were incubated with a secondary antibody (horseradish peroxidase conjugated mouse anti-rabbit antibody), the antibody binding detected

with ECL chemiluminescent detection reagent as described by the supplier (GE Healthcare).

A further serum stability assay was carried out to investigate the functional stability of the resulting CPG2 proteins. 0.1µg/µl of purified free CPG2, PEG Xen-CPG2and HSA Xen-CPG2 proteins were incubated with serum samples from a normal donor at 37$_{o}$C for more than12 days. A sample was taken every 2 days and the catalytic activity of the glucarpidase moieties was measured using the MTX hydrolysis assay described above. The percentage of remaining activity at each point was calculated and plotted against the time of sample taking.

Ex-vivo immunogenicity

The immunogenicity of the resulting purified proteins was investigated using a proliferation assay for human peripheral blood mononuclear cells (PBMCs) from normal healthy donors. Total blood samples were collected and the PBMCs separated using ficoll solution (Sigma) and density centrifugation. The isolated PBMCs were cultured at 1 x 10$_{6}$ cells/ml of X-vivo medium in 96 well plates. Cells were incubated for 48 hours at 37 °C with the purified endotoxin-free proteins (free

Xen-CPG2, PEG Xen-CPG2, and HSA Xen-CPG2) (10µg/ml). Pierce LAL Chromogenic Endotoxin Quantitation Kit was used to detect the level of endotoxin in the purified CPG2 protein samples and, where necessary, endotoxin levels were reduced to > 0.1EU/ml using Pierce™ High Capacity Endotoxin Removal Resin. Following incubation for 48 hours, 10µl of Cell Counting Kit-8 solution (CCK-8) (Sigma) was added to each well and incubated for 3 hours at 37 °C. The absorbance of resulting color was measured at 450 nm using Infinite M200 PRO NanoQuant Plate Reader. Endotoxin level of the resulting purified proteins was lowered to <0.1EU/ml

using Pierce™ High Capacity Endotoxin Removal Resin, followed my measuring endotoxin level using Pierce™ LAL Chromogenic Endotoxin

Quantitation Kit.

Statistical analysis

The resulting data are presented as means a ± standard deviation of the means from at least three independent experiments. Significance was obtained by statistical analysis using student t-test (two-tailed). Graph Pad Prism software was used for all analysis and the significance level was set at ≤0.05.

Results

Production of CPG2 Modifications

a. HSA fusion protein design, expression, and purification

The Xen-CPG2 gene was fused in-frame to the 3' end of a gene encoding HSA (Fig 2a) as described in the Experimental Section. The fusion gene was then sub-cloned into the pET28a expression vector and transformed into E. coli BL21 (DE3)RIL. Following induction of expression, recombinant HSA Xen-CPG2 protein was purified using Ni-affinity chromatography. SDS-PAGE suggested that the protein was >90 % pure (Fig 2b).

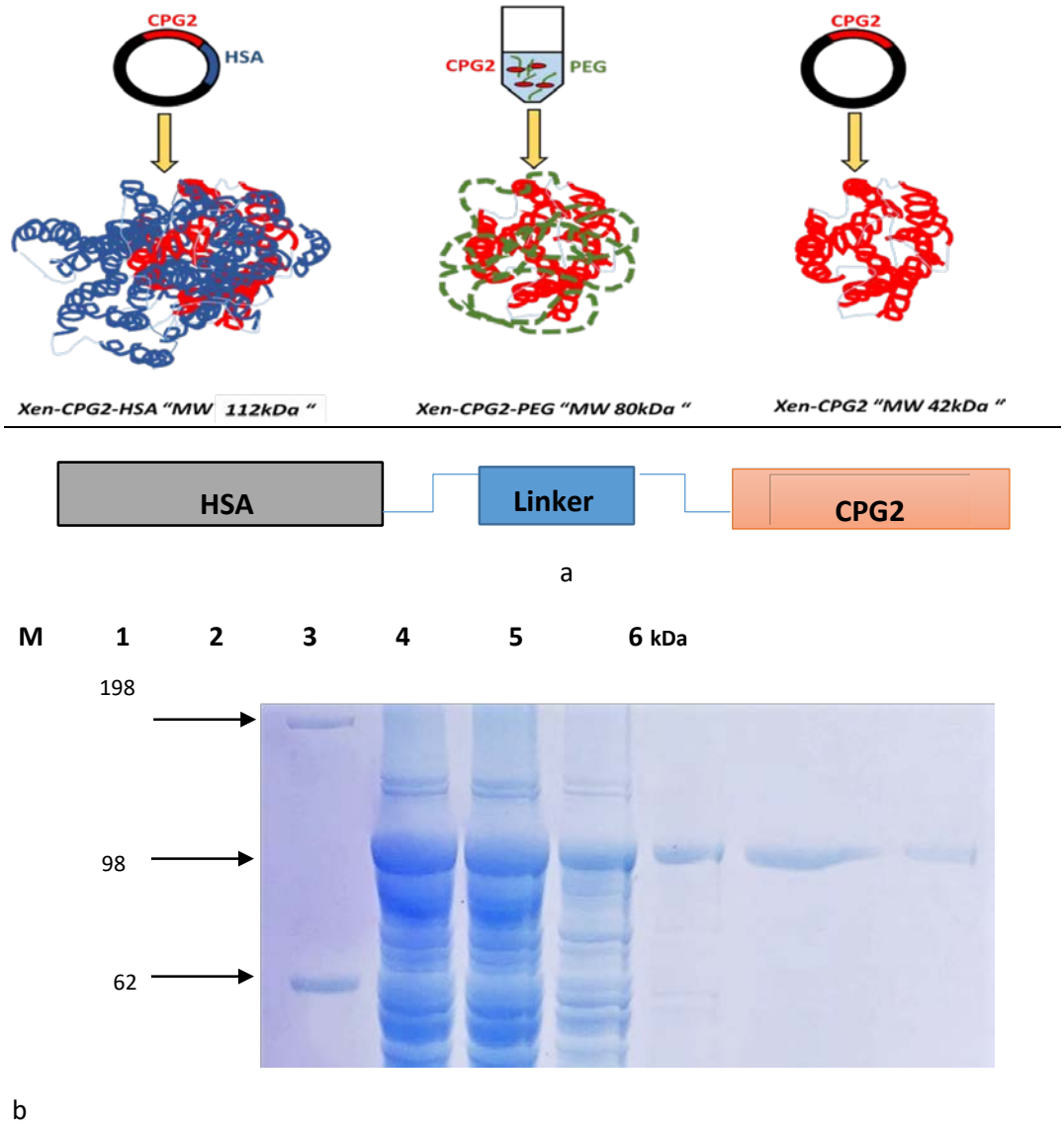

Fig 2. Design and purification of the HSA-Xen-CPG2 fusion protein. **a)** Standard recombinant DNA techniques were used to create an in-frame fusion between the 5' end of the Xen-CPG2 gene and the 3' end of the human HSA gene. A sequence encoding a linker (YGGGGSGGGGSGGGG) was inserted between the HSA and CPG2 genes. **b)** The HSA Xen-CPG2 fusion protein was expressed in *E. coli*, purified using Ni-NTA affinity chromatography, and analysed by SDS-PAGE. Lane M showed the SeeBlue Plus2 Prestained Protein Standard (198-3 kDa). Lane 1, total soluble protein; lane 2, flowthrough during Ni-NTA affinity purification; lane 3, proteins released during washing of Ni-NTA beads; lanes 4-6, eluted fractions. Proteins were visualized by Coomassie blue staining, indicating >90% purity of the eluted protein. As expected, the fusion protein had an MW of ≈ 112 kDa.

b. PEGylation technology of Xen-CPG2

To extend the half-life and protein stability of Xen-CPG2, and hence improve ADEPT and cancer treatment, polyethylene glycol (PEG) chains were tethered to Xen-CPG2

using PEGylation technology, thereby increasing its hydrodynamic size. PEGylation was achieved by employing a Y-shaped (MPEG20K)2 succinimidyl carboxymethyl ester of MW 40,000 (JenKem Technology) that reacts with the amino groups of lysine side chains on the target protein. To reduce the formation of different PEGylated chain lengths on the protein and to maximize the degree of protein PEGylation, the reaction condition was first optimized in trials that systematically varied the time of exposure to the PEGylation reagent. The PEGylated protein was then purified by Ni-affinity chromatography and further purified by gel filtration prior to comparison with non-PEGylated CPG2 by SDSPAGE analysis (Fig 3, Appendix A).

The purity of the resulting purified protein is crucial for further investigations as the presence of any non-modified, native CPG2 might interfere and affect the end result. Thus, the purity of the PEGylated- and HSA-fused CPG2 was confirmed by western blot analysis (Fig 4). The results indicated that the engineered and purified proteins were suitable for application studies.

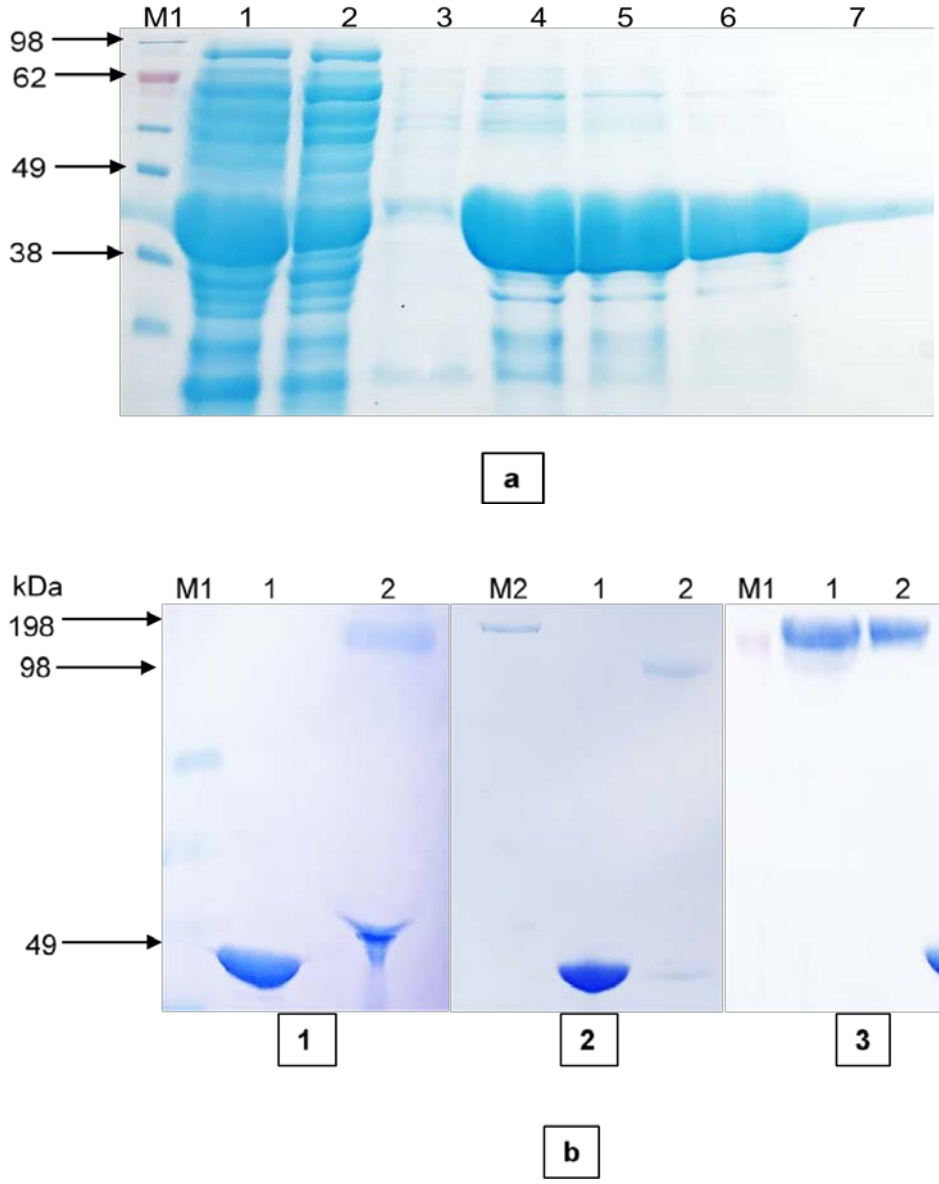

Fig 3. PEGylation of Xen-CPG2 using SCM reagent.

a) SDS-PAGE of Xen-CPG2 at different stages of purification. Xen-CPG 2 was purified as described in the Materials & Methods section. Lane M1 shows a SeeBlue Plus prestained protein marker (3 to 198 kDa) while lane M2 showed a PageRuler Unstained Protein Ladder (10 kDa to 200 kDa). Lane 1, total soluble protein; lane 2, flowthrough during NiNTA affinity purification; lane 3, proteins released during washing of Ni-NTA beads; lanes 4-7, eluted fractions.

b) SDS-PAGE of Xen-CPG2 at different stages of PEGylation. Panel 1. Lanes 1 and 2, pure non-PEGylated Xen-CPG2 and PEGylated Xen-CPG2, before removal of PEGylation reagent. Panel 2. Lanes 1, and 2, pure non-PEGylated Xen-CPG2 and PEGylated XenCPG2, respectively, after removal of PEGylation reagent by affinity purification. Panel 3. PEGylated Xen-CPG2 and non-PEGylated CPG2 after purification and concentration. Lanes 1 and 2, PEGylated Xen-CPG2 at two different concentrations; lane 3,nonPEGylated Xen-CPG2.

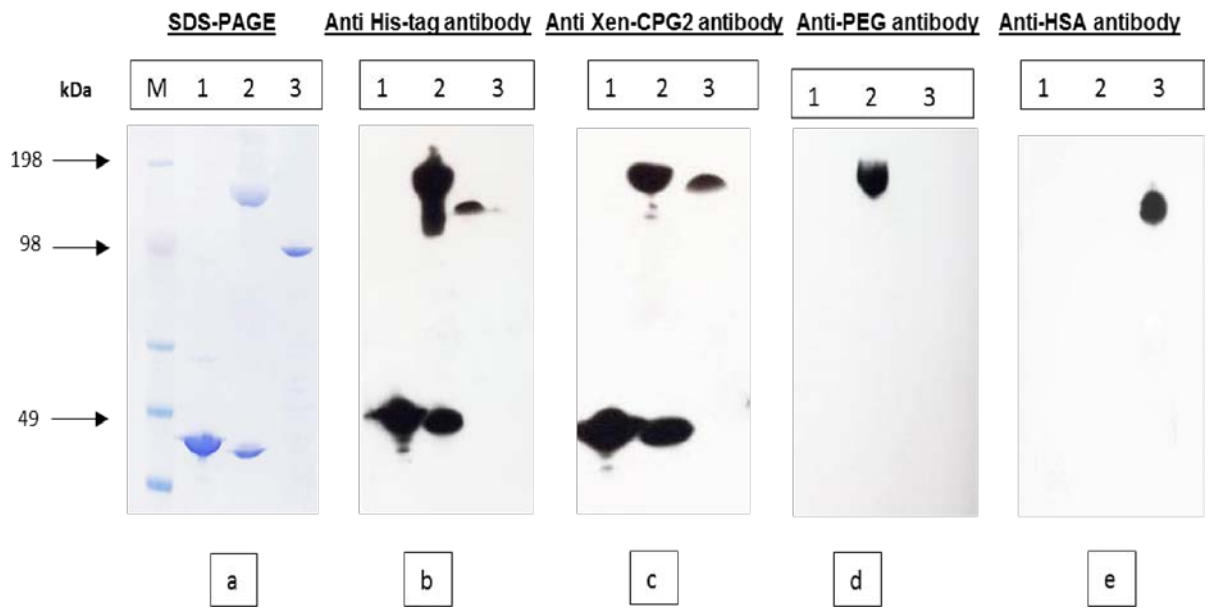

Fig 4. Western blot analyses of different forms of CPG2 relative to the wt. Lane M, SeeBlue Plus2 Prestained ladder (198-10 kDa), while lanes 1-3 are free Xen-CPG2, PEGylated XenCPG2 and HSA-Xen-CPG2, respectively. Panel a shows SDS-PAGE of the three purified proteins while panels b-e show the results of immunoblots with anti-His-tag antibody, anti-CPG2 antibody, anti-PEG antibody and anti-HSA antibody, respectively.

PEGylation and HSA-fusion affects the hydrolytic activity of CPG2

E. coli cells expressing the HSA-CPG2 fusion protein were tested for glucarpidase activity by assessing the degree of folate hydrolysis using agar plates supplemented with folate in the growth medium. Colonies were dark orange color and were surrounded by clear zones suggesting that fusion with HSA did not grossly affect the glucarpidase activity of CPG2 (Fig 5).

The catalytic activity of PEGylated- and HSA-fused CPG2 proteins was further investigated by measuring the rate of MTX hydrolysis by the purified proteins (Fig 6). The derived kinetic parameters for Xen-CPG2, PEG-Xen-CPG2 and HSA-XenCPG2 were, respectively: Vmax values: 24.35 ±1.91, 20.69 ±1.428, 48.72 ± 4.389 µM/min; Km values, 50.56 ± 10.71, 69.97 ± 17.12, 66.14 ± 21.85 µM; and Kcat values: 11.49 ± 0.1947, 9.759 ± 0.2093, and 8.4 ± 0.2401 S-1.

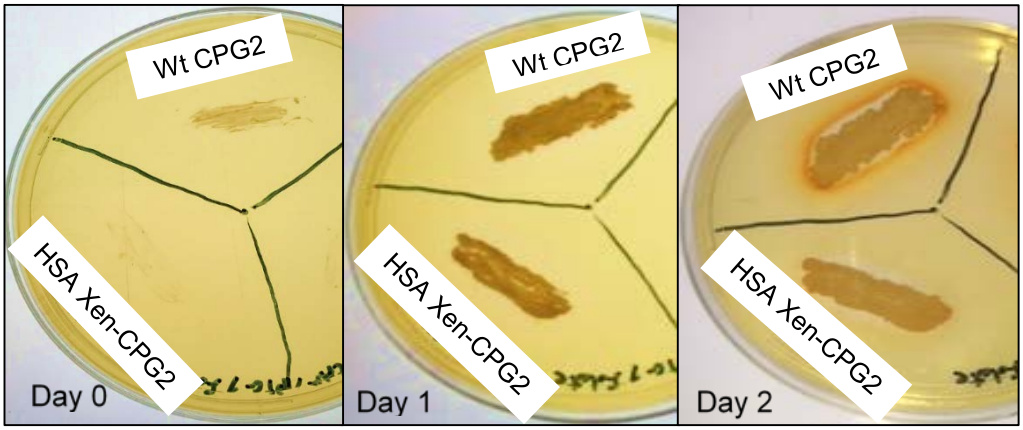

Fig 5. Development of folate-specific hydrolytic activity of *E. coli* expressing recombinant fused HSA-Xen-CPG2 or wild-type Xen-CPG2. Cells were inoculated on LB agar supplemented with folate and IPTG, and the relevant antibiotics. Their growth and coloration were recorded at daily intervals.

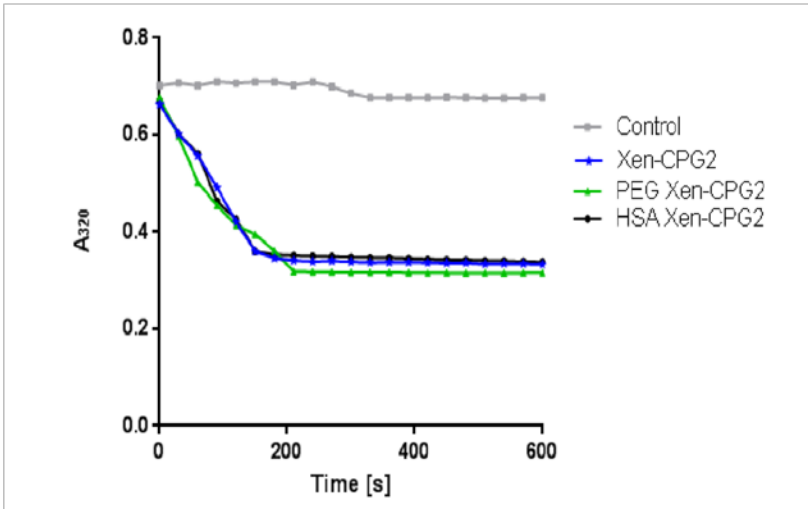

Fig 6. Activity assay of different forms of XenCPG2 on hydrolysis of methotrexate (MTX). The activity of free XenCPG2 (blue), the activity of HSA-Xen-CPG2 (black) and activity of PEG-Xen-CPG2 (green) relative to the buffer control (line in gray). See Materials & Methods for further details.

PEGylation and HSA conjugation enhance the structural and functional stability of CPG2

To investigate the stability of the PEGylated and HSA-conjugated CPG2 proteins, they were incubated with serum from healthy donors at 37$_0$C. Samples were taken every 2 days and tested for CPG2 enzymatic activity. The resulting remaining percentage activity (Fig 7) indicates that PEGylated and HSA conjugated CPG2 proteins retained

more than 50% of their enzyme activity after 14 days. In contrast, Xen-CPG2 retained less than 40% of its activity.

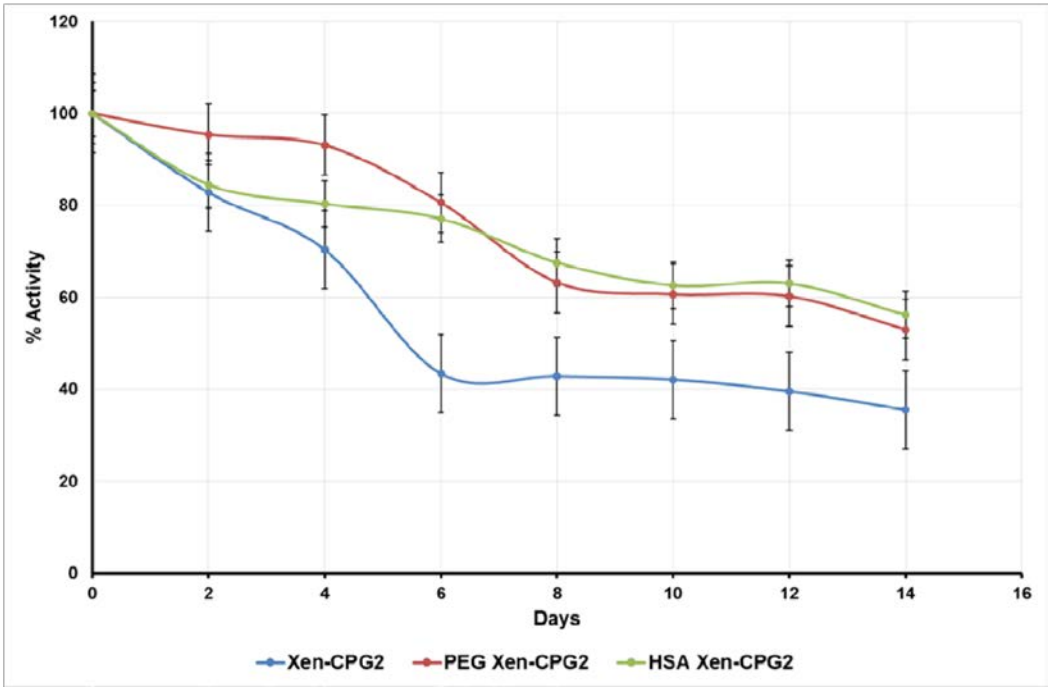

Fig 7. Remaining catalytic activity of different CPG2 variants following incubation in human serum. The proteins (0.1 mg/ml) were incubated in serum at 37oC for 14 days and the remaining methotrexate hydrolysis activity was measured at 48 hour intervals.

The results suggest that genetic fusion of CPG2 with HSA was better at stabilizing CPG2 activity in serum (with ~60% of activity maintained at day 14), compared with the PEGylated form. To further investigate the structural stability of the proteins, samples were incubated in serum prior to separation by native PAGE and analysis by immunoblotting using anti-CPG2 antibodies. Free CPG2 was progressively degraded as the incubation time increased from Day 10 to Day 15 (Fig 8). In contrast, PEGylated and HSA-conjugated CPG2 remained relatively intact from Day 0 to Day15, indicating that the engineered proteins have enhanced stability in serum (Fig 8).

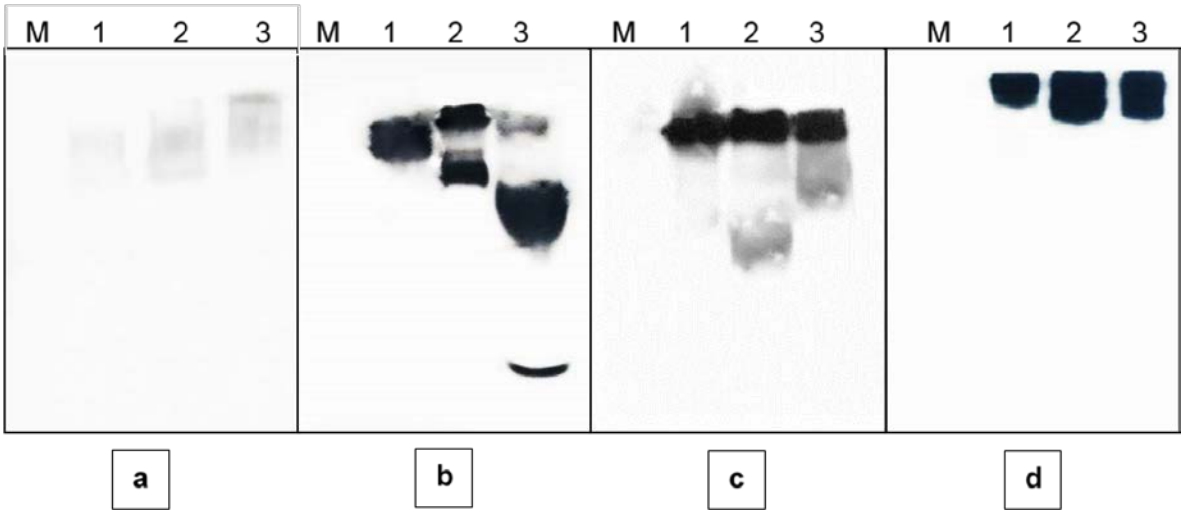

Fig 8. Stability of different CPG2 variants in normal human serum. The proteins were incubated in serum and samples were taken on days 0, 10 and 15. The samples were separated by native PAGE and analyzed by western blotting using anti Xen-CPG2 antibody. Lane M, SeeBlue Plus2 Prestained ladder (198-10 kDa); lanes 1, 2, and 3 , samples taken on days 0, 10, and 15, respectively. Panel a: serum only as control; panel b: Xen-CPG2; panel c: PEG-Xen-CPG2; and panel d: HSA-Xen-CPG2.

Circular dichroism spectral analysis

Circular dichroism (CD) spectroscopy was used to obtain information on how PEGylation or fusion with HSA might affect the overall structure of CPG2 (Fig 9). CD is based on the principle that the differential absorption of polarized light by a chiral molecule (i.e. right- and left-handed rotation of circularly polarized light induced by optically active molecules in the sample) provides structural information. The obtained CD data was deconvoluted to give the predicted secondary structure as shown in Table 1.

The percent composition of the four main secondary structure components calculated by CDNN deconvolution analysis of the obtained spectra (Fig 9.), consists of 69.3% alpha helix, 1.2% antiparallel, 3.2% parallel, 11.3% beta turn, and 14.9% random coil for Xen-CPG2 [24] . In contrast, and 81.7% helix, 0.6% antiparallel, 1.6% parallel, 9.1% beta turn, and 6.7% random coil for PEG-CPG2 and 30.9% parallel, 11.1% antiparallel, 8.9% parallel, 17.4% beta turn and 31.5% random coil for HSA-CPG2, respectively.

Table 1 - Comparison of secondary structures of Xen-CPG2, PEG-CPG2, and HSA-CPG2

Protein / Secondary structure component (%) [1]	Xen-CPG2	PEG-CPG2	HSA-CPG2
Alpha helix	69.3	81.7	30.9
Anti-parallel	1.2	0.6	11.1
Parallel	3.2	1.6	8.9
Beta-turn	11.3	9.1	17.4
Random coil	14.9	6.7	31.5
Total Sum	99.9	99.7	99.8

[1] The relative amounts of different secondary structures in Xen-CPG2, PEG-CPG2, and HSA-CPG2 were calculated from the spectral data shown in Fig 8 by CDNN deconvolution analysis. The average values of each secondary structure component following four sets of measurements is shown as percentages.

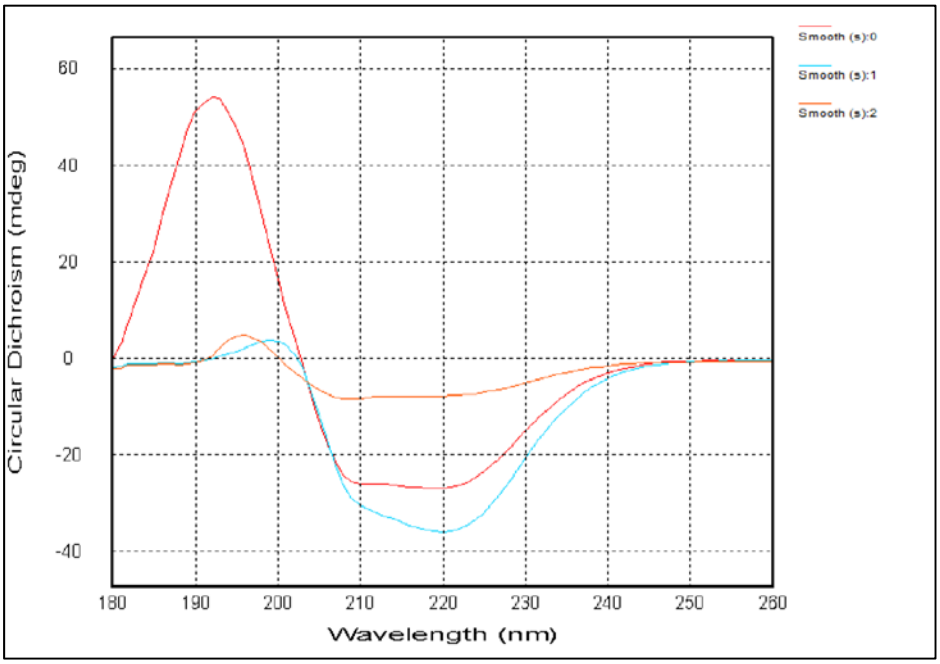

Fig 9. Far UV spectroscopy of free Xen-CPG2, PEG-Xen-CPG2, and HSA-Xen-CPG2 using CHIRASCAN. The lines labeled Smooth 0, 1, and 2 represent the CD spectra for Xen-CPG2, PEG Xen-CPG2, and HSA Xen-CPG2, respectively

In vitro immunogenicity of PEGylated and HSA conjugated CPG2 proteins

The immunogenicity of the produced proteins was examined using PBMCs from healthy donors. The proliferation of the cells was detected following incubation with

either the vehicle (negative control), LPS (positive control) or the endotoxin low produced proteins (CPG2, PEGylated, and HSA conjugated Xen-CPG2). As shown in Fig 10. PEG-Xen-CPG2 was significantly low in immunogenicity compared to the positive control. Fusion with HSA also lowered CPG2 immunogenicity significantly in most of the samples.

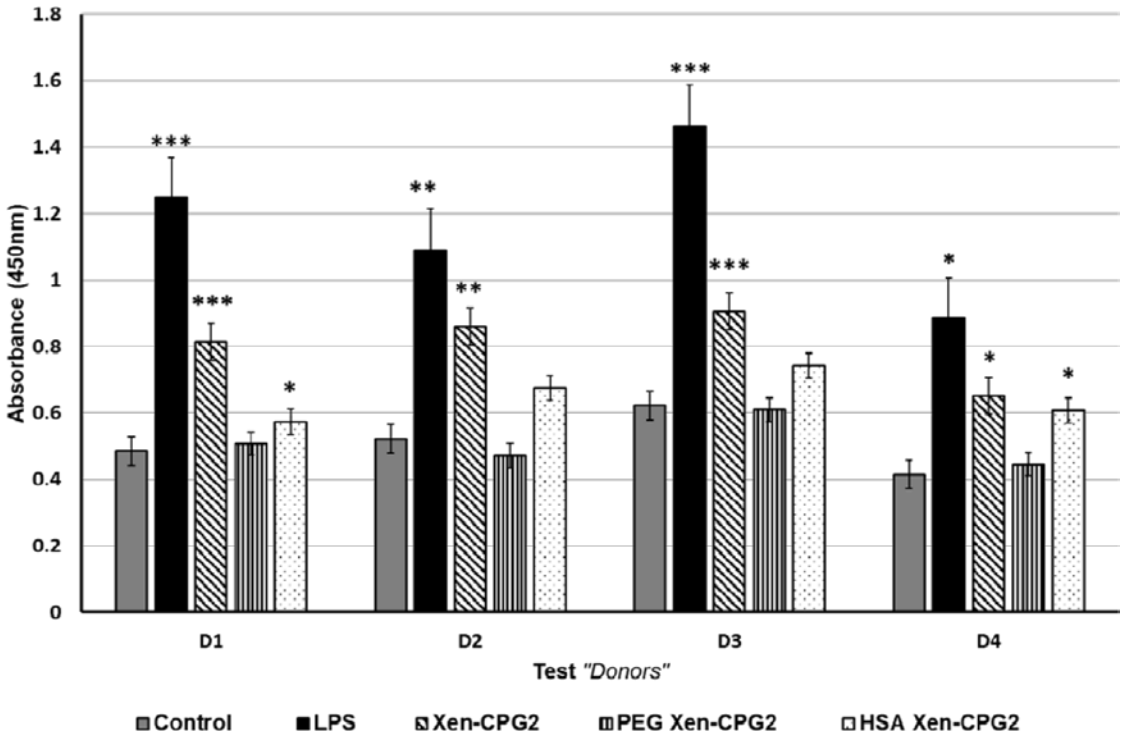

Fig 10. Human PBMC proliferation assay (Immunogenicity). PBMC from healthy donors incubated with purified proteins followed by determining their proliferation. A significant increase was found in the positive control, Lipopolysaccharide (LPS) compared with all control groups with the vehicle only. When comparing with negative control, PEG XenCPG2 treated cells in all groups showed no significant increase in proliferation, whereas HSA Xen-CPG2 treated cells showed similar result except in two donors. ** $P < 0.01$, *** $P < 0.0001$, an unpaired test was used to analyze data. $P < 0.05$ was considered statistically significant.

Discussion

Antibody directed enzyme prodrug therapy (ADEPT) is an effective strategy for targeted cancer treatment. The technique, however, suffers from two significant drawbacks; namely, the patient immune system will progressively generate antibodies

against the enzyme due to the repeated injection of CPG2, thereby limiting its efficacy, and the enzyme will be liable to degradation by the patient's proteases.

In our previous work [13] we isolated a novel glucarpidase whose raised antibodies did not cross-react with the one in clinical use. In principle, therefore, it would be possible to delay the production of antibodies in a patient by alternating the use of the two versions of CPG2. However, this strategy may not totally solve the problem and in any case does not address the issue of limited protein stability in a patient's blood, e.g. due to proteolytic degradation [26]. In this study, therefore, we adopted a different approach to produce biobetter glucarpidases, which should both reduce the potential for antibodies production and also protect the protein against endogenous proteases.

PEGylation of proteins and other biomolecules is one of the most effective strategies to produce biobetter therapeutics. It improves the pharmacokinetics and pharmacodynamics of the conjugated molecules in relation to the non-conjugated one, increases water solubility and also protects against proteolytic degradation. On the other hand, human serum albumin has a long half-life in the body and proteins fused to this protein also have extended half-lives [27, 28].
Modifications of glucarpidase by PEGylation or by genetic fusion to HSA is thus a promising strategy to allow these molecules to be used optimally in drug detoxification or in ADEPT.

The data presented in Figs 2-6 and appendix A indicate that the production of pure and active PEG-CPG2 and HSA-CPG2 was successfully achieved. The mass spectra analysis confirmed the formation of the HSA-CPG2, Appendix B. However, it was important to verify that the conjugated forms of CPG2 retained enzyme activity – it remained possible that attachment of large additional molecules might sterically

hinder access to the active site of CPG2. Surprisingly, enzyme activity studies indicate that HSA-CPG2 has slightly increased catalytic activity relative to free CPG2 – the V_{max} of the former was 48.72 ±4.389 µM/min whereas unconjugated CPG2 has a V_{max} of 24.35 ±1.91 µM/min [13]. In the case of PEGylated CPG2, the catalytic activity found to be slightly lower than that of unconjugated CPG2 (Vmax value of PEG-CPG2: 20.69 ±1.428 µM/min). Thus, the attached PEG may slightly restrict the access of the substrate to the enzyme active site or slightly alter the enzyme's conformation. The results of far UV spectroscopy (CD) suggest that significant structural changes in secondary structure components of each protein from induced by PEGylation and/or HSA conjugation compared with the CD scan and its deduced secondary structure results of free Xen-CPG2 recently published by our group [13].

To compare the stability of the modified forms of CPG2 with the free enzyme, we incubated them with human blood serum for a total of 14 days. Fig 7 and fig 8 confirm that both HSA-CPG2 and PEG-CPG2 are significantly more stable than free CPG2 and that they also have longer half-lives. In the latter case, PEGylation (incorporation of PEG negative charged molecules) is known to stabilize the conformation of proteins by increasing the intramolecular hydrogen bonding and increasing the hydrophilicity [29, 30]. Increasing protein conformation also restricts access of proteases to the conjugated protein. On the other hand, HSA, which is well known to be non-immunogenic and biocompatible, also extends the half-life of the HSA-protein therapeutics [31].

A PBMC proliferation assay, where T-cell (in the PBMCs) proliferation and differentiation is induced upon exposure to their cognate antigens, is considered to be a helpful tool during preclinical safety assessment and is used efficiently to evaluate

and predict immunological effects of biopharmaceuticals [32]. To assess the potential immunotoxicity of the modified CPG2s relative to the free CPG2, we, therefore, carried out an *ex-vivo* lymphocyte proliferation assay. Our results (Fig.9) indicated that in case of PEG-CPG2 no significant induction of T-cell proliferation was observed, indicating that the attached PEG molecules are able to mask the immunogenic epitopes in CPG2 that react with immune cells and induce immunogenicity. In contrast, HSA-CPG2 triggered a significant increase in T-cell proliferation compared with the negative control. This unexpected result, which apparently contradicts the protein stability results (Figs 7 and 8), could be explained by the presence of endotoxin impurities, which might induce immunogenicity. We, however, carried out further purification steps to remove any remaining endotoxin but obtained the same results. Further study is needed to establish the cause of the observed immunogenicity.

Collectively, our results show that conjugation of CPG2 with HSA or with PEG has a significant effect on CPG2 structural and functional stability *in vitro* and *ex-vivo*. Furthermore, PEGylated CPG2 was shown to have a reduced immunogenic effect on PBMCs compared with free CPG2. Our findings pave the way for *in vivo* studies and possible clinical investigation using modified forms of CPG2.

Conclusion

Glucarpidase (CPG2) is an important enzyme used in antibody directed enzyme prodrug therapy (ADEPT) for cancer treatment but with several pitfalls such as host immune response and proteases degradation. The Human serum albumin and PEG molecules are good half-life extenders with several beneficial features, such as resistance to proteases degradation and low immune response. In this work we successfully carried out conjugation of HSA and PEG molecules to our newly isolated

glucarpidase (CPG2), generating two novel glucarpidase conjugates, HSACPG2 and PEG-CPG2. We demonstrated that both HSA and PEG molecules could be conjugated to glucarpidase without compromising the critical property of the target protein such as enzyme activity. Our work shows that both glucarpidase conjugates have serum half-lives much higher than the free glucarpidase. We also show that PEG-CPG2 have a reduced immunogenic effect on PBMCs compared with free CPG2. Our work paves the way for the *in vivo* clinical investigation and clinical trials using our novel modified forms of CPG2 for cancer treatment and drug detoxification.

Appendices

Appendix A

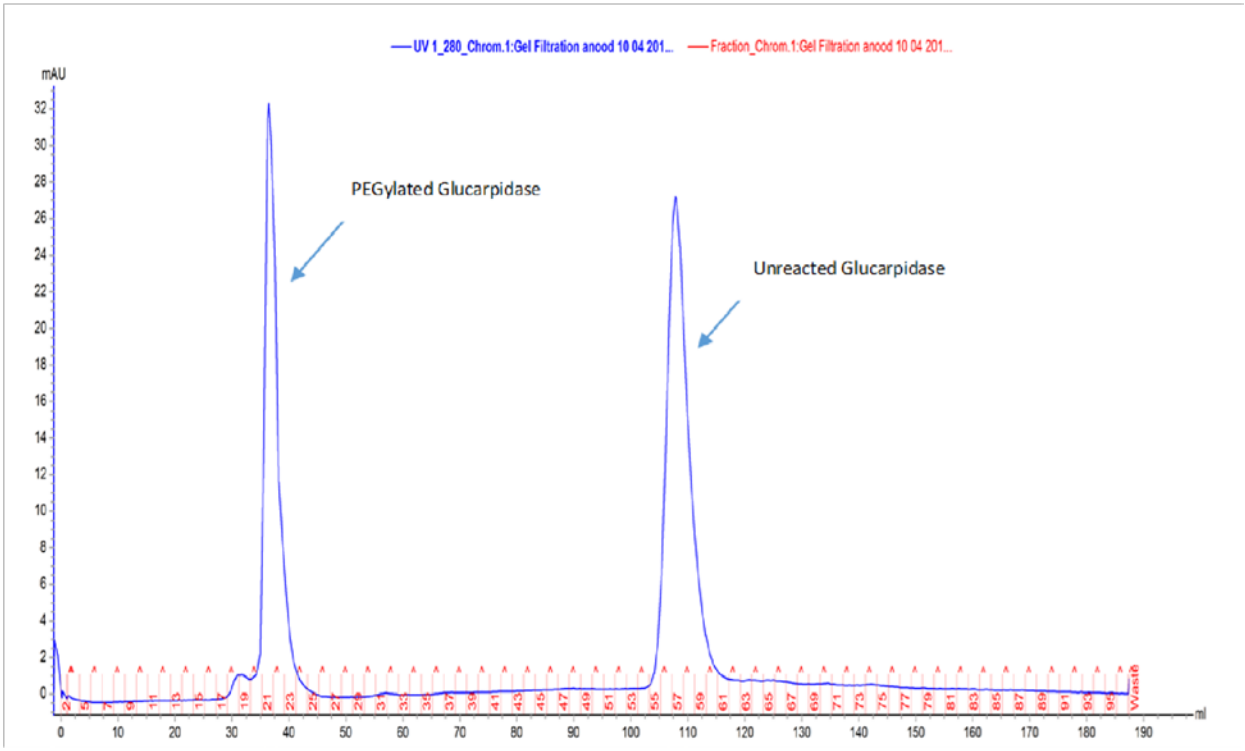

Appendix A.1: Size exclusion of PEG-CPG2 under high-resolution conditions using AKTA purifier.

Appendix B

Protein List

Protein Group	Protein ID	Accession	-10lgP	Coverage (%)	#Peptides	#Unique	PTM	Avg. Mass	Description
4	1	P02768|ALBU_HUMAN	287.76	47	35	7	Y	69367	Serum albumin OS=Homo sapiens GN=ALB PE=1 SV=2
40	20750	P02769|ALBU_BOVIN	194.30	13	10	3	Y	69294	Serum albumin OS=Bos taurus GN=ALB PE=1 SV=4
109	20920	P06621|CBPG_PSES6	146.32	16	7	7	Y	43932	Carboxypeptidase G2 OS=Pseudomonas sp. (strain RS-16) GN=cpg2 PE=1 SV=1
total 3 proteins									

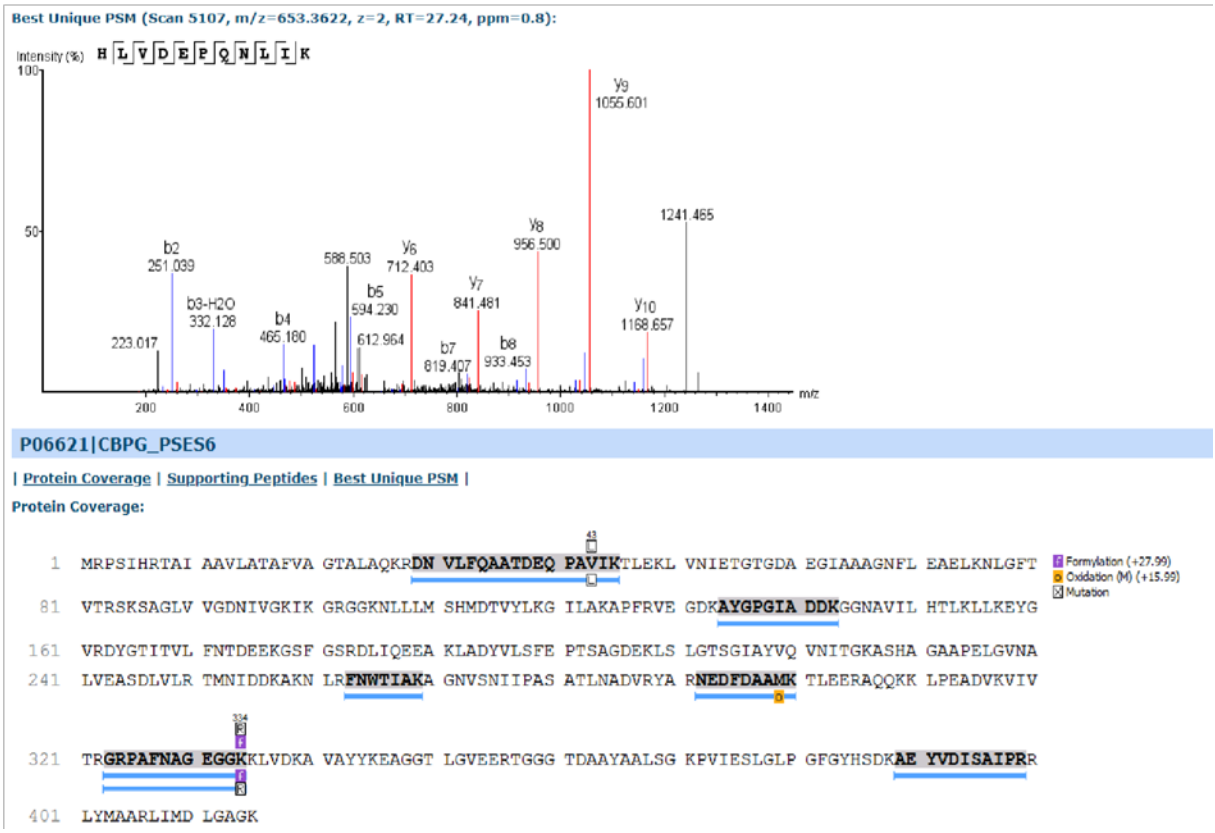

Appendix B.1: Mass spectra and matching peptide sequences for Carboxypeptidase G2 (matching peptides are highlighted)

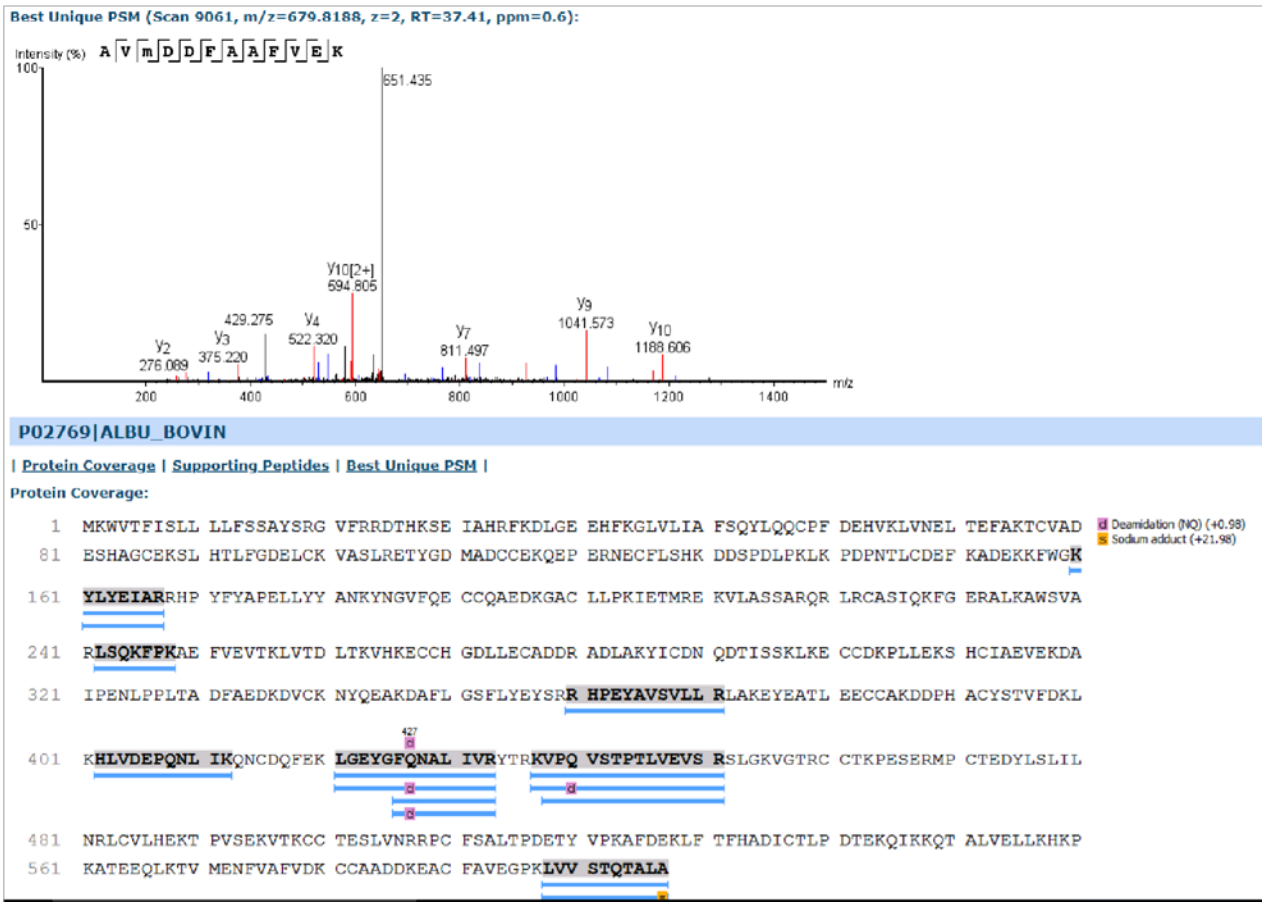

Appendix B.2: Mass spectra and matching peptide sequences for human serum albumin (matching peptides are highlighted)

Acknowledgment

- QNRF grant number NPRP6-065-3-012, Qatar National Research Fund, Doha Qatar for funding this work with grant number NPRP No.:NPRP6065-3-012.

- Professor C. David O'Connor, Xi'an Jiaotong-Liverpool University for reading and reviewing the manuscript.

- TMPL Lab, Anti-Doping Lab, Doha, Qatar for carrying out the mass spectra analysis of HSA-glucarpidase

Ethics approval and consent to participate

The study was approved by the Anti-Doping Lab-Qatar Institutional Review Board, Ethical approval number: E2017000205. All blood samples used in this study were taken from authors involved in the work.

References

1. Werle, M.; Bernkop-Schnurch, A. Strategies to improve plasma half life time of peptide and protein drugs. *Amino acids* **2006,** *30*, (4), 351-67.
2. Thompson, J. D.; Higgins, D. G.; Gibson, T. J. CLUSTAL W: improving the sensitivity of progressive multiple sequence alignment through sequence weighting, position-specific gap penalties and weight matrix choice. *Nucleic acids research* **1994,** *22*, (22), 4673-80.
3. Kamlage, B. Methods for General and Molecular Bacteriology. Edited by P. Gerhardt, R. G. E. Murray, W. A. Wood and N. R. Krieg. 791 pages, numerous figures and tables. American Society for Microbiology, Washington, D.C., 1994. Price: 55.00 £. *Food / Nahrung* **1996,** *40*, (2), 103103.
4. Minton, N. P.; Atkinson, T.; Sherwood, R. F. Molecular cloning of the Pseudomonas carboxypeptidase G2 gene and its expression in Escherichia coli and Pseudomonas putida. *Journal of bacteriology* **1983,** *156*, (3), 1222-7.
5. Kalghatgi KaB, J. Folate-degrading enzymes: a review with special emphasis on Carboxypeptidase G. In: Enzymes as drugs. *Wiley* **1981,** *J Holcenberg and J Roberts, eds,*, 77-102.
6. Sherwood, R. F.; Melton, R. G.; Alwan, S. M.; Hughes, P. Purification and properties of carboxypeptidase G2 from Pseudomonas sp. strain RS-16. Use of a novel triazine dye affinity method. *European journal of biochemistry* **1985,** *148*, (3), 447-53.
7. Bagshawe, K. D.; Springer, C. J.; Searle, F.; Antoniw, P.; Sharma, S. K.; Melton, R. G.; Sherwood, R. F. A cytotoxic agent can be generated selectively at cancer sites. *British journal of cancer* **1988,** *58*, (6), 700-3.
8. Sharma, S. K.; Pedley, R. B.; Bhatia, J.; Boxer, G. M.; El-Emir, E.; Qureshi, U.; Tolner, B.; Lowe, H.; Michael, N. P.; Minton, N.; Begent, R. H.; Chester, K. A. Sustained tumor regression of human colorectal cancer xenografts using a multifunctional mannosylated fusion protein in antibody-directed enzyme prodrug therapy. *Clinical cancer research : an official journal of the American Association for Cancer Research* **2005,** *11*, (2 Pt 1), 814-25.
9. Martin, J.; Stribbling, S. M.; Poon, G. K.; Begent, R. H.; Napier, M.; Sharma, S. K.; Springer, C. J. Antibody-directed enzyme prodrug therapy: pharmacokinetics and plasma levels of prodrug and drug in a phase I clinical trial. *Cancer chemotherapy and pharmacology* **1997,** *40*, (3), 189-201.
10. Bagsgawe, K., Sharma, SK, Springer, CJ, and Antoniw, P . . Antibodydirected enzyme prodrug therapy: A pilot clinical trial. *Tumor Targeting* **1995,** *1*, 17–29
11. Rappold, H.; Bacher, A. Bacterial degradation of folic acid. *Journal of general microbiology* **1974,** *85*, (2), 283-90.

12. Goda, S. K.; Rashidi, F. A.; Fakharo, A. A.; Al-Obaidli, A. Functional overexpression and purification of a codon optimized synthetic glucarpidase (carboxypeptidase G2) in Escherichia coli. *The protein journal* **2009,** *28*, (9-10), 435-42.
13. Rashidi, F. B.; AlQhatani, A. D.; Bashraheel, S. S.; Shaabani, S.; Groves, M. R.; Dömling, A.; Goda, S. K. Isolation and molecular characterization of novel glucarpidases: Enzymes to improve the antibody directed enzyme pro-drug therapy for cancer treatment. *PLoS ONE* **2018,** *13*, (4), e0196254.
14. Schellenberger, V.; Wang, C. W.; Geething, N. C.; Spink, B. J.; Campbell, A.; To, W.; Scholle, M. D.; Yin, Y.; Yao, Y.; Bogin, O.; Cleland, J. L.; Silverman, J.; Stemmer, W. P. A recombinant polypeptide extends the in vivo half-life of peptides and proteins in a tunable manner. *Nature biotechnology* **2009,** *27*, (12), 1186-90.
15. Herndon, T. M.; Demko, S. G.; Jiang, X.; He, K.; Gootenberg, J. E.; Cohen, M. H.; Keegan, P.; Pazdur, R. U.S. Food and Drug Administration Approval: Peginterferon-alfa-2b for the Adjuvant Treatment of Patients with Melanoma. *The Oncologist* **2012,** *17*, (10), 1323-1328.
16. Barnard, D. L. Pegasys (Hoffmann-La Roche). *Current opinion in investigational drugs (London, England : 2000)* **2001,** *2*, (11), 1530-8.
17. Maullu, C.; Raimondo, D.; Caboi, F.; Giorgetti, A.; Sergi, M.; Valentini, M.; Tonon, G.; Tramontano, A. Site-directed enzymatic PEGylation of the human granulocyte colony-stimulating factor. *The FEBS journal* **2009,** *276*, (22), 6741-50.
18. Peters, T., Jr. Serum albumin. *Advances in protein chemistry* **1985,** *37*, 161-245.
19. Ru, Y.; Zhi, D.; Guo, D.; Wang, Y.; Li, Y.; Wang, M.; Wei, S.; Wang, H.; Wang, N.; Che, J.; Li, H. Expression and bioactivity of recombinant human serum albumin and dTMP fusion proteins in CHO cells. *Applied microbiology and biotechnology* **2016,** *100*, (17), 7565-75.
20. Kim, Y. M.; Lee, S. M.; Chung, H. S. Novel AGLP-1 albumin fusion protein as a long-lasting agent for type 2 diabetes. *BMB reports* **2013,** *46*, (12), 60610.
21. Muller, D.; Karle, A.; Meissburger, B.; Hofig, I.; Stork, R.; Kontermann, R. E. Improved pharmacokinetics of recombinant bispecific antibody molecules by fusion to human serum albumin. *The Journal of biological chemistry* **2007,** *282*, (17), 12650-60.
22. Tian, S.; Li, Q.; Yao, W.; Xu, C. Construction and characterization of a potent, long-lasting recombinant human serum albumin-interferon alpha1 fusion protein expressed in Pichia pastoris. *Protein expression and purification* **2013,** *90*, (2), 124-8.
23. Zhao, H. L.; Xue, C.; Wang, Y.; Sun, B.; Yao, X. Q.; Liu, Z. M. Elimination of the free sulfhydryl group in the human serum albumin (HSA) moiety of human interferon-alpha2b and HSA fusion protein increases its stability against mechanical and thermal stresses. *European journal of pharmaceutics and biopharmaceutics : official journal of Arbeitsgemeinschaft fur Pharmazeutische Verfahrenstechnik e.V* **2009,** *72*, (2), 405-11.
24. Melder, R. J.; Osborn, B. L.; Riccobene, T.; Kanakaraj, P.; Wei, P.; Chen, G.; Stolow, D.; Halpern, W. G.; Migone, T. S.; Wang, Q.; Grzegorzewski, K. J.; Gallant, G. Pharmacokinetics and in vitro and in vivo anti-tumor response of an interleukin-2-human serum albumin fusion protein in mice. *Cancer immunology, immunotherapy : CII* **2005,** *54*, (6), 535-47.

25. Batra, J.; Robinson, J.; Mehner, C.; Hockla, A.; Miller, E.; Radisky, D. C.; Radisky, E. S. PEGylation extends circulation half-life while preserving in vitro and in vivo activity of tissue inhibitor of metalloproteinases-1 (TIMP1). *PLoS One* **2012,** *7*, (11), e50028.
26. Lawrence, P. B.; Price, J. L. How PEGylation influences protein conformational stability. *Current opinion in chemical biology* **2016,** *34*, 88-94.
27. Aggarwal, S. What's fueling the biotech engine? *Nature biotechnology* **2007,** *25*, (10), 1097-104.
28. Kontermann, R. E. Strategies for extended serum half-life of protein therapeutics. *Current opinion in biotechnology* **2011,** *22*, (6), 868-76.
29. Davidson, W. S.; Jonas, A.; Clayton, D. F.; George, J. M. Stabilization of alpha-synuclein secondary structure upon binding to synthetic membranes. *The Journal of biological chemistry* **1998,** *273*, (16), 9443-9.
30. Robotta, M.; Braun, P.; van Rooijen, B.; Subramaniam, V.; Huber, M.; Drescher, M. Direct evidence of coexisting horseshoe and extended helix conformations of membrane-bound alpha-synuclein. *Chemphyschem : a European journal of chemical physics and physical chemistry* **2011,** *12*, (2), 267-9.
31. Cho, J.; Lim, S. I.; Yang, B. S.; Hahn, Y. S.; Kwon, I. Generation of therapeutic protein variants with the human serum albumin binding capacity via site-specific fatty acid conjugation. *Scientific reports* **2017,** *7*, (1), 18041.
32. Lim, S. I.; Hahn, Y. S.; Kwon, I. Site-specific albumination of a therapeutic protein with multi-subunit to prolong activity in vivo. *Journal of controlled release : official journal of the Controlled Release Society* **2015,** *207*, 93100.

Chapter 6:

Studies on Vascular Response to Full Superantigens and Superantigen Derived **Peptides:** possible production of novel superantigen variants with less vasodilation effect for tolerable cancer immunotherapy**.**

Sara S Bashraheel[1,2], Alanod D Al Qahtani[1,2], Fatma B Rashidi[3], Haya Al-Sulaiti[1,2], Alexander Domling[2], Nelson N Orie [4] and Sayed K Goda[1,3]

[1]Protein Engineering Unit, Life and Science Research Department, Anti-Doping Lab-Qatar (ADLQ), Doha, Qatar.
[2]Drug Design Group, Department of Pharmacy, University of Groningen, Groningen, Netherlands.
[3]Cairo University, Faculty of Science, Giza, Egypt.
[4]Vascular Laboratory, Life and Science Research Department, Anti-Doping LabQatar (ADLQ), Doha, Qatar.

Accepted at **Biomedicine & Pharmacotherapy 2019**

Studies on Vascular Response to Full Superantigens and Identification of potential Novel Antihypertensive Peptides Drugs

1. Codon Optimization, cloning, overexpression and purification of four Superantigens, SEA, SEB, TSST-1 and SPEA

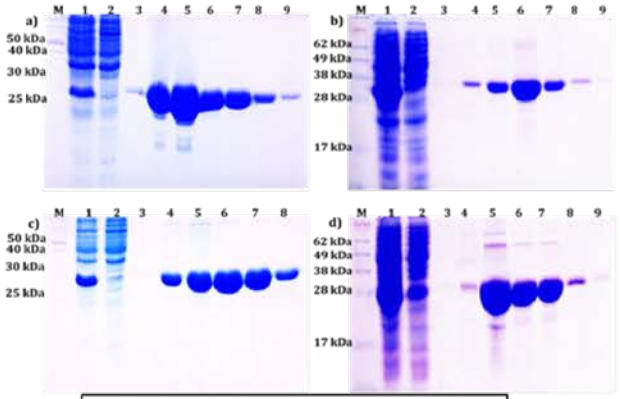

Vascular Response Assessment

2. Studies on vascular response to SEA and SPEA were carried out and the mechanism of action

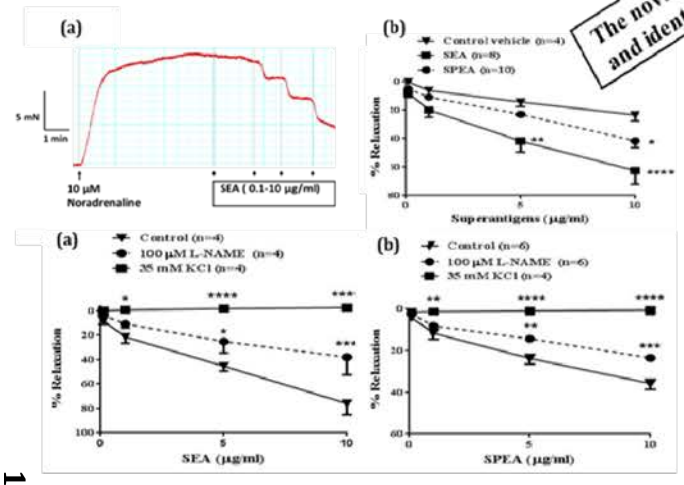

The novel data on full molecule led to mapping and identification of antihypertensive peptides

3. Synthesis of 20 overlapped peptides covering the whole molecule

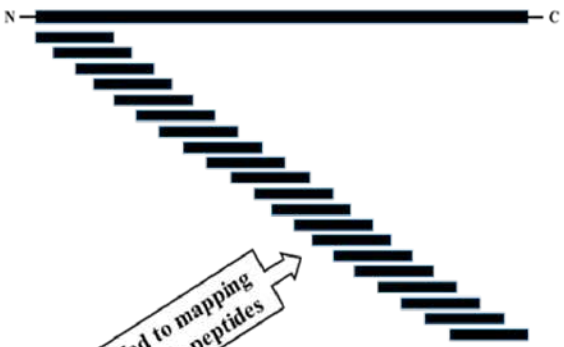

Vascular Response Assessment

4. Identification of functional region that are involved in causing the vasodilation

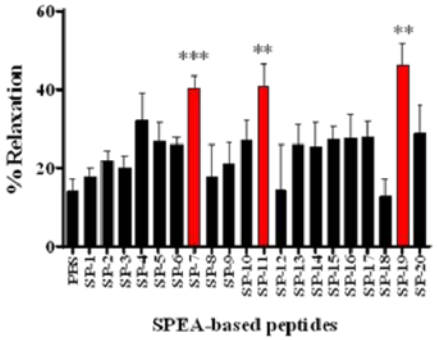

Outcome

Outcome

Outcomes:

1. The direct effects on vascular tone were assessed for SEA and SPEA using ovine skeletal muscle (SKM): Both SEA and SPEA caused dose-dependent relaxation of the ovine SKM arteries.
2. The functional regions of the superantigens, SPEA, that are involved in causing the vasodilation and the hypotension by superantigens were identified.
3. Our novel isolated region could be used as Antihypertensive therapeutics.
4. This work might pave the way for production of superantigens with less side effects for tolerable cancer immunotherapy.

Abstract

Superantigens (SAgs) are a class of antigens that cause non-specific activation of T-cells resulting in polyclonal T cell activation and massive cytokine release and causing symptoms similar to sepsis, e.g. hypotension and subsequent hyporeactivity. We investigated the direct effect of SAgs on vascular tone using two recombinant SAgs, SEA and SPEA. The roles of Nitric Oxide (NO) and potentially hyperpolarization, which is dependent on the K_+ channel activation, were also explored. The data show that SEA and SPEA have direct vasodilatory effects that were in part NO-dependent, but completely dependent on activation of K_+ channels. Our work also identified the functional regions of one of the superantigens, SPEA, that are involved in causing the vasodilation and possible hypotension. A series of 20 overlapping peptides, spanning the entire sequence of SPEA, were designed and synthesized. The vascular response of each peptide was measured, and the active peptides were identified. Our results implicate the regions, (61100), (101-140) and (181-220) which cause the vasodilation and possible hypotension effects of SPEA. The data also shows that the peptide 181-220 exert the highest vasodilation effect. This work therefore, demonstrates the direct effect of SAgs on vascular tone and identify the active region causing this vasodilation. We propose that these three peptides could be effective novel antihypertensive drugs. We also overexpressed, in *E.coli*, four superantigens from codon optimized genes.

Keywords

Superantigen based peptides, Superantigenicity, T-cell activation, Vasodilation, Hypotension, Potassium Channel, Hyperpolarization and antihypertensive drugs.

Introduction

Superantigens (SAgs) comprise a large family of disease-associated microbial proteins with potent non-specific T-cell stimulatory activity. SAgs can non-specifically activate up to 20% of resting T-cells, while conventional antigen presentation results in the activation of only 0.001 - 0.0001% of the T-cell population. In this process, SAgs promote various intracellular signal transduction pathways, activating protein kinase C, protein tyrosine kinase (PTK), NF-κB and AP-1 transcription factor signaling, resulting in the release of high levels of specific proinflammatory cytokines by activated T-cells [1]. Subsequently, certain secreted cytokines may attract and activate additional immune cells, including macrophages and polymorphonuclear leukocytes (PMNs)[2]. Activated PMNs may produce excessive amounts of reactive oxygen species (ROS) and release destructive hydrolytic enzymes that contribute to multi-organ failure and lethal shock.

Patients with infective endocarditis (IE), staphylococcal pneumonia, and some patients after surgery develop sepsis due to infections. It has been shown that SAgs; SEA, TSST-1 and SEC are overexpressed in patients with sepsis compared to patients without sepsis [3-5], raising the possibility that these SAgs contribute to the manifestations of the disease. A recent study confirmed the contribution of SAgs to the development of IE, sepsis and acute kidney injury [6] and *S. aureus* strains that cause sepsis and IE in rabbits, produce TSST-1, SEB, and SEC [7]. The most severe manifestation of sepsis is the septic shock, which is characterized by low systemic vascular resistance and severe hypotension. These abnormal vascular conditions are caused by both excessive vasodilatation and vascular hyporeactivity to circulating catecholamines. The hypotension is often resistant to high doses of catecholamines [8] but can be responsive to vasopressin [9-11] or to inhibition of Nitric Oxide (NO) synthase [11]. Excess NO production, through both constitutive and

inducible NO synthase isoforms (NOS), low vasopressin secretion and abnormal potassium channel activation [9, 12, 13], have all been suggested to contribute to the excessive vasodilation associated with this condition. Thus, apart from provoking cytokine release, SAgs appear to stimulate the production of NO, which is a vasodilator produced by the endothelium and in that way induces hypotension and the hyporeactivity characteristic for sepsis. We, therefore, investigated the direct effect of SAgs on vascular tone and the roles of NO and potentially hyperpolarization on the observed effects. This was followed by the determination of the region(s) on the whole superantigen which causes the vasodilatory effect.

Hypertension is a global health problem and is associated with increased mortality of cardiovascular diseases, stroke and diabetes [14]. More than 17.5 million people die every year from cardiovascular disease. Hypertension was projected to affect 29.2% of the global adult population by 2025 [15], and therefore, it has become one of the leading cause of death globally [16].

There are many antihypertensive drugs in the market. In this work; however, we report novel superantigen derived peptides with vasodilatory bioactivity which could be effective antihypertensive drugs.

This work describe the effects of selected SAgs on vascular tone and to shed light on the mechanism of action and to discover the region with the hyporeactivity.

Our study paves the way for in vivo investigation of the novel peptides as antihypertensive drugs and the possible production of superantigen variants with less or no vasodilatory effect for tolerable cancer therapy.

Material and Methods

Bacterial strains, Plasmid and Chemicals

Prokaryotic IPTG-inducible expression vector, pET28a plasmid and compatible *E. coli* host *Rosetta (DE3)* genetically engineered with T7 polymerase were purchased from Novagen (Madison, WI). DLD-1 was obtained from ATCC collections, DLD-1 (ATCC® CCL221). Ni^{2+}-NTA resin was purchased from Sigma-Aldrich (Dorset, England). L. Broth Miller and L. Broth Agar were purchase from Formedia (Devon, England). Kanamycin and chloramphenicol were purchased from Sigma-Aldrich.

Reagents and Antibodies

Restriction enzymes and T4 DNA ligase were purchased from Biolabs (London, England) and used as described in the manufacturer's instructions. Standard SEB was purchased from Sigma-Aldrich (labeled as SEBsig throughout the manuscript). Human anti CD3-FITC, anti CD25-PE and Annexin V- FITC were purchased from ImmunoTools (Friesoythe, Germany). All peptides were synthesized and supplied by GenScript.

Codon optimization of SAgs

The genes for SAgs; SEA, SEB, SPEA and TSST-1, were codon optimized for expression in the yeast, *Saccharomyces cerevisiae* (see Results and Discussion sections). Several unique restriction enzyme sites (*Bam*HI, *Nde*I at the 5' end and *Hin*dIII at the 3' end) were introduced into the gene to facilitate insertion into the cloning vector digested by the same restriction enzymes. The SAg genes, codon optimized for yeast, were synthesized by Geneart GmbH (Regensburg, Germany). The sequences of the codon optimized SAg genes have been deposited in the GenBank database with accession numbers: SEA (KY594411) SEB (KY594412) TSST-1 (KY594413) and SPEA (KY594414).

Sub cloning of SAgs into the expression vector pET28a

The codon optimized SAgs genes were excised by digestion using *Nde*I and *Hin*dIII and ligated into the identically digested vector pET28a using T4 DNA ligase. Each of the ligation mixtures were transformed into competent *E. coli* and grown on LB media agar plates containing kanamycin (33 µg/ml) at 37°C. DNA sequence analysis confirmed the correct sequence of the full coding sequence and in-frame fusion to the region of pET28a encoding an N-terminal His-tag. The constructs were then transformed into competent *E. coli Rosetta (DE3)* cells for protein expression studies.

Overexpression of SAgs in *E. coli*

Single colony picks of *Rosetta (DE3)* cells transformed with pETSAgs were grown in LB medium containing the relevant antibiotics (33 µg/ml kanamycin and 34 µg/ml chloramphenicol) at 37°C until the OD reached 0.45-0.60 at 600 nm. Expression of the SAgs was induced by addition of 1 mM IPTG at 37°C. After 4 h of induction, the bacterial cells were collected by centrifugation at 4000 rpm for 15 min.

Purification of soluble SAgs using Ni^{2+}-NTA chromatography

Recombinant SAgs were isolated from the harvested *E. coli* cells. Cell pellets from 1 L culture were resuspended in 25 ml of 1 mM Tris buffer, pH 7 and sonicated on ice for 5 x 2 min cycles using an MSE Soniprep 150 Plus (1 min sonication pulse followed by 1 min cooling on ice). The soluble protein fraction was separated from the insoluble fraction by centrifugation at 15000 rpm. The soluble proteins were purified via their N-terminal His-tag by Ni-NTA affinity chromatography. Recombinant SAgs were eluted from the

column using 500 mM imidazole containing buffer, pH 7.5. The purified SAgs were dialyzed against 1 mM Tris buffer pH 7, with three exchanges, for 48 h.

Superantigenicity assay

The superantigenicity of purified soluble SAg was determined by treating Peripheral Blood Mononuclear Cells (PBMCs) freshly isolated from human blood using Lymphoprep (Stemcell Technologies, Germany) with the SAgs. In short, PBMCs were seeded (3 x 10_6 cells/well) into 24 well plates and incubated (37°C, 5% CO_2) in the presence or absence of the SAg under study (10 µg/ml in 1 mM Tris buffer, pH 7) for 48 h. Culture supernatants were evaluated for cytokines, IL-2, IL-4, IL-5, IL-10 and IFNγ, produced by PBMCs in response to SAgs, using a Th1/Th2 Human 5-Plex Panel for Luminex Platform.

MTT Assay

To evaluate cell cytotoxicity of superantigens, we prepared PBMCs as above and seeded 5x10_5 cells/well in a 96 well plate. Cells were treated with either Media as a control, or with 10_2ng/ml SAg and 10_4ng/ml SAg and incubated at 37°C, 5% CO_2 for 48 h. The cells were then incubated with MTT reagent (5 µg/mL final concentration) at 37°C for 3 h. 170 µl of DMSO was added into each well to solubilize the formed formazan. The level of formazan production was measured by Infinite M200 PRO Nano Quant Plate Reader at 570 nm.

Assessment of T- Cell activation

To determine T-cell activation, PBMCs, isolated as above, were seeded into a 48 well plate (5 x 10_5 PBMCs/well) and treated with different concentrations (1 ng/ml, 10_2 ng/ml, and 10_4 ng/ml) of SEA, SEB, SPEA, TSST-1 or a commercial preparation of SEB purchased from Sigma-Aldrich (SEBsig). Cells were incubated at 37°C, 5% CO_2 for 72 h prior to

harvesting and staining with anti-CD3 and anti-CD25 antibodies tagged with fluorescent dyes FITC and PE, respectively. T-cell activation analysis was carried out using an Accuri C6 flow cytometer (BD Biosciences) by gating for the lymphocyte subset and measuring the percentage of $CD3^+$ $CD25^+$ cells.

Assessment of apoptosis induction

The ability of the SAgs to kill tumor cells was determined using mixed cultures in 48 well plates containing per well 1.7 x 10^5 PBMCs and 3.5 x 10^4 DLD-1 colon tumor cells (obtained from the ATCC: ATCC CCL221). The mixed cultures were incubated at 37°C in 5% CO_2 for 48 h with different concentrations of SAgs (1 ng/ml, 10^2 ng/ml, and 10^4 ng/ml). After 48 h cells were harvested, stained with Annexin V- FITC and analyzed by flow cytometry.

Synthesis of SPEA based overlapped peptides

We produced peptides covering the complete amino acid sequence of SPEA (Fig.1 and Table 1) , They overlap by thirty amino acids SP1 (1-40), SP2 (11-50), SP3 (21-60), SP4 (31-70), SP5 (41-80), SP6 (51-90), SP7 (61-100), SP8 (71-110), SP9 (81-120), SP10 (91-130), SP11 (101-140), SP12 (111-150), SP13 (121-160), SP14 (131-170), SP15 (141-180), SP16 (151190), SP17 (161-200), SP18 (171-210), SP19 (181-220), SP20 (191-222).

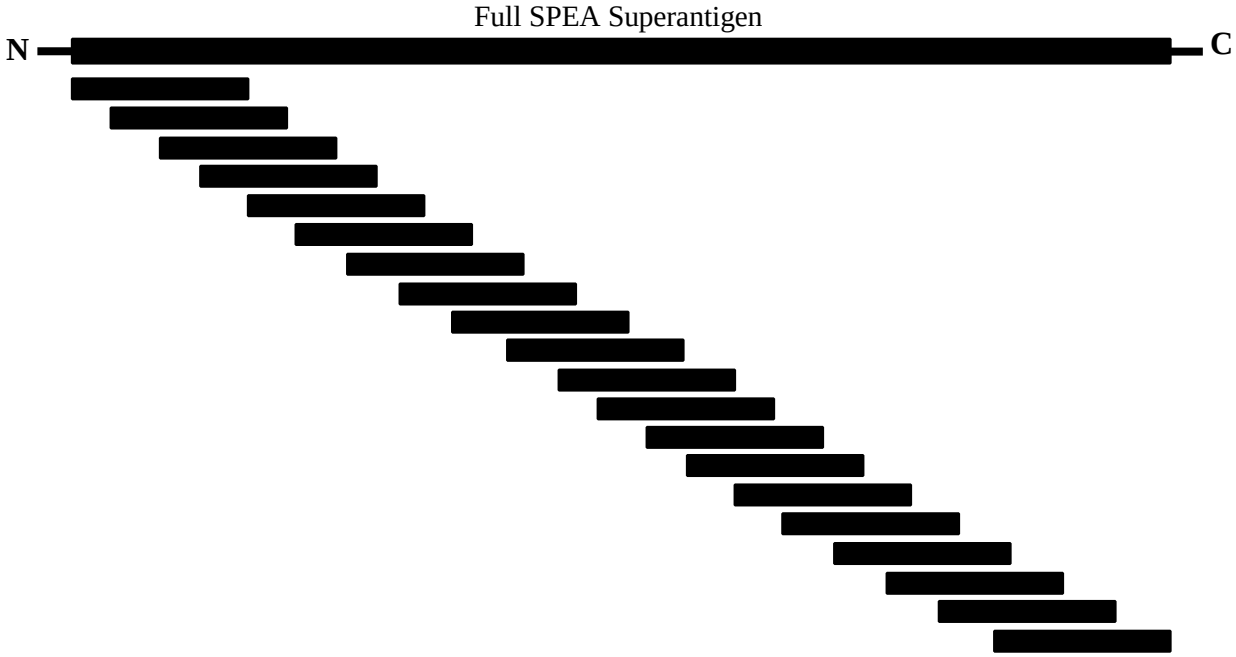

Fig. 1 Design and synthesis of overlapping peptides (SP1 – SP20) based on the SPEA superantigen sequence.

Table 1 Peptides, overlapping by thirty amino acids and corresponding to the whole amino acid sequence of SPEA, the amino acid in red is the start of the overlapping with the next peptides.

Peptide Name	Sequence	Peptide range
SP1	MQQDPDPSQLHRSSLVKNLQNIYFLYEGDPVTHENVKSVD	1-40
SP2	HRSSLVKNLQNIYFLYEGDPVTHENVKSVDQLLSHDLIYN	11-50
SP3	NIYFLYEGDPVTHENVKSVDQLLSHDLIYNVSGPNYDKLK	21-60
SP4	VTHENVKSVDQLLSHDLIYNVSGPNYDKLKTELKNQEMAT	31-70
SP5	QLLSHDLIYNVSGPNYDKLKTELKNQEMATLFKDKNVDIY	41-80
SP6	VSGPNYDKLKTELKNQEMATLFKDKNVDIYGVEYYHLCYL	51-90
SP7	TELKNQEMATLFKDKNVDIYGVEYYHLCYLCENAERSACI	61-100
SP8	LFKDKNVDIYGVEYYHLCYLCENAERSACIYGGVTNHEGN	71-110
SP9	GVEYYHLCYLCENAERSACIYGGVTNHEGNHLEIPKKIVV	81-120
SP10	CENAERSACIYGGVTNHEGNHLEIPKKIVVKVSIDGIQSL	91-130
SP11	YGGVTNHEGNHLEIPKKIVVKVSIDGIQSLSFDIETNKKM	101-140
SP12	HLEIPKKIVVKVSIDGIQSLSFDIETNKKMVTAQELDYKV	111-150
SP13	KVSIDGIQSLSFDIETNKKMVTAQELDYKVRKYLTDNKQL	121-160
SP14	SFDIETNKKMVTAQELDYKVRKYLTDNKQLYTNGPSKYET	131-170
SP15	VTAQELDYKVRKYLTDNKQLYTNGPSKYETGYIKFIPKNK	141-180

SP16	RKYLTDNKQLYTNGPSKYETGYIKFIPKNKESFWFDFFPE	151-190
SP17	YTNGPSKYETGYIKFIPKNKESFWFDFFPEPEFTQSKYLM	161-200
SP18	GYIKFIPKNKESFWFDFFPEPEFTQSKYLMIYKDNETLDS	171-210
SP19	ESFWFDFFPEPEFTQSKYLMIYKDNETLDSNTSQIEVYLT	181-220
SP20	PEFTQSKYLMIYKDNETLDSNTSQIEVYLTTK	191-222

Assessment of vascular response

Small arteries were isolated from samples of ovine abdominal muscle obtained from male sheep at the slaughter house in Doha. The arteries were dissected under the LINTRON microscope (BidSpotter, UK) and cut into segments (~2 mm long). Each segment was mounted on 2 wires (40 µm diameter) in an isometric myograph (510 A; JP Trading, Aarhus, Denmark) containing normal physiological salt solution (PSS). The PSS contained 112 mM NaCl, 5 mM KCl, 1.8 mM $CaCl_2$, 1 mM $MgCl_2$, 25 mM $NaHCO_3$, 0.5 mM KH2PO_3, 0.5 mM NaH_2PO_3, and 10 mM glucose, bubbled with 95% O_2/5% CO_2 to pH 7.4. The arterial segments were continuously aerated at 37°C and pre-tensioned to an equivalent of 100 mm Hg (13.3 kPa). The normalized luminal diameter of each segment was obtained as described previously [17]. An equilibration period of at least 1 h was allowed during which tissues were contracted with KCl (90 mM) and noradrenaline (10100 µM) to optimize tissue response.

Following the equilibration period, the arteries were pre contracted with noradrenaline (10 µM) to achieve a stable tone. After that, SAgs were applied cumulatively, starting from 0.1 µg/ml to a maximum of 10 µg/ml final bath concentrations, to generate dose response curves. Relaxation curves were generated for two of the SAgs (SEA and SPEA). A control curve was also generated for the PBS in which the SAgs were diluted to determine any superantigen unrelated effect. The roles of NO or K ion channels were determined by pretreating the vessels with 100 µM Nω-Nitro-L-arginine methyl ester

(L-NAME, an inhibitor of NO synthase), for at least 30 min or by raising the K ion concentration in the bathing fluid to 35 mM (to block the opening of K ion channels/potential hyperpolarization) prior to applying the superantigens. Data were acquired with a Powerlab acquisition system and LabChart software version 7 (DMT, Denmark). Changes in tone were expressed as the percentage of initial contraction by noradrenaline just before the addition of the lowest concentration of the SAgs. The assessment of the twenty overlapped SPEA based peptides was carried out individually, as mentioned above.

Statistical analyses

Data are presented as mean ± standard error of mean (S.E.M) of "n" observations. All graphs were constructed using GraphPad Prism 6 software (San Diego, CA, USA). Statistical analysis was performed using Student's t-test or ANOVA, as appropriate. P values < 0.05 were considered statistically significant.

Results

Overexpression and purification of recombinant SAgs

Codon optimised genes encoding the SAgs SEA, SEB, SPEA and TSST-1 were inserted into expression vector pET28a and transformed into *E. coli Rosetta (DE3)* cells for overexpression. Following expression, soluble protein fractions were purified by Ni^{2+}-NTA affinity chromatography (Fig 2), which was sufficient to obtain proteins with high purity

Superantigenicity assay

The superantigenicity of purified SAgs was investigated by treating PBMCs with the various SAgs (at 10µg/ml) or with solvent only prior to measuring the levels of five cytokines, IL-2, IL-4, IL-5, IL-10 and IFNγ, excreted into the growth media. As expected while IL-2 and IFNγ (hallmarks of superantigenicity) were produced at significantly elevated levels from cells incubated with SAgs (Fig 3), none of the cytokines was detected in the control. There were no significant levels of IL-5, IL-10 and IL-4 detected. Also, the MTT assay was carried out which shows that SAgs have no cytotoxicity on PBMCs (Fig. 4) and cells proliferation were detected in response to 10^2 ng/ml and 10^4 ng/ml of SAgs.

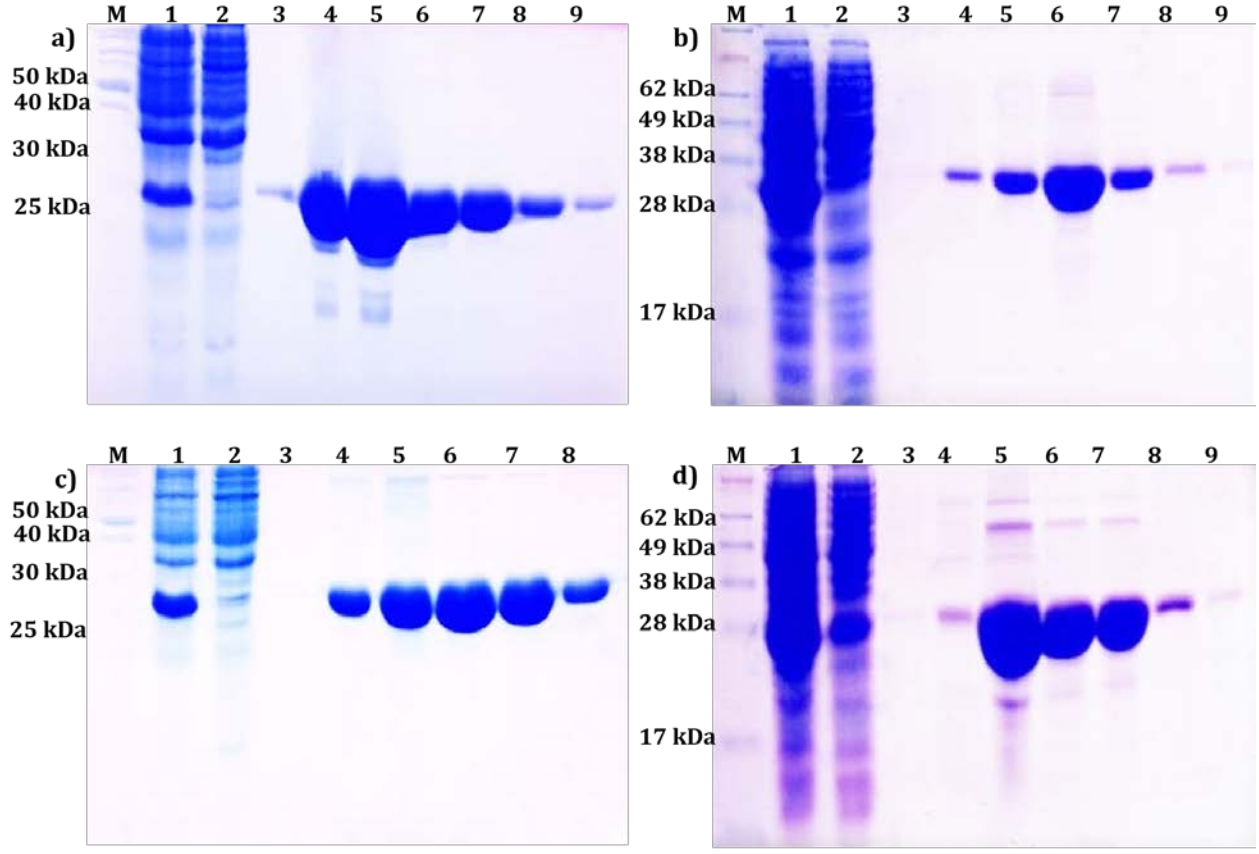

Fig. 2 Purification of recombinant SAgs expressed from synthetic codon optimized genes. 10% SDS-PAGE gels of soluble SEA, SEB, SPEA and TSST-1 (Panels a-d, respectively) protein purification. M is Pre-Stained Protein Marker. Lanes 1- 3 are total soluble fraction, flow through and wash 5, respectively. Lanes 4-9 are elution fractions.

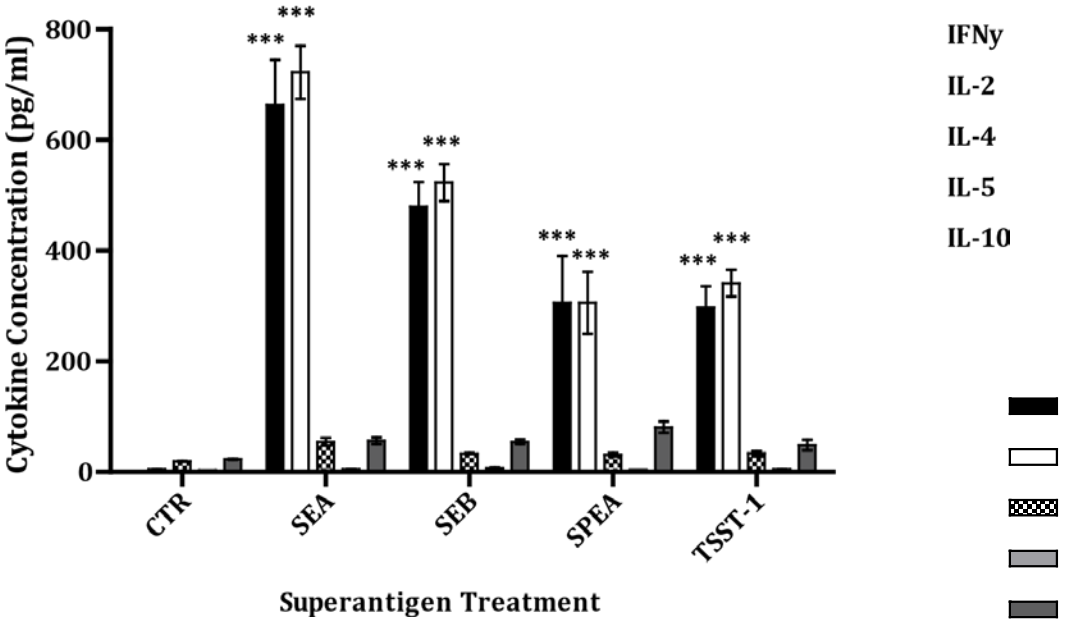

Fig. 3 Concentration of IFNγ, IL-2, IL-4, IL-5 and IL-10 produced by PBMC cells in response to treatment with 1 mM Tris control, SEA, SEB, SPEA or TSST-1. Data are presented as mean ± standard error of the mean (S.E.M) of 3 independent experiments (n=3).*p<0.05, **p<0.01, ***p<0.001, compared to the buffer control.

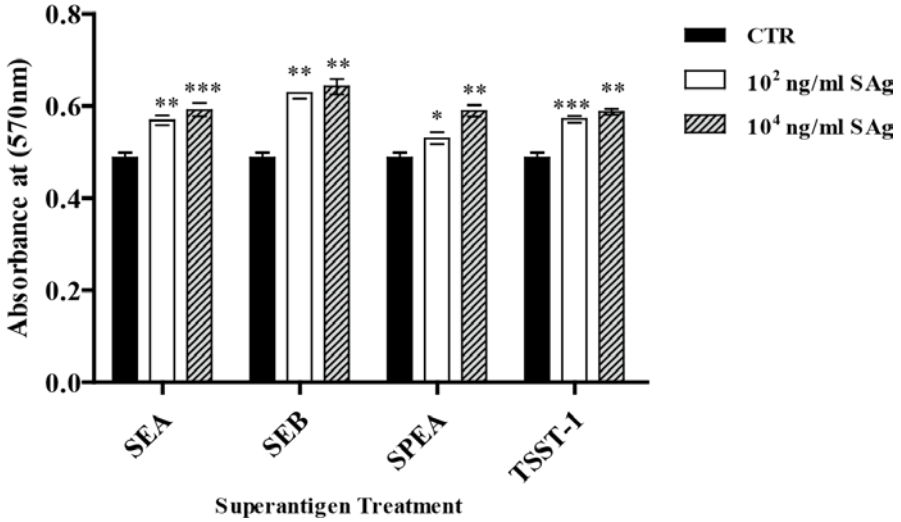

Fig. 4 MTT assay on PBMCs exposed to treatment with different concentrations of SEA, SEB, SPEA or TSST-1 for 48 h. Data are presented as mean ± standard error of the mean (S.E.M) of 3 experiments (n=3). *p<0.05, **p<0.01 and ***p<0.001, compared to the media control.

T-cell activation

The ability of the various recombinant SAgs to activate T-cells was investigated. PBMCs were treated with increasing concentrations of SEA, SEB, SPEA, TSST-1 or commercial SEB, prior to staining with fluorescently labeled anti-CD3 and anti-CD25 antibodies and flow cytometric analysis. Fig 5 shows that both media and buffer controls had no significant effect on T-cells, while up to 20% of T-cells were activated by 1 ng/ml of SAgs SEB, TSST-1 or SEA. All recombinant SAgs dose-dependently increased T-cell activity up to 60%, including SEBsig. There was no significant difference between the standard SEB from sigma (SEBsig) and the recombinant SEB in T-cell activation.

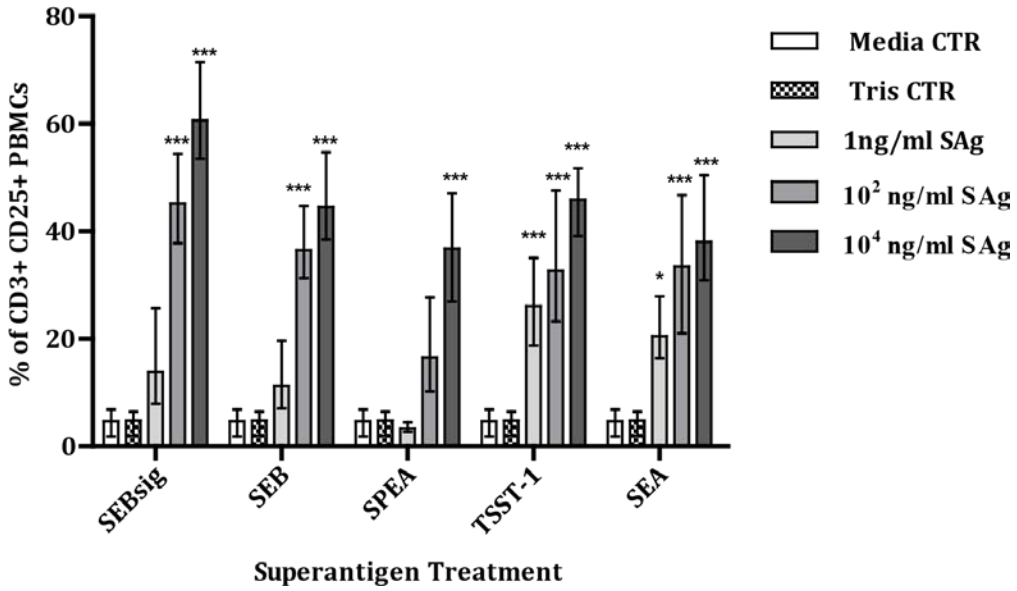

Fig. 5 Percentage of CD3+ CD25+ PBMCs (activated T-cells) in response to treatment with different concentrations of SEBsig, SEB, SPEA, TSST-1, or SEA. Data are presented as mean ± standard error of the mean (S.E.M) of 3 independent experiments (n=3).*p<0.05, **p<0.01, ***p<0.001, compared to the buffer control.

Tumor cell apoptosis

SAgs alone were not efficient in tumor cell killing (Fig 6), but promoted tumor cell killing by activating T-cells and production of cytokines. Treatment of a mixed culture of PBMCs and DLD-1 tumor cells with different doses of SAg resulted in tumor cell killing up to 80%. Fig 6 shows a higher percentage of dead tumor cells with higher SAg concentration, (from 1 ng/ml to 10 µg/ml). When a mixed culture of DLD-1 and PBMCs was treated with media or Tris buffer controls, no significant killing was detected. Comparison between SEBsig and recombinant SEB in tumor killing showed no significant difference.

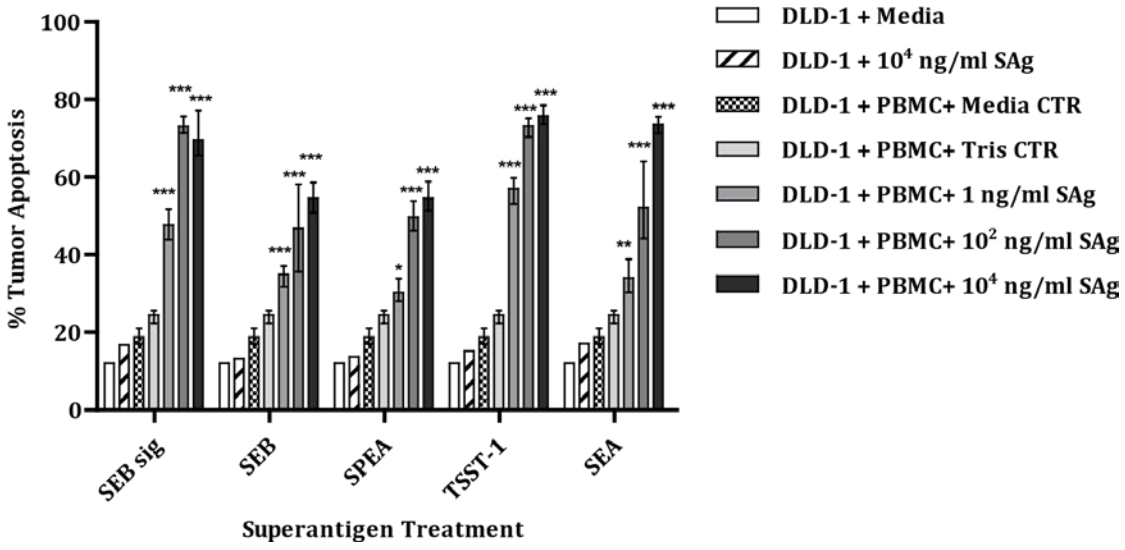

Fig. 6 Percentage of apoptotic tumor cells in response to treatment with different concentrations of SEBsig, SEB, SPEA, TSST-1, or SEA in a mixed culture with PBMCs. Negative controls include: DLD-1 tumor cells with Media, DLD-1 cells with Tris buffer, DLD-1 cells with media, and DLD-1 cells with 10_4ng/ml of SAg. Data are presented as mean ± standard error of the mean (S.E.M) of 3 observations (n=3). *p<0.05, **p<0.01, ***p<0.001, compared to the DLD-1+PBMC+ Tris control sample.

Vascular response to the SAgs

A total of 16 ovine skeletal muscle arteries, with the mean normalized internal diameter of 318±20 µm, were studied for the direct relaxant effects of the SAgs SEA and SPEA. Both SEA and SPEA caused dose-dependent relaxation of these arteries. A typical tracing of the relaxation response to SEA is shown in Fig 7a and a summary of the responses to both superantigens is shown in Fig 7b. SEA caused significantly greater relaxation of the arteries compared with SPEA ($p<0.01$) in the dose range tested, with 62±10% and 42±5% relaxation, respectively, following administration of 10 µg/ml of these SAgs.

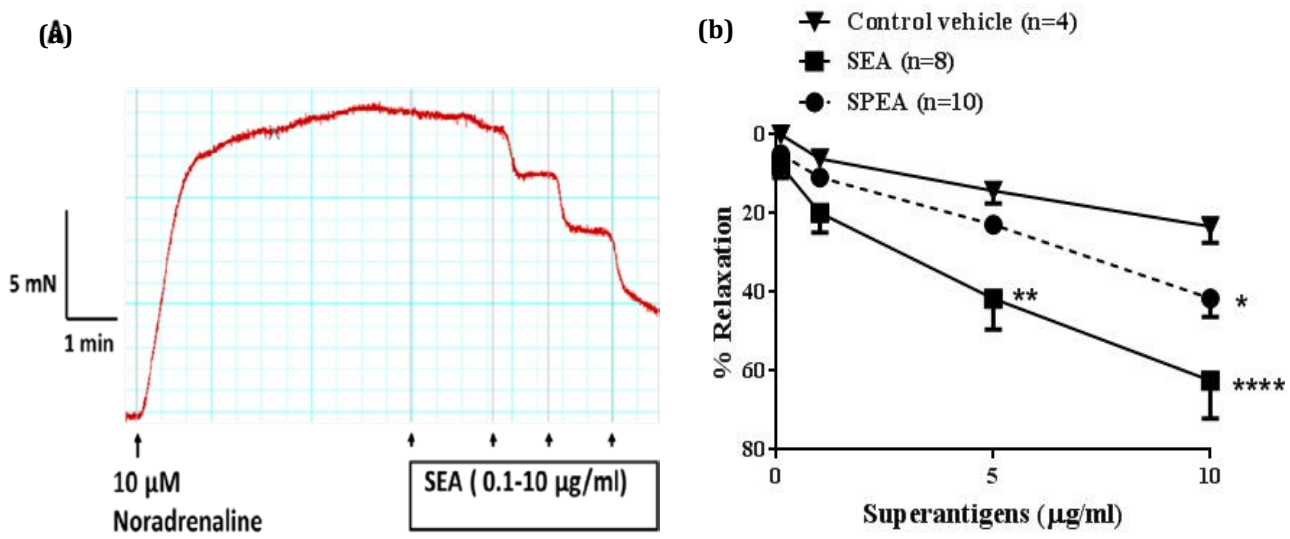

Fig. 7 (a) Typical trace of superantigen -induced relaxation. (b) Vasodilation induced by the two superantigens SEA and SPEA. Both superantigens induced dose-dependent dilation of small skeletal muscle (SKM) arteries. Data are presented as mean ± standard error of the mean (S.E.M). *$p<0.05$, **$p<0.01$, ****$p<0.0001$, compared with control vehicle (PBS buffer).

Roles of NO and K^+ channel activation in the superantigen-induced vasodilation

Endotoxins can induce the release of NO from the vascular endothelium, which in turn causes relaxation of the underlying vascular smooth muscle. Accordingly, we investigated whether NO also contributes to vasodilation induced by SAgs. In the presence of the NO synthase inhibitor, L-NAME, the relaxation induced by both SEA (Fig 8a) and SPEA (Fig 8b) was significantly attenuated ($p<0.01$) compared with the respective controls, indicating that NO was involved in their relaxation effects.

To determine whether the relaxation induced by the SAgs also involved the opening of K^+ channels/potential hyperpolarization of the vascular smooth muscle, experiments were carried out in the presence of increased K^+ concentration (35 mM) in the solution bathing the arteries, to prevent opening of these channels. This treatment abolished the relaxation mediated by both SAgs (Fig 8a and 8b), suggesting dependence of the SAg-induced relaxation on activation of K^+ channels and potentially hyperpolarization of the vascular smooth muscle.

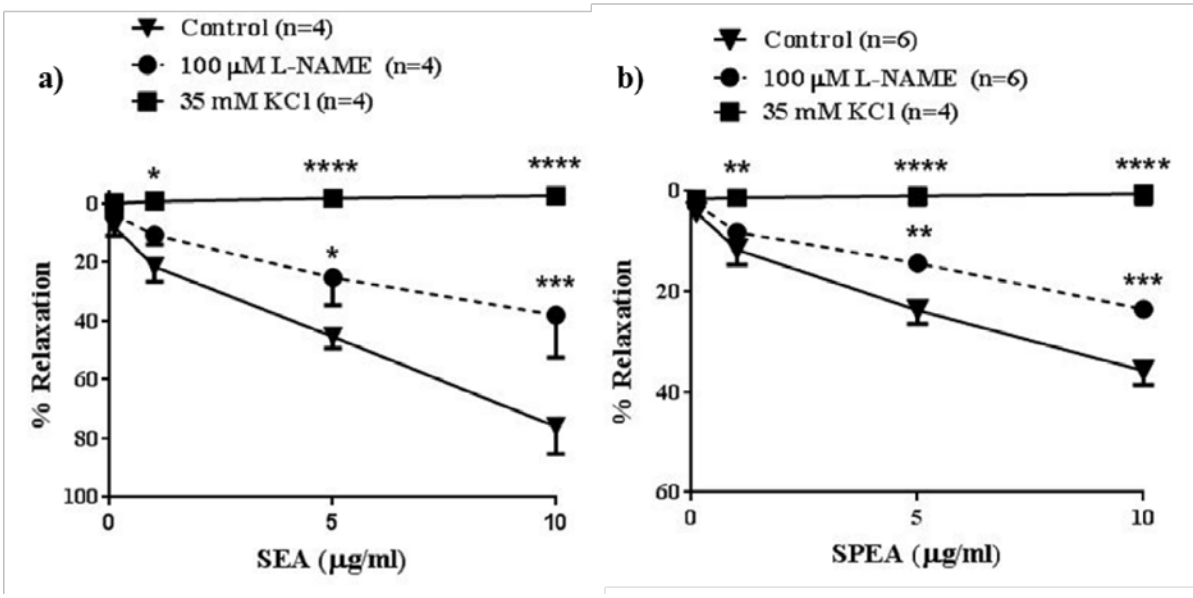

Fig. 8 The effects of 100 µM L-NAME and 35 mM KCl on the relaxation induced by (a) superantigen SEA and (b) superantigen SPEA. Relaxation to these superantigens was partially inhibited by L-NAME and completely abolished by high KCl. Data are presented as mean ± standard error of the mean (S.E.M). *p<0.05, **p<0.01, ***p<0.001, ****p<0.0001, compared with control (SAg) responses.

Localization of regions of the SAg SPEA involved in the vascular response

To map region(s) of SPEA involved in the vascular response, we produced a series of peptides spanning the complete amino acid sequence of SPEA. Each peptide overlapped with the next by thirty amino acids (Table 1). The peptides were then tested for their effects on the vascular response as described in the experimental section. SP7 (61-100), SP11 (101140) and SP19 (181-220) consistently showed marked vasodilator effects above the threshold level, while SP19 showed the highest effect of the three (Fig 9).

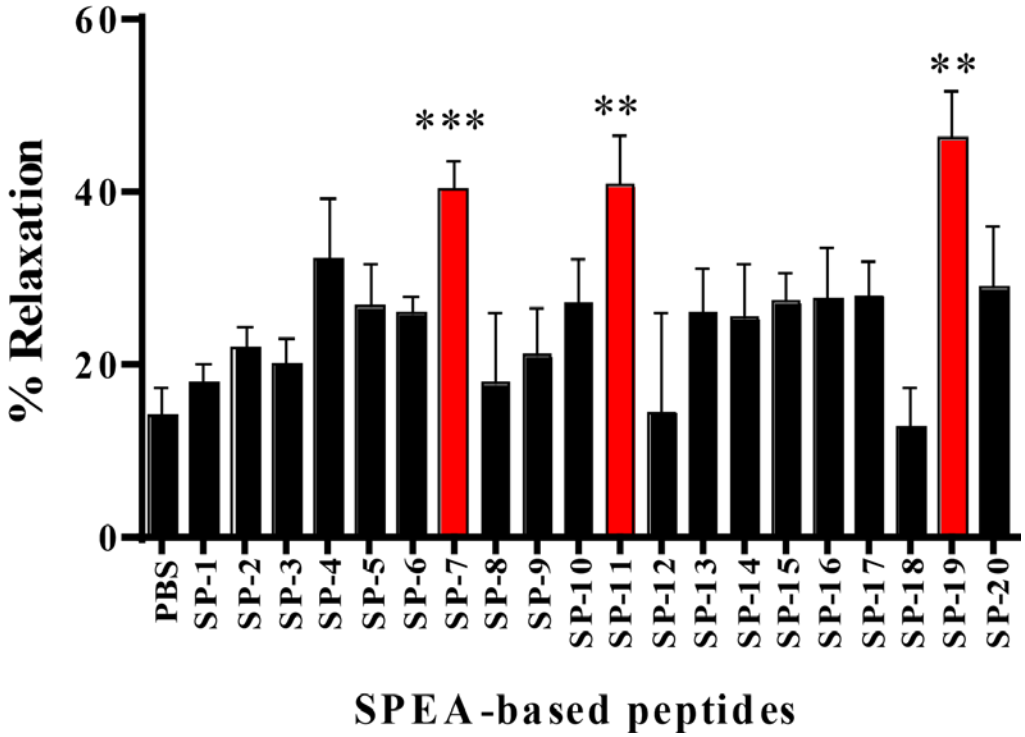

Fig. 9 Identification of peptides derived from superantigen SPEA that induced relaxation. The chart shows the % vasodilation induced by each peptide (n=5). Three peptides SP7, SP11 and SP19 (red column) induced significant dilation of small skeletal muscle with peptide SP19 showing the greatest effect. Data are presented as mean ± standard error of the mean (S.E.M). *p<0.05, **p<0.01, ***p<0.001, compared to the buffer control.

Discussion

The paper describes the production of recombinant superantigens in *E. coli* from codon optimized genes, and their use to investigate the mechanism of action involved in vascular responses. Although cloning and expression of superantigen genes derived from the chromosomal DNA of the pathogens, has been reported previously, this work used codon optimized synthetic gene versions to produce recombinant superantigens. . This approach allowed the large scale production of recombinant superantigens in *E. coli*. Of note, the SAgs genes were codon optimized for expression in yeast but, as we previously serendipitously discovered, this often yields high expression levels of soluble

heterologous protein in *E. coli* [18, 19]. In the present study, the yeast codon optimized SAgs genes were indeed highly expressed in *E. coli*, with the corresponding proteins accounting for up to 50% of the total protein content after IPTG induction. Purification by Ni^{2+} ion column chromatography (Fig 2) confirmed that each recombinant SAg was equipped with an N-terminal His-tag.

The antitumor effect of the superantigens is believed to be mainly due to their activation of T-lymphocytes, which leads to the production of cytokines and hence to cytotoxicity effects on tumors [20, 21]. We therefore, evaluated the purified recombinant SAgs for their superantigenicity activity towards human PBMCs by measuring proinflammatory cytokines (IL-2, IFNγ). The data shown in Fig 3 confirmed the induction of IFNγ and IL2. On the other hand Fig. 4 shows that there is no cytotoxicity effect of SAgs on PBMCs. Moreover, the purified recombinant SAgs induced potent T-cell activation (Fig 5). The T cell activation by the recombinant SAgs was at least 66% of the activation carried out by commercially available SEB.

Subsequently, we evaluated the anticancer activity of the recombinant SAgs. The data in Fig 6 show the capability of the recombinant superantigens for killing DLD-1 cancer cells through the activation of the T-cell and the production of cytokines. The data in Fig 6 show that all four recombinant superantigens induced T-cell mediated killing of DLD-1 tumor cells when mixed with PBMCs. In contrast, the recombinant superantigens had no killing effect on tumor cells in the absence of PBMCs (Fig. 6) or killing effect on PBMCs alone (Fig. 4). Collectively, this part of the work demonstrated that recombinant SEA, SEB, SPEA and TSST-1 produced from synthetic codon optimized genes, are biologically active and have potent antitumor capacities.

SAgs have been implicated in some forms of sepsis, which is a major cause of mortality and morbidity. Its most severe manifestation is the septic shock, which is characterized by low systemic vascular resistance and severe hypotension. These abnormal vascular conditions are caused by both excessive vasodilatation and vascular hyporeactivity to circulating catecholamines.

Our data demonstrate that the SAgs, SEA and SPEA have direct vasodilatory effects that are partly NO-dependent, and fully dependent on activation of K^+ channels. Both NO production and potassium channel activation have been implicated in sepsis induced hypotension [22, 23]. K^+ channels regulate the resting membrane potential of vascular smooth muscle cells and can, therefore, influence vascular tone and blood pressure. The opening of K^+ channels on the arterial smooth muscle membrane allows K^+ to leave the cell and as a result, the cell membrane becomes hyperpolarized. This change in membrane hyperpolarization inhibits the voltage dependent calcium channels, thereby lowering intracellular calcium level and causing arterial dilation [24]. Indeed, abnormal activation of either the ATP-sensitive or the large conductance calcium-activated potassium channels could account for a cardiovascular collapse in shock states [9, 25].

The partial role of NO in the SAg-induced relaxation suggests the vascular endothelium also plays a part in these responses. When NO is released from the endothelium, it diffuses into the underlying vascular smooth muscle and activates soluble guanylyl cyclase enzyme to convert guanosine triphosphate to cyclic guanosine monophosphate (cGMP), an important mediator of vasodilation [25].

Due to the above finding, we extended our study in an attempt to identify the region(s) on one of the superantigens, SPEA superantigen that causing vasodilation and therefore

possible hypotension. Our results indicate that three peptides, SP7, SP11 and SP19, had a direct vasodilatory effect, with SP19 showing the highest effect (table 1 and Fig. 9). Previous studies have identifies peptides from milk and other food sources with possible antihypertensive bioactivities [26-31]. Our work presents the isolation of novel superantigen based peptides with vasodilatory effect and possible antihypertensive bioactivity.

The localized dilation of a vessel by peptides as shown in this study does not necessarily lead to the development of systemic changes in blood pressure. Also, previous studies have shown that for peptides, which are taken orally or by intravenous infusion to exert their antihypertensive bioactivity on their targets in vivo they must be absorbed in the intestine and also be resistant to any peptidases degradation [32, 33]. Testing in animal models, therefore, is required to establish whether the vasodilation shown by the new peptides could lead to a change in blood pressure and to demonstrate the bioactivity of our new peptides as antihypertensive drugs.

One of the ultimate aims of this part of the study was to produce superantigen variants (with less or no hypotension effect) that have tolerable therapeutic potential, e.g. in cancer immunotherapy. The identification of the regions on superantigen which causes vasodilatory effect could lead to the production of safer superantigen variants to improve the tumor-targeted superantigens (TTSs) technique. TTS is a promising strategy for cancer immunotherapy. Typically, TTSs are constructed by fusing a superantigen to a tumor-specific antibody or ligand that binds to targets that highly or uniquely expressed on cancer cells. TTSs have been applied successfully in several cases [34-40]. This therapy however, was achieved at the cost of severe side effects, such as high superantigenicity, toxicity and severe hypotension. Our discovery of the region(s) that

are implicated in the vasodilatory response, and therefore potential hypotension, may allow the production of novel superantigen variants which lack this region, with less or no vasodilatory effect. These novel superantigen variants could be used for tolerable cancer immunotherapy. Equally, the peptides themselves may be useful starting points for therapies where vasodilation is desirable.

Conclusion

We show that the SAgs SEA and SPEA induce arteriolar dilatation, which is partly NOdependent and completely dependent on opening of K_+ channels and potentially hyperpolarization of the vascular smooth muscle, consistent with the potential to cause hypotension. We also identified regions on one of the superantigens, SPEA, which might cause this arteriolar dilatation. Our findings pave the way for the construction and production of superantigen variants with reduced vasodilatory side effects, which could be used for tolerable cancer immunotherapy. Our work may also lead to in vivo investigation of our novel peptides as novel antihypertensive drugs.

Acknowledgments

- The Anti-doping Lab for funding this work and for funding the PhD of the first author (SB), the main contributor to this work.
- Professor C. David O'Connor, Xi'an Jiaotong-Liverpool University for reading and commenting on the manuscript.

Conflict of Interest

- The authors declare that they have no conflict of interest.

Ethics approval and consent to participate

The study was approved by the Anti-Doping Lab-Qatar Institutional Review Board, Ethical approval number: E2017000205. All blood samples used in this study were taken from authors involved in the work.

Funding

- Internal funding obtained from the ADLQ.

References

1. Krakauer T. Therapeutic down-modulators of staphylococcal superantigeninduced inflammation and toxic shock. Toxins. 2010;2(8):1963-83. Epub 2010/08/01. doi: 10.3390/toxins2081963. PubMed PMID: 22069668; PubMed Central PMCID: PMCPMC3153276.
2. Luster AD, Alon R, von Andrian UH. Immune cell migration in inflammation: present and future therapeutic targets. Nature immunology. 2005;6(12):1182-90. Epub 2005/12/22. doi: 10.1038/ni1275. PubMed PMID: 16369557.
3. Dauwalder O, Thomas D, Ferry T, Debard AL, Badiou C, Vandenesch F, et al. Comparative inflammatory properties of staphylococcal superantigenic enterotoxins SEA and SEG: implications for septic shock. J Leukoc Biol. 2006;80(4):753-8. Epub 2006/08/04. doi: 10.1189/jlb.0306232. PubMed PMID: 16885504.
4. Ferry T, Thomas D, Genestier AL, Bes M, Lina G, Vandenesch F, et al. Comparative prevalence of superantigen genes in Staphylococcus aureus isolates causing sepsis with and without septic shock. Clin Infect Dis. 2005;41(6):771-7. Epub 2005/08/19. doi: 10.1086/432798. PubMed PMID: 16107972.
5. Becker K, Friedrich AW, Lubritz G, Weilert M, Peters G, Von Eiff C. Prevalence of genes encoding pyrogenic toxin superantigens and exfoliative toxins among strains of Staphylococcus aureus isolated from blood and nasal specimens. J Clin Microbiol. 2003;41(4):1434-9. Epub 2003/04/12. PubMed PMID: 12682126; PubMed Central PMCID: PMCPMC153929.
6. Salgado-Pabon W, Breshears L, Spaulding AR, Merriman JA, Stach CS, Horswill AR, et al. Superantigens are critical for Staphylococcus aureus Infective endocarditis, sepsis, and acute kidney injury. MBio. 2013;4(4). Epub 2013/08/22. doi: 10.1128/mBio.00494-13. PubMed PMID: 23963178; PubMed Central PMCID: PMCPMC3747586.
7. Spaulding AR, Satterwhite EA, Lin YC, Chuang-Smith ON, Frank KL, Merriman JA, et al. Comparison of Staphylococcus aureus strains for ability to cause infective endocarditis and lethal sepsis in rabbits. Front Cell Infect Microbiol. 2012;2:18.

Epub 2012/08/25. doi: 10.3389/fcimb.2012.00018. PubMed PMID: 22919610; PubMed Central PMCID: PMCPMC3417574.
8. Bone RC. The pathogenesis of sepsis. Ann Intern Med. 1991;115(6):457-69. Epub 1991/09/15. PubMed PMID: 1872494.
9. Landry DW, Oliver JA. The pathogenesis of vasodilatory shock. N Engl J Med. 2001;345(8):588-95. Epub 2001/09/01. doi: 10.1056/NEJMra002709. PubMed PMID: 11529214.
10. O'Brien A, Clapp L, Singer M. Terlipressin for norepinephrine-resistant septic shock. Lancet. 2002;359(9313):1209-10. Epub 2002/04/17. doi: 10.1016/S01406736(02)08225-9. PubMed PMID: 11955542.
11. Grover R, Zaccardelli D, Colice G, Guntupalli K, Watson D, Vincent JL. An openlabel dose escalation study of the nitric oxide synthase inhibitor, N(G)-methyl-Larginine hydrochloride (546C88), in patients with septic shock. Glaxo Wellcome International Septic Shock Study Group. Crit Care Med. 1999;27(5):913-22. Epub 1999/06/11. PubMed PMID: 10362413.
12. Thiemermann C. Nitric oxide and septic shock. Gen Pharmacol. 1997;29(2):159-66. Epub 1997/08/01. PubMed PMID: 9251894.
13. Clapp LH, Tinker A. Potassium channels in the vasculature. Curr Opin Nephrol Hypertens. 1998;7(1):91-8. Epub 1998/01/27. PubMed PMID: 9442369.
14. Cornelissen G, Delcourt A, Toussaint G, Otsuka K, Watanabe Y, Siegelova J, et al. Opportunity of detecting pre-hypertension: worldwide data on blood pressure overswinging. Biomedicine & pharmacotherapy = Biomedecine & pharmacotherapie. 2005;59 Suppl 1:S152-7. Epub 2005/11/09. PubMed PMID: 16275485; PubMed Central PMCID: PMCPMC2581881.
15. Kearney PM, Whelton M, Reynolds K, Muntner P, Whelton PK, He J. Global burden of hypertension: analysis of worldwide data. Lancet (London, England). 2005;365(9455):217-23. Epub 2005/01/18. doi: 10.1016/s0140-6736(05)17741-1. PubMed PMID: 15652604.
16. Faria M, da Costa EL, Gontijo JA, Netto FM. Evaluation of the hypotensive potential of bovine and porcine collagen hydrolysates. Journal of medicinal food. 2008;11(3):560-7. Epub 2008/09/20. doi: 10.1089/jmf.2007.0573. PubMed PMID: 18800907.
17. Orie NN, Fry CH, Clapp LH. Evidence that inward rectifier K+ channels mediate relaxation by the PGI2 receptor agonist cicaprost via a cyclic AMP-independent mechanism. Cardiovasc Res. 2006;69(1):107-15. Epub 2005/09/27. doi: 10.1016/j.cardiores.2005.08.004. PubMed PMID: 16183044.
18. Goda SK, Rashidi FA, Fakharo AA, Al-Obaidli A. Functional overexpression and purification of a codon optimized synthetic glucarpidase (carboxypeptidase G2) in Escherichia coli. Protein J. 2009;28(9-10):435-42. Epub 2009/11/17. doi: 10.1007/s10930-009-9211-2. PubMed PMID: 19911261.
19. Goda SK, Abu Aqel YW, Al-Aswad MR, Rashedy FA, Mohamed AS. Production of synthetic methionine-free and synthetic methionine-limited alpha casein: protein foodstuff for patients with homocystinuria due to cystathionine beta-synthase deficiency. Protein J. 2010;29(1):44-9. Epub 2009/12/25. doi: 10.1007/s10930009-9219-7. PubMed PMID: 20033268.
20. Terman DS, Bohach G, Vandenesch F, Etienne J, Lina G, Sahn SA. Staphylococcal superantigens of the enterotoxin gene cluster (egc) for treatment of stage IIIb

nonsmall cell lung cancer with pleural effusion. Clin Chest Med. 2006;27(2):321-34. Epub 2006/05/24. doi: 10.1016/j.ccm.2006.01.001. PubMed PMID: 16716821.
21. Sundstedt A, Celander M, Hedlund G. Combining tumor-targeted superantigens with interferon-alpha results in synergistic anti-tumor effects. International immunopharmacology. 2008;8(3):442-52. Epub 2008/02/19. doi: 10.1016/j.intimp.2007.11.006. PubMed PMID: 18279798.
22. Russel JA. The current management of septic shock. Minerva Med. 2008;99(5):431-58. Epub 2008/10/31. PubMed PMID: 18971911.
23. Annane D, Bellissant E, Cavaillon JM. Septic shock. Lancet. 2005;365(9453):6378. Epub 2005/01/11. doi: 10.1016/S0140-6736(04)17667-8. PubMed PMID: 15639681.
24. Nelson MT, Patlak JB, Worley JF, Standen NB. Calcium channels, potassium channels, and voltage dependence of arterial smooth muscle tone. Am J Physiol. 1990;259(1 Pt 1):C3-18. Epub 1990/07/01. doi: 10.1152/ajpcell.1990.259.1.C3. PubMed PMID: 2164782.
25. Buckley JF, Singer M, Clapp LH. Role of KATP channels in sepsis. Cardiovasc Res. 2006;72(2):220-30. Epub 2006/09/12. doi: 10.1016/j.cardiores.2006.07.011. PubMed PMID: 16963005.
26. Morales-Camacho JI, Espinosa-Hernandez E, Rosas-Cardenas FF, SemeriaMaitret T, Luna-Suarez S. Insertions of antihypertensive peptides and their applications in pharmacy and functional foods. Applied microbiology and biotechnology. 2019. Epub 2019/01/30. doi: 10.1007/s00253-019-09633-1. PubMed PMID: 30693404.
27. Martinez-Leo EE, Martin-Ortega AM, Acevedo-Fernandez JJ, Moo-Puc R, SeguraCampos MR. Peptides from Mucuna pruriens L., with protection and antioxidant in vitro effect on HeLa cell line. Journal of the science of food and agriculture. 2019. Epub 2019/02/20. doi: 10.1002/jsfa.9649. PubMed PMID: 30779130.
28. Li G, Liu W, Wang Y, Jia F, Wang Y, Ma Y, et al. Functions and Applications of Bioactive Peptides From Corn Gluten Meal. Advances in food and nutrition research. 2019;87:1-41. Epub 2019/01/27. doi: 10.1016/bs.afnr.2018.07.001. PubMed PMID: 30678813.
29. Li B, Habermann D, Kliche T, Klempt M, Wutkowski A, Clawin-Radecker I, et al. Soluble Lactobacillus delbrueckii subsp. bulgaricus 92059 PrtB proteinase derivatives for production of bioactive peptide hydrolysates from casein. Applied microbiology and biotechnology. 2019. Epub 2019/01/23. doi: 10.1007/s00253018-09586-x. PubMed PMID: 30666364.
30. Amorim FG, Coitinho LB, Dias AT, Friques AGF, Monteiro BL, Rezende LCD, et al. Identification of new bioactive peptides from Kefir milk through proteopeptidomics: Bioprospection of antihypertensive molecules. Food chemistry. 2019;282:109-19. Epub 2019/02/04. doi: 10.1016/j.foodchem.2019.01.010. PubMed PMID: 30711094.
31. Aderinola TA, Fagbemi TN, Enujiugha VN, Alashi AM, Aluko RE. In vitro antihypertensive and antioxidative properties of trypsin-derived Moringa oleifera seed globulin hydrolyzate and its membrane fractions. Food science & nutrition. 2019;7(1):132-8. Epub 2019/01/27. doi: 10.1002/fsn3.826. PubMed PMID: 30680166; PubMed Central PMCID: PMCPMC6341156.

32. Li GH, Le GW, Liu H, Shi YH. Mung-bean Protein Hydrolysates Obtained with Alcalase Exhibit Angiotensin I-converting Enzyme Inhibitory Activity. Food Science and Technology International. 2005;11(4):281-7. doi: 10.1177/1082013205056781.
33. Li G. LG, Shi Y., & Shrestha S. . Angiotensin I – converting enzyme inhibitory peptides derived from food proteins and their physiological and pharmacological effects. 2004;24:469–86. doi: 10.1016/j.nutres.2003.10.014.
34. Dohlsten M, Hansson J, Ohlsson L, Litton M, Kalland T. Antibody-targeted superantigens are potent inducers of tumor-infiltrating T lymphocytes in vivo. Proceedings of the National Academy of Sciences of the United States of America. 1995;92(21):9791-5. Epub 1995/10/10. PubMed PMID: 7568219; PubMed Central PMCID: PMCPMC40888.
35. Shaw DM, Connolly NB, Patel PM, Kilany S, Hedlund G, Nordle O, et al. A phase II study of a 5T4 oncofoetal antigen tumour-targeted superantigen (ABR-214936) therapy in patients with advanced renal cell carcinoma. British journal of cancer. 2007;96(4):567-74. Epub 2007/02/08. doi: 10.1038/sj.bjc.6603567. PubMed PMID: 17285137; PubMed Central PMCID: PMCPMC2360042.
36. Xu Q, Zhang X, Yue J, Liu C, Cao C, Zhong H, et al. Human TGFalpha-derived peptide TGFalphaL3 fused with superantigen for immunotherapy of EGFRexpressing tumours. BMC biotechnology. 2010;10:91. Epub 2010/12/24. doi: 10.1186/1472-6750-10-91. PubMed PMID: 21176167; PubMed Central PMCID: PMCPMC3018390.
37. Sun J, Zhao L, Teng L, Lin F, Zhang H, Li Z, et al. Solid tumor-targeted infiltrating cytotoxic T lymphocytes retained by a superantigen fusion protein. PloS one. 2011;6(2):e16642. Epub 2011/02/12. doi: 10.1371/journal.pone.0016642. PubMed PMID: 21311755; PubMed Central PMCID: PMCPMC3032773.
38. Hedlund G, Eriksson H, Sundstedt A, Forsberg G, Jakobsen BK, Pumphrey N, et al. The tumor targeted superantigen ABR-217620 selectively engages TRBV7-9 and exploits TCR-pMHC affinity mimicry in mediating T cell cytotoxicity. PloS one. 2013;8(10):e79082. Epub 2013/11/07. doi: 10.1371/journal.pone.0079082. PubMed PMID: 24194959; PubMed Central PMCID: PMCPMC3806850.
39. Forsberg G, Skartved NJ, Wallen-Ohman M, Nyhlen HC, Behm K, Hedlund G, et al. Naptumomab estafenatox, an engineered antibody-superantigen fusion protein with low toxicity and reduced antigenicity. Journal of immunotherapy (Hagerstown, Md : 1997). 2010;33(5):492-9. Epub 2010/05/14. doi: 10.1097/CJI.0b013e3181d75820. PubMed PMID: 20463598.
40. Yousefi F, Siadat SD, Saraji AA, Hesaraki S, Aslani MM, Mousavi SF, et al. Tagging staphylococcal enterotoxin B (SEB) with TGFaL3 for breast cancer therapy. Tumour biology : the journal of the International Society for Oncodevelopmental Biology and Medicine. 2016;37(4):5305-16. Epub 2015/11/13. doi: 10.1007/s13277-015-4334-x. PubMed PMID: 26561468.

Chapter 7

Summary and Future Prospects

Summary and Future Prospects:

Targeted cancer therapies are currently the focus of many anticancer drug treatments with the ability to interfere with cancer cell growth or survival. Many targeted cancer therapies have been approved by the Food and Drug Administration (FDA) to treat specific types of cancer. Others are being studied in clinical trials, and many more are in preclinical testing. Targeted therapies on cancer cells may have limitations, possibly involving drug resistance, or lack of dug specificity. Each chapter below focuses on a possible limitation of the treatment, and provides a new approaches that can be applied to overcome these limitations.

In **Chapter 2,** we carried out a review of different strategies to produce long acting therapeutic drugs in cancer, and their benefits for drug delivery. PEGylation and albumin fusion have provided a particular focus and represent the most widely used and discussed. The application of the two forms in therapeutic proteins and their use in cancer treatment and improving drug delivery are crucial and are the future for therapeutic proteins. The modified therapeutic agents have been demonstrated to have increased serum half-life and solubility, and an improved potential for drug delivery while maintaining their activity. Our studies suggest roles in immunotherapy as well in targeted cancer therapy and in a manner that protects the protein/enzyme from the immune system.

In **chapter 3,** we discuss how we managed to isolate a novel CPG2 variant. Despite the close similarity between the new and the conventional enzyme, the polyclonal antibody raised against our new form of CPG2 did not react with the CPG2 from Pseudomonas strain RS-16 that is currently in clinical use. This indicates that the two enzymes are antigenically distinct. This feature may have advantages in that administration of the two drugs consecutively in the ADEPT protocol could minimize the antibody responses that hampers repetitive administration of the current treatment with Ps CPG2. The availability of the new glucarpidase could be of great importance in improving

its therapeutic usefulness in cancer therapy and will provide the opportunity for dose studies that, in turn, might lead to the escalation of methotrexate doses for more efficient treatment. Future studies should carry out in vivo studies to investigate if the patient's immune system will react favorably, if the two enzymes are given consecutively comparing to one enzyme only.

In **Chapter 4,** we discuss how with DNA shuffling we created new CPG2 variants with mutations that produced 110-200% more activity than the wild type glucarpidase. Analysis of the DNA sequences indicated that single point mutation occurred in each variant causing amino acid substitutions I100T, T239A, and G123S. CD study of the shuffled CPG2 showed a higher alpha helix content than the wild type. This work indicates a basis for economical production of a new recombinant glucarpidase with enhanced enzyme activities for the potential use in ADEPT and/or the detoxification of drugs. The application of the newly generated glucarpidase could be extended to clinical applications other than cancer. The new glucarpidase with higher activity that we have produced could be of value in detoxification, in cases of methotrexate overdose. Modified drugs (as discussed below in **chapter 5**) could be applied with the new shuffled variants to produce a longer active drug with even higher activity using the PEGylation techniques and also the genetic fusion of HSA.

In **Chapter 5,** the aim was to produce a long-acting glucarpidase. We created two longacting forms of CPG2: a mono-PEGylated glucarpidase, and a HSA-fused glucarpidase.

Biochemical and bioactivity analyses indicated that each form had an improved half-life, and the functional activities of the glucarpidase conjugates were maintained. They also exhibited high stability in human serum and were more resistant to key human proteases than the native glucarpidase. To our knowledge, this study is the first to report stable and less immunogenic glucarpidase variants produced by PEGylation and fusion with HSA. Our findings suggest that they

might have greater efficacy in drug detoxification and ADEPT. The two forms can be given to patients consecutively to prolong the cycle administration, thereby, significantly improving the cancer treatment strategy. Our work paves the way for clinical investigation, and clinical trials using our novel modified forms of CPG2 for cancer treatment and drug detoxification. Production of different modifiers to glucarpidase (CPG2) and its new variants should allow novel CPG2 forms to be produced for more cycle of administration of the enzyme. Animal testing will be a crucial bridge to clinical studies, and permit an initial assessment of the half-lives of the different forms of CPG2, *in vivo*, their immunogenicity and stability.

In **Chapter 6,** we used different molecules for cancer treatment, superantigens. The aim is to identify the region(s) on these molecules, which cause the severe hypotension if the host was injected by superantigen. The identification of the region causing this hypotension will then lead to the production of modified superantigen by the removal of these regions. The novel superantigen molecules will then be used for targeted cancer treatment with less side effects. We first overexpressed four codon optimized superantigens, SEA, SEB, TSST-1 and SPEA. These had the ability to activate the T cells to an extent at least 66% greater than that with the available SEB. The recombinant superantigens had the ability to kill DLD1 cancer cells when mixed with PBMCs which activated T cells and triggered the production of cytokines. We showed, using two of the superantigens (SEA and SPEA), that they cause vasodilation which could lead to hypotension, and creating an unwanted side effect. We then designed and synthesized nineteen overlapping peptides from SPEA, and were able to identify peptides which contribute to the superantigen-induced hypotension. Removing the amino acids identified should pave the way for production of superantigen variants with reduced potential for the side effect of vasodilation.

Chapter 8:

Samenvatting en toekomstperspectieven

Samenvatting en toekomstperspectieven :

Gerichte kanker therapieën zijn momenteel middelpunt van veel geneesmiddel gerichte kanker behandelingen, met de eigenschap tot het hinderen van kanker celgroei of overleving. Veel geneesmiddel gerichte kanker behandelingen zijn goedgekeurd door de Amerikaanse Inspectie van voedsel- en geneesmiddelen (FDA) voor de behandeling van verschillende soorten kanker. Andere behandelingen worden getest in klinische trials en vele zijn momenteel in de preklinische fase. Gerichte therapieën op kanker cellen hebben hun beperkingen, mogelijk door medicijn resistentie, of gebrek aan specificiteit. Elk hieronder beschreven hoofdstuk richt zich op een mogelijke beperking van behandeling en levert nieuwe benaderingen welke in de toekomst toegepast kunnen worden om dit in de te ondervangen.

In **Hoofdstuk 2** hebben we een evaluatie uitgevoerd van verschillende strategieën om langwerkende therapeutische geneesmiddelen bij kanker te produceren en de voordelen ervan voor drug delivery. De resultaten leggen een bijzondere nadruk op PEGylatie en albumine-fusie en vertegenwoordigen de gevallen die het meest gebruikt en genoemd worden. De toepassing van de twee vormen in therapeutische eiwitten en hun bij de behandeling van kanker en het verbeteren van de medicijnafgifte zijn cruciaal en vertegenwoordigen de toekomst voor therapeutische eiwitten. Van de gemodificeerde therapeutische middelen is aangetoond dat ze een verhoogde halfwaardetijd en oplosbaarheid in serum hebben en een verbeterd potentieel voor drug delivery met behoud van activiteit. Onze studies suggereren een rol in zowel immunotherapie en gerichte kankertherapie, dusdanig op een manier die het eiwit / enzym beschermt tegen het immuunsysteem.

In **Hoofdstuk 3**, wordt besproken hoe het gelukt is om een nieuwe CPG2 variant te isoleren. Ondanks de sterke gelijkenissen tussen het nieuwe en het conventionele enzym, reageerde het gekweekte polyklonale antilichaam tegen onze nieuwe vorm van CPG2, niet tegen CPG2 van Pseudomonas stam RS-16 dat momenteel in klinisch gebruik is. Dit geeft aan dat de twee enzymen antigeen verschillend zijn. Dit kenmerk kan voordelen hebben doordat toediening van twee geneesmiddelen achtereenvolgens in het ADEPT-protocol, de antilichaamreacties die repetitieve toediening van de huidige behandeling met Ps CPG2 belemmeren, kan minimaliseren. De beschikbaarheid van nieuwe glucarpidase zou van grote betekenis kunnen zijn in de verbetering van de therapeutische bruikbaarheid tijdens kankertherapie en levert de mogelijkheid tot dosis studies, welke vervolgens kunnen leiden tot de escalatie van methotrexaat dosering voor efficiëntere behandeling. Toekomstige studies zouden kunnen onderzoeken in hoeverre welke antilichamen, in de circulatie van patiënten die behandeld zijn met de Ps CPG2, anders of zelf niet reageren met de nieuwe variant van CPG2, en zodoende een klinisch voordeel bieden.

In **Hoofdstuk 4** bespreken we hoe we met DNA-shuffling nieuwe CPG2-varianten creëerden met mutaties die 110-200% meer activiteit produceerden dan het wildtype glucarpidase. Analyse van de DNA-sequenties liet zien dat een mutatie op een enkel punt optrad in elke variant die aminozuursubstituties I100T, T239A en G123S veroorzaakte. CD-onderzoek van het geshuffelde CPG2 vertoonde een hoger alfa-helixgehalte dan het wildtype. Dit werk vormt de grondslag voor economische productie van een nieuw recombinant glucarpidase voor het potentiële gebruik in ADEPT en / of de ontgifting van geneesmiddelen. De toepassing van de nieuw gegenereerde glucarpidase kan worden uitgebreid naar andere klinische toepassingen dan kanker. Het nieuwe geïsoleerde

glucarpidase met hogere activiteit, zou van waarde kunnen zijn bij ontgifting bij een overdosis met methotrexaat. Gemodificeerde geneesmiddelen (zoals hieronder besproken in **Hoofdstuk 5**) kunnen worden toegepast met de nieuwe geshuffelde varianten om een langer actief medicijn te produceren met een nog hogere activiteit.

In **Hoofdstuk 5** was het de doel om een langwerkende glucarpidase te produceren. We ontwikkelden twee langwerkende vormen van CPG2: een mono-gePEGyleerde glucarpidase en een HSA-gefuseerde glucarpidase. Biochemische en bioactiviteitsanalyses wezen erop dat elke vorm een verbeterde halfwaardetijd had en de functionele activiteiten van de glucarpidase conjugaten werden gehandhaafd. Ze vertoonden ook een hoge stabiliteit in menselijk serum en waren meer resistent tegen belangrijke humane proteasen dan het lichaamseigen glucarpidase. Voor zover ons bekend is, is deze studie de eerste die melding maakt van stabiele en minder immunogene glucarpidase-varianten geproduceerd door PEGylation en fusie met HSA. Onze bevindingen suggereren dat ze mogelijk een grotere werkzaamheid hebben bij het ontgiften van medicijnen en ADEPT. De twee vormen kunnen achtereenvolgens aan de patiënt worden gegeven om de cyclus toediening te verlengen, waardoor de kankerbehandelingsstrategie aanzienlijk wordt verbeterd. Ons werk baant de weg voor klinisch onderzoek en klinische trials met behulp van onze nieuwe gemodificeerde vormen van CPG2 voor de behandeling van kanker en ontgifting van geneesmiddelen. De productie van verschillende modifiers voor glucarpidase (CPG2) en variaties ervan zouden het mogelijk moeten maken dat nieuwe CPG2-vormen worden geproduceerd voor meer cycli van toediening van het enzym. Dierproeven zullen een cruciale brug vormen

naar klinische onderzoeken en een eerste beoordeling toelaten van de halfwaardetijden van de verschillende vormen van CPG2 in vivo, hun immunogeniciteit en stabiliteit.

In **Hoofdstuk 6** hebben we verschillende moleculen gebruikt voor de behandeling van kanker, namelijk superantigenen. Het doel is om de regio's op deze moleculen te identificeren die de hypotensie veroorzaken als een bijwerking van superantigenen. Dit zal op zijn beurt leiden tot de productie van een gemodificeerd superantigeen door de verwijdering van deze regio's met minder bijwerkingen. We brachten eerst vier met codons geoptimaliseerde superantigenen, SEA, SEB, TSST-1 en SPEA tot over expressie. Deze hadden het vermogen om de T-cellen te activeren in een mate die ten minste 66% groter was dan die met de beschikbare SEB. De recombinante superantigenen hadden het vermogen om DLD1-kankercellen te doden wanneer gemengd werden met PBMC's, die T-cellen activeerden en zo de productie van cytokinen activeerden. We hebben aan de hand van twee van de superantigenen, SEA en SPEA aangetoond dat ze vasodilatatie veroorzaken, wat zou kunnen leiden tot hypotensie, een mogelijke ongewenste bijwerking. Vervolgens hebben we 19 overlappende peptiden van SPEA ontwikkeld en gesynthetiseerd en konden we peptiden identificeren die bijdragen aan de door superantigen geïnduceerde hypotensie. Het verwijderen van de geïdentificeerde aminozuren zou de weg moeten banen voor de productie van superantigen varianten met een lagere potentie voor de vasodilatatie bijwerkingen.

Chapter 9:

الملخص والرؤيه المستقبليه

الملخص والرؤيه المستقبليه:

العلاجات السرطانية المستهدفة هي حاليا محور العديد من العلاجات المضادة للسرطان مع القدرة على التدخل في نمو الخلايا السرطانية أو البقاء على قيد الحياة. تمت الموافقة على العديد من العلاجات السرطانية المستهدفة من قبل إدارة الغذاء والدواء (FDA) لعلاج أنواع معينة من السرطان. تتم دراسة البعض الآخر في التجارب السريرية ، والعديد منها في الاختبارات قبل السريرية. العلاجات المستهدفة على الخلايا السرطانية قد يكون لها قيود ، وربما تنطوي على مقاومة للأدوية ، أو عدم وجود التخصيص المطلوب. يركز كل فصل أدناه على القيود وتوفير البدائلا لحلها وإظهار العمل المستقبلي الذي يمكن المضي فيه.

في **الفصل الثاني** ، أجرينا مراجعة لاستراتيجيات مختلفة لإنتاج الأدوية العلاجية طويلة المفعول في السرطان ، وفوائدها لتسليم المخدرات. ويعد ال PEGylation و الاتحاد بال Albumin ذوي تركيزا خاصا وتمثل الأكثر استخداما ومناقشه علميا. إن استخدام الشكلين في البروتينات العلاجية واستخدامها في علاج السرطان وتحسين توصيل الدواء لهما أهمية حيوية وهما مستقبل البروتينات العلاجية. وقد ثبت أن العوامل العلاجية المعدلة قد زادت من فترة نصف عمر المصل وقابلية الذوبان ، وتحسين القدرة على توصيل الدواء مع الحفاظ على نشاطها. تقترح دراستنا أدوار في العلاج المناعي وكذلك في علاج السرطان المستهدف وبطريقة تحمي البروتين / إنزيم من الجهاز المناعي.

في **الفصل الثالث** ، نناقش كيف نجحنا في عزل متغيرجديد لل CPG2. على الرغم من التشابه الوثيق بين الإنزيم الجديد والتقليدي ، لم يتفاعل الأجسم المضاده من CPG2 الجديد مع ال CPG2 من Pseudomonas sp. سلالة RS-16 التي هي حاليا في الاستخدام السريري. هذا يدل على أن الانزيمات الاثنين مستقلين بالتصرف. قد يكون لهذه الميزة مزايا في أن تناول دوائين على التوالي في بروتوكول ADEPT يمكن أن يقلل من استجابات الأجسام المضادة التي تعيق الجرعات المتكررة للمعالجة الحالية مع Ps CPG2. إن توفر الCPG2 الجديد يمكن أن يكون ذو أهمية كبيرة في تحسين فائدته العلاجية في علاج

السرطان وسيوفر فرصة لدراسات الجرعة التي قد تؤدي بدورها إلى تصعيد جرعات الميثوتريكسيت لعلاج أكثر فعالية. يجب على الدراسات المستقبلية أن تبحث في مدى تفاعل الأجسام المضادة من المرضى الذين عولجوا بالـ PSG2 بطريقة مختلفة أو لا تتفاعل مع الشكل الجديد لـ CPG2 ، وبالتالي تمتلك مزايا الكلينيكيه. في **الفصل الرابع** ، ناقشنا كيف قمنا عن طريق خلط الحمض النووي DNA بإنشاء متغيرات جديدة لـ CPG2 مع طفرات أنتجت نشاطًا أكثر من 110-200٪ من الCPG2 المستخدم. يشير تحليل تسلسلات الدنا إلى حدوث طفرة أحادية النقطة في كل متغير يسبب استبدال الحمض الأميني I100T و T239A و G123S. أظهرت دراسة ال CD من الـ CPG2 المختلط أن محتوى اللولب ألفا أعلى من النوع المستخدم. ويشير هذا العمل إلى أساس للإنتاج الاقتصادي لغلوكاربيداز المؤتلف الجديد للاستخدام المحتمل في ADEPT و / أو إزالة السموم من المخدرات. يمكن توسيع تطبيق الCPG2 الذي تم تكوينه حديثًا ليشمل تطبيقات اكلينيكيه أخرى غير السرطان. يمكن للجلوكاربيديز الجديد ذو النشاط الأعلى الذي تم عزله في **الفصل الثالث** أن يكون ذا قيمة في إزالة السموم في حالات جرعة زائدة من الميثوتريكسيت. يمكن تطبيق العقاقير المعدلة (كما هو موضح أدناه في **الفصل الخامس**) علي المتغيرات المختلطة الجديدة لإنتاج دواء طويل الفاعليه مع نشاط أعلى. في **الفصل الخامس** ، كان الهدف هو إنتاج CPG2 طويل الفاعليه. نجحما بإنشأنا شكلين من CPG2: CPG2 مرتبط أحاديا مع ال PEG ، و CPG2 متحد مع HSA. أشارت التحليلات البيوكيميائية والنشاط الحيوي إلى أن كل شكل كان له عمر نصف محسّن ، وتم الحفاظ على الأنشطة الوظيفية للجلوكاربيداز. كما أظهروا ثباتًا عاليًا في مصل الدم البشري وكانوا أكثر مقاومة لبروتيز الإنسان من الCPG2 الأصلي المستخدم. على حد علمنا ، هذه الدراسة هي أول من نوعها علي مستوي ال CPG2 واثبت بأنه مستقر وأقل استدامة من الشكلين ال PEGylated والمتحد بال HSA. وتشير النتائج التي توصلنا إليها أن قد يكون لها فعالية أكبر في إزالة السموم من العقاقير و ADEPT. يمكن إعطاء الشكلين للمريض على التوالي لإطالة دورة العلاج ، وبالتالي تحسين استراتيجية علاج السرطان بشكل كبير. يمهد عملنا الطريق للتحريات الكلينيكيه والتجارب

السريرية باستخدام هذه الأشكال الجديدة المعدلة من CPG2 لعلاج السرطان وإزالة السموم من العقاقير. إن إنتاج مُعَدِلات مختلفة إلى CPG2 ومتغيراته الجديدة بإنتاج أشكال جديدة من ال CPG2 لمزيد من دورات العلاجيه بكميات اقل اسبوعيا. سيكون اختبار الحيوانات جسراً حاسماً للدراسات الكلينيكيه ، ويسمح بإجراء تقييم أولي لنصف عمر الأشكال المختلفة للـ CPG2 في الجسم الحي ، واستجابتها واستقرارها.

في **الفصل السادس** ، استخدمنا جزيئات مختلفة لعلاج السرطان، superantigens. الهدف هو تحديد المنطقة (المناطق) على هذه الجزيئات التي تسبب انخفاض ضغط الدم باعتباره أحد الآثار الجانبية لل superantigen. وسيؤدي ذلك إلى إنتاج superantigen المعدلة عن طريق إزالة هذه المناطق مع أقل الآثار الجانبية. لقد عزلنا أكثر من أربعة مناطق محسنه الـ codon علي ال SEA و SEB و TSST-1 و SPEA. هؤلاء الاربعه لديهم القدرة على تنشيط الخلايا التائية إلى حد ما على الأقل 66 ٪ من ال SEB المتاحة. كان لدى superantigens القدرة على قتل الخلايا السرطانية DLD1 عند مزجه مع PBMCs التي تنشط الخلايا التائية وتؤدي إلى إنتاج السيتوكينات. أظهرنا ، باستخدام اثنين من superantigens، SEA و SPEA أنها تسبب توسع الأوعية التي يمكن أن تؤدي إلى انخفاض ضغط الدم ، وهذا يمكن أن يكون أحد الآثار الجانبية غير المرغوب فيها. ثم قمنا بتصميم وتوليف تسعة عشر ببتيد متداخل من SPEA ، وتمكننا من تحديد الببتيدات التي تساهم في انخفاض ضغط الدم المستحث. إزالة الأحماض الأمينية التي تم تحديدها يجب أن تمهد الطريق لإنتاج أنواع مختلفة من الخلايا ذات الإمكانات المنخفضة للأثر الجانبي لتوسع الأوعية.

Chapter 10:

Appendix

Propositions

It is a continuous battle between science and nature, who is going to win the war?

Al-Anod D. Al-Qahtani

- “Man is either your brother in faith or your equal in humanity.”-Ali bin Abii Taleb.
- “Only two things are infinite, the universe and human stupidity, and I'm not sure about the universe.” - Albert Einstein
- “A person who never made a mistake, never tried anything new.”- Albert Einstein
- “One, remember to look up at the stars and not down at your feet. Two, never give up work. Work gives you meaning and purpose and life is empty without it. Three, if you are lucky enough to find love, remember it is there and don't throw it away.” - Stephen Hawking
- “There may be times when we are powerless to prevent injustice, but there must never be a time when we fail to protest.”- Elie Wiesel
- “You do not write your life with words...You write it with actions. What you think is not important. It is only important what you do.”-Patrick Ness
- “The definition of insanity is doing the same thing over and over and expecting different results.” - Albert Einstein
- “Such studies might also open a rational pathway for further changes.” - this thesis
- “modification can lead to slight denaturation which may generate a significant immune response” - this thesis
- “If you genuinely believe it ... It will happen. Just aim towards it.”- Myself
- “If you are not doing what you love, you are wasting your time.”- Billy Joel
- What nature have done in millions of years could be done in laboratories in several days.- my view
- Science can beat nature and yield biobetter products than the wild type. – my view
- Naturally lethal, but could be therapeutics. – my view

- “Question and criticism yourself as if you are your worst enemy.”- Prof. Sayed Goda
- “If you want to worship God be good to all mankind first regardless their religions, skin colors or political beliefs then do the rest such as praying and others.” - Prof. Sayed Goda
- “Poverty and ignorance of peoples are the true wealth of the tyrants, dictators and terrorists, without which they cannot commit their crimes.” - Prof. Sayed Goda

Conferences:

- American Society for Biochemistry and Molecular Biology, 26-30 Apr. **2014**, San Diego, CA, USA. (Poster presentation)
- The Medicinal Chemistry & Bioanalysis symposium (MCB 2014), 25-26Aug. **2014**, Groningen, The Netherlands. (Poster presentation).
- American Society for Biochemistry and Molecular Biology, March 28- April 1, **2015**, Boston, USA 2015(Poster presentation)
- 10th Annual Proteins & Antibodies Congress, 24- 25 Apr. **2017**, London, UK (Poster presentation)
- PEGS Europe Protein and antibody engineering summit 13-17 Nov. **2017**, Lisbon, Portugal (Poster presentation)
- Anti Doping Lab QATAR Annual Junior symposiums **2013, 2014, 2015, 2016,** and **2017**, Doha, Qatar. (Lecture)
- AntiDoping Lab QATAR Annual Junior symposiums **2018**, Doha, Qatar. (Poster presentation)
- Qatar Foundation Annual Research Conference, **2015**, **2016** and **2017**, Doha, Qatar (Poster presentation)

Acknowledgment

لَئِن شَكَرْتُمْ لَأَزِيدَنَّكُمْ

(If you are thankful, surely I will increase you) 7 Ibrahim

Thank you Allah الحمد والشكر لله عز وجل

To My Parents

Thank you for believing in me

Thank you for making it possible

Thank you for being my biggest supporters I

am nothing without you.

I truly give you both all my success

I would like to express my deep appreciation to my PhD supervisors,

Professor Sayed K Goda and Professor Alex Dömling

Thank you for your guidance, encouragement and critiques. Thank you for pushing me and believing in me, when I felt down and discouraged. Thank you for teaching me to be more than just a scientist, but to become a humble and intuitive person. You are both the best example of a true scientist. I would especially thank Dr Sayed for his persistence and patience with me. Thank you for teaching me that science is not only obtaining a degree, but it's a life style and a plan for the future. I thank you for being a father figure to me. I can loudly say:

Dr. Sayed you are my Guru.

I would like to thank my sister (**Noora**), and my brothers (**Ahmad, Hamad, & Abdulla**). You are my solid wall.

To my daughter, my beautiful baby, my pride and joy, my princess

(**Maryam**)

It is you who made me realize that I have to do my best to be your best. It is you who made me wake up and realize that I can be more than just a mother.

To (**Prof, David O'Conner)** I can't thank him enough for making the time to proof read my papers, even though he is very busy, he managed go through them and criticism it as if they were his own.

I would like to thank **(Dr. Mohammad AlMaadeed)** for initiating and supporting the PhD program in the ADL Q.

My appreciative thanks are also extended to **(Dr. Matthew Groves).** The first person in Groningen who was patient enough to stand with me hand in hand and teach me the basics and trick of molecule biology and always encouraging me to do better.

I would liket o thank **(Dr.Mohammad AlSayrafi** and **Prof. Aisha Lattif)** for their continuous support durning my PhD journey.

Our lab manager in GU, (**André**) Thank you for giving me your time in translating my English thesis summary to Dutch.

I would also like to extend my appreciations to both the **Protein Engineering Lab** especially **Sara Bashraheel** and the ADLQ as a whole and everyone in the **Drug Discovery Unit** in GU. Both labs have become by second family, holding some of the best memories between those walls.

I would like to give an exceptional thank you to my friends and loved ones without for being supportive, understanding and baring with me at all times.

I would like to acknowledge **QNRF** for funding and **ADLQ** for giving me a chance to work full time on my PhD.

After a journey of ups and downs and memories filled with mixed emotions, I can now stand proudly and say it was the best experience of my life. I am happy to have taken the initiative to make a difference in my life and add my part in the pool of science.